Dorso-ventral differences in gene expression and Brachyury chromatin binding in *Xenopus*

University College London (UCL)

Cell and Developmental Biology

Rita S. Monteiro

The Francis Crick Institute

formerly

MRC — National Institute for Medical Research

A dissertation submitted in partial fullfilment

of the requirements for the degree of

Doctor of Philosophy

of

University College London

March 21, 2018

I, Rita S. Monteiro, confirm that the work presented in this thesis is my own. Where information has been derived from other sources, I confirm that this has been indicated in the work.

_____

Rita Monteiro

This thesis is dedicated to Pedro and my parents. Obrigada por tudo!

Acknowledgments

First I would like to thank Jim Smith for giving me the opportunity to do this work and for his supervision during the project. I would like to thank everyone from the Smith's lab, past and present members, for the support and for being a positive influence during my PhD.

Special thanks to George Gentsch, who guided me through all the project and was a mentor and an inspiration for the researcher that I thrive to be. I would also like to thank Kevin Dingwell for keeping the lab going and all of his assistance.

I would like to thank members of the Gilchrist lab with whom I shared eggs and frustrations. A special thanks to Rosa, my PhD companion with whom I share the nationality and had many discussions on ChIP-Seq analysis. Having a fellow 'tuga' going through the same difficulties made the journey easier.

I spent many hours looking down a scope, sorting and counting thousands of frog embryos. Although it might be silly, I feel like I have to thank the frogs for providing me my studying material. This acknowledgement is extended to the Aquatics staff whose work was essential and made the process easier.

My project was part of a Marie Curie ITN, at a time when EU funding for UK research was still a reality! I would like to thank all of the supervisors that organised workshops and seminars. They were essential to provide me with skills to complete the PhD. Oh! And the travelling was also great!

I also want to thank everyone that I've crossed paths with during my Bachelor and Masters, who have taught me something along the way. It all contributed to me getting here!

I would like to thank my parents, although they will never understand what it is that I do, they have always supported me in all matters. Finally, I want to thank Pedro,

my life partner, for always being there for me even when I was absolutely unbearable complaining about failed experiments. Although sometimes it did not look like, you have kept me sane.

Abstract

The main question developmental biologists pursue is the understanding of the processes involved in transforming a single cell into a whole organism with distinct tissues.

In this thesis, I addressed this question, using the frog embryo and focusing on tissue-specific regulation by transcription factors. As an approximation for dorsal and ventral tissues, I used UV and LiCl treatments, that resulted in ventralised and dorsalised embryos, respectively. In a first instance, I did a whole poly(A)-transcriptome comparison of LiCl- and UV-treated embryos which validated the use of this approach as a proxy for dorsal and ventral cell types. Furthermore, I characterised these cell types, identified and characterise new genes, with a special focus in a dorsally expressed gene activated by the canonical Wnt signalling.

To study cell-specific regulation at the chromatin level I compared the chromatin landscape of dorsalised and ventralised embryos. I observed that both RNAPII and the putative enhancer marker p300 bind the chromatin differently in a way that correlated with gene expression. I also compared the binding of Brachyury, a zygotic transcription factor expressed in both cell types. Although the majority of sites were bound similarly, a small subset was differentially bound in the two condition. I showed evidence that these differences could be due to absence/presence of co-factors that mediated the binding to these sites.

Finally, I compared Brachyury morpholino(MO)-mediated KD (knockdown) and KO (knockout) embryos and showed, that whilst phenotypically are similar, transcriptionally there was a group of genes misregulated only in MO-injected embryos. I further explored the nature of these genes and revealed new insights into the use of morpholinos in loss of gene function experiments.

Contents

List of Figures

List of Tables

Abbreviations

Abbreviations for measurement units were used based on the International System of Units (SI). For chemical elements and formulae standard notations were used. Protein and gene names abbreviations were used in accordance with the *Xenopus* model organism database, Xenbase. Other abbreviations used in this work are described below:

3'	3-prime
5'	5-prime
BCNE	blastula chordin and noggin expressing centre
ChIP	Chromatin immunoprecipitation
CNS	Central nervous system
CRISPR	Clustered regularly interspaced short palindromic repeats
DC	Destruction complex
DNA	Deoxyribonucleic acid
GO	Gene ontology
HA	Hemagglutinin
HAT	Histone acetyltransferases
HDAC	Histone deacetylase
hESC	Human embryonic stem cell
iPS	Induced pluripotent stem cells
MBT	Midblastula transition
miRNA	micro RNA
MO	Morpholino oligonucleotide
mRNA	messenger RNA
NC	Nieuwkoop center
NLS	Nuclear localisation signal

PCR	Polymerase chain reaction
RNA	Ribonucleic acid
RT-qPCR	Reverse transcription quantitative polymerase chain reaction
SO	Spemann organiser
TALEN	Transcription activator-like effector nuclease
TF	Transcription factor
UV	Ultraviolet
WT	Wild-type

Chapter 1

Introduction

1.1 Signalling pathways and the role in development

Embryonic development can be summarised as the process of transforming one cell, the mature zygote, into a organism composed of many different cell types. It is a highly complex process that relies on interaction and communication between different cells. An early observation of this cell-cell communication (then called embryonic induction) was by Hans Spemann in amphibians, firstly with optic cup and later with grafting experiments of the dorsal lip, which I shall discuss later.

The identification of cell communication as an essential process in development preceded, by several decades, the identification of the molecules responsible for these interactions and the mechanisms involved. We now know that cell-cell communication is achieved by the transduction of a signal from one cell to the other: a cell secretes a ligand to the extracellular space, other cells with the proper receptor will then transduce the signal through a series of intermediates, which will lead to changes in the receiving cell. During development, the most common effect of signal transduction between cells is on transcription, either activation or repression. From the 1980s onwards, as different molecules have been identified by their role and molecular nature, they have been grouped into families based on their similarities and capacities to activate certain pathways. In metazoa, about 17 signalling pathways have been identified, but only 5 of these families seem to have an essential role in early development. These are: (i) wingless related (Wnt), (ii) TGF-β, Hedgehog, (iv) signalling by receptor-tyrosine kinase and (v) Notch signalling. In the next sections I will expand on Wnt and TGF-β

signalling and refer to their role in development because these are the pathways more relevant to my thesis.

1.2 Wnt Signalling

1.2.1 History

The Wnt signalling pathway provides a powerful example of the link between developmental biology and cancer, and why studying the former will greatly inform the latter. The Wnt ligand was discovered in the late 1980s and early 1990s both as a developmentally relevant gene in *Drosophila*, *wingless*, (Baker, 1987; Cabrera et al., 1987) and as an oncogene in mouse, *int-1* (Nusse and Varmus, 1982). With the realisation that the genes belonged to the same family of extracellular signalling molecules (Rijsewijk et al., 1987) the names were merged into Wnt (*wingless+int*).

Through the 1990's more components of the pathway were identified. These included *Frizzled*(*Fzd*), *Dishevelled* (*Dsh*,*Dvl*) (Sussman et al., 1994; Sokol et al., 1995; Noordermeer et al., 1994), *β-catenin*/*Armadillo* (Noordermeer et al., 1994; Peifer et al., 1991), *T cell factor* (*TCF*)/*Pangolin* (Brunner et al., 1997) and *Glycogen synthase kinase 3b* (*GSK3-β*) (Dominguez, Itoh, and Sokol, 1995). Many of these genes were identified through forward genetic screens and found to be conserved between species. Epistasis experiments allowed the assembly of a model for the mechanism of Wnt signalling by identifying where in the pathway each component acted (Siegfried, Wilder, and Perrimon, 1994; Noordermeer et al., 1994).

In classifying the different Wnt proteins based on function, Wnt signalling was divided into 'canonical' and 'non-canonical'. Canonical Wnt was able to induce the formation of a secondary anterio-posterior (AP) axis in *Xenopus* embryos (McMahon and Moon, 1989) and trigger morphological changes in mouse mammary cells (Wong, Gavin, and McMahon, 1994). The activity responsible for these phenotypes is the accumulation of β-catenin in the nucleus and the activation of the β-catenin/TCF complex (Shimizu et al., 1997). I shall focus on this canonical signalling in this Introduction.

1.2.2 Canonical Wnt signal transduction

The canonical signal transduction pathway comprises of different components that can be separated into major groups: ligands (the Wnt proteins), the Frizzled transmembrane receptors, the LRP co-receptors, agonists and antagonists of the pathway, the

APC/Axin/GSK3-β destruction complex (determines β-catenin stability) and nuclear effectors (such as TCFs). A summary of the Wnt signal transduction cascade is represented in Fig.1.1. Wnt ligand binds the primary receptor Frizzled leading to the association of Axin2 to the phosphorylated co-receptor LRP. This results in the disassembly of the destruction complex and the stabilisation and accumulation of β-catenin which enters the nucleus, binding to TCF leading to changes in gene expression. In the absence of a Wnt ligand, β-TrCP binds β-catenin, resulting in its phosphorylation and ubiquitination and thus its degradation. In the nucleus, the transcriptional repressor Groucho (Gro) regulates gene expression negatively. I will briefly refer to each of these components in the following subsections.

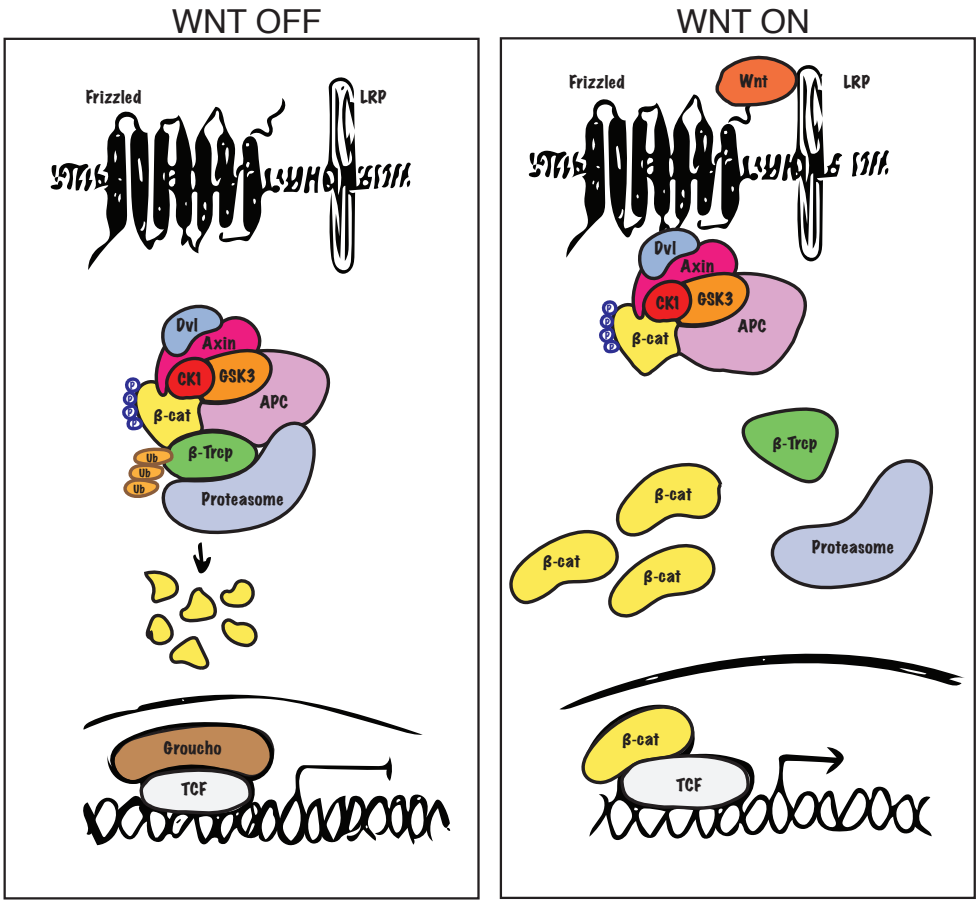

Figure 1.1: **Diagram of active and inactive canonical Wnt/β-catenin signalling**

The left panel is a representation of a cell in the absence of a Wnt ligand: the destruction complex (composed of Dvl, Axin, CK1α, APC, GSK3-β) binds β-catenin which is marked for degradation by β-TrCP via ubiquitination (Ub) and phosphorylation (p). The right panel is a representation of cell upon binding of a Wnt ligand to the Frizzled receptor which leads to the association of Axin2 to the phosphorylated LRP. The destruction complex is disassembled resulting in the accumulation and nuclear transport of β-catenin. In the nucleus β-catenin bind the effector TCF and activates the expression of target genes. This figure was adapted from (Nusse and Clevers, 2017). APC - adenomatous *polyposis coli*, CK1α - Casein kinase 1 alpha, Dvl - Dishevelled, GSK3-β - Glycogen synthase kinase 3 beta.

1.2.3 The Wnt ligands

Wnt ligands belong to an evolutionary conserved family, only present in metazoans, of which there are 19 known genes in vertebrates. The ligands are around 40kDa in size, and act mostly as short-range intercellular signals. During synthesis, Wnt proteins undergo major modifications: these include N-glycosylation that facilitates secretion and lipidation/acylation (Doubravska et al., 2011; Komekado et al., 2007; Kurayoshi et al., 2007; Tang et al., 2012) that confers the ability to bind Fzd receptors (Janda et al.,

2012). In the endoplasmatic reticulum (ER), Wnts are lipid modified by a palmitoyl transferase, Porcupine (Porc) (Hofmann, 2000; Zhai, Chaturvedi, and Cumberledge, 2004). Following the post-translation modifications in the ER, Wnts are trafficked to the Golgi assisted by the p24 cargo adaptor family (Buechling et al., 2011; Port, Hausmann, and Basler, 2011). Once in the Golgi, Wnts bind Wntless/Evi/Sprinter (WLS), a seven-pass transmembrane protein, (Bartscherer et al., 2006; B nziger et al., 2006; Goodman et al., 2006) via their palmitate modifications, and are then transferred to the plasma membrane. Wls is a sorting receptor that facilitates trafficking of Wnts to the membrane after which it is recycled back to the Golgi by the retromer complex (Belenkaya et al., 2008; Franch-Marro et al., 2008; Port et al., 2008). This recycling step is essential for the maintenance of active Wnt signalling as shown in both *Drosophila* (Herr and Basler, 2012) and in mammalian cells (Belenkaya et al., 2008). Although not yet fully understood, some evidence suggests that Wnts, together with Wls, are incorporated into exosomes and subsequently secreted (Gross et al., 2012; Korkut et al., 2009), reviewed by (McGough and Vincent, 2016). However, a cell-bound mechanism has been proposed to occur in the intestinal stem cell niche, in which direct cell contact promotes Wnt transfer mediated by Fzd and E3 ligases Rnf43/Znrf3 (Farin et al., 2016). In these examples, the signal is propagated not by diffusion but through cell division (Farin et al., 2016).

In summary, the synthesis and secretion of Wnt proteins is a complex process that it still not fully understood, but one that is essential for the start of signal transduction. Although this mechanism seems to be shared between most Wnt proteins, additional factors including the cell/developmental context and rate of signal diffusion will also impact upon signal transduction.

1.2.4 Wnt receptors and co-receptors

After secretion, Wnt ligands bind their corresponding receptor and initiate a signal transduction cascade in the receiving cell. The main receptors are part of the Frizzled (Fzd) family, but, other receptors and co-receptors include the lipoprotein receptor-related protein (LRP) (Wehrli et al., 2000; Pinson et al., 2000; Tamai et al., 2000), Ror/Ryk (Masiakowski and Carroll, 1992), the muscle-specific kinase (MuSK) (Baner-

jee et al., 2011) and the protein tyrosinase kinase 7 (PTK7) (Hayes et al., 2013) family members. Generally, canonical Wnt/β-catenin pathway ligands (i.e. Wnt1, Wnt3a and Wnt8) bind to the Fzd/Lrp5/6 complex, while non-canonical Wnts (i.e. Wnt5a, Wnt11) bind the co-receptors Ror2 and PTK7.

The seven-pass-transmembrane receptor Fzd was first identified in *Drosophila* as a regulator of tissue polarity (Vinson and Adler, 1987). There are 10 Fzds encoded in the mammalian genomes all of which resemble, structurally, the G-protein coupled receptors. Fzds are composed of an extracellular cysteine rich domain (CRD) which interacts with the Wnts (Bhanot et al., 1996), the transmembrane domain (TMD) and 4 intracellular domains (ICDs) that can interact with other components of the pathway and regulate Wnt signalling.

A few years ago the structure of the Wnt-Fzd complex was resolved (Janda et al., 2012). Besides other observations, the structural analysis revealed a two-domain Wnt structure resembling a 'hand' with 'thumb' and 'index fingers' extended to grasp Fzd8-CRD at two sites (Janda et al., 2012). Furthermore, the CRD contains a hydrophobic pocket that establishes the contact with the Wnt palmitoyl moiety. The same group has shown more recently that upon Wnt binding, LRP5/6 and Fzd dimerise, leading to conformational changes of the receptors (Janda et al., 2017).

The most common mechanism of signal transduction through Fzd is via Dishevelled's (Dvl) interaction with the ICD (Tauriello et al., 2012). Upon phosphorylation, the intracellular tail of LRP5/6, a long single-pass-transmembrane co-receptor, interacts with the scaffold protein Axin (Liu et al., 2003; Mao et al., 2001; Tamai et al., 2004; Tolwinski et al., 2003). The complex of LRP5/6 with Fzd and consequently DVL and Axin has been characterised as a signalsome (Bilic et al., 2007).

The next step in the cascade is the transduction of the signal from the membrane, through the cytoplasm and finally to the nucleus. The next section will focus on the cytoplasm, specifically β-catenin and the destruction complex.

1.2.5 The destruction complex

At the core of the canonical Wnt pathway is β-catenin, which is synthesised in the cytoplasm and degraded by the destruction complex (DC). It is the balance between

these two processes that determines the stabilisation and accumulation of β-catenin and consequently its nuclear entry and target gene activation. Proteins with different roles make up the DC: the scaffold proteins Axin and adenomatous polyposis coli (APC) and the kinases GSK3-β and CK1α.

β-catenin was discovered in *Drosophila* as the segment polarity gene *Armadillo* (Nüsslein-Volhard and Wieschaus, 1980) and later in *Xenopus* as part of the adherens junction (McCrea, Turck, and Gumbiner, 1991). The protein is composed of 42 amino-acid armadillo repeats (Huber, Nelson, and Weis, 1997) that foster protein-protein interaction (Graham et al., 2000; Huber, Nelson, and Weis, 1997; Xing et al., 2004; Xing et al., 2003).

The main scaffold protein Axin, identified in mice, (Zeng et al., 1997) assembles the components of the DC, interacting with all its proteins. It has also been proposed that Axin acts as an anchor to keep β-catenin from moving to the nucleus (Peterson-Nedry et al., 2008; Tolwinski and Wieschaus, 2001). Axin plays an important role in regulating Wnt signalling; it is present at low concentration in cells, and therefore the limiting factor for the DC (Lee et al., 2003). APC acts to promote Wnt transduction by downregulating Axin (Takacs et al., 2008).

GSK3-β is a serine-threonine (Ser/Thr) kinase with roles in numerous cellular processes. In the DC, GSK3-β phosphorylates β-catenin, APC, Axin and LRP (Rubinfeld et al., 1996). Similarly, the Casein kinase 1 (CK1) family of Ser/Thr kinases has many roles and targets in the cell (Knippschild et al., 2005). CK1 family members regulate Wnt signalling both positively and negatively by phosphorylating different components of the cascade: Dvl, LRP5, β-catenin, APC, Axin and TCF (Yanagawa et al., 2002; Zeng et al., 2005; Zhang et al., 2006; Sakanaka et al., 1999; Hämmerlein, Weiske, and Huber, 2005; Rubinfeld, Tice, and Polakis, 2001; Lee, Salic, and Kirschner, 2001).

APC was first identified as a tumor suppressor in colon cancer cells (Kinzler et al., 1991; Nishisho et al., 1991), and it too has many roles independent of Wnt signalling. In the DC, APC phosphorylation by CK1, protein kinase 4 (PK4) and GSK3-β (Morin et al., 1997; Rubinfeld et al., 1996), and ubiquitination and deubiquitination by Trabid, USP15 or HECT D1 E3 ligase, control its capacity to regulate Wnt signalling. In the absence of Wnt ligand, CK1 and GSK3β phosphorylate β-catenin, which is bound to

Axin (Liu et al., 2002). The phosphorylated motif is recognised by the E3 ubiquitin ligase β-TrCP resulting in β-catenin poly-ubiquitination and degradation (Aberle et al., 1997; Kitagawa et al., 1999).

Upon Wnt ligand engagement with Fzd/LRP, Axin binds LRP and together with the adaptor protein Disheveled (DVL) the DC is recruited to the membrane promoting the disintegration of the complex. Under these circumstances, β-catenin is not degraded and its subsequent accumulation leads to nuclear transport.

1.2.6 Nuclear effectors -TCFs

T-cell factors (TCFs) were first discovered in lymphocytes (Laudet, Stehelin, and Clevers, 1993) and are the main family of transcription factors that associate with β-catenin in the nucleus, bringing it to the chromatin. These proteins act on the genome both to activate and repress gene expression, depending on the co-factor they bind to. TCFs contain a high mobility group (HMG) domain that enables them to bind DNA in a sequence-specific manner (Giese, Amsterdam, and Grosschedl, 1991; Love, Huber, and Anders, 2014). The N-terminal portion of TCF binds to β-catenin and is therefore essential for its positive activity on transcription (Wetering et al., 1997; Molenaar et al., 1996).

In vertebrates, the number of TCF genes differs between species: frogs and mice both have 4 genes: TCF1, LEF1, TCF3 and TCF4. The diversity of TCF genes provides a mechanism for either activating or repressing gene transcription. For example, LEF1 acts only as an activator (Kratochwil et al., 2002; Reya et al., 2000; Genderen et al., 1994), while TCF3 is a repressor (Kim et al., 2000; Liu et al., 2005; Merrill et al., 2004). TCFs bind gene regulatory regions classified as Wnt responsive elements (WREs) which have been shown to respond both positively and negatively to the binding of TCF (Brannon et al., 1997; Hikasa and Sokol, 2011).

In the absence of Wnt signalling, TCF3 binds co-repressors, inhibiting the activation of Wnt targets. However, when β-catenin is stabilised and becomes present in the nucleus, it induces the phosphorylation of TCF3 removing it from the DNA. In this context, TCF1 binds β-catenin, replacing TCF3 resulting in the activation of Wnt the target genes (Hikasa and Sokol, 2011; Hikasa et al., 2010). This process is also known as

'TCF exchange' and was shown to play a role during development in *Xenopus* (Hikasa et al., 2010).

The most common mechanism for repressing Wnt target expression is by recruiting co-repressors, such as Groucho (Gro), to the chromatin. *Gro* was first discovered in *Drosophila* (Schrons, Knust, and Campos-Ortega, 1992) as part of a family of co-repressors, the transducin-like Enhancer of split (TLE). Gro/TLE binds to a variety of transcription factors (TFs), including TCFs, and represses expression by recruiting histone deacetylases (HDACs) to the target chromatin (reviewed by (Zhang and Cadigan, 2014). Gro/TLE (and other co-repressors, such as Corepressor of Pangolin (Coop) in *Drosophila* (Song et al., 2010) and myeloid translocation gene (MTG) in mammals (Barrett et al., 2012; Moore et al., 2008)) competes with β-catenin for the binding to TCFs (Arce, Pate, and Waterman, 2009; Daniels and Weis, 2005; Moore et al., 2008; Song et al., 2010). Another repressive mechanism of Wnt target genes is disruption of the β-catenin/TCF interaction by proteins such as the inhibitor of ?-catenin and TCF-4 (ICAT) (Hasegawa et al., 2007; Tago et al., 2000), the Sry-type HMG box containing protein 9 (Sox9) (Akiyama et al., 2004; Topol et al., 2009), and Chibby (Cby) (Love et al., 2010; Li et al., 2008; Takemaru et al., 2003).

Conversely, there are also factors that facilitate the activation of Wnt target genes, the so-called co-activators. Some proteins strengthen the interaction between TCF and β-catenin, such as transducin β-like protein 1 (TBL1), TBL1-related protein (TBLR1), (Li and Wang, 2008) and the ring finger protein 14 (RFN14) (Wu et al., 2013). Other proteins act as co-activators by specifically binding to the C-terminal transactivation domain of β-catenin: histone acetyl transferases (HATs), Creb binding protein (CBP) and p300 (Hecht et al., 2000; Takemaru and Moon, 2000; Li et al., 2011; Sun et al., 2000), and the ATPase subunit of the Swi/Snf chromatin remodelling complex (Brg-1) (Barker et al., 2001). In addition to HATs, β-catenin has also been shown to interact with other components of epigenetic regulation, including proteins responsible for depositing histone markers. There are reported interactions with MLL1/2 (responsible for H3K4me3) (Chen et al., 2010), protein arginine methyltransferase 2 (PMRT2) (H3R8me) (Blythe et al., 2010), SET8 (H3K20me) (Li et al., 2011), CARM1 (H3R17me2) (Ou et al., 2011) and DOTL1/DOT1 (H3K79m3) (Mahmoudi et al., 2010;

Mohan et al., 2010; Sierra et al., 2006).

1.2.7 Wnt signalling in early *Xenopus* development

Wnts are involved in many cellular processes and are essential during development as morphogens, impacting cell polarity, cell division and gene expression that ultimately will lead to cell identity. In amphibians, Wnt plays a crucial role in early development and in *Xenopus*, embryos have become 'test tubes' to study Wnt signalling and its components. In this section, I will refer to specific developmental processes where Wnt is involved.

The dorso-ventral (DV) axis in *Xenopus*, determined by the sperm entry point, has at its core the differential activation of Wnt signalling in the early embryo. The determination of the dorsal side of the embryo, where the blastopore is formed, gastrulation starts and from where the most anterior structures originate is a hub of active Wnt signalling (the organiser). Exogenous activation of Wnt signalling in the opposite side, the ventral side, will cause the formation of a secondary axis (head and trunk), by simulating the organiser activity. This characteristic has made *Xenopus* a model in which to study Wnt signalling, and in particular to test the role of a gene in the cascade based on its capacity to induce a secondary axis (Christian et al., 1991; Funayama et al., 1995; Yost et al., 1996).

In summary, dorsal determination occurs upon fertilisation; as the embryo undergoes cortical rotation 'dorsal determinants' are transported to the prospective dorsal side resulting in β-catenin enrichment. Throughout the 1990s this process was well studied, but the nature of the 'dorsal determinants' was still a mystery. The hypothesis was that some Wnt component would be involved in the stabilisation of β-catenin dorsally. Initial experiments looked at Wnts expressed maternally in the vegetal pole, since cortical rotation would 'bring' the determinants from this region to the prospective dorsal side. *Wnt11* was the first candidate, given the desired expression, but when it was tested, *Wnt11* was not capable of inducing a secondary axis (Ku and Melton, 1993). It was only in 2005 that maternal *Wnt11* was shown to be important for dorsal determination as *Wnt11*-depleted embryos lacked the capacity to make dorsal structures (Tao et al., 2005). Further studies have shown that Wnt11 forms a heterodimer

with Wnt5a and only the region of co-expression has dorsalising capacity (Cha et al., 2008). While Wnt5a is present throughout the whole embryo, Wnt11 is only vegetal, but cortical rotation relocates it to the dorsal side where it forms the heterodimer. Fzd7 and LRP6 are also maternally inherited and ubiquitously expressed; they are activated by the Wnts resulting in the stability and accumulation of β-catenin in the nucleus where it interacts with one of the three maternal effectors: TCF1, 3 and 4 (reviewed by (Sokol and Hoppler, 2014)). Recent studies have identified, by means of chromatin immunoprecipitation followed by deep-sequencing (ChIP-Seq), where in the genome β-catenin binds at this and later stages of development (Nakamura et al., 2016; Nakamura and Hoppler, 2017). These well characterised and relevant targets include the homeodomain TFs *siamois1* (*sia1*) and *twin*, as well as the *nodal related 3* (*xnr3* or *nodal3.1*) (Brannon and Kimelman, 1996; Hikasa and Sokol, 2013; Ishibashi et al., 2008; Laurent et al., 1997; Lemaire, Garrett, and Gurdon, 1995; Lustig et al., 1996). The activation the of these genes is the starting point of induction of the Nieuwkoop centre and later the organiser.

The other major roles of Wnt signalling during development occur after zygotic activation of the genome and during gastrula stage. Wnt regulates two major processes: patterning of the mesoderm in the DV axis and patterning of the neuroectoderm in the antero-posterior (AP) axis. For both processes, Wnt is not the sole player, as there is crosstalk with other signalling pathways. For example, BMP is essential for DV patterning as discussed in the next section.

Wnt8 is the main player at this developmental stage, a zygotic activated gene expressed in the prospective ventrolateral mesoderm and repressed dorsally by Wnt antagonists Dickkopf-1 (Dkk1) and Frzb1. Its role in mesodermal patterning is to induce *MyoD* (a paraxial/posterior mesoderm marker) and to repress axial mesoderm (notochord) via the inhibition of *goosecoid* (*gsc*) (reviewed by (Hikasa and Sokol, 2013). The dorsal centre continues to have active Wnt signalling, maternally activated, that is simultaneously repressed ventrally by sizzled (szl) (Salic et al., 1997).

The role of Wnt in regulating the patterning of the neuroectoderm involves mostly Wnt3a that posteriorises the neural tube (Ulloa and Martí, 2010). Kiecker and Niehrs have shown that Wnt signalling is necessary and sufficient to pattern the AP neural

axis by a posterior to anterior gradient acting on the neural plate (Kiecker and Niehrs, 2001).

Although not referred to in this Introduction, non-canonical Wnt signalling also plays an important role in early development regulating the process of convergent extension during gastrulation.

1.3 TGF-β Signalling

1.3.1 History

Transforming growth factors (TGFs) were discovered around a decade before Wnts in the 1970s, whilst studying the C-type RNA tumor virus and its transforming activity in cells (Larco and Todaro, 1978). In the 1970s, research started to focused on cancer cells, and the initial concept was that some molecule was secreted and cause a 'normal' cell to 'transform' into a cancer cell. An example of such a transforming factor was the RNA of type-C tumor viruses, that, when expressed in 'normal' cells, caused the transformation into a cancer cell (Todaro and Huebner, 1972).

Initially, the transforming growth factors (TGFs) were described as sarcoma growth factors (sGFs), proteins secreted by murine sarcoma virus (MuSV) transformed cells that would bind ectodermal growth factor (EGF) receptors (Larco and Todaro, 1978). By the late 1970s, the sGFs were renamed TGFs because they were secreted factors that lead to growth of cells and were thought, incorrectly, to be produced by transformed cancer cells. Early on, two kinds of TGFs were described, TGF-α and TGF-β, the distinction between them being that only TGF-α was capable of binding EGF receptors. For the purpose of this work I will focus solely on the TGF-β family of dimeric growth factors, as they have a critical role during development.

Other components of the TGF-β signalling pathway were subsequently discovered and described in the 1980s. Competitive assays showed that TGF-β family members bind with high affinity (Frolik et al., 1984; Tucker et al., 1984) to what were later characterised as type I and type II receptors, and type III co-receptors (also known as betagycan) (Massague and Like, 1985). Historically, the next major step was the cloning of the TGF-β gene in 1985, a 2439bp precursor mRNA from human cDNA (Derynck et al., 1985). The gene was called TGF-β1 and discovered to be produced not only by cancer cells, as previously described, but also by normal cells, although at higher levels in tumors (Derynck et al., 1985; Derynck and Rhee, 1987). Other TGF-β homologs were identified in the 1980s: the homodimeric TGF-β2 and the heterodimeric TFG-β1:TGF-β2 (Cheifetz et al., 1987). TGF-β2 was found to have different affinities with the three types of receptors, specifically lower affinity to the type II receptor

(López-Casillas, Wrana, and Massague, 1993; Cheifetz et al., 1987). These three homologs are the only TGF-β genes found in the mammalian genome, but when reference is made to TGF-β signalling it usually refers to a larger group of proteins, known as the TGF-β superfamily. Members of this family share sequence homology, specifically the 'cysteine knot', the last six cysteines of the proteins (McDonald and Hendrickson, 1993). TGF-β genes were identified in other model organisms and were shown to have a role during development: *decapentaplegic* (*dpp*) in *Drosophila* has a role in patterning (Padgett, St Johnston, and Gelbart, 1987); *Vg1* in *Xenopus* is important for mesoderm induction (Padgett, St Johnston, and Gelbart, 1987; Birsoy et al., 2006). Other members of the superfamily include the bone morphogenetic proteins (BMPs); also identified in the 1980s and isolated from bone tissue, BMP2 and BMP3 (Wozney et al., 1988).

The remaining components of the pathway, the effector proteins that act both in the cytoplasm and in the nucleus, are the Smads. Smads were discovered in the early 1990s, initially in *Drosophila* when studying Dpp. There, *mothers against dpp* (*mad*) was identified as a downstream component of the Dpp signalling pathway (Raftery et al., 1995). Similarly, in *C.elegans*, 3 genes, *Sma 2-4*, were shown to be required for the activation of the homolog of the BMP2/4 receptor (Savage et al., 1996). Smads became Smads in 1996 by combining mad and sma (Derynck et al., 1996) and many homologs have been found since then. In total we now know 33 genes that encode for human proteins that belong to the TGF-β superfamily, having many distinct roles in development and disease. In the next sections I will summarise what is understood about the general mechanism of signal transduction and its components while giving examples of the role of the pathway in early *Xenopus* development.

1.3.2 TGF- β signalling cascade - the commonly accepted model

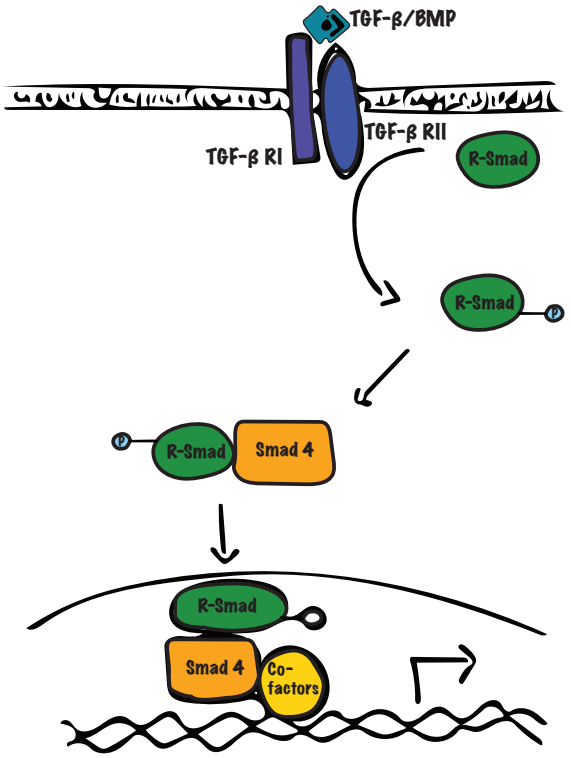

Figure 1.2: **Diagram of TGF-β/Smad signalling**

This figure represents a cell with active TGF-β signalling. TGF-β ligands bind as dimers to type I and type II receptors leading to the phosphorylation of the R-Smad. Active R-Smad binds Smad4 forming an heteromeric complex that is translocated to the nucleus. In the nucleus, this complex binds co-factors and regulates the activation of target genes. The figure was adapted from (Luo, 2017).

The TGF-β signalling cascade starts with the binding of the dimeric ligands to type I and type II transmembrane receptors, which are assembled as a heterodimeric complex. After binding, the cascade can take different paths; I will focus here on the Smad-dependent pathway, which is the more relevant to this thesis. Upon binding, the type II receptor activates the type I receptor which in turn phosphorylates the receptor-regulated Smad (R-Smad) proteins via its intracellular kinase domain. Once activated, R-Smads bind other R-Smads plus a common Smad (Co-Smad), Smad4, forming a heteromeric complex. This complex is then translocated to the nucleus where it binds co-factors and regulates transcription of target genes by interacting with the chromatin (Fig. 1.2). The complexity of the TGF- β signalling pathway is conveyed by the different types of components (ligands, receptors, smads) which in different combinations can lead to different transcriptional outputs. In the next sections, I shall refer to these different components and how they are regulated.

1.3.3 TGF-β sub-families

The members of the TGF-β superfamily are generally subdivided into two large groups, the TGF-β-like (includes TGF-β, activin, nodals and some growth differentiation factors (GDFs)) and the BMP-like (BMPs, most GDFs and the anti-Muellerian hormones (AMH)). What distinguishes the two families is their differing affinities for the receptors and the R-Smads that are in turn activated. TGF-β and activins have a higher affinity for type II receptor and activate Smad2/3, while Smad1/5/8 are phosphorylated upon BMP binding to type I receptor (reviewed by (Massagué, 2012; Heldin and Moustakas, 2016). The higher affinity binding of BMPs requires both types of receptors (Sebald et al., 2004; Feng and Derynck, 2005; Kirsch, Sebald, and Dreyer, 2000). These rules are commonly accepted, although many of the conclusions derived from overexpression studies that may mask the endogenous activities of both ligands and receptors.

1.3.4 TGF-β ligands and its regulation in the extracellular space

There are more than 30 proteins in the TGF-β superfamily and 19 homologs in *Xenopus* (summarised in table 1.1). Biochemically, these proteins are cytokines with 6 conserved cysteine residues known as the 'cysteine knot'. The synthesis process includes the conversion of a precursor protein by furins (and other convertases) into the dimeric active protein (Constam, 2014; Taylor, Van De Ven, and Creemers, 2003). Dimerisation is mediated by the 7th cysteine and while homodimers are the most common active ligands, heterodimers have also been described to be active. Lefty is the exception as it does not contain the 7th cysteine and is active as a monomer (Meno et al., 1996).

After synthesis and release into the extracellular space, different mechanisms can act to regulate TGF-β signalling. For example, several antagonists have been identified, including molecules capable of binding the ligands and sequestering them from the receptors. The first to be identified was follistatin (FS), that binds activin (Bragdon et al., 2011), and others include the BMP binding proteins Noggin, Chordin, Twisted gastrulation, Cerberus1 and Gremlin 1/2 (reviewed by (Zakin and Robertis, 2010; Umulis, O'Connor, and Blair, 2009; Bragdon et al., 2011)). The accessibility of ligands to bind the receptors is controlled by the so-called ligand binding traps. These traps occur as a result of the action of the antagonists. The ligand traps are a type of TGF-β

TGF-β family members in Xenopus
BMP2
BMP4
BMP7
Gdf6
Vg1, Derriere
Admp
Xnr1-4
Activin-β A
Activin-β B
Activin-β C
Activin-β D
TGF-β5
TGF-β2
Lefty-A
Lefty-B

Table 1.1: TGF-β family members present in *Xenopus*. The four Xnr1-4 proteins are homologous to Nodal in humans and Vg1 and Derriere are the only proteins without human homology

inhibition that functions to regulate excess of BMPs, and a well described example is the BMP7-Noggin ligand trap (Groppe et al., 2002).

1.3.5 TGF-β receptors

In vertebrates there are 7 type I receptors (Activin A receptor like type I (ACVRLI also known as Activin like kinase 1 (ALK1)), Activin A receptor type I (ACVRI/ALK2), BMP receptor type I A (BMPRIA/ALK3), Activin A receptor type I B (ACVRIB/ALK4), TGF-β receptor I (TGFβRI/ALK5) , BMP receptor type I B (BMPRIB/ALK6), Activin A receptor type I C (ACVRIC/ALK7)), and 5 type II receptors (TGF-β receptor type II (TGFβRII), Activin receptor type II A (ACVRIIA), Activin receptor type II B (ACVRIIB), BMP receptor type I (BMPRII) and anti-Muellerian homone receptor type II (AMHRII). Both kinds of receptors have a small cysteine-rich extracellular domain, a single transmembrane portion, a juxtamembrane domain and a cytoplasmic domain with kinase activity.

As referred to above, the commonly accepted model of signal transduction involves the initial binding of ligand to type II receptors. Type II receptors are thought to be constitutively active (Lin and Wang, 1992; Lin et al., 1992) with ligand binding leading

to the formation of a type I and type II complex that in turn leads to the phosphorylation of the juxtamembrane domain of type I by type II. The juxtamembrane domain is also known as the 'GS' domain because of its rich composition of glycine and serine residues (Wrana et al., 1994). The receptor complex formed upon ligand binding is composed of two type I and two type II receptors, and since the ligands are dimeric, it forms a 2:2:2 heterotetrameric complex (Wrana et al., 1992; Moustakas et al., 1993; Henis et al., 1994; Wells et al., 1999; Yamashita et al., 1994; Massague, 1998). Moreover, the receptor-receptor interaction increases the stability of the receptor-ligand binding (Radaev et al., 2010). When the receptors are inactive that is, not bound by TGF-β ligands, they exist in the membrane as monomers, homodimers and heterodimers (Chen and Derynck, 1994; Henis et al., 1994; Gilboa et al., 1998; Zhang et al., 2009; Ehrlich et al., 2012).

Regulation of TGF-β signalling in the membrane

The receptors can be regulated by different mechanisms such as post-translational modification, co-receptors, microRNAs (miRNAs) and other interacting proteins. Phosphorylation is the most common form of modification since this is how the receptors are activated. Besides the phosphorylation process already described, type II receptors, specifically TGFβRII, are autophosphorylated, maintaining an active form (Luo and Lodish, 1997). Dephosphorylation of the receptors also occurs in order to inhibit signal transduction.

At this point, I should introduce a distinct type of Smad protein, known as I-Smad, for its inhibitory role in TGF-β signalling. These I-Smads compete with R-Smads by binding to the receptors and blocking access. Smad7, an I-Smad, can also promote dephosphorylation of the TGFβRI by recruiting GADD34, a subunit of protein phosphatase 1 (PP1), to the type I receptor (Shi et al., 2004). In a developmental context, another protein phosphatase, Dullard, has been shown to dephosphorylate BMPRIA, which in turn results in the degradation of the BMPRII, a process required for neural induction (Satow et al., 2006).

The Smad ubiquitin regulatory factors (Smurfs) are a family of E3 ubiquitin ligases that can bind to Smad7 and mark TGFβRI for degradation by polyubiquitination

(Kavsak et al., 2000; Ebisawa et al., 2001). This regulatory mechanism is part of a feedback loop, since Smurf2 and Smad7 are activated by TGF-β. SUMOylation is a modification, analogous to ubiquitination that involves the addition of small ubiquitin-like modifiers (SUMOs). Upon TGF-β stimulation, TGFβRI is modified by the addition of SUMOs, enhancing R-Smad phosphorylation (Kang et al., 2008). Another kind of modification, Neddylation, is provided by the neural precursor cell-expressed developmentally down-regulated 8 (NEDD8), a ubiquitin-like molecule that stabilises TGFβRII (Zuo et al., 2013). Deubiquitination of the receptors also occurs, resulting in a positive effect on signal transduction. Examples of proteins involved include the ubiquitin carboxy-terminal hydrolase 37 (UCH37) (Wicks et al., 2005), the ubiquitin-specific protease 4 (USP4) (Zhang et al., 2012a), USP11 (Al-Salihi et al., 2012) and USP15 (Zhang et al., 2013).

Smad7 is the most studied example of an I-Smad that interacts with and regulates type I receptors (Hayashi et al., 1997; Nakao et al., 1997) in ways other than recruiting protein modifiers to the receptor. The mode of action of this protein also includes blocking R-Smad recruitment and inhibition of the Smad-DNA interaction in the nucleus (reviewed by (Yan and Chen, 2011)).

Other molecules can also interact with the receptor and regulate the pathway, with one example being the BMP and Activin membrane-bound inhibitor (BAMBI), a transmembrane protein that directly binds to either the ligands TGF-β/Activin or the BMP receptors (Grotewold et al., 2001; Loveland et al., 2003; Onichtchouk et al., 1999). Additionally, BAMBI binds Smad7 reinforcing its inhibitory role on the TGF-β type I receptor (Yan et al., 2009). It is part of a negative feedback loop, as *Bambi* is activated by TGF-β signalling (Xi et al., 2008; Sekiya et al., 2004). In *Xenopus*, BAMBI has an important role in regulating anterio-posterior (AP) patterning, which I will refer to below.

Finally, receptor control also occurs at the mRNA level, which can be targeted by miRNAs, causing downregulation. The most pertinent example is the role of the miR-15 family members (miR-15 and miR-16) in early *Xenopus* development, regulating Nodal signalling. The miRNAs act to restrict Nodal signalling to the organiser by targeting the ACVRIIA; moreover, the miRNAs are inhibited by Wnt/β-catenin sig-

nalling, resulting in its ventral expression (Martello et al., 2007). Many other miRNAs have been shown to regulate TGF-β in other contexts: miR-302/miR-372 in induced pluripotent stem cells (iPSc) (Subramanyam et al., 2011) and miR-520/miR-373 in cancer cells (Keklikoglou et al., 2012), the cluster miR-17-92 (Mestdagh et al., 2010) and miR-140-5p (Yang et al., 2013).

1.3.6 TGF-β effectors - the Smads

The basic structure of R-Smads and Co-Smads is of two globular domains: the mad homology 1 (MH1) domain on the amino-terminus (N-terminus) and the mad homology 2 (MH2) domain at the carboxyl-terminus (C-terminus). The MH1 domains contain the nuclear localisation signal (NLS) and the DNA-binding domain, a β-hairpin structure. The MH2 domain contains an L3 loop, a series of hydrophobic surface patches, essential for the interaction with the type I receptor (Lo et al., 1998). Upon ligand binding, phosphorylation of the type I receptor by the type II receptor creates a binding site for the basic surface patch of the MH2 domain of R-Smads (Wu et al., 2000). The subsequent phosphorylation of the C-terminal end of R-Smads allows for the association with Smad4, the Co-Smad; an acidic knob allows the binding of homologous MH2 domains (Abdollah et al., 1997; Kretzschmar, Doody, and Massague, 1997; Liu et al., 1997; Souchelnytskyi et al., 1996). Smad4 is not able to interact with type I receptors since its MH2 domain lacks the required C-terminal serine residues (SXS). Once in the nucleus, the MH1 domain binds to DNA whilst MH2 interacts with other nuclear factors to modulate transcription (reviewed by (Massagué, 2012; Moustakas and Heldin, 2009; Weiss and Attisano, 2013)). MH1 and MH2 domains are coupled by a non-conserved linker region. This linker region can be phosphorylated by a variety of kinases (such as the cyclin C-cyclin dependent kinase 8 (CDK8) and CDK9) that, among other things, control the maintenance of Smads in the nucleus and create docking sites for nuclear proteins (Alarcón et al., 2009). I-Smads do not contain an MH1 domain nor the SXS motif. Rather they have only the MH2 domain which allows the binding to the type I receptor .

The Smad-receptor interaction can be modulated by Smad-interacting proteins that either promote or repress it. The best studied examples are the Smad anchor for

receptor activation (SARA) and the hepatic growth factor-regulated tyrosine kinase substrate (Hrs)(Hgs); FYVE-motif proteins that recruit Smad2 and 3 to the type I receptor (Tsukazaki et al., 1998). Other proteins include the serine/threonine kinase receptor associated protein (STRAP) and the destruction complex component Axin (Datta and Moses, 2000; Furuhashi et al., 2001; Guo et al., 2008).

The nuclear transport of Smads can also be modulated in order to influence the outcome of signal transduction. Although R-Smads and Co-Smads have a NLS in their MH1 domain, nuclear transport is processed differently for each kind of Smad. Smad3 interacts with importin-β, whereas Smad4 interacts with importin-α for nuclear transport (Xiao, Latek, and Lodish, 2003; Xiao, Liu, and Lodish, 2000; Kurisaki et al., 2001). However, Smads3, 4 and 2 can also interact with nucleoporin proteins for import, such as the nucleoporin 153 (Nup153) and Nup214 (Xu et al., 2002; Xu et al., 2003). In *Drosophila* it has been shown that importin 7 and 8 can also mediate nuclear import of Smad1, 2 and 3 (Xu et al., 2007). In the presence or absence of a TGF-β signal, Smads continuously shuttle between the cytoplasm and the nucleus via interaction with the nuclear pore complex (Xu et al., 2002).

Although all R-Smads have a nuclear export signal in the linker region, only Smads1 and 4 use it for this purpose (Watanabe et al., 2000). Furthermore, Smad4 export can also be mediated by exportin 1 (CRM1) (Xiao et al., 2003; Xiao et al., 2001; Pierreux, Nicolás, and Hill, 2000). Translocation of Smad3 from the nucleus to the cytoplasm is mediated by exportin 4 and a Ras related nuclease (Ran) GTPase (Kurisaki et al., 2006).

Smads in the nucleus

In the nucleus, the Smad complex binds with low affinity to DNA regions called Smad-binding elements (SBE), present near TGF-β/Smad target genes, that are commonly enriched for the AGAC or GTCT sequence (Zawel et al., 1998; Jonk et al., 1998; Dennler et al., 1998). Smad1 has the particularlity of a hairpin structure in the MH2 domain that might be responsible for the affinity of the protein to the CG-rich sequences (Korchynskyi and Dijke, 2002). The low affinity of Smads to DNA sequences is overcome by the presence of other TFs that act as co-factors to increase binding

affinity. These co-factors include cell-type specific transcription factors or nuclear factors such as histone acetyltransferases (HATs) and histone deacetylases (HDACs). In the nucleus there is also cross-talk between signalling pathways. One example is the co-operation with Wnt via co-occupancy of Smad target enhancers by LEF1 and TCF7L2 (Labbé et al., 2007; Labbé, Letamendia, and Attisano, 2000; Nakano et al., 2010). The need for co-factors adds another layer of regulation to TGF-β signalling, as different cell types will have different co-factors which in turn will influence the activation of distinct target genes. This results in distinct roles for TGF-β/Smad signalling in the cell, from differentiation to self-renewal. Once in the nucleus, several mechanisms occur to maintain Smads and allow accumulation. Such mechanisms include the association with DNA and proteins like Fast1/Foxh1 (Xu et al., 2002) and TAZ (Varelas et al., 2008). Association of phosphorylated-Smad3 (pSmad3) (active form) with Smad4 blocks its interaction with CRM1 and consequently its export from the nucleus (Chen et al., 2005).

1.3.7 TGF-β in early *Xenopus* development

The main TGF-β superfamily members that play an important role in early frog development are the *Xenopus*-related nodal (Xnr) 1-6, Derriere, Vg1 and Activin from the Nodal family and BMP2, 4 and 7 from the BMP family. Nodals are involved in regulating endoderm and mesoderm specification and patterning, gastrulation movements and left-right asymmetry, while BMPs regulate ventral and lateral mesoderm patterning and determine ectodermal cell fate. I will refer to some of these processes here, but they will be described in more detail in the section related to early *Xenopus* development.

The first zygotic genes to be expressed are the Nodal members *xnr5* and *xnr6*. The activation of these genes occurs by the blastula stage in the most dorsal cells of the embryo, a region where both β-catenin and maternal VegT (T-box transcription factor present in the vegetal pole of the embryo) are present and cooperate in the activation (Takahashi et al., 2000) (Fig. 1.3). By itself, maternal VegT is capable of inducing low levels of both genes in the prospective endoderm. Other members of the Nodal family, *xnr1*, *xnr2* and *xnr4* are subsequently induced by xnr5 and xnr6 (Agius et

al., 2000). Simultaneously, *Derrière*, another TGF-β member, starts to be expressed in the marginal zone, a similar pattern to that of zygotic *VegT*, with slightly higher levels dorsally (Sun et al., 1999; Stennard et al., 1999). Hence, a coarse gradient of Activin-like TGF-β signalling is formed, higher in the dorsal side, which will pattern the mesoderm and endoderm. Other molecules act to better define the gradient, for example, Cerberus1 (Cer1) which is an antagonist of both TGF-β and Wnt signalling (Piccolo et al., 1999).

Interestingly, BMPs have the opposite gradient in the early embryo, with higher expression in ventral cells. BMP is also expressed in the prospective ectoderm where lower levels determine neural tissue (Graff, 1997). BMP4 is the main player at this point in development and its expression is restricted ventrally as the result of antagonist signals and diffusion limitations (Fainsod, Steinbeisser, and Robertis, 1994; Hemmati-Brivanlou and Thomsen, 1995). The other two BMPs, BMP2 and BMP7, share expression domains in the ectoderm and mesoderm (Piccolo et al., 1996). Other antagonists that constrain BMP expression are Chordin and Noggin, both expressed dorsally, keeping these cells BMP-free (Zimmerman, De Jesús-Escobar, and Harland, 1996; Jones and Smith, 1998). Bambi, the pseudo-receptor described above (first identified in *Xenopus*) is activated by BMP4 and expressed in the same cells, associating with TGF-β receptors and repressing the signal (Onichtchouk et al., 1999).

The anti-dorsalising morphogenetic protein (Admp), a TGF-β ligand, was first identified in *Xenopus* in a screen for genes expressed in the Spemann organiser and is related to human BMP3 (Moos, Wang, and Krinks, 1995). *Admp* expression is activated by low levels of BMP and despite being expressed dorsally it has a ventralising activity, conserved in chicken and fish (Moos, Wang, and Krinks, 1995; Joubin and Stern, 1999; Dosch and Niehrs, 2000; Lele, Nowak, and Hammerschmidt, 2001; Willot et al., 2002). ADMP signals through Alk-2 but it does not do so dorsally, as it is repressed by Chordin (Reversade and Robertis, 2005).

In relation to the Smads, in *Xenopus*, xSmad1 and xSmad5 are activated by BMPs (Graff, Bansal, and Melton, 1996; Suzuki et al., 1997) and, as observed in other vertebrates, xSmad2 and xSmad3 are activated by Activin and Nodals (Howell, Mohun, and Hill, 2001). SARA was also identified in *Xenopus* as the xSmad2 recruiter to the

type I receptor (Tsukazaki et al., 1998). Interestingly, the co-Smad Smad4, is encoded by two genes in the *Xenopus* genome: *xSmad4α* and *xSmad4β* (*Smad10*). The former is the human orthologue; it is expressed maternally and its expression decreases with the onset of gastrulation when *xSmad4α* starts to be expressed (Masuyama et al., 1999; LeSueur and Graff, 1999; Howell et al., 1999). Another distinction between the two is that Smad10 does not contain a NES domain, making it constitutively nuclear (Watanabe et al., 2000; Pierreux, Nicolás, and Hill, 2000). I-Smads are also present in *Xenopus*: xSmad6 (Nakayama et al., 1998) and xSmad7 (Nakao et al., 1997); their expression mimics that of BMP4 and they act to inhibit some TGF-β signals.

Although the Smad proteins are ubiquitously and uniformely present in the embryo, their active phosphorylated (p) forms are not. pSmad1 and pSmad2 have an assymetric distribution, the former higher ventrally and lower dorsally (Faure et al., 2000; Kurata et al., 2001), and the spatial and temporal localisation of pSmads follows that of the corresponding activator ligands. By stage 9, pSmad1 is localised in dorsal and ventral cells becoming enriched ventrally by stage 9.5 until stage 12.5 (early neurula) (Faure et al., 2000; Kurata et al., 2001). pSmad2 is initially dorsally enriched and by stage 9.5 has spread through the marginal zone and the endoderm, moving from dorsal to ventral, with higher levels vegetally and absence in animal cap cells (Lee, Heasman, and Whitman, 2001).

Active forms of Smads in the nucleus interact with co-factors and bind DNA to activate target genes. Early targets of TGF-β have been identified in *Xenopus* such as the *mix paired-like homeobox* (*mixl1* or *mix.2*) which contains a Activin responsive element in its promoter and requires xFast1/Foxh1 as a co-factor (Chen, Rubock, and Whitman, 1996; Chen et al., 1997). Other transcription factors, mostly homeodomain-containing like Mixer, Milk and Bix3, have been shown to act as co-factors and recruit Smad2/4 to the genome (Germain et al., 2000). At present, in the era of whole-genomics, most genomic targets of TGF-β have been identified in different animal models and at different stages by ChIP-Seq using antibodies against pSmad2/3 or pSmad1 and cofactors like Foxh1 (Gupta et al., 2014; Kim et al., 2011; Yoon et al., 2011; Wills and Baker, 2015; Chiu et al., 2014; Charney et al., 2017).

1.4 Early amphibian development

Xenopus unfertilised eggs are polarised in the animal-vegetal axis, both in pigmentation and in cytoplasmic yolk content: the animal pole is darker and has less yolk content, the vegetal pole is rich in yolk and lighter. The polarity is broken at fertilisation as a consequence of the rotation of the cortex in relation to the core of the egg, in the direction of the animal pole. Given the differences in pigmentation, rotation leads to the formation of the 'grey crescent', a region with an intermediate pigmentation, on the opposite side of the sperm entry point (SEP). As I will discuss below, this is the earliest, and one of the most important processes in development, as it determines the dorsal-ventral (DV) axis. Amphibian embryos cleave holoblastically: the first cleavage goes through the SEP and the mid-line of the grey crescent, and the second is perpendicular to this first. The first division takes longer to occur (timing depends on the species and temperature) while the following divisions are roughly every 30 minutes. Initially, the embryo is single layered, as all divisions are perpendicular to its surface, but becomes multilayered as it cleaves. The cell divisions are synchronous up until cell cycle 13 when the midblastula transition (MBT) occurs (Newport and Kirschner, 1982a; Newport and Kirschner, 1982b).

1.4.1 Dorsal-Ventral Axis Determination

The dorsal-ventral (DV) axis of amphibians is established early in development, just after fertilisation. The sperm entry point will determine the dorsal side of the embryo as a result of cytoplasmic rearrangements, called cortical rotation (reviewed by (Harland and Gerhart, 1997) (Fig. 1.3) . After fertilisation, the egg cortex rotates 30° relative to the central core of the egg cytoplasm (Vincent, Oster, and Gerhart, 1986). During cortical rotation, microtubules localised between the core and the cortex align in parallel to the direction of rotation, towards the prospective dorsal side (Elinson and Rowning, 1988), reviewed by (Gerhart et al., 1989). Elinson et al. further showed that cortical rotation is a microtubule dependent event by using inhibitors of microtubule polymerisation (UV irradiation and colchicine) that lead to the impairment of rotation. This disruption of microtubule polymerisation leads to deficiencies in axis determination, specifically the lack of dorsal determination and development of solely

ventral structures (ventralised) (reviewed by (Gerhart et al., 1989)). Additional studies showed that microtubules are responsible not only for cortical rotation, but their alignment allows for a rapid and efficient transport system for molecules to the plus end (prospective dorsal side) (Rowning et al., 1997). Further experiments have shown that the molecules transported by the microtubules to the dorsal side (herein called dorsal determinants) come from the vegetal pole of the amphibian embryo (Sakai, 1996) (Fig. 1.3). Although it was understood that cortical rotation was essential for the determination of the dorsal side of the embryo, the molecular nature of the process was not understood at the time. It was not until the mid-90s that it was shown that the main consequence of cortical rotation is the asymmetrical activation of the Wnt/β-catenin signalling pathway and the enrichment of β-catenin (ctnnb1) in the dorsal nuclei (Larabell et al., 1997; Schneider et al., 1996). The molecular components began to emerge and included Dishevelled and the GSK-3β binding protein GBP, all components of the Wnt signalling pathway (Miller et al., 1999; Weaver, 2004). The nuclear translocation of β-catenin in dorsal cells marks the earliest molecular event in DV asymmetry and is also responsible for the formation of two signalling centres at blastula stage: the Nieuwkoop center and the Spemann organiser.

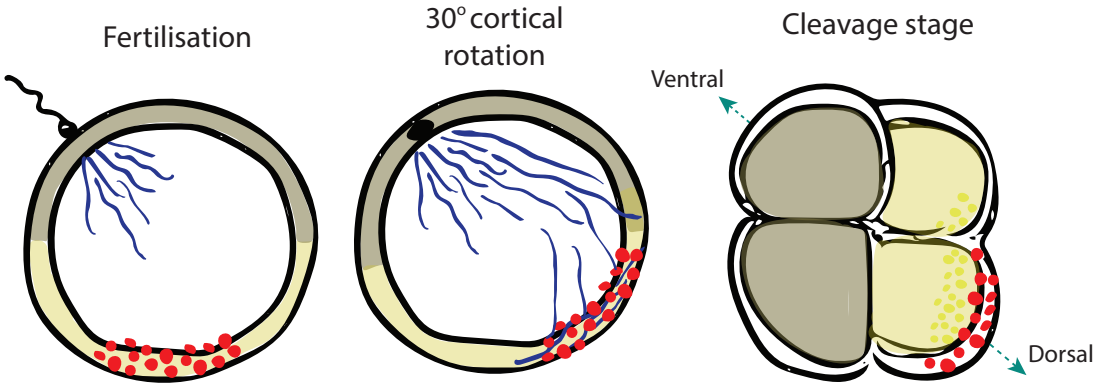

Figure 1.3: **Diagram representing determination of the dorsal-ventral axis by cortical rotation**

The frog egg has maternally deposited dorsal determinants (red circles) enriched in the vegetal pole. Fertilisation triggers reorganisation of the microtubule cytoskeleton and leads to microtubule polymerisation in the vegetal cortex. The egg cortex rotates 30° in relation to the core displacing the maternal determinants to the prospective dorsal side. Here, these determinants activate the canonical Wnt signallings resulting in the accumulation of nuclear β-catenin (yellow circles). The figure was adapted from (Wolpert and Tickle, 2011) and (De Domenico et al., 2015)).

1.4.2 Spemann organiser and Nieuwkoop center

The Nieuwkoop center (NC) is formed on the dorsal vegetal region and it is characterised by the expression of nodal related factors (xnr), activated by β-catenin, together with *chordin* and *noggin*, BMP-signalling antagonists (Wessely et al., 2001) (Fig. 1.4, 1.5). This region is also known as the BCNE centre (blastula chordin and noggin expression center) (De Robertis and Kuroda, 2004) (Fig. 1.4) . Both centres are formed at the blastula stage and both require β-catenin, however the NC further requires other maternal mRNAs. The BCNE centre will give rise to neural tissue and regulates neurulation, whilst the NC functions as a endoderm regulator (reviewed by (De Robertis and Kuroda, 2004)). In addition to the expression of BMP antagonists, the BCNE also expresses *siamois* (homeobox gene), *foxa4a/pintallavis* (winged-helix protein) and *xnr3* (nodal related-3) (Kuroda, Wessely, and Robertis, 2004; Wessely et al., 2004). The NC is characterised by the expression of *cerberus* (a secreted antagonist) and nodal related factors (*xnr1,2,4,5, and 6*), the latter being mesoderm inducers, specifically of dorsal mesoderm (Agius et al., 2000; Takahashi et al., 2000). The equatorial cells overlying the NC are only induced to become dorsal during the gastrula stage (reviewed by (Harland and Gerhart, 1997)).

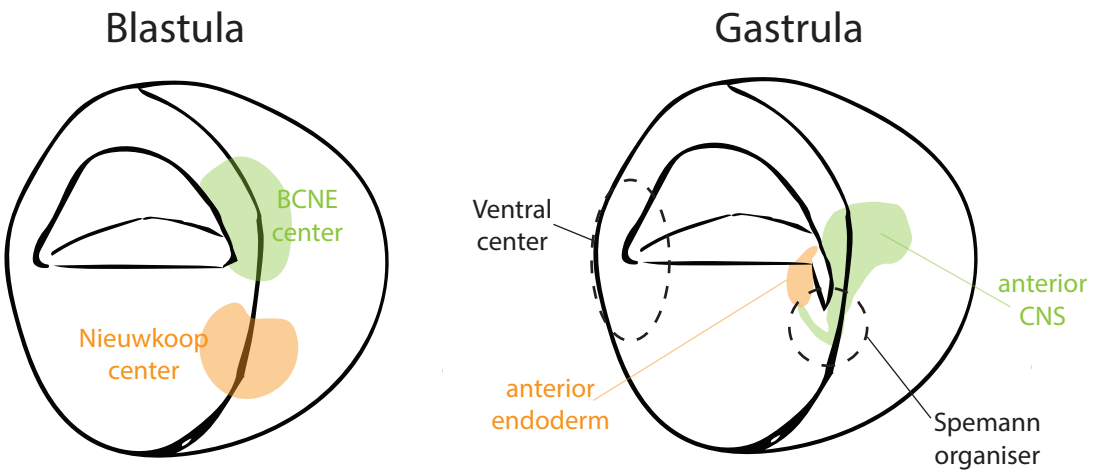

Figure 1.4: **Diagram of the BCNE and Nieuwkoop center at blastula stage that give rise to the Spemann organiser at gastrula stage**

At blastula stage the BCNE centre is located in the dorsal-most part of the animal cap and it is characterised by the expression of the BMP antagonists, *chordin* and *noggin*. In the dorsal vegetal region the Nieuwkoop centre (NC) is formed and characterised by the expression of β-catenin and VegT targets, the nodal related proteins. The BCNE gives rise to neural tissue while the NC is essential for dorsal mesoderm induction, including the Spemann organiser at early gastrula. Also at the gastrula stage the ventral signalling organiser is established. The figure was adapted from (De Robertis and Kuroda, 2004).

The organiser is characterised by three properties: induction, morphogenesis and self differentiation. It is responsible for organising embryonic development by signalling to neighbouring cells to differentiate as different cell types, whilst organising the scale, placement and orientation of the tissues (reviewed by Harland and Gerhart, 1997). The amphibian organiser is also known as the Spemann organiser (SO), as a result of the 1924 experiments conducted by Hans Spemann and Hilde Mangold. They transplanted a small fragment of the dorsal side of a newt gastrula into the ventral side resulting in the formation of 2 conjoined embryos (Spemann and Mangold, 1924). The transplanted cells were able to change the neighbouring cells of the host and make them differentiate into central nervous system (CNS), somites and other axial components (dorsal tissues). This indicated that the transplanted cells (Spemann graft) behave as an organiser and inducer. We now know that these cells secrete paracrine factors that change the fate of the surrounding cells.

Although the function of the SO has long been known, the molecular players were only discovered many years later. The SO is characterised by the secretion of several proteins, that regulate different molecular signalling pathways, including TGF-β, Wnt and FGF signalling, such as *chordin*, *noggin* and *xnr3*. Xnr3, contrarily to the

other nodal related proteins, is not a mesoderm inducer but acts as a BMP antagonist (Haramoto et al., 2004). The organiser also secretes Wnt antagonists, such as Frizzled-related proteins (*frzb-1*, *crescent*, *sfrp-2*) (Leyns et al., 1997), and *dkk1* (Mao et al., 2001). *Cerberus* is highly expressed in the dorsal mesoderm (the organiser), where it acts as a Nodal, BMP and Wnt antagonist (Piccolo et al., 1996) and is required for head induction (Kuroda, Wessely, and Robertis, 2004). Overall, the SO secretes mostly BMP, Wnt and Nodal antagonists which promote head development whilst repressing trunk-tail tissues (Niehrs, 2001; Piccolo et al., 1999). As referred to above, the cells that form the Spemann organiser are in the equatorial region of the embryo and will become the dorsal mesoderm. However, the inductive properties of the organiser influence all three germ layers. The organiser is able to anteriorise the endoderm, dorsalise the mesoderm and induce neurulation in the ectoderm.

1.4.3 Germ layer determination

The use of fate maps, labelling cells early in development with a marker and observing later in development which cells are marked has allowed for the identification of cells which will give rise to the different germ layers and tissue types. In a simplified way, at the pre-gastrula stage, the animal cap (AC) represents the presumptive ectoderm, the vegetal pole will give rise to endoderm and the region in between, the marginal zone, will form mesoderm.

For the purpose of this work, I will further discuss the process of mesoderm induction, but first I will refer to the developmental process responsible for the segregation of the germ layers: gastrulation.

1.4.4 Gastrulation movements

Gastrulation starts on the dorsal side of the embryo and it is identifiable by Nieuwkoop and Faber stage (NF) 10-10.5 (Nieuwkoop and Faber, 1994) with the formation of a pigmented lip, called the dorsal lip of the blastopore. However, cell movements involved in the process start before this structure is visible, with the formation of bottle cells. Bottles cells gained the name from their shape and they are essential for

gastrulation (Keller, 1991; Keller and Danilchik, 1988; Keller, 1984). These cells are formed and, by invagination, are transported inside the embryo and by contracting they pull the associated cells inwards. Cells from the marginal zone and the vegetal pole will ingress through the blastopore whilst AC cells (prospective ectoderm) spread vegetally replacing the involuting cells. The marginal zone cells can be categorised into involuting marginal zone (IMZ) and non involuting marginal zone (NIMZ). The IMZ has many layers that involute as sheets inside the gastrula and will form mostly axial mesoderm: somites and notochord. The NIMZ and AC will give rise to neural ectoderm, with the latter contributing to the brain and the former to the posterior hindbrain and spinal cord. As the first cells ingress (the prospective neural tissue), they extend and narrow toward the dorsal midline resulting in lengthening in an AP orientation. This movement, essential for neural tube morphology, is called convergent extension. Gastrulation starts on the dorsal side and then continues laterally and ventrally, terminating with the blastopore closure.

1.5 Mesoderm Development

1.5.1 Mesoderm Induction - the three-signal model

As described above, the organiser is able to dorsalise mesoderm, however mesoderm induction happens earlier in development, at blastula stage. The equatorial cells of the blastula are induced to become mesoderm, instead of ectoderm, by signals secreted by the underlying cells, the endoderm (Fig. 1.5). This phenomenon was tested and observed when cells of the animal pole (Animal cap), prospective ectoderm, were cultured juxtaposed to vegetal pole cells and become mesoderm (Nieuwkoop and Ubbels, 1969). In the 1980s Jonathan Slack's lab described mesoderm induction as the result of a series of inducing signals, known as the 3-signal model. It postulated that two signals arise from the vegetal pole cells, one that induces ventral-like mesoderm in the marginal zone and a second signal restricted to the dorsal side (from the Nieuwkoop center) that induces dorsal mesoderm (Spemann organiser). These signals differ qualitatively between dorsal and ventral vegetal cells (Dale, Smith, and Slack, 1985; Smith and Slack, 1983), dividing the marginal zone into dorsal and ventral prospective mesoderm (Fig. 1.5). The organiser then secretes the third signal that dorsalises some of the mesoderm pre-specified as ventral. Due to diffusion limitations this signal does not reach the ventral-most region of the marginal zone that will still form the ventral most mesoderm (Dale, Smith, and Slack, 1985; Slack and Forman, 1980; Smith and Slack, 1983; Smith, Dale, and Slack, 1985).

This model is still accepted to this day as the principle behind mesoderm induction, although some modifications and additions to the model have been made. Moon and colleagues suggested that the two signals from the vegetal pole should be separately characterised, one being a dorsal competent modifier (resultant from cortical rotation) that modifies the interpretation of the second signal from the vegetal cells. The two initial signals were then classified as two types; a generic meso-endoderm inducing signal and a dorsal modifying signal that is superimposed (Christian and Moon, 1993; Kimelman, Christian, and Moon, 1992).

A 4th signal was added as a result of work done in Edward de Robertis' lab; BMPs secreted by the ventral and lateral regions of the gastrula embryo that antagonise the

organiser (reviewed by (De Robertis and Kuroda, 2004; Harland and Gerhart, 1997; Heasman, 1997). This region was classified as the gastrula ventral centre that establishes a gradient of BMP activity across the marginal zone determining dorsal/ventral mesodermal fates (Dosch et al., 1997). The secretion of BMPs leads to the expression of ventral specific genes *ventx* (*vent-homeobox1-3*) and *evx1* (*even-skipped homeobox-1*) (Gawantka et al., 1995; Joly et al., 1993; Kawahara et al., 2000). The same lab added another modification to the model, accounting for the dorsal-to-ventral gradient of vegetally expressed nodal related proteins (Agius et al., 2000) (Fig. 1.5). The maternal *vegt* (a T-box transcription, below) and *vg1* (a TGF-β member) together with β-catenin are responsible for this gradient. High levels of β-catenin and nodals induce dorsal mesoderm (organiser) whilst lower levels of nodals (which are induced by *vegt* and *vg-1* only) lead to the expression of *bmp4* and *wnt8a* on the ventral side of the embryo (Agius et al., 2000; De Robertis and Kuroda, 2004).

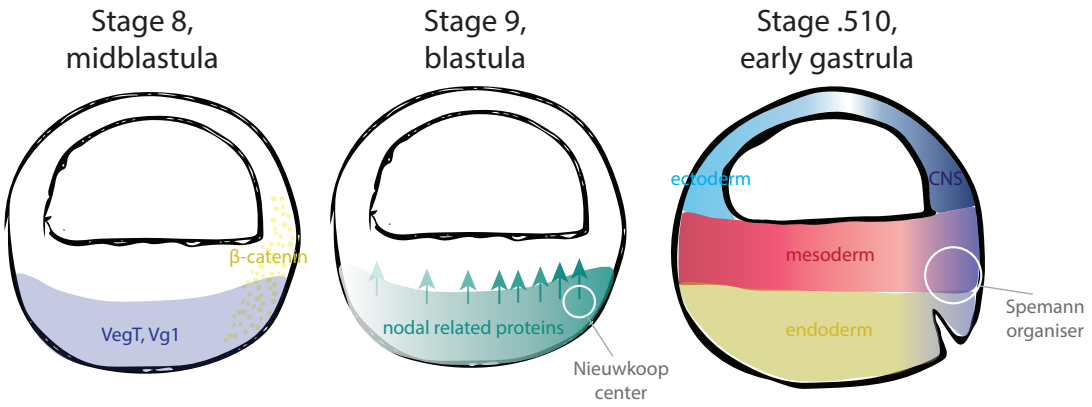

Figure 1.5: **Diagram representing mesoderm induction in early *Xenopus* development**

Mesoderm induction is initiated at stage NF8, maternal T-box VegT together with dorsal activated β-catenin induce the expression of nodal related protein that establish a gradient in the vegetal pole of the animal. Higher levels in the dorsal side induce dorsal mesoderm and lower levels lead to the expression of ventral markers, such as *bmp4* and *wnt8a*. This initial gradient will give rise to the distinct types of mesoderm within the dorsal-ventral axis. The figure was adapted from (Wolpert and Tickle, 2011). CNS - central nervous system.

The nature of the mesodermal inductive signals has mostly been identified using techniques such as the animal cap assay. The animal cap assay is similar to the technique described above where animal cap cells are juxtaposed to vegetal cells, changing their fate to mesoderm. By substituting the vegetal pole with a soluble molecule, or

injecting the embryos with mRNA of the inducing agent, it was possible to discover several molecules capable of inducing mesoderm (Jones and Smith, 1999). Different mesoderm inducers were independently identified, many of which were members of the TGF-β family, including nodals, Activin, Vg1 and BMPs (Asashima et al., 1991; Kimelman and Kirschner, 1987; Smith, 1987; Smith et al., 1990; Weeks and Melton, 1987). FGF was also shown to have some mesoderm-inducing activity (Kimelman and Kirschner, 1987; Slack et al., 1987). Induction of mesoderm is characterised by the expression of specific genes that are required for the further development of this germ layer. Brachyury is one of these genes. It encodes a T-box transcription factor and it is a key protein for mesoderm formation and patterning. In the next section I will discuss further this family of TFs.

1.6 T-box transcription factors during early development

Brachyury (also known as T) was the first member of the T-box gene family to be discovered, in 1927 by Dobrovolskaïa-Zavadskaïa, when describing heterozygous mutant mice with a short tail and embryonic defects (Dobrovolskaia-Zavadskaia, 1927). In the 1990s when the gene was cloned and sequenced, it was classified as a transcription factor and its role in mesoderm regulation identified (Herrmann et al., 1990; Kispert and Herrmann, 1993). It was also in the mid-1990s that the T-box gene family was categorised, with the identification of novel genes in the mouse that shared a protein motif, the T-box domain (Bollag et al., 1994).

The T-box is a 200 amino acid DNA-binding domain that binds in a sequence specific manner (reviewed by (Papaioannou, 2014; Smith, 1997; Smith, 1999; Gentsch, Monteiro, and Smith, 2016)). The T-box domain binds a 20 nucleotide partially palindromic sequence T[G/C] ACACCTAGGTGTGAAATT, made of two half-sites and described to be bound by the protein as monomer (Kispert and Herrmann, 1993). Other T-box proteins can bind the consensus half site AGGTGTGAA also known as the TBE (T-box binding element) (reviewed by (Papaioannou, 2014)). The crystal structure of the *Xenopus* Bachyury bound to a palindromic sequence derived from the *in vitro* selected consensus sequences, was analysed and revealed that it binds as a

dimer (Müller and Herrmann, 1997).

There are 5 T-box subfamilies, categorised in relation to their DNA-binding domain: T, Tbx1, Tbx2, Tbx6 and Tbr1. With the exception of *tbx2* (Carreira et al., 1998) T-box transcription factors have been shown to act as transcriptional activators, although this is not yet completely understood. The members of this family of transcription factors have a variety of roles during development: *t*, *vegt* and *eomesodermin* (*eomes*) are essential during early development in regulation of mesoderm and endoderm (reviewed by (Showell et al., 2006)), *tbx6* is important later in the presomitic mesoderm, *tbx4/5* exerts its role in limb development and *tbx20* is important for cardiogenesis. For the purpose of this project I will focus on the role in early amphibian development, specifically mesoderm formation and regulation by *t*, *Eomes* and *Vegt*.

1.6.1 *Eomes* and *Vegt*

Eomes and *Vegt* are the earliest T-box genes to be expressed during *Xenopus* development. Both act as transcription factors and are essential for mesoderm induction and regulation.

The *eomes* gene was isolated in *Xenopus* and shown to be expressed in the prospective mesoderm (Fig. 1.6), before *Brachyury* induction, in a dorsal to ventral gradient (Ryan et al., 1996). Later in development the gene is expressed in a subset of cells of the central nervous system (Ryan et al., 1996) (Fig. 1.6). Expression of *Eomes* mRNA in animal caps induces the expression of mesodermal markers like *brachyury gsc* and *wnt8a*. These genes are induced in a dose-dependent manner, higher levels of *Eomes* induce high level of *gsc* but less of *brachyury* and *wnt8a*. Furthermore, overexpression of *Eomes* induces *gsc* and changes the fate of ventral to dorsal mesoderm (Ryan et al., 1996). Overexpression of Eomes mRNA fused to the repressor domain Engrailed resulted in gastrulation defects and reduction of mesodermal markers and muscle actin (Ryan et al., 1996). Together, these experiments have shown that *Eomes* is essential for mesoderm induction, regulation and patterning.

There are two VegT alternative splice isoforms in *Xenopus*, one that is maternally deposited in the vegetal pole of the egg and the other is expressed upon zygotic genome activation. I referred to maternal VegT and its role in inducing the SO and dorsal meso-

derm. VegT was identified as a transcription factor capable of activating transcription (Zhang and King, 1996). Similar to *Eomes* and *Brachyury*, zygotic *VegT* is expressed in the prospective mesoderm but, by the end of gastrulation the gene is no longer expressed dorsally and it is later confined to a few cells of the neural tube (Zhang and King, 1996; Lustig et al., 1996) (Fig. 1.6). VegT acts in a non cell autonomous manner and is capable of inducing both mesoderm and endoderm (Clements et al., 1996; Horb and Thomsen, 1997; Lustig et al., 1996; Stennard, Carnac, and Gurdon, 1996; Zhang and King, 1996; Zhang et al., 1998a). VegT is a master regulator of endoderm, which in turn is involved in the induction of mesoderm. Loss of maternal *VegT* results in embryos with head defects as well as reduction of endodermal and mesodermal gene markers (Zhang et al., 1998a). Zygotic *VegT* can be activated by /TGF-β factos, FGFs, Brachyury and Eomes, although it is not known if the effect is direct (Horb and Thomsen, 1997; Lustig et al., 1996; Stennard, Carnac, and Gurdon, 1996).

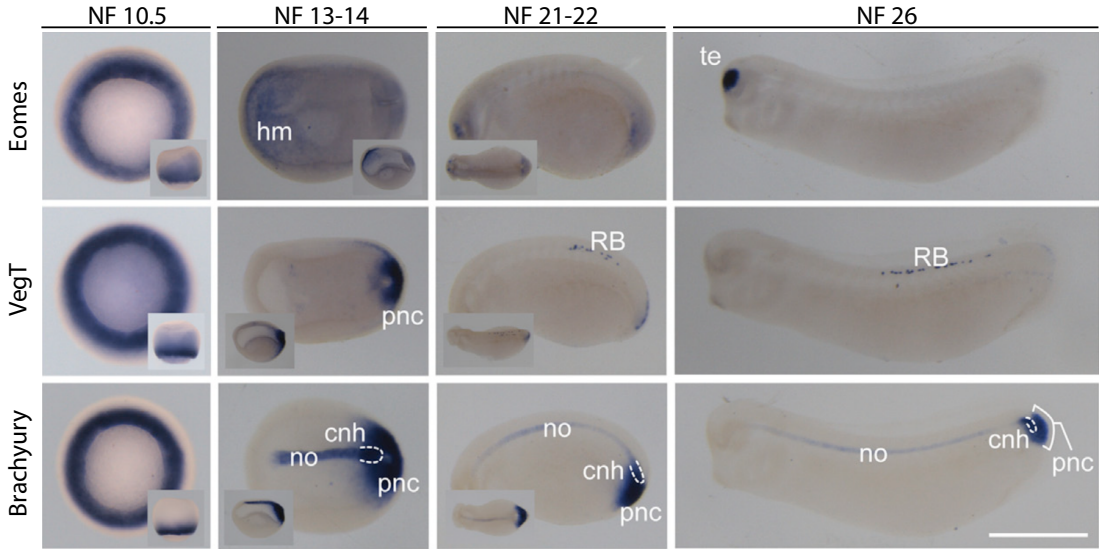

Figure 1.6: **Expression of *Eomes*, *VegT* and *Brachyury* in gastrula and tailbud stage *Xenopus* embryos**

Expression pattern of *Eomes*, *VegT* and *Brachyury* by whole mount *in situ* hybridasation in gastrula and tailbud stages of the *Xenopus tropicalis* embryo. NF - Nieuwkoop and Faber stage.The image was adapted from Figure 4 of (Gentsch et al., 2013).

1.6.2 The role of Brachyury in mesoderm formation and maintenance

T is necessary and sufficient for mesoderm formation. This was shown in animal cap assays where overexpression of *t* is sufficient for the conversion of ectoderm to a

mesodermal fate (Cunliffe and Smith, 1992). Furthermore *t* acts in a dose-dependent manner with low concentrations inducing the formation of smooth muscle and higher concentrations inducing skeletal muscle (O'Reilly, Smith, and Cunliffe, 1995; Tada, O'Reilly, and Smith, 1997). In the experiments by O'Reilly et al they showed that the notochord is only induced when *t* is coexpressed with *pintallavis/foxa4a* (dorsally expressed gene), an example of how *t* can act synergistically with other TFs to specify cell fates (O'Reilly, Smith, and Cunliffe, 1995).

1.6.3 Induction and regulation of *t* in the mesoderm

T is induced in mesodermal cells in the equatorial region of the embryo. Activation occurs in response to mesoderm-inducing signals (discussed above) derived from the vegetal hemisphere of the embryo (Slack, 1994). Mesoderm is formed only in the equatorial cells of the embryo, which can be explained by the threshold response of *t* to Activin, a strong *Brachyury* inducer. The activation of *t* occurs in a narrow window of Activin levels, either high (vegetal pole) or low levels (animal pole) of Activin represses *t* (Green, New, and Smith, 1992; Gurdon et al., 1994; Gurdon, Mitchell, and Mahony, 1995). The repression of *t* by high levels of Activin was shown to be indirect, through *goosecoid* (*gsc*). Ectopic expression of *gsc* leads to down-regulation of *t* through a direct interaction with the gene promoter (Artinger et al., 1997; Latinkic and Smith, 1999).

Another gene that is capable of inducing *Brachyury* expression and regulating mesoderm formation is *vegt*. *VegT* is maternally expressed in the vegetal hemisphere of the amphibian egg, a region that will form the endoderm (*vegt* also acts as an endodermal regulator) (Horb and Thomsen, 1997; Lustig et al., 1996; Stennard et al., 1999; Zhang and King, 1996). Zygotic *vegt* is expressed throughout the mesoderm in a broader pattern compared to *t*, and its expression is later downregulated in the notochord (Stennard, Carnac, and Gurdon, 1996) (Fig. 1.6). Depletion of maternal vegt impairs endoderm formation and mesodermal cells differentiate as ectoderm while the animal pole gives rise only to epidermis (no neural tissue) (Zhang et al., 1998b).

Expression of *brachyury* is also regulated by Wnt signalling. Overexpression of canonical Wnt signalling inhibitors revealed that *brachyury* requires ligand-dependent

activity of Wnt in order to be expressed (Vonica and Gumbiner, 2002). However, Wnt by itself is not capable of inducing mesoderm, so it can only induce *t* in the presence of TGF-β and FGF signalling. Analysis of the *t* promoter revealed elements that respond to Activin and FGF signalling (Latinkic et al., 1997) as well as TCF-binding sites (mediated by Wnt signalling) (Vonica and Gumbiner, 2002). Interestingly, FGF has an additional role in maintaining *Brachyury* expression at later developmental stages (Schulte-Merker and Smith, 1995) attained by an autoregulatory loop between these two genes (Casey et al., 1998; Isaacs, Pownall, and Slack, 1994). This was shown using the expression of Xbra-Enr (engrailed repressor domain) fusion construct that resulted in a lack of expression of embryonic FGF (eFGF) in the notochord. Furthermore, FGF is a direct target of *t*; binds as a monomer to two Brachyury consensus sites in the FGF promoter (Casey et al., 1998).

Besides *eFGF*, other genes have been identified as Brachyry targets, most of them activated, which has led to the idea that Brachyury mostly acts as a transcriptional activator (Conlon et al., 1996). The first Brachyury targets were identified by analysis of cDNA libraries from embryos injected with a hormone-inducible version of Brachyury (Tada, O'Reilly, and Smith, 1997; Tada et al., 1998). Among the genes induced, within a short period of brachyury activation, there was a family of four genes encoding proteins containing a paired-type homeodomain. These genes were related to the mix family of homeobox-containing genes (Rosa, 1989) named *bix1-4* (brachyury induced homeobox containing genes). Bix are activated by both *t* and *vegt* and are expressed in the prospective mesoderm and the vegetal hemisphere (Tada et al., 1998). Both bix1 and bix4 are responsive to mesoderm-inducing factors of the TGF-β family and they direct ectoderm to mesodermal fates (Casey et al., 1999; Tada et al., 1998). As well as being regulated by Wnt signalling, *xwnt11* was also shown to be a Brachyury target and mediates convergence during gastrulation (Tada and Smith, 2000).

In the era of whole genome analysis, the discovery of T-box targets has become easier and more thorough. New techniques have allowed us to focus on defining the gene regulatory networks (GRNs) initiated by these T-box transcription factors and that regulate mesoderm development. In zebrafish, a chromatin immunoprecipitation-microarray approach (ChIP- chip) allowed the identification of more than 200 potential

targets of No-tail (Ntl, Brachyury homolog) (Morley et al., 2009). In *Xenopus tropicalis*, a detailed ChIP-Seq analysis of binding of Brachyury, Eomesodermin and VegT at gastrula and tailbud stage led to significant insights into the role of these T-box transcription factors in the regulation of neuromesodermal progenitors (Gentsch et al., 2013). I shall discuss this work further in Chapter 4.

1.7 Chromatin regulation in early embryonic development

1.7.1 Studying the chromatin; introduction to ChIP-Seq

Developmental fates are established during development as a result of complex gene regulatory networks (GRNs) that lead to changes in gene expression. The main players in these GRNs are proteins that are capable of binding chromatin, specifically regulatory regions (promoters and enhancers), leading to changes in the regulation of genes by modulating transcription and ultimately gene expression. Proteins that are capable of binding DNA, and that influence gene regulation are known as transcription factors (TFs). There is also an epigenetic layer, mainly involving histone modifications, that contributes to regulation (establishment and maintenance) of the cell-specific gene expression.

There are several techniques that allow the study of protein-DNA interactions, such as the electrophoretic mobility shift assay (EMSA) (Garner and Revzin, 1981) and DNA-pulldown (Roberts and Green, 1996). These are however, *in vitro* techniques and require *a priori* knowledge of the DNA sequence. For the purpose of this Introduction, I will focus on the most commonly used technique, Chromatin Immunoprecipitation (ChIP), that allows the *in vivo* identification of DNA-protein interaction and their genomic location. I will review how the technique has evolved throughout the years and give examples of how it has contributed to the field of developmental biology, specifically in the study of GRNs and the identification of regulatory regions.

In 1984 Gilmour and Lis made the first attempt to study protein-DNA intereactions (Gilmour and Lis, 1984). They developed a method to covalently bind proteins to DNA by irradiating *E.coli* with UV light. Using an antibody against RNA polymerase, the authors pulled down DNA which was then purified and studied using hybridisation assays. This experiment showed that RNA polymerase is bound to genes which are constitutively active. A year later, the same group applied the method to eukaryotic DNA, in *Drosophila melanogaster*, where they showed that recruitment of RNA polymerase II to heat shock genes increased as a response to increasing temperatures (Gilmour and Lis, 1985). Three years later, Solomon et al. (Solomon, Larsen, and Varshavsky, 1988) improved the technique by using formaldehyde to crosslink DNA

to protein. This form of crosslinking is still the most widely used today. This work was also done in *D.melanogaster* and they studied the positioning of histone H4 in the heat shock gene hsp70. In 1993 the technique was first applied in developmental biology, to study the homeotic bithorax complex (BX-C) in *D.melanogaster*. Orlando and Paro (Orlando and Paro, 1993) used crosslinked chromatin and an antibody against the Polycomb group (Pc-G) to map its binding sites. To identify the locations of the binding sites they coupled ChIP with PCR to amplify chromatin fragments using linker modifiers. This allowed them to identify Pc-binding sites with 1 kilobase (kb) resolution, and showed that Pc is a major component of a large repressive domain; regions being actively transcribed were negative for Pc binding.

The next big development in the technique came seven years later, in 2000, in the era of microarrays. The technique was pioneered in Richard Young's lab which developed a microarray method that revealed the genome-wide location of DNA-bound proteins. They first used it to monitor binding of gene specific transcription factors in yeast (Ren et al., 2000). The technique came to be known as ChIP-chip (or ChIP-on-chip). Kim and colleagues then used this technique in human fibroblast cells and identified more than 10,000 active promoters, including more than 1,000 that were previously unannotated (Kim et al., 2005), and predicted insulator regions by analysing the binding of CCCTC binding factor (CTCF) (Kim et al., 2007).

With the increasing power of next generation sequencing such as Solexa/Illumina and 454, the next step in ChIP evolution was possible. These sequencers were able to obtain millions of short reads which would facilitate the direct measurement of the sequence content that was pulled down by ChIP. Combining ChIP with high-throughput sequencing is better known as ChIP-Seq and it was first introduced in 2007. Several groups published work introducing ChIP-Seq during this time, the first being on yeast, *Saccharomyces cerevisiae*, where they studied nucleosomes containing the histone variant H2A.Z (Albert et al., 2007). A few months later, the first work using the technique in human cells was published, using the term ChiP-Seq for the first time (Barski et al., 2007). In this work they created maps for the genome-wide distribution of 20 histone modifications (lysine and arginine methylations), the histone variant H2A.Z, RNA polymerase II and CTCF, a protein which binds insulator regions. They were

able to show that H3K27me, H3K9me, H4K20me, H3K79me and H2BK5me modifications are associated with gene expression while repressed regions are characterised by H3K27me3, H3K9me3, and H3K79me marks.

Similar analyses were undertaken in mouse embryonic stem cells, neural progenitors and embryonic fibroblasts, where the histones modifications were mapped (Mikkelsen et al., 2007) confirming the previous findings. Additionally, they identified H3K36me3 as a mark of primary coding and non coding transcripts (gene annotation) and H4k9me3 and H4K20me3 as telomeric and satellite markers (active long-terminal repeats). In the same period, two other papers where published describing the technique in human cell lines (Johnson et al., 2007; Robertson et al., 2007).

1.7.2 Bioinformatic Tools

The rapid application of ChIP-Seq in different fields, but mostly in stem cell research and developmental biology, led to advancements in computational tools to facilitate the analysis of the genome-wide data being produced. From softwares of short-read mapping, such as Bowtie (Langmead, 2010) and Burrows-Wheeler Aligner (BWA) (Langmead et al., 2009), to tools that identify regions with a high probability of binding, called peaks (Model-based analysis for ChIP-Seq (MACS) (Zhang et al., 2008), SPP (Kharchenko, Tolstorukov, and Park, 2008) and ultimately tools that allow visualisation of the data like IGV (Robinson et al., 2011; Thorvaldsdottir, Robinson, and Mesirov, 2013). The use of ChIP-Seq to compare the binding of transcription factors in different cell types or conditions lead to the development of tools that allow this kind of analysis, such as DiffBind (Ross-Innes et al., 2012) and MAnorm (Shao et al., 2012).

1.7.3 Derivations of ChIP-Seq

In a manner analogous to the transition from ChIP-chip to ChIP-Seq, the ChIP-Seq has had improvements and derivations. One example is ChIP-Exo (Rhee and Pugh, 2011; Rhee and Pugh, 2012) which was developed to improve the resolution of ChIP-seq by combining ChIP with 5' to 3' exonuclease digestion. Another adaptation widely used in developmental studies to investigate cell-type specific binding of TFs or his-

tone modifications is the batch isolated tissue specific-ChIP (BiTS-ChIP) (Bonn et al., 2012b; Bonn et al., 2012a) and the isolation of nuclei tagged in specific cell types (INTACT) (Deal and Henikoff, 2010a; Deal and Henikoff, 2010b). More recently, Schmidl and colleagues developed a technique that reduces the input requirements for library preparation by combining ChIP with *tn5* transposase (as used in ATAC-Seq), termed chiPmentation (Schmidl et al., 2015).

1.7.4 Applications of the technique in developmental biology - mesendoderm GRNs

There is a wide range of studies focused on early germ layer specification in different model animals, here I'll provide examples of research that have contributed to the assembly of the mesendoderm GRN in zebrafish and the frog (*Xenopus tropicalis/laevis*).

The main players in early mesendoderm development are effectors of the Nodal/TGF-β signalling pathway (Smad2/3), Foxh1 and members of the T-box family of transcription factors (*Eomes*, *VegT* and *Brachyury*). Researchers have studied the DNA binding profile of these proteins in order to identify their targets and better understand the GRN that governs mesendoderm development. An early study in *X.laevis* focused on anterior endoderm, and they found that Foxh1 together with Smad2 binds to the promoter of an early endoderm marker, hhex (Rankin et al., 2011). More recently, genome-wide analysis of the binding of Foxh1 and Smad2/3, together with loss-of-function experiments and RNA-Seq, has identified most of the early Nodal target genes regulated by Foxh1 and Smad2/3 (Chiu et al., 2014). Integration of these analyses with ChIP-seq for histone modifications that mark active enhancers (H3K4me1, H3K27ac), has led to the hypothesis that Foxh1 acts as a pioneer factor in establishing Nodal enhancers and, as a consequence, the start of the mesendoderm program (Gupta et al., 2014). These two publications reinforce the importance of implementing different techniques, ChIP-seq for TF and histone modifications, RNA-Seq and loss-of-function (morpholino or small molecules treatments) in a genome-wide approach to allow a better understating of the processes that regulate early development.

Similar experiments were performed in early zebrafish embryos to identify genomic targets of Smad2 and Eomes. Nelson et al showed that these two proteins have common

genomic targets, genes involved in both endoderm and mesoderm development and that they both interact with Foxh1 (Nelson et al., 2014).

Regarding mesoderm formation and regulation, much effort has been put into identifying the genomic targets of the T-box TFs in zebrafish, frog and mouse (Garnett et al., 2009; Gentsch et al., 2013; Lolas et al., 2014; Morley et al., 2009). Most of the studies referred to above are focused on individual TFs and identification of their targets, but it is the merging of these ChIP data that will allow the construction of the GRN that governs development.

Chapter 2

Materials and methods

2.1 Materials

2.1.1 Buffers and solutions

Xenopus embryo culture media

Marc's modified Ringer (MMR): 1M NaCl, 20mM KCl, 20mM $CaCl_2$, 10mM $MgSO_4$, 50mM Hepes pH 7.8, 1mM EDTA.

Normal amphibian medium (NAM): 1.1M NaCl, 20mM KCl, 10mM $Ca(NO_3)_2$, 10mM $MgSO_4$, 1mM EDTA.

Whole mount *in situ* hybridasation buffers

Phosphate buffered saline, PBS (10x) : 137mM NaCl, 2.7m KCl, 10mM Na_2HPO_4, 1.8mM KH_2PO_4 pH7.4.

Phosphate buffered saline with tween-20, PBT (1x): 1x PBS, 0.1% (v/v) tween-20.

MEM salts: 137 mM NaCl, 2.7mM KCl, 10mM Na_2HPO_4.

MEMFA fixative: 3.7% Formaldehyde pH 7.5, 10mM MEM salts (10x)

Saline sodium citrate (SSC) (20x): 17.5% NaCl, 8.8% Sodium citrate pH 7.

Hybridisation solution: 50% Formamide, 5x SSC (20x), 1mg/ml Torula yeast RNA, 100ug/ml Heparin, 1x Denhart?s solution (50x), 0.1% Tween-20, 0.1% CHAPS, 10mM EDTA.

Maleic acid buffer (MAB) (2x): 200mM Maleic Acid, 300mM NaCl.

Staining Solution, Alkaline phosphatase buffer: 100µM Tris, 100µM NaCl, 0.1% Tween-20, 40mM $MgCl_2$.

Protein immunoprecipitation and Western Blot

SDS loading buffer: 250mM Tris pH6.8, 10% (w/v) SDS powder, 50% glycerol, 25% β-mercaptoethanol, 0.02% bromophenol blue.

IP buffer: 50mM Tris, pH7.5, 150mM NaCl, 1mM EGTA, 1% (v/v) Igepal CA-630, 0.25% (w/v) Sodium deoxycholate.

SDS running buffer (10x) : 25mM Tris Base, 192mM Glycine, 0.1% SDS.

Transfer Buffer: 25 mM Tris Base, 190mM Glycine, 2% MeOH.

Chromatin immunoprecipitation buffers

E1: 50 mM HEPES-KOH pH 7.5, 150 mM NaCl, 1 mM EDTA. 10% glycerol, 0.5% Igepal CA-630, 0.25% Triton X-100).

E2: 10 mM Tris-HCl pH 8.0, 150 mM NaCl, 1 mM EDTA, 0.5 mM EGTA.

E3: 10 mM Tris-HCl pH 8.0, 150 mM NaCl, 1 mM EDTA, 1% Igepal CA-630, 0.25% Na-Deoxycholate, 0.1% SDS.

RIPA buffer: 50 mM HEPES-KOH pH 7.5, 500 mM LiCl, 1 mM EDTA, 1% Igepal CA-630, 0.7% Na-deoxycholate.

TEN buffer: 10 mM Tris-HCl pH 8.0, 1 mM EDTA, 150 mM NaCl.

SDS elution buffer: 50 mM Tris-HCl pH 8.0, 1 mM EDTA, 1% SDS.

2.1.2 Other buffers

Tris-acetate EDTA buffer (TAE) : 40mM Tris base , 20mM Glacial acetic acid, 1mM EDTA pH 8.

Elution buffer (EB) : 10 mM Tris-Cl, pH 8.5.

2.1.3 Oligonucleotides

All oligonucleotides were designed using the Primer3 online software (http://primer3.ut.ee) (Untergasser et al., 2012). Desalted nucleotides were synthesised by Sigma and a re-ssuspended in distilled water to a final concentration of 100mM and stored at -20°.

Gene	Forward primer (5'-3')	Reverse primer (5'-3')	Amplicon size, bp	Source
gsc	AGAGAACAGCTGGCAAGGAG	TTTCTGCCTCCTCCACTTTG	90	(Gentsch et al., 2013)
noggin	CGGAGGAGAGACTTGGAGTG	TTTGATTTCTGCTGGCATTG	89	(Gentsch et al., 2013)
not	ACAGCAGCCAATGAGGATG	AGGGTTCATGGAACCATTTG	106	(Gentsch et al., 2013)
bmp4	ATGGAGTACCCGGAGAGACC	TCCATTTTCTGCTGTGCTTG	99	(Gentsch et al., 2013)
wnt8a	AAGATGCCAGAGCCCTAATG	CCAGATATTCCATGGCACTTG	100	(Gentsch et al., 2013)
msgn1	TCACTTAGCCAGACCCCATC	GAATGGCATCTCCTCCAGAC	105	(Gentsch et al., 2013)
mespa	TCTCCAGACCAGGGATTTTG	GGCTGAAATGATGTCCACAG	86	(Gentsch et al., 2013)
xcad3	ACTCACCCAGCGATCTTAGC	CACCCGGTATTTTTCTTTGG	101	(Gentsch et al., 2013)
szl	CACACAAGACAGTTTTGGAAGC	GAACTCAACTGGGCCTTCTG	119	(Gentsch et al., 2013)
K00726	GGAGTCACCCCAACATCTCA	ACCCGTCCGACTTCTTATCTC	79	this work
72022004	TGCACTTGTTACAGGATTCCT	ACACAGCGGTAGGTCTCATT	117	this work
cpe	GAGCCCGGTGAACCAGAAT	TCCCTCTGGTACTCATTGCA	113	this work
odc	GGGCAAAAGAGCTTAATGTGG	CATCGTGCATCTGAGACAGC	103	(Gentsch et al., 2013)
c8orf4	CAGCCAACATCTTCCAAGGG	GTCCTGGTCGATGCAGAAGA	113	this work

2.1.4 Chemicals

All chemicals used were of molecular biology grade and purchased from Sigma or Roche.

2.1.5 DNA molecular size markers

The DNA molecular size markers used for DNA separation in gel electrophoresis was either a 100bp DNA ladder or 1Kb DNA ladder from NEB.

2.1.6 Enzyme

Restriction endonucleases

All restriction enzymes used were obtained from Roche or NEB.

Other enzymes

Other enzymes used and its source are summarised in the table below:

Enzyme	**Company**	**Catalogue number**
Turbo DNase	ThermoFisher Scientific, Life technologies	AM2238
Proteinase K	ThermoFisher Scientific, Life technologies	AM2546
T7 RNA polymerase (Dig labeling)	Roche	11175025910
SP6 RNA polymerase (Dig labeling)	Roche	11175025910
T7 RNA polymerase (cap)	ThermoFisher Scientific	AM1344
SP6 RNA polymerase (cap)	ThermoFisher Scientific	AM1340
KAPA HiFi HotStart ReadyMix	KAPA Biosystems	KK2601
GoTaq HotStart Polymerase	Promega	M5132
T4 DNA ligase	Promega	A3600
KAPA2G Fast ReadyMix	KAPA Biosystems	KK5103
Pfx50 polymerase	ThermoFisher Scientific, Invitrogen	12355-012

Table 2.1: Other enzymes used during this project

2.2 Methods

2.2.1 Embryo culture and manipulation

Egg and testes collection

Animal procedures were performed under license, as required by Animals (Scientific Procedures) Act 1986 (UK). *Xenopus tropicalis* and *Xenopus laevis* embryos were generated via *in vitro* fertilisation (IVF). Female *Xenopus laevis* frogs were primed for ovulation a week prior to IVF by injection of 50 units of hCG (Human chorionic gonodatropin) subcutaneously in the dorsal lymph sac. *Xenopus tropicalis* females were primed similarly but with a lower dose, 10 units, and around 20 hours prior to IVF. To induce ovulation, *Xenopus laevis* were boosted by injecting 500-800 units of hCG 20 hours prior to IVF while *Xenopus tropicalis* were boosted 4 hours prior with 100 units of hCG. Egg collection differs between the two species; *Xenopus laevis* females were kept in isolation for 8 hours in a 1x Marc's modified Ringer (MMR) while collection of *Xenopus tropicalis* eggs was done manually by gently squeezing the lower abdomen of the female frogs. For IVF, testes isolation was processed similarly in both species with the exception of the maintenance, *X.laevis* testes were kept up to 10 days in Leibovitz's L-15 Medium (Sigma L5520) + 10% fetal bovine serum (FBS, Sigma 12003C) at 4°C while *X.tropicalis* were used fresh. For testes isolation, male frogs were sacrificed according to schedule 1 guidelines by immersion in fresh 0.2% Ethyl 3-aminobenzoate methanesulfonate (MS222, Sigma E10521), for 30 minutes to 1 hour followed by decapitation. Frogs were placed belly up and with a pair of scissors a small cut was done in the lower abdomen in order to expose the viscera. Blunt forceps were used to push aside the liver, stomach and intestine in order to reach the testes, which were connected to the fat body, on the back. Using forceps and scissors, the testes were removed from the fat body and cleaned from the surrounding connective tissue and place in the appropriate media.

in vitro fertilisation (IVF)

Eggs were collected in petri dish with 0.1x MMR and before IVF the majority of the liquid was removed to facilitate fertilisation. Either the whole testes (*X.tropicalis*)

or a piece (*X.laevis*) were put in a 1.5 ml Eppendorf tube containing L-15/FBS (*X.tropicalis*) or 0.1x MMR (*X.laevis*) and were crushed with a pestle. Testes solution was mixed with the eggs and allowed to fertilise for 5 minutes after which the *Xenopus tropicalis* and *Xenopus laevis* eggs were flooded with either 0.05x MMR or 0.1x normal amphibian medium (NAM), respectively. Prior to all kinds of manipulation referred to in this work, the thick protective jelly membrane that surrounds the embryo was removed. This process was known as dejellying and can be done 10 minutes post-fertilisation by washing the embryos in 2.2% L-cysteine at pH 8.0, diluted in the appropriate media for 5-8 minutes. Embryos were washed in the media without cysteine and were ready for manipulation: microinjection, LiCl treatment or UV irradiation. Prior and post manipulation, the embryos were kept in agarose-coated Petri dished in 0.05x MMR at 25-28°C in the case of *Xenopus tropicalis* and *Xenopus laevis* embryos were incubated at 14-22°C in 0.1X NAM.

Microinjection

Embryos were manually injected with either mRNA, DNA (plasmid) or morpholinos at either 1-cell, 2-cell or 4-cell stage embryos. Depending on the experiment, embryos were also co-injected with a lineage tracer such as fluorescin dextran (10.000MW, Anionic; D1821, Thermo Scientific) at a concentration of 1-2% (250-500pg/nl). *Xenopus tropicalis* embryos were injected at 1-cell stage with 2nl or with 1nl at the other two stages, in each cell. The volume of injection was higher for *Xenopus laevis*: 1-cell stage embryos were injected with 10nl while 2/4-cell stage embryos were injected with 5nl in each cell. Needles used for microinjection were produced from glass capillaries (GC120-15, Harvard Apparatus) that were pulled using a micropipette puller (Sutter p97). The settings used for needle pulling were the following: pull 55, velocity 55, time 10 and heat 580-590 (determined each time the procedure was done). Prior to microinjection the tip of the needle was cut open using fine forceps and the needle mounted into a fixed micromanipulator (Micro Instruments, LTD.) connected to a microinjector (Narishige IM-300, Intracel). Injection volume was calibrated by injecting water into mineral oil (Sigma 330779) and measuring the water bubble diameter at 5x magnification using the eyepiece micrometer in a Leica MZ75 binocular stereomicroscope. Embryos were

put into a 'injection dish': a petri dish with a circle sheet of 800um mesh Nitex screen 'glued' to the bottom using chloroform. During and a couple of hours after injection, embryos were kept in 4% Ficoll (diluted in the appropriate media) which allows the vitelline membrane to collapse, reducing pressure and therefore preventing leakage. Ficoll was replaced by 0.05x MMR or 0.1x NAM and embryos incubated at the desired temperature. Death embryos were removed from the plate and the media was replaced every 12 hours.

LiCl treatment

Xenopus tropicalis embryos, after being dejellied, were incubated at room temperature for 2h30-3 hours until they reached 32/64-cell stage. At this stage, embryos were transferred to a agarose-coated petri dish containing 0.3M LiCl (Sigma) in 0.05x MMR and incubated for 4.30-5 minutes and swirled in the plate. The treatment was done in batches of a maximum of 750-900 embryos. After the treatment, the embryos were transferred using a plastic Pasteur pipette to another agarose-coated plate containing fresh 0.05xMMR. Embryos were washed in the media by being swirled around in the plate and this process was repeated 4-5 times (see Figure 3.2). Upon completion of the washes, the embryos were transferred again to another agarose-coated plate and incubated in 0.05x MMR at 25-28°C. Embryos were harvested at stagNF11.5 or NF12, depending on the experiment, however around 10% were kept developing to assess phenotype at tailbud stages. Only treatments that resulted in embryos with an average DAI score of 9.4-10 were considered for further analyses.

UV treatment

In order to be an efficient treatment, UV irradiation into the vegetal pole of *Xenopus tropicalis* embryos has to occur within the first 30 minutes post fertilisation. Upon dejellying, embryos were transferred (no more than 200 embryos) into a 50 ml Falcon conical centrifuge tube and the tube containing 0.05x MMR to the top. The tube was closed by wrapping Saran wrap around the top using rubber bands and turned upside down allowing the embryos to be placed on top of the Saran wrap (see Figure 1.1). Embryos were centred and allowed to be positioned with its vegetal pole down.

The tube in positioned on top of a hole (same diameter as the falcon tube opening) of a styrofoam platform (2cm high) which in positioned on top of the UV lamp (UVP, LLC, UVGL-25). This allowed the embryos to be at the desired distance from the UV source. The embryos were irradiated with an UV short-wave (254nm) for 2 minutes. Upon irradiation, the tube was transferred in the same orientation to the incubator as embryos must not be moved until the first cell division. After this, embryos were transferred to an agarose-coated plate containing 0.05x MMR and incubated at 25-28°C until the desired harvesting stage. Similarly to the LiCl treatment, around 10% of the UV-treated embryos were kept after collection in order to assess the treatment efficiency by tailbud stage. Only treatments that resulted in embryos with an average DAI score of 0.5-0.8 were considered for further analyses.

Animal cap explants

mRNA was injected into the top of the animal pole of 1/2-cell stage *Xenopus laevis* embryos and developed at 14°C in 4 %Ficoll in 0.1xNAM. By stage NF8-9 embryos were placed in a agarose-coated petri dish containing 0.7xMMR where 'capping' was performed. Animal caps were cut using a micro wire tip cautery electrode (1mm loop) (13-Y1, Protech International Inc.) connected to a micro cautery instrument (Protech International Inc.) at medium voltage (setting 2). After dissection, caps were transferred to a fresh agarose-coated plate containing 0.07x MMR and incubated at 18°C alongside with whole sibling embryos in order to track the stage. Animal caps were collected at corresponding stage NF15 and processed for total RNA extraction.

2.2.2 Cloning

Throughout this work different cloning techniques were used depending on each project objective. Here I will refer to the three kinds used: Gateway® cloning in order to insert the gene of interest in an expression vector; to generate WMISH RNA probes the pGEM-T-Easy vectors were used for easy cloning from PCR products; and for the dual-luciferase assay, genomic regions of interest were cloned into pGl3-Basic vectors.

Cloning into expression vector using Gateway®

The first step of the Gateway cloning system was to produce an entry clone with the gene of interest. For this I used directional TOPO® cloning that utilises the *attL* sites in the pENTR™/TOPO® vector that allow for efficient recombination with the destination vector that contains *attR* sites. The first step was to design primers compatible with the pENTR directional TOPO cloning: forward primer must start with CACC, complementary to the overhang of the cloning vector, GTCC, and the reverse primer should end with or without a STOP codon depending on the position (C- or N-terminus) of the tag on the destination vector. All genes were amplified using *Pfx50* polymerase (12355-012, Invitrogen, Thermo Fisher Scientific) and a final concentration of 0.4µM of each of the following primers:

Cloning of K00726 from stage NF10-12 of *Xenopus tropicalis* cDNA (Chapter 3).

K00726 (1285bp)

Forward primer:

5'-CACCATGGAGAGTTCCTCCGGCCT-3',

Reverser primer including STOP codon, for N-terminal tag:

5'-TTATCACAGGTATACTCTGCGTA-3',

Reverser primer without a STOP codon, for C-terminal tag:

5'-TCACAGGTATACTCTGCGTA-3'.

Cloning of wild-type and mutant *t* and *t2* for expression in embryos. t^{wt}, $t^{e1.2D}$ and $t2^{e3.7D}$ were cloned from synthetic genes assembled from synthetic oligonucleotides and manufactured by GeneArt® (Invitrogen, Thermo Fisher Scientific) and $t2^{wt}$ from IMAGE clone 5307982 (Gentsch et al., 2013) (Chapter 5).

t ^{wt} **and** ***t*** $^{tm2.2}$ **N-terminal**:

5'-CACCATGAGTGTAAGTGCCACCGAGA-3',

5'-TTAGATTGACGGCGGTGCAAC-3';

t ^{wt} **and** ***t*** $^{tm2.2}$ **C-terminal**:

5'-CACCATGAGTGTAAGTGCCACCGAGA-3',

5'-GATTGACGGCGGTGCAACTG-3';

t2 ^{wt} **N-terminal**:

5'- CACCATGAGTACAGGAACAGCTG-3',

5'-CTATAATGATGGAGGTGTCACAGA-3';

t2 ^{wt} **C-terminal**:

5'-CACCCAGAAGAGGCATCAGCAATAC-3',

5'-TAATGATGGAGGTGTCACAGAAG-3';

t2 $^{tm1.2}$ **N-terminal**:

5'-CACCATGAGCACAGGCACAGCTGAGA-3',

5'-CTATAATGATGGAGGTGTCACAGA-3';

t2 $^{tm1.2}$ **C-terminal**:

5'- CACCATGAGCACAGGCACAGCTGAGA -3',

5'- TAATGATGGAGGTGTCACAGAAGC -3'.

Amplification parameters were the following: 2 minutes at 94°C, 35 cycles of 15 seconds at 94°C, 60°C for 30 seconds, 68°C for 1 minutes and 30 seconds; and 5 minutes at 68°C and kept at 4°C. Part of the amplification reaction was used to verify the size of the amplicon on a 1% agarose/TAE gel (containing 1:50,000 RedSafe, Ecogen, 21141) gel. If the correct fragment was amplified I proceeded to the pENTR directional TOPO cloning as follows: 1µl of fresh PCR product, 0.5µl of salt solution (1.2M NaCl, 0.06M $MgCl_2$, 1µl of H_2O and 1µl of pENTR™/TOPO®vector. The reaction was gently mixed and incubated at room temperature for 20 minutes to 1 hour. 1µl of this reaction was used to transform 50µl of TOP10 competent cells (Life Technologies, C4040-06). The cells and reaction were mixed and incubated on ice for 30 minutes followed by heat-shock for 30 seconds at 42°C. Cells were transferred back to ice for a few minutes and 75µl of super optimal broth with catabolite repression (SOC) was added followed by an incubation at 37°C for 1 hour, shaking. The whole volume of SOC, with competent cells, was spread in a pre-warmed lysogeny broth (LB) agar plate containing 50µg/ml of kanamycin. Plates were incubated overnight at 37°C and in the next day 3 colonies from each transformation were picked and resuspended in 50µl of Tris-EDTA buffer (TE) for a PCR colony reaction. The PCR reaction was as follows: 1µl of resuspended colony, 0.4µl of 10µM of each primer (see above, or M13 forward or M13 reverse), 3.6µl of H_2O and 5µl of 2x KAPA2G Fast ReadyMix (KK5103, KAPA Biosystems). The

reaction in run on a 1% agarose/TAE gel (containing 1:50,000 RedSafe, Ecogen, 21141) gel. The resuspended colonies that have the insert were inoculated in 5ml of LB with 50µg/ml kanamycin and incubated overnight at 37°C shaking (1250rpm).

On the following day, the bacteria cultures were transferred to a 2ml Eppendorf tube and centrifuged at RT for 2 minutes at 12,000xg to pellet bacteria. The media was removed and the process was repeated until the whole culture was collected on the bottom of the tube. The plasmid DNA was isolated using the Plasmid MiniPrep kit (Qiagen, 27106) and eluted in 50µl of elution buffer (EB) (10 mM Tris-Cl, pH 8.5). The next step was the recombination with the destination vector containing the *attR* sites. The destination vectors used were produced by Kevin Dingwell and besides being compatible with the Gateway® Cloning system (contains *att* sites) they have pCS2$^+$ as backbone (contains a CMV minimal promoter and a SV40 polyA terminatior) and contain 3x HA to tag the gene either C- or N-terminally (pCS2$^+$-N-3xHA and pCS2$^+$-C-3xHA). The recombination was known as LR recombination since it uses a LR clonase™that catalyses the reaction between the entry clone containing the *att*L-flanked gene and the *att*R-containing destination vector, which results in an *att*B-containing expression clone. The LR recombination reaction was as follows: 1µl of pENTR/D-TOPO containing the insert (150ng), 1µl of destination vector (pCS2$^+$-N-3xHA or pCS2$^+$-C-3xHA, 150ng), 2µl of TE (pH8.0) and 1µl of LR clonase™II enzyme mix (Life Technologies, 11791-020). The reaction was gently mixed and incubated at 25°C for 1 hour. After this, 0.5µl of proteinase K (Life technologies, AM2546) was added to the mix proceeded by an incubation at 37°C for 10 minutes. The reaction was put one ice and 1µl used to transform TOP10 competent cells, as described above. The destination vector has ampicillin resistance, so the SOC media was spread in pre-warmed LB agar plates containing 100µg/ml ampicillin. On the following day, three colonies from each transformation were picked and each inoculated in 5 ml of LB with 50µg/ml ampicillin and grown at 37°C overnight. The following day, the plasmid DNA was isolated as described above and eluted in 50µl of EB. In order to confirm cloning of the gene of interest, right orientation and that no mutations occurred during the PCR amplification, the DNA was Sanger sequenced (GENEWIZ) using primers on each end of the insert, forward SP6 primer and reverse T3P primer. Results of

the sequencing were analysed using the software SeqMan Pro™(DNASTAR®). The plasmids containing the correct sequence were used for capped mRNA synthesis (see below).

Cloning into pGEM®-T-Easy for WMISH probes

To clone genes to generate WMISH RNA probes I used the pGEM®-T-Easy plasmids as they contain single 3'-T overhangs at the insertion site compatible with overhangs produced by DNA polymerase (such as Taq) during PCR reaction, allowing for an efficient and rapid ligation of PCR products. I have cloned full-length coding sequences of the gene of interest from stage NF11-12 *Xenopus tropicalis* cDNA. Fragments were amplified using GoTaq® Hot start polymerase (M5132, Promega) in a 25µl reaction: 1µl of 10µM forward and reverse primer, 2µl of cDNA and 8.5µl of H20. The following primer pairs were used:

***K00726* (1285bp)**:
forward: 5'- ATGGAGAGTTCCTCCGGCCT-3',
reverse: 5'- TCACAGGTATACTCTGCGTA-3';
***72022004* (814bp)**:
forward: 5'- ATGGAAAACGCCATTCTCAGT-3',
reverse: 5'- TTAGTGGGAAATATTAAGTAC-3';
***cpe* (1392bp)**:
forward: 5'- ATGATGGCAGGAGTATGGGC-3',
reverse: 5'- TCAAAAATTCAAGGTCTGTGACA-3';
***c8orf4* (291bp)**:
forward: 5'- ATGTCCGTCTCTCTGAGAGTCAG-3',
reverse: 5'- TCAGGTCATGACCTTGAGAGGAATC-3'.

To verify that the correct fragment was amplified, 12µl of the reaction was run on a 1% agarose/TAE gel (containing 1:50,000 RedSafe, Ecogen, 21141) gel. The PCR product was purified from the remaining reaction using the QIAquick PCR Purification kit (QIagen, 28194) and the concentration measure using NanoDrop™1000 (Thermo Scientific). The ligation reaction was as follows: 5µl of 2x Rapid Ligation Buffer, T4

DNA ligase, 1µl of pGEM-T Easy® vector (50ng) (A3600, Promega), 50ng of the purified PCR product, 1µl of T4 DNA ligase (3 Weiss units/µl) (M1801, Promega) and deionised water to a final volume of 10µl. The reaction was gently mixed and incubated at RT for 1 hour. 2µl of the ligation reaction were used to transform 50µl of JM109 competent cells (L2005, Promega). As described above, the competent cells plus the ligation product were kept on ice for 20-40 minutes followed by a 30 seconds heat-shock at 42°C, upon which, the cells were returned to ice for a few minutes. At this point, 950µl of SOC was added and incubated for 1h30 minutes at 37°C while shaking. 100µl of each transformation culture was plated in pre-warmed LB plated containing Ampicilin (100µg/ml)/6-Chloro-3-indolyl-β-D-galactopyranoside (Salmon-Gal) (80µg/ml/ isopropyl β-D-1-thiogalactopyranoside (IPTG) (0.5mM). The plates were incubated at 37°C overnight and the following day white colonies (3-6) from each plate were picked and re-suspended in 50µl of TE buffer. 1µl of each resuspension was used for PCR colony as described above. The selected colonies were inoculated into 5 ml of LB with 50µg/ml ampicillin and grown at 37°C overnight. On the following day, plasmid DNA was isolated from the cultures using the Plasmid MiniPrep kit (Qiagen, 27106) and eluted in 50µl of elution buffer (EB) (10 mM Tris-Cl, pH 8.5). In order to confirm that no mutations occur during the amplification of the transcripts and verify the orientation of the gene in the vector, the plasmid DNA was sequenced (Sanger Sequencing, GENEWIZ) using the forward primer T7P and the reverse primer M13-26. The plasmids were linearised and used to generate anti-sense RNA probes for WMISH (see below).

Cloning into pGl3-Basic for Dual Luciferase Assay

In order to understand whether certain genomic regions were capable of driving expression and hence were potential regulatory regions for the nearest genes I used the Dual-Luciferase® Reporter Assay System (Promega). The system uses the luciferase activity of firefly (*Photinus pytalis*) and *Renilla* (*Renilla reniformis*) which were measured sequentially in the same sample. I used the pGL3 Luciferase reporter vector (Promega, E1751) that contains the *luc*$^+$ firefly luciferase expression and two multi-cloning sites (MLS) that allow the insertion of up to two sequences, such as a pro-

moter and an enhancer. In the context of this experiment I had 6 distinct versions of the pGL3-Basic vectors: (1) pGL3-*K00726* promoter, (2) pGL3-*K00726*promoter-e1, (3) pGL3-*K00726* promoter-e2, (4) pGL3-*K00726* promoter-e3, (5) pGL3-*K00726* promoter-Neg.Reg. and (6) pGL3-Basic. Vector (1) contains only the gene promoter, vectors (2)-(5) contain the same promoter plus the specific regulatory region to be tested and vector (6) was also called empty vector as it does not contain any genomic region.

The first step was to design primers that span the region of interest and include the restriction site and a GATC region to ensure that restriction occurs efficiently. Promoter was inserted into a HindII site and the 'enhancers' into a BamHI site. The sequences were amplified from genomic DNA (gDNA) of *Xenopus tropicalis* embryos in the following reaction: 200ng of gDNA, 2µl of forward and reverse primer mix at 10µM, 25µl of KAPA HiFi HotStart ReadyMix (KAPA Biosystems, KK2601) and H_2O to final reaction volume of 50µl.

The following primer pairs were used to amplified the regions of interest:

K00726 promoter (133bp), containing a HindII restriction site

forward: 5'- GATCAAGCTTGACATTTTATCTGGTTTTACAG-3',

reverse: 5'- GATCAAGCTTATTTTCCAACAGGTGGGTGA-3';

K00726 e1 (306bp)

forward: 5'- GATCGGATCCCTGGTGATTGGTTGCTGTTG-3',

reverse: 5'- GATCGGATCCGGGGTAGGTAAATGCCGAAA-3';

K00726 e2 (583bp)

forward: 5'- GATCGGATCCAAATCAAGCGCCTCTCAGAC-3',

reverse: 5'- GATCGGATCCAAGGTGGCCATACACCAATC-3';

K00726 e3 (441bp)

forward: 5'- GATCGGATCCAACAACTGCATAAGGAATGTGC-3',

reverse: 5'- GATCGGATCCCCCAGCCAGTGAATAGCATTA-3';

K00726 Neg. Region (953bp)

forward: 5'- GATCGGATCCAAACCCCATCTGAAGCCTCT-3',

reverse: 5'- GATCGGATCCGGGGGTTATTCTTCCCCTTT-3'.

The reaction was added to a thermocycler (T100 Thermal Cycler, BioRad) and amplified: pre-incubation for 45 seconds at 98°C, 35 cycles of; 10 seconds at 98°C, 10 seconds at 63°C and 30 seconds at 72°C; followed by a final extension at 72°C for 20 seconds. 5µl of the amplification reaction was used to verify the size of the amplicon on a 1% agarose/TAE gel (containing 1:50,000 RedSafe, Ecogen, 21141). The remaining 45µl were used to purify the DNA fragment using the QIAquick PCR purification kit (Qiagen, 28106) and following the manufacturer's instructions. The PCR amplicons were digested overnight in a 100µl reaction: 46µl of purified PCR amplicon, 10µl of 10x restriction buffer, 10U of the appropriate restriction enzyme (HindIII or BamHI) and and H_2O. The vector (20µg) to which the sequence was going to be inserted (either pGL3-Basic, if inserting the promoter ,or pGL3-*K00726* promoter when inserting the 'enhancer' sequence) was also also linearised overnight with the appropriate restriction enzyme (30U) in a similar reaction. Both reactions were incubated overnight at 37°C and the next day the digested PCR amplicon and linearised vector were purified using the QIAquick PCR purification kit (Qiagen, 28106), as before, and the concentration measured. Prior to ligation, the vector was dephosphorylated using the Rapid DNA Dephosphorylation and Ligation kit (Roche, 04898117001) for 10 minutes at 37°C: 1µg of linearised vector, 2µl of 10x phosphatase buffer, 1µl of 1U alkaline phosphatase and H_2O to a final volume of 20µl; followed by inactivation by incubating at 75°C for 2 minutes.

Both the vector and the insert were prepared for the ligation reaction. The ligation was done with a vector:insert ratio of 1:3 and the amount insert used for 50ng of vector was calculated accordingly (amount of insert (ng) = 50ng/4800bp*3 *[insert size,bp]). The ligation used the reagents of the Rapid DNA Dephosphorylation and Ligation kit (Roche, 04898117001) as follows: 50 ng of linearised-dephosphorylated vector, insert (appropriate amount), 2µl of 5x DNA dilution buffer, H_2O to a volume of 8µl, 10µl of 2x DNA dilution buffer and 1µl of 5U T4 DNA ligase. The reaction was incubated at room temperature for 20-40 minutes. Following ligation, TOP10 competent cells were transformed as described above and the cells were spread on LB agar plates containing 100µg/ml ampicillin. Colonies were picked and inoculated and DNA was purified from the cultures as described above. The plasmids were ver-

ified for the right orientation and presence of mutation by Sanger sequencing (GENEWIZ) using GLprimer2 (5'-CTTTATGTTTTTGGCGTCTTCCA-3'), RVprimer4 (5'-GACGATAGTCATGCCCCGCG-3') and RVprimer3 (5'-CTAGCAAAATAGGCTG TCCC-3'). Once the promoter was cloned into the pGL3-Basic vector, the processed was repeated using this vector (pGL3-*K00726* promoter) to insert the 'enhancer' regions. The plasmids were co-injected with *Renilla* mRNA into *Xenopus tropicalis* embryos for the dual-luciferase reporter assay (see below).

2.2.3 Synthesis of capped mRNA for micro-injection

For the synthesis of capped mRNA for injections into *Xenopus* embryos, 10µg of plasmid containing the cloned cDNA of interest was linearised by the appropriate restriction digest overnight at 37°C (Table 2.1). The linearised plasmid was purified using the QIAquick PCR purification kit (QIAGEN, 28106) according to the manufacturer's guidelines and quantified using a NanoDrop™1000 (Thermo Scientific). 1µg of linearised plasmid was used for *in vitro* transcription using the mMESSAGE mMACHINE®SP6 Transcription Kit (Life technologies AM1340) in the following reaction: 2µl of 10x reaction buffer, 10µl of 2x NTP/CAP, 2µl of SP6 enzyme mix and H_2O to final reaction volume of 20µl. The reagents were carefully mixed and the samples were incubated at 37°C for 2 hours. 1µl of TurboDNase (Ambion, AM2238) was added and the sample incubated for 15 minutes at 37°C to allow the digestion of the DNA template. RNA was precipitated by adding 30µl of LiCl and 30µ H_2O and an overnight incubation at -20°C. On the following day the samples was centrifuged at full speed for 15 minutes at 4°C, the pellet was washed once with 80% EtOH and air-dried for 5 minutes at room temperature. The RNA was re-suspended in RNase-free water, the concentration was measured on the NanoDrop™1000 (Thermo Scientific). To assess the RNA integrity and correct size, 200ng of pre-warmed (65°C) RNA was run on a 1.4% agarose/TAE gel (containing 1:50,000 RedSafe, Ecogen, 21141). The sample was diluted to stock solutions of 1ng/nl or 0.5ng/nl, aliquoted and stored at -80°C.

mRNA	Size	Vector	Restriction Enzyme	Polymerase	Origin
HA-t	1.8kb	N-terminal 3xHA pCS2$^+$	ApaI	SP6	this work
t-HA	1.8kb	C-terminal 3xHA pCS2$^+$	ApaI	SP6	this work
HA-t2	1.8kb	N-terminal 3xHA pCS2$^+$	ApaI	SP6	this work
t2-HA	1.8kb	C-terminal 3xHA pCS2$^+$	ApaI	SP6	this work
HA-t$^{e1.2D}$	1.8kb	N-terminal 3xHA pCS2$^+$	ApaI	T7	this work
t$^{e1.2D}$-HA	1.8kb	C-terminal 3xHA pCS2$^+$	ApaI	SP6	this work
HA-t$^{e3.7D}$	1.8kb	N-terminal 3xHA pCS2$^+$	ApaI	SP6	this work
t$^{e3.7D}$-HA	1.8kb	C-terminal 3xHA pCS2$^+$	ApaI	SP6	this work
HA-K00726	1.5kb	N-terminal 3xHA pCS2$^+$	ApaI	SP6	this work
K00726-HA	1.5kb	C-terminal 3xHA pCS2$^+$	ApaI	SP6	this work
fam83g-myc	3kb	C-terminal MYC pCS2$^+$	PvuII	SP6	this work
β-catenin-GFP	2.3kb	pCS2$^+$	NotI	SP6	Addgene (#16839)

Table 2.2: Constructs used to make capped mRNA to inject into embryos

2.2.4 Generation of anti-sense RNA probes

This protocol was very similar to the synthesis of capped mRNA for micro-injection, so here the steps were summarised, for more detail refer to it. For the synthesis of anti-sense RNA probes for WMISH, 10µg of plasmid containing the cloned cDNA of interest was linearised by the appropriate restriction digest overnight at 37°C (Table 2.2). The linearised plasmid was purified using the QIAquick PCR purification kit (QIAGEN, 28106) according to the manufacturer's guidelines and quantified using a NanoDrop™1000 (Thermo Scientific). 1µg of linearised plasmid was used for *in vitro* transcription with the appropriate RNA polymerase (Table 2.2) to create the Digoxigenin-labelled antisense (AS) RNA probe. For this purpose, the DIG-RNA Labeling Mix (Roche 11277073910) was used following the manufacturer's instructions. The DNA template was removed by treating the reaction with TurboDNase (Ambion, AM2238). The RNA probe was precipitated with LiCl overnight at -20°C and cleaned with 80% EtOH. RNA was re-suspended in RNase-free water, the concentration was measured on the NanoDrop™1000 (Thermo Scientific) and a 10x stock of the RNA probe was made by diluting it with hybridisation buffer to 10 ng/ml and stored at -20°C.

Probe	Size	Vector	Restriction Enzyme	Polymerase	Origin
t	2.2kb	pSP73	BglII	T7	(Smith et al., 1991)
cav1	1.4kb	pExpress1	BglII	T7	IMAGE clone: 7024946
actc1	0.4kb	pSP21	EcoRI	SP6	(Mohun et al., 1984)
not	1.1kb	pCS2(+)	XhoI	T7	(Dassow, Schmidt, and Kimelman, 1993)
msgn1	1kb	pCMV-Sport6.ccdB	EcoRI	T7	IMAGE clone: 699331
tal1	1.3kb	pGEM-7Zf(+)	XhoI	SP6	European Xenopus Resource Centre
myh6	0.4kb	pGEM	NcoI	SP6	(Gentsch et al., 2013)
hoxd8	1kb	pCR2.1-TOPO	HindIII	T7	(Gentsch et al., 2013)
noggin	0.7kb	pGEM-5Zf(-)	EcoRI	T7	(Smith and Harland, 1992)
goosecoid	1.1kb	pBS-SK(-)	EcoRI	T7	(Cho et al., 1991)
chordin	1kb	pBS-SK(-)	EcoRI	T7	(Sasai, 1994)
wnt8a	1.42kb	pGEM1	BamHI	T7	(Christian et al., 1991)
bmp4	1.4kb	pBS-SK(+)	EcoRI	T7	(Köster et al., 1991)
c8orf4	0.3kb	PGEM®-T Easy	NdeI	T7	this work
7202004	0.8kb	pGEM®-T Easy	SacI	T7	this work
K00726	1.3Kb	pGEM®-T Easy	SacI	T7	this work
cpe	1.4kb	pGEM®-T Easy	ApaI	SP6	this work

Table 2.3: List of WMISH probes and specific enzymes used to generated them.

2.2.5 WMISH

Embryos of the desired stage were fixed in MEMFA overnight at 4°C or for 2h at room-temperature (RT) in glass vials. After fixation embryos were washed 2-3 times in 100% absolute Ethanol (EtOH) to keep them dehydrated and stored at -20°C at least overnight (o/n). On the first day of the WMISH protocol, embryos were gradually rehydrated by washing 5 minutes in 75% EtOH/25% PBT (PBS + 0.1% Tween-20), 50% EtOH/50% PBT followed by 25% EtOH/25% PBT and finally two washed in 100% PBT. Embryos were permeabilised: embryos under NF22 were washed 5x in PBT for 5 to 10 minutes; embryos over NF22 were incubated in 10ug/ml proteinase K (Sigma) in PBT, washed once for 5 minutes in PBT, re-fixed for 20 minutes in MEMFA and washed again 5 times, for 10 minutes, in PBT. The protocol described here uses baskets (2ml Eppendorf tube whose conical bottom was cut off and replaced by a fine mesh that allows liquid to go in and embryos to be submerged in solution), although glass vials were also permissible. Embryos were transferred to an agarose-coated plate and under a stereomicroscope selected and distributed into the different baskets (each for a different RNA probe) fitted into holes of a 1.5ml tube storage box containing PBT. All subsequent washes were performed using the baskets submerged into the 1.5ml tube storage box holes containing the different solutions. Following the last PBT wash, baskets were transferred to pre-warmed hybridisation solution (pre-hyb solution) and incubated at 60°C for 2-5 hours, in a hybridisation oven. After this, pre-hyb solution

was saved and replaced by 500µl of DIG labelled antisense RNA probe was added at 1µg/ml and the embryos were incubated overnight at 60°C. The following day, the AS probe was replaced by the previous day's pre-hyb solution and the embryos washed for 5 minutes at 60°C. The AS probe was stored at -20°C and re-used up to 5 times. Embryos were washed 3 times, for 20 minutes, in pre-warmed 2xSSC/Tween at 60°C followed by two washes, 30 minutes each, in 0.2xSSC/Tween still at 60°C. Since SSC was the main component of the hybridisation solution these washes were a gradual washing off of the hybridisation solution. Embryos were transferred to RT and washed 2 times (5 minutes each) in MAB before blocking for 1 hour in MAB containing 2% BMB Blocking Reagent (BR) (Roche 11096176001). Embryos were incubated for 4 hours at RT in antibody solution: 1:2000 anti-DIG alkaline-phosphatase(AP)-conjugated antibody in 2% BMBBR/MAB containing 10% of lamb serum. Upon antibody incubation, embryos were washed in MAB 4-6 times for 10 minutes at RT and kept overnight in MAB at 4°C with gentle shaking. The following day embryos were washed at RT 3 times in MAB for 15 minutes, 2 times in freshly prepared AP buffer for 5 minutes. At this point, embryos were removed from the baskets, returned to glass vials and to each was added the staining solution (AP buffer + 3.4µl/ml NBT (100mg/ml) + 3.5µl/ml BCIP (50mg/ml) + 4mM levamisole) and embryos were incubated at RT and protected from light (using aluminium foil). The duration of incubation varies depending on the probe (from 15 minutes to 24 hours) and staining was checked initially every 15 minutes and every hour after that. For a slower staining reaction embryos were incubated at 4°C. The staining reaction was stopped by washing the embryos in MAB 2-3 times at RT. Embryos were re-fixed in Bouin's solution for 1 hour at room temperature or overnight at 4°C. Upon fixation, embryos were washed 3-4 times in 70% EtOH/PBT and rehydrated back to 100% PBT in 2 gradual steps. Embryos were bleached by incubating them for 2-4 hours in bleaching solution on top of a light box while covered with aluminium foil. Bleaching removes the pigmentation of the embryos allowing for a better visualisation of the staining. Embryos were washed and stored in PBS at 4°C. For image acquisition, embryos were placed in a petri dish coated with a thick agarose layer and pictures taken under the stereomicroscope (Leica M165FC).

2.2.6 ChIP-grade polyclonal antibody production

In experiments described in Chapter 4, two distinct ChIP-grade antibodies against *t* were used. One antibody was previously described (Gentsch et al., 2013) and a second antibody was produced during the duration of this project. An anti-rabbit polyclonal antibody was produced by Cambridge Research Biochemicals using 1-1.75mg of t (Xbra) full length protein previously derived from *Baculovirus* expression system (Gentsch et al., 2013). The crude antisera of two rabbits was purified by affinity chromatography on thiopropyl sepharose 6B and NHS sepharose coupled with the antigen, the native form of the protein. I were supplied with a glycine eluate (11ml) at 0.5mg/ml protein in PBS and a TEA eluate (14ml) at 0.03mg/ml protein in PBS. Before purification 4 bleeds from the rabbits were tested by Dotblot (see below) and once the antibody was purified it was validated by Immunoprecipitation followed by Western Blot (IP/WB) (see below) and by whole mount immunohistochemistry (WMIHC) (see below).

2.2.7 Dotblot

A Polyvinylidene fluoride (PVDF) membrane was cut into rectangular shape and in each, small circles (dots) were drawn with a pencil, about 2 cm apart. The PVDF membrane was pre-wet in 100% Methanol (MeOH) and washed one time in H_2O. The membrane was placed on top of PBT-wet Whatman® filter paper inside an 'humid chamber'. The 'humid chamber' was composed, from bottom to top of: paper tissue, one sheet of dried filter paper and the wet filter paper with the PVDF membrane on top. To each circle, 1µl of different dilutions of the Brachyury purified protein (3ng, 1.5ng and 500pg) was added, the 'chamber' was closed and incubated for 1 hour at room temperature. The PVDF membranes were blocked with 5% (w/v) non-fat milk powder (Cell Signalling Technology, 9999S) in PBT for 40 minutes at room temperature. The bleeds/antibody were diluted 1:500 in 5% non-fat milk/PBT and incubated with the membranes for 1 hour at room temperature. The membranes were washed 3 times with PBT and the secondary antibody was added, goat α-rabbit, horse radish peroxidase (HRP) conjugated (ThermFisher Scientific,) at 1:2000 (diluted in 5%(w/v) non-fat milk powder/PBT) and incubated for 1 hour at room temperature.

The membranes were washed 3 times with PBT and once with PBS. The peroxidase activity was detected by chemiluminescence reaction (BioFX® Chemiluminescent Ultra Sensitive HRP membrane substract, Surmodics) and captured with ChemiDoc™XRS+ imager (BioRad).

2.2.8 Protein Immunoprecipitation followed by Western Blot (IP/WB)

X.laevis and *X.tropicalis* embryos were homogenised in 6µl/embryo of PhosphoSafe™ Extraction Buffer (Novagen) supplemented with cOmplete™ EDTA-free protease inhibitors (Roche Life Sciences, 11873580001). In order to remove yolk from the embryonic extract the homogenate was mixed with the same volume of FREON and centrifuged for 5 minutes at 4°C. This initial step was the same whether continuing with protein IP or just for Western blot (see below). In the case of an IP, aliquots of the supernatant were saved to use as input and the remaining used for IP. For the IP, 0.5µg of Brachyury antibody ((Stennard et al., 1999), this work) was added to the embryonic extract and incubated for 1 hour on a rotator (10 rpm) at 4°C. Dynabeads® M-280 sheep anti-rabbit IgG (Thermo Scientific, 11203D) were washed with IP buffer (50mM Tris, pH7.5, 150mM NaCl, 1mM EGTA, 1% (v/v) Igepal CA-630, 0.25% (w/v) Sodium deoxycholate), and 30µl were added to the embryonic extract and incubated in a rotator (10 rpm) at 4°C overnight. The following day, the beads were washed 5 times, 5 minutes each, with IP buffer, using the rotator and a magnetic rack to bind the beads. The immunoprecipitaed protein was eluted by re-suspending the beads in SDS loading buffer (250mM Tris pH6.8, 10% (w/v) SDS powder, 50% glycerol, 25% β-mercaptoethanol, 0.02% bromophenol blue) by warming up the sample to 65°C while shaking (1000 rpm) for 5 minutes. Using the magnetic stand the supernatant was removed and it was ready to be used for Western Blot.

Western Blot

The initial step of obtaining embryonic extract was described above. SDS loading buffer was added to the embryonic extract in a 1:5 ratio and the samples were denatured by incubating at 70°C for 5 minutes. The samples were loaded into mini-PROTEAN® precast polyacrylamide gels (Bio-Rad, 456102, 4569035) (7.5% and AnykD™) submerged

in 1x SDS running buffer in a BioRad tank (BioRad, Mini-PROTEAN® Tetra Cell). The samples were loaded alongside 5µl of Precison Plus Protein™WesternC™Blotting standard (BioRad, 1610376) a pre-stained ladder. Gels were run at 100V for the first 5 minutes and the voltage was increased to 200V until the running front reached the bottom of the gel. The gel cassette was taken from the tank and opened to removed the gel which was trimmed off at the bottom and at the top. The Immobilon-P PVDF membrane (Millipore, IPVH00010) was activated by submerging it in 100% MeOH for 2 minutes, washed one time in H_2O and finally in transfer buffer (25mM Tris Base, 190 mM Glycine, 20% (v/v) MeOH). Before mounting the 'transfer sandwich', the gel was briefly rinsed in transfer buffer in order to remove SDS as well as four sponges and 4 Whatman® filter papers. The 'transfer sandwich' was set up, inside a holder, with the following order from the positive pole (red): two sponges, two Whatman® filters, the PVDF membrane, the polyacrylamide gel, two Whatman® filters and two sponges. Bubbles were carefully removed by rolling a Western Blot roller on top of the filter papers. The holder was placed inside a BioRad tank filled with transfer buffer, with the correct orientation: gel to the negative pole (black) side and the membrane towards the positive pole (red). An ice pack was added to the tank to keep the transfer from overheating. The blot was transferred for 40 minutes at 200mA. After this, the holder was removed and opened, and the membrane checked for complete transfer by observing the ladder (pre-stained) transference. If the transfer was successful the membrane was removed and placed in between two sheets of Saran Wrap to cut in half if different antibodies were to be used. The membrane(s) was placed inside a 50 ml Falcon conical centrifuge tube containing 5-10 ml of 5% (w/v) non-fat milk powder (Cell Signalling Technology, 9999S) in PBT (MPBT) and incubated (while rolling) for 1 hour at room temperature or overnight at 4°C. The primary antibodies were added at the appropriate dilution in MPBT and incubated for 1 hour at room temperature or overnight at 4°C. The membranes were washed 3 times, 15 minutes each, with PBT, at room temperature and the secondary antibody was added and incubation was similar to the primary. Finally, the membrane was washed three times (15 minutes) with PBT and one time with PBS. The secondary antibodies used were all HRP-conjugated, and peroxidase activity was detected by chemiluminescence reaction (BioFX ® Chemilu-

minescent Ultra Sensitive HRP membrane substract, Surmodics) and captured with ChemiDoc™ XRS+ imager (BioRad). On the ChemiDoc™ XRS+ imager the images were captured using the Chemiluminescence High Sensitivity detector, without filter and with the aperture opened to the maximum (100). The membrane was exposed from 1 second to 5 minutes in order to detect signal, depending on the experiment.

Primary antibodies: rabbit polyclonal anti-Xbra serum (Cunliffe and Smith, 1994) at 1:5,000, rabbit polyclonal anti-t at 1:5000 (this work), mouse monoclonal anti-α-tubulin(Sigma, T5168) at 1:5,000, mouse monoclonal anti-c-Myc (Sigma, M5546) at 1:5,000 and mouse monoclonal anti-HA (Sigma, H9658) at 1:10,000

Secondary antibodies: goat anti-rabbit IgG horse radish peroxidase (HPR) conjugate (TrueBlot®) 1:1000, goat anti-mouse IgG (H+L) HRP conjugate (Thermo Fisher Scientific, 31430) and goat anti-rabbit IgG (H+L) HRP conjugate (Thermo Scientifc, 30954)

Semi-quantitative WB

Next to the embryonic extracts, a serial dilution of known concentrations of Brachyury protein were load in the gel. This allowed to design a standard curve and quantified the amount of Brachyury in embryonic extracts based on the luminescence. The analysis was done using the Quantity One 1-D Analysis Software (BioRad) associated with the ChemiDoc™ XRS+ imager (BioRad).

2.2.9 Whole mount immunohistochemistry in *Xenopus* embryos

Stage NF12 *Xenopus* embryos were fixed in MEMFA for 10 or 15 minutes at room temperature. The embryos were washed in 100% EtOH and incubated overnight at -20°C. On the following day, embryos were rehydrated in 3 steps to 100%PBT and washed once in PBT. If needed, the embryos were bisected, through the blastopore, using a disposable scalpel (Swann-Morton®, 0501) under a stereomicroscope. Upon dissection embryos were transferred to a glass vial and fixed for 5 more minutes in MEMFA and washed once with PBT (PBS + 0.1% Triton X-100). Bisected embryos were blocked by washing 3 times, 10 minutes each, with PBT (PBS + 0.1% Triton X-100) with 2mg/ml BSA (bovine serum albumin). The primary antibody was added (diluted in PBT/BSA)

and incubated overnight at 4°C. On the following day, embryos were further incubated for 1 hour at room temperature and washed five times (10 minutes each) in PBT. Embryos were blocked again for one hour at room temperature and incubated overnight at 4°C with the secondary alkaline phosphatase (AP)-conjugated antibody. On the next day, the embryos were washed in PBT for 10 minutes, 3-4 times. Embryos were washed one time in AP buffer (100mM NaCl, 100mM Tris, pH9.5, 50mM $MgCl_2$ and 1% Tween-20) for 10 minutes. The AP buffer was replaced by AP buffer containing 3.4µl/ml of NBT (100mg/ml) and 3.5µl/ml BCIP (50mg/ml) and the glass vials were kept in the dark and incubated at room temperature for 30-40 minutes. To stop the reaction, the embryos were washed a couple of times with PBS, for 10 minutes each, and fixed overnight in MEMFA at 4°C. Embryos were bleached and pictures taken as described in the WMISH section.

Primary antibody: rabbit polyclonal anti-t at 1:500 (this work) Secondary antibody: Alkaline Phosphatase AffiniPure F(ab')$_2$ Fragment Goat Anti-Rabbit IgG (H+L) (Jackson ImmunoResearch Laboratories, Inc, 111-056-045)

2.2.10 Extraction and purification of total RNA from *Xenopus* embryos

Embryos (10-20 embryos) of the desired stage or animal caps (15-20) were collected in 1.5ml Eppendorf tubes and the media removed using a pipette with a fine tip. The appropriate volume (200µl for animal caps, 1-10 *Xenopus tropicalis* embryos or 5 *Xenopus laevis* and 400µl for 15-20 *Xenopus tropicalis* and 10 *Xenopus laevis*) of TRIzol (Thermo Fisher Scientific, 15596018) was added and the embryos were homogenised by vortexing for 10 minutes, at room temperature. The samples were snap-frozen in liquid nitrogen and stored at -80°C or processed for total RNA extraction. The homogenate was transferred to a 1.5 ml Phase-lock gel heavy tube (5 Prime) (prespun at 12,000x g for 30 seconds) and 80/40µl of chloroform (1/5 of TRIzol volume) was added and shake vigorously. Samples were incubated at room temperature for 2 minutes followed by 15 minutes of centrifugation at 4°C at full speed. After centrifugation, the upper phase was transferred to a clean 1.5ml Eppendorf tube. RNA was precipitated using the RNA Zymo Clean and concentrator™-5 (Zymo Research, R1016), as follows. To the tube

containing the upper-phase it was added one volume of 100% EtOH and after mixing, the mixture was transferred to the Zymo-Spin™ IC column in a collection tube which was spinned for 1 minute at 12,000x *g*. The flow-through was discarded and 400µl of RNA Wash Buffer added to the column and centrifuged for 30 seconds at 12,000x *g* and the flow-through discarded. The samples were treated with DNAse in order to remove any remaining DNA by adding 50µl of DNaseI cocktail (5µl of Turbo DNase, 5µl of 10x Turbo Dnase Reaction Buffer and 40µl of RNA Wash Buffer) directly to the column's matrix. The samples were incubated at room temperature for 20-30 minutes. To each column 400µl of RNA Prep Buffer was added, the column centrifuged for 30 seconds at the same speed as before and the flow-through discarded. This step was repeated with, first with 700µl and then with 400µl of RNA Wash Buffer. After discarding the flow-through, the columns were spun at full speed for 2 minutes to remove all of the remaining liquid, the collection tube was discarded and the column transferred to a clean 1.5ml Eppendorf tube. To the centre of each column, 10µl of RNAse-free water was added and incubated at room temperature for 5 minutes. Finally, the column was centrifuged at 10,000x *g* for 30 seconds, the eluate RNA collected at the bottom of the tube and kept on ice for a few minutes. The RNA concentration was determined in 1µl of sample using a a NanoDrop™ 1000. Furthermore, the RNA integrity was assess by running 200ng of RNA on a 1% agarose/TAE (containing 1:50,000 RedSafe) and, in intact RNA, the 18S and 28S ribosomal RNA bands were clearly visible.

2.2.11 Extraction of RNA and DNA from single *Xenopus tropicalis* embryos

For genotyping and RNA extraction of single embryos the initial steps of the protocol were similar to the ones described in the section Extraction and purification of total RNA from *Xenopus* embryos. The exception being that, instead of 1.5 ml Phase-lock gel heavy tube (5 Prime) I have used 1.5 ml Eppendorf tubes that allowed us to use the lower phase for DNA extraction.

The RNA extraction was processed as described above.

For DNA extraction from single embryos I have used the Back Extraction (BE) protocol, as follows. After removing all of the aqueous phase overlying the interphase,

250µl of BE buffer (4M of Guanidine Thiocyanate, 1M Tris Base and 50mM of Sodium Citrate) was added and mixed well. The mixture was incubated at room temperature for 10 minutes followed by a centrifugation at 12,000x g for 30 minutes at room temperature. The aqueous phase, containing DNA, was transferred to a new tube and one volume of wasopropanol (100%) was added and mixed. The sample was further incubated for 30 minutes to 1 hour at room temperature and before spinning it for 15 minutes at 4°C at full speed, 0.5µg of GlycoBlue™ (Thermo Scientific, AM9516) was added. The DNA pellet was washed 2 times with 500µl of 70% EtOH followed by a spin at 4°C at 12,000x g for 15 minutes. The supernatant was removed and the pellet air-dried for 10 minutes at room temperature. The pellet was dissolved in 20µl of H_2O and incubated for 5 minutes at 55°C to help dissolve DNA. The DNA yield from single embryos ranges from 15-40ng/µl which was used for genotyping (see below).

2.2.12 Extraction of genomic DNA

This protocol for DNA extraction was distinct from the above, since the embryos were pulled and used solely for DNA extraction. Whole embryos or clipped tails from anaesthetised tadpoles were digested in 60µl of lysis buffer (50mM Tris pH8.5, 1mM EDTA, 0.5% [v/v] Tween-20 and 100µl/ml of proteinase K) and incubated at 55°C for 2 hours. To inactivate proteinase K samples were incubated at 95°C for 5 minutes, briefly centrifuged and the supernatant was used for genotyping.

2.2.13 Genotyping

For this work, embryos and tadpoles were genotyped for the *t* and *t2* locus in order to identify wild-types, homozygous and heterozygous mutants. The genomic DNA was extracted as described above and 2µl of the lysate was mixed in the PCR reaction containing 5µl of 2x KAPA HiFi HotStart ReadyMix (KAPA Biosystems, KK2600), 3.6µl of water and 0.4µl of each pair of primers:

***t* exon 1**

forward: 5'- AATCAGAGGAAGAGCTGCTG-3'

reverse: 5'-CATTGGTGAGCTCCTTGAAC-3'

***t2* exon 3**

forward:5'-TCACATCATTAAAATAGTGGCCTGCT-3'

reverse:5'-TCCATGAAATGTGAATTGTGGGCT-3'

The primers were designed to span the targeted site of mutagenesis and the region was amplified with the following PCR conditions: 45 seconds at 98°C, 36 cycles of (10 seconds at 98°C, 10 seconds at 58°C (t) or 63°C(($t2$), 10 seconds 72°C) and 20 seconds at 72°C. Following amplification, the fragments were digested with either SacI (t) or EcoRI ($t2$) overnight and separated by gel electrophoresis. An example of fragment distribution for each kind of genotype was shown in Figure 5.8.

2.2.14 Synthesis of complementary DNA (cDNA) from total RNA

For the reverse transcription (RT) reaction, 1µg of total RNA was used to synthesise first-strand cDNA using the Superscript® III kit (Invitrogen, 18080-051). To the total RNA, 10µM random hexamers, 500µM of each dNTP and RNAse-free water were added to a final volume of 13µl. Samples were incubated in a thermocycler at 65°C for 5 minutes and chilled on ice. To each sample the following reagents were added: 4µl of 5x First-strand buffer, 2µl of 0.1M DTT, 1µl of RiboLock RNase Inhibitor (Thermo Fisher Scientific, E00381) and 1µl of Superscript® III reverse transcriptase. The contents were gently mixed and incubated in a thermocycler: 5 minutes at 25°C, 50 minutes at 50°C and 15 minutes at 70°C (to inactivate the polymerase). Samples were kept at 4°C and diluted in RNAse-free water to a final volume of 100µl. To assess the synthesis efficiency, 1µl of diluted cDNA was added to 3.6µl of H_2O, 5µl of 2x KAPA2G Fast ReadyMix (KK5103, KAPA Biosystems) and 0.4µl of 10µM *odc* primers and amplified: pre-incubation at 94°C for 60 second, 35 cycles of; 15 seconds at 94°C, 15 seconds at 60°C and 15 seconds at 72°C; followed by a final extension at 72°C for 5 minutes. The product of this diagnostic PCR was loaded into a 2% agarose/TAE (containing 1:50,000 RedSafe, Ecogen, 21141) gel and fragment separated by electrophoresis.

2.2.15 Quantification of transcription

Expression levels were quantified in real-time (real time quantitative PCR, RT-qPCR) relative to a gene or locus-specific standard curve using the LightCycler LC480 II (Roche). For each primer pair a master mix was prepared: 5μl of SYBR Green I master

mix (Roche, 04707516001), 0.4µl of 10µM reverse and forward primer mix and 3.6 H_2O. The master mix was pipetted into a 384-well plate and 1µl of diluted cDNA was added to each well. The LC480 II carried 55 cycles of amplification with the following conditions: 10 seconds at 94°C, 60°C and 72°C with ramp rates of 4.8(°C/s), 2.5 (°C/s) and 4.8(°C/s), respectively. Each sample was amplified in technical triplicates and the standard curve for each primer set was calculated from 1:3 dilution series, of 8, of wild-type cDNA. The LC480 II software calculated the concentration of each sample based on the crossing point (CP) value and the standard curve calculated in each experiment. Microsoft® Excel was used to normalise the concentrations to the control gene (a house-keeping gene, *odc*), design plots and statistical analysis (Student's T test).

2.2.16 Dual Luciferase Assay

Xenopus laevis at 2-cell stage were injected with 50pg of firefly luciferase construct (pGl3 constructs, see Cloning, Dual Luciferase Assay, pGl3-Basic) and 5pg of *Renilla reniformis* luciferase mRNA into each blastomere. Embryos were incubated overnight at 14°C and 3 times 8 embryos were harvested at stage NF10-11 in 1.5ml Eppendorf tubes. Most of the media was removed from the tubes which were snap-frozen in liquid nitrogen and stored at -80°C.

To detect luminesce from the luciferase construct I used the Dual-Luciferase® Reporter Assay System (Promega, E1910) kit. Embryos were homogenised in 100µl of 1x Passive Lysis Buffer (PLB) (made from 5x PLB, diluted in water) and the tubes centrifuged for 3 minutes at 4°C at 16,000x g. 20µl of the supernatant was used for luminescence detection, which was added to a well from a 96-well plate with solid white bottom (Perkin Elmer, OpiPlate™-96). Each sample was read in triplicate (3x 20µl in EnVision 2102 MultiLabel Reader (Perkin Elmer) using the EnVsion Manager 1.12 Software. The appropriate protocol was previously set up in the software (shaking, 0.2 seconds reading.). To each 20µl of samples 50µl of Luciferase Assay Reagent II (LARII) (previously prepared by re-suspending lyophilised Luciferase Assay Substract in 10ml of Luciferase Assay Buffer II) was added and the plate was immediately transferred to the EnVision 2102 MultiLabel Reader and the first measurements made. Once finished,

to each well I added 50µl of Stop & Glo® reagent (previously diluted in Stop & Glo® 1x buffer from 50x Stop & Glo® substract) and the plate was again transferred to the plate reader that proceeded to make the second measurement. The first luminescence signal was originated from the firefly luciferase while the second if from the *Renilla* luciferase, which was co-injected and acts as an internal control. The measurement data was exported as a .csv file and analysed on Microsoft® Excel: luminescence from firefly (from the pGl3 constructs injected in *Xenopus* embryos) was normalised to the *Renilla* luminescence measurements.

2.2.17 Chromatin immunoprecipitation

The protocol was carried out as described in (Gentsch et al., 2013; Gentsch and Smith, 2014). I will refer to some alterations to the protocol and to the specific times and amounts used. To create the ChIP-Seq library from Brachyury/RNA polymerase II/p300 immunoprecipitated DNA, approximately 750-3000 *X. tropicalis* UV- and LiCl-treated embryos were harvested at stage NF10.5-11.5. Embryos were cultured in 0.05x MMR and prior to chromatin crosslinked transferred to a glass vial and washed 2 times in 0.01x MMR. Embryos were fixed at room temperature by adding 225µl of 36.5-38.% of formaldehyde (Sigma, F8775) to the glass vial containing 8ml of 0.01x MMR (final concentration of 1% (v/v)) and incubating for 20 minutes. Fixation was stopped by quickly and carefully washing the embryos with ice-cold 0.01X MMR 3-5 times. Batches of 250 embryos were transferred to 2ml Eppendorf tubes, excess media was removed, tubes were snap-frozen in liquid nitrogen and stored at 80°C for future use. Three distinct extraction buffers were used for chromatin extraction: E1 (50 mM HEPES-KOH pH 7.5, 150 mM NaCl, 1 mM EDTA. 10% glycerol, 0.5% Igepal CA-630, 0.25% Triton X-100), E2 (10 mM Tris-HCl pH 8.0, 150 mM NaCl, 1 mM EDTA, 0.5 mM EGTA), and E3 (10 mM Tris-HCl pH 8.0, 150 mM NaCl, 1 mM EDTA, 1% Igepal CA-630, 0.25% Na-Deoxycholate, 0.1% SDS). Prior to extraction, 1mM of DTT and protease inhibitor, in the form of tablets (Roche,11836170001), were added to each buffer. The buffers were used sequentially and 50 to 80 embryos per ml of extraction buffer. The nuclear extraction was either done in 2 ml tubes or in 50 ml Falcon conical centrifuge tubes. The embryos were first homogenised with E1 buffer by pipetting up and down

followed by a 2-5 minutes centrifugation (depending on the volume) at 4°C at 1,000x g. The nuclei were in the pellet together with dark insolubilise pigment granules. The supernatant was aspirated and the homogenisation with E1 repeated, however, before centrifugation, the samples were incubated on ice for 10 minutes. This process was repeated using the buffer E2 (homogenisation, centrifugation, aspiration of supernatant, homogenisation, ice incubation, centrifugation and aspiration of supernatant). The pellet was re-suspended in E3 buffer and incubated on ice for at least 10 minutes, followed by centrifugation and the supernatant discarded. At this point the pellet was smaller as the anionic detergents in E3 removed most of the yolk platelets. After the last step of nuclear extraction the pellet was resuspended in E3 buffer, and when using several tubes for extraction, all the material was pulled together to a final volume of 2.5-3ml. The next step was the solubilisation and fragmentation of cross-linked chromatin by sonication.

The solution containing the cross-linked nuclei was transferred to polystyrene tube previously clipped to fit the sonication probe. During sonication, the conical tube in kept on icy water in a plastic beaker attached via a short thermometer clamp. Sonication was done with a 1.6 mm microtip connected to a Misonix Sonicator 3000 Ultrasonic Liquid Processor. The microtip was inserted into the tube and immersed in the sample to about two-thirds of the volume depth while keeping it centered and away from the tube wall. Sonication consisted of 15-18 cycles of 30 seconds shock waves with power of 1.5-2 until it reached 6-9W with interruptions of 60 seconds to allow the sample to cool down. Upon sonication, the chromatin solution was returned into a 1.5ml Eppandorf tube and centrifuged for 10 minutes at 4°C at maximum speed; this removed the debris. The supernatant contained the solubilised and sheared chromatin and it was transferred to a new 1.5 ml low-retention microcentrifuge tube (Ambion, AM12450).

Before proceeding to chromatin immunoprecipitation, the efficiency of the chromatin shearing was checked by collecting 50µl. While processing this aliquot to check shearing efficiency, the remaining chromatin was kept at 4°C for one day or stored at -80°C for a longer period. To the 50µl of sheared chromatin it was added 1 volume of SDS elution buffer (50 mM Tris-HCl pH 8.0, 1 mM EDTA, 1% SDS), 4µl of 5M NaCl

and 1µl of proteinase K (Ambion, AM3548) that, in combination with an overnight incubation at 65°C results in the de-crosslinking of the chromatin. On the following day, de-crosslinked chromatin was purified using the QIAquick PCR Purification kit (QIagen, 28194) and according to the manufacturer's instructions. The DNA was eluted twice in 11µl of EB buffer, treated with 0.4µl of RNase A (Invitrogen, 12091-039) by incubating a few minutes at room temperature. To check the DNA fragment distribution, the sample was loaded into a 1.4% agarose/TAE gel (containing 1:50,000 RedSafe, Ecogen, 21141) gel and ran by electrophoresis. The ideal distribution should be in the range 0f 100-500 bp with a highest concentration at 200-300 bp. If this distribution was not achieved by the first round of sonication the process would be repeated for 4-8 cycles. If the shearing was successful I proceed to the immunoprecipitation of the sheared chromatin using a ChIP-grade antibody against Brachyury ((Stennard et al., 1999; Gentsch et al., 2013) or this work, see ChIP-grade polyclonal antibody production), p300 (Santa Cruz Biotechnologies, sc585) or RNA polymerase II (BioLegend, MMS-126R).

Before the chromatin IP, an aliquot corresponding to 2-5% of the total volume was kept at 4°C to be used as imput sample. For the IP, approximately 1µg/million cells of T antibody was added to the chromatin and incubated overnight at 4°C on a rotator (10rpm). DynaBeads® M-280 Sheep Anti-Rabbit IgG (Invitrogen, 11203D) were washed with E3 buffer, using a magnetic rack and a rotator, and 30µl/µ of antibody was added to the chromatin. The IP'ed chromatin was incubated with the beads for at least 4 hours at 4°C in a rotator (10rpm). On the following day the beads were extensively washed, 10 times for 5 minutes, with cold RIPA buffer (50 mM HEPES-KOH pH 7.5, 500 mM LiCl, 1 mM EDTA, 1% Igepal CA-630, 0.7% Na-deoxycholate) and once with cold TEN buffer (10 mM Tris-HCl pH 8.0, 1 mM EDTA, 150 mM NaCl). After the washed, the beads were resupsended in 50µl of TEN buffer and transferred to a new 1.5 ml low-retention microcentrifuge tube (Ambion, AM12450). The beads were collected at the bottom of the tube by using the magnetic rack and a short centrifugation at 1,000x g and most of the liquid was discarded. To strip the ChIP material from the beads, 100µl of SDS elution buffer was added and mixed by continously vortexing using a thermomixer at 1,000rpm for 15 minutes at 65°C. The sample was centrifuged

at room temperature, for 5 minutes at maximum speed for 30 sec and the supernatant, containing the ChIP eluate, was transferred to a new tube. The stripping process was repeated to recover a total of 200µl of ChIP eluate.

The next step was to reverse crosslink the ChIP and the input chromatin (stored at 4°C). SDS elution buffer was added to the input chromatin sample to a reach a total volume of 200µl, same as the ChIP. To both the ChIP and input samples was added 10µl of 5M NaCl (1/20 of the volume) and the samples were incubated overnight at 65°C. On the following day, the samples were diluted with 200µl of TE (1 volume) and treated with RNAse A at 200µl/ml and incubated at 37°C for 1 hour. This was followed by a treatment with proteinase K (200µl/ml) for 2 to 4 hours at 55 °C. The DNA was purified by phenol:chloroform:wasoamyl alcohol extraction followed by ethanol precipitation. The DNA was transferred to a 1.5 ml Phase-lock gel heavy tube (5 Prime) (prespun at 12,000x g for 30 seconds) and mixed with 1 volume of phenol:chloroform:wasoamyl alcohol (24:24:1, pH7.9). The tubes were centrifuged at full speed for 5 minutes at room temperature and the upper aqueous phase was transferred to a new microcentrifuge tube. To this, 1/25 of the volume of 5M NACl, 2 volumes of 100% ethanol and 1µg of GlycoBlue™ (Thermo Scientific, AM9516) were added. The samples were mixed by inverting the tube a few times and incubated at -20°C for, at least, 16 hours. Samples were centrifuged at full speed for 1 hour at 4°C. The supernatant was discarded without disrupting the blue DNA pellet which was washed with 500µl of 80% EtOH followed by a 3 minute full-speed spin at 4°C. The supernatant was carefully removed and air-dried for 5-10 minutes at room temperature. Finally, 32µl of H_2O was added to the pellet and samples were left in ice for at least 2 hours to allow the pellet to completely dissolve. The concentration of the co-immunoprecipitated DNA was measured with Qubit™dsDNA HS Assay.

2.2.18 Preparation of Solid Phase Reverse Immobilisation (SPRI) beads

Throughout this project SPRI beads were used to clean DNA, specifically to select certain fragment ranges, e.g. in preparation of DNA libraries for highthroughput sequencing these were used to remove smaller fragments, usually to remove adapter dimers, or

longer fragments that impair cluster formation prior to sequencing. For some experiments, I have used the Agencourt® AMPure® XP (Beckman Coulter, A63880) but for others I have used 'homemade' SPRI beads and here I will refer to its preparation and validation.

TE buffer was prepared in a 50 ml Falcon conical centrifuge tube by adding 500µl of 1M Tris pH8.0, 100µl of 0.5M EDTA and filling up with distilled water to the 50ml mark. The Sera-Mag SpeedBeads™ Carboxylate-Modified Magnetuc Particles (GE Healthcare Life sciences, 65152105050250) were mixed and 1ml was transferred to a 1.5ml Eppendorf tube. The tube containing the beads was placed in a magnetic rack (ABI Applied Biosystems DYNAL MPC-S) and supernatant was removed using a pipette. The beads were washed twice with 1ml of TE and re-suspended in 1ml of TE. To a new 50 ml Falcon conical tube it was added: 9g of Polythylene glycol (PEG) 8000 (Amresco, 0777), 10ml of 5M NaCl, 500µl of 1M of Tris-HCl, 100µl of 0.5M EDTA and distilled water(dH_2O) to around 49ml. The tube was placed in a tube roller for 5 minutes to allow the PEG to go into solution, until tube was clear. To this solution it was added 27.5µl of Tween-20 and mixed gently. The Sera-Mag beads re-suspended in TE were transferred (1ml) to the tube containing PEG and the tube was filled with dH_2O to a final volume of 50ml.

The beads were tested against the AMPure XP beads® using aliquots of GeneRuler 50bp DNA ladder (Thermo Fisher Scientific, SM0371). The DNA ladder was diluted by adding 2µl to 18µl of dH_2O and different volumes of SPRI 'homemade' beads were added depending on the fragment range to include or exclude, e.g. a ratio of 0.9x (20µl of DNA to 18µl of beads), should remove most fragments shorter than 300bp and a 1.2x ratio (20µl of DNA to 24µl of beads) removes fragments shorter 200bp. Beads were incubated with the DNA in a well of a 96-well microplate with V-bottom (Greiner Bio-One International, 651101) for 5 minutes at room temperature. The plate was placed on a magnetic stand-96 (Ambion, AM10027) for a few seconds to allow the beads to separate from the supernatant which was removed and the beads washed twice with 500µl of 70% EtOH. Following the last wash, the supernatant was removed and the beads air-dried for 5 minutes at room temperature and re-suspended in 20µl of dH_2O by mixing up and down. The plate was returned to the magnetic stand

and the supernatant was transferred to a new 1.5ml Eppendorf tube. The DNA was mixed with 5x loading buffer (0.01g Orange G Dye (Sigma, O3756), 3ml 50% Glycerol, 0.6ml of 0.5M EDTA pH8.0 and 1.2ml of H_2O) and loaded in a 1.5% agarose/TAE gel (containing 1:50,000 RedSafe) and the fragments separated by electrophoresis.

2.2.19 Preparation of Paired-End indexed library for Illumina sequencing - RNA-Seq

This protocol refers to the library RNA-Seq libraries in Chapter 3.

Poly(A)$^+$ RNA-Seq libraries, for sequencing, were made from 2µg of total RNA (see section **Extraction and purification of total RNA from *Xenopus*** embryos) using the version 2 of the TruSeq RNA low sample kit (Illumina, RS-122-2001) following the manufacturer's instructions. In summary, the RNA was first purified using oligo-dT attached to magnetic beads and fragmented by enzymatic reaction. This step was followed by the first stand cDNA synthesis and the second strand cDNA synthesis after which the DNA was washed with AMPure® XP beads. The following step was to perform end repair which converts the overhangs into blunt ends and subsequently the 3' ends were adenylated (addition of an 'A' nucleotide to prevent fragments to bind each other and, in addition, adaptors contain a 'T' on the 3' end for adapter-fragment ligation). The next step was the ligation of indexed adapters to the end of the double strand DNA which will be used for hybridisation to the flow cell. The final step was an amplification, of 15 cycles, to enrich the DNA fragments followed by purification with AMPure XP beads®. The final cDNA library was quantified using the Qubit fluorometer and Qubit dsDNA high sensitivity reagents (Thermo Fisher Scientific, Q3285) and fragment distribution checked on the Agilent 2100 Bioanalyzer. Libraries were sequenced on an Illumina HiSeq 4000 to produce paired end reads of 50 bases

2.2.20 Preparation of Paired-End indexed library for Illumina sequencing - ChIP-Seq

A library was generated from 2-15ng of each ChIP and input using the KAPA Hyper Prep kit (KAPA Biosystems, KK8502) for Illumina® platforms. Some modifications

were done to the protocol. The amount of adaptors used and the number of amplification steps varied based on the starting amount of ChIP (see Table ,below). For adapter ligation, the TruSeq DNA adapters (15µM) were diluted to the appropriate concentration and used for the reaction.

Starting DNA	**TruSeq DNA adaptors**	**PCR cycles**
1ng	300nM	5+8
5ng	1.5µM	5+7
15ng	4.5µM	5+6

Table 2.4: Conditions for paired-ended ChIP-Seq library preparation.

To the protocol a pre-amplification step (5 cycles of amplification of denature for 15" at 98°C, annealing at 60°C for 30" and elongation 30" for 72°C) using Illumina primers was added after adapter ligation was added. This step was used to convert the Y-shaped Illumina adapters to dsDNA. This allowed for a proper size-selection of fragments of the desired length (when running the samples on agarose gel) and also reduces adapter dimer contamination (Ford et al., 2014). After the pre-amplification, the DNA fragments were cleaned using the SPRI beads (Agencourt® AMPure® XP beads, or 'homemade' SPRI beads (see above)).

The DNA clean-up using SPRI beads was also altered from the protocol from KAPA Hyper Prep kit. The appropriate amount of SPRI beads (the protocol includes 0.8x and 1.0x bead cleaning steps) were added to each V-bottom well from a 96-well plate (Greiner Bio-One International, 651101) containing the DNA sample and mixed by pipetting up and down. The mixture was incubated at room temperature for 2 minutes. The plate was transferred to a magnetic stand (Ambion, AM10027) and incubated for 3 minutes or until the beads were completely separated from the supernatant. The supernatant was removed by pipetting with a fine tip and the beads washed twice with 80% EtOH. Finally, the supernatant was removed and the plate sealed with an adhesive PCR film (4titude, 4ti-0500) and centrifuged for 1 minutes at 200x *g*. The plate was returned to the magnetic stand, the film removed, the remaining supernatant was removed and the beads allowed to dry at room temperature for 5 minutes or until pellets showed cracks. The dried beads, were eluted in 20µl of Elution buffer (EB) (10mM Tris-HCl, pH8.5) by removing the plate from the magnetic stand and pipetting

the beads up and down several times. The beads were incubated at room temperature for 2 minutes, re-suspended again and the plate placed in the magnetic stand. When the beads were completely separated, the supernatant containing the DNA was transferred to a new tube to be used in the next step of the protocol.

Size-selection of the library fragments was done using an electrophoresis-based method, using the E-gel® iBase™ Power System dock with the E-gel® EX agarose gel, 2% and selected bands from 250-450bp. I proceeded to do DNA purification using the MinElute Gel Extraction Kit Protocol (Qiagen) following the manufacturer's instructions. The recovery DNA was amplified for the appropriate number of cycles in a thermocycler followed by a post-amplification cleanup, as described in KAPA Hyper Prep kit guide. The concentration of the library was assessed with Qubit™dsDNA HS Assay (Thermo Fisher Scientific, Q32851) (ranged from 4µg/ml to 48µg/ml) and the integrity of the library was checked on the Agilent 2100 Bioanalyzer. Libraries were read single-end along 50-100 bases on the HiSeq 2000 machine (Illumina®).

2.2.21 Bioinformatic analysis

Sequenced libraries were provided by the Advance Sequencing Facility (The National Institute for Medical Research (NIMR) and the The Francis Institute, core facilities) in fastq file format and were analysed for sequencing quality control using the software FastQC. The software provides information on the number of sequenced reads, the read quality score and the percentage of duplication. This information is essential to evaluate the quality of the sequenced library and decide whether to proceed or not with the analysis.

RNA-Seq

The sequenced reads were aligned to the *Xenopus tropicalis* transcriptome assembly JGI7.1 using Tophat2 (Kim et al., 2013) with the following parameters: `-p 12 --transcriptome-index= xenTro7 --no-novel-juncs --no-coverage-search`. The transcriptome index was previously generated using version 2 of gene models of assembly JGI7.1 using the following command: `tophat2 -G JGI7.1_genes7.2_updated.gtf --transcriptome-index=xenTro7 indexes/xentrov7`. The average alignment percentage was around 80%. The resulting

aligned reads were in sequence alignment/map (SAM) format which where converted to binary alignment/map (BAM) and sorted by reads name using SAMtools (Li et al., 2009). The library was paired-end sequenced to obtain the correct fragment size, which meant reads were mapped in pairs and, after sorting the BAM file, unpaired reads were removed. The goal of the RNA-Seq experiment was to identify differentially expressed genes between the different conditions which implicated quantification of transcripts. To this end, I used HTSeq (Anders, Pyl, and Huber, 2015), a tool to count reads in features, in this case in genes using the following command : `htseq-count -s no -m intersection-nonempty -t gene -i Name -f bam .bam genes.gff3`. The result was a text file with raw counts for each gene in each condition. The file was used to identify differentially expressed genes using the R package (R Core Team, 2013; Maechler et al., 2013) DESeq2 which performs a test based on a negative binomial distribution resulting a data frame with adjusted p values (Benjamin-Hochberg correction) or false discovery rate (FDR) and $\log_2$ fold changes for each genes. From here I selected genes based a adjusted p-value smaller or equal to 0.01 (1% change of a false positive) and a fold change equal or bigger than 2. The PCA plot was produced using DESeq2, the MA-plot was designed using the R package 'ggpubr' and the produce the other graphs I used Ipython (Fernando Pérez, 2007), using the libraries 'pandas' ("pandas: a Foundational Python Library for Data Analysis and Statistics") and 'seaborn' (Waskom et al., 2014); Microsoft® Excel for Mac OS X and GraphPad Prism 7 for Mac OS X.

ChIP-Seq

ChIP-Seq single-end sequenced libraries were aligned to *Xenopus tropicalis* genome assembly JGI7.1 using Bowtie with the following parameters: `--best -m 1 -p 12 --chunkmbs 512`. The resulting SAM file was converted to BAM file, sorted and duplicated were marked using 'MarkDuplicates' from Picard Tools (http://broadinstitute.github.io/picard). To identify regions of high probability of chromatin binding, peaks I used MACS2 (Feng et al., 2012) with the following command: `macs2 callpeak -t <sorted.bam> -c <inputs_sorted.bam> -n <> -g 1.16e+09 -B --SPMR -q5e-4`. The peak files, table of genomic intervals were in the BED format are were manipulated and compared using Linux commands ('grep', 'awk') and BEDTools (Quinlan and Hall, 2010). For example, peaks

summits were filtered based on fold enrichment and extended 150bp on each direction with this command: `awk 'print $1"\t"$2+$10"\t"$2+$10+1"\t"$7' .narrowPeak | awk 'if ($4 >= 5) print' | bedtools slop -i - -g genome.txt -b 150 > 5fe_300bp.bed`. Peaksets were compared using the tool 'intersect' from BEDtools (`bedtools intersect -wa -wb -a <.bed> -b <.bed> (-v)`) and annotated with the nearest using using Homer (Heinz et al., 2010) (`annotatePeaks.pl xenTro7 -gtf <.gtf> <.bed> > <annotated.txt>`.

Heatmaps were created using deepTools (Ramírez et al., 2016); correlation heatmap: `multiBamSummary BED-file --BED <.bed> --bamfiles <sorted.bam> <> -out <results.npz> --ignoreDuplicates -p max` and `plotCorrelation -in <results.npz> --whatToPlot heatmap -o <correlation.pdf> --skipZeros --plotNumbers --corMethod pearson`. The reads coverage heatmaps were produced with the following commands: `bamCoverage -b <sorted.bam> <> -o <.bw> --normalizeTo1x 1160000000 --ignoreDuplicates`, `computeMatrix reference-point -S <.bw> <> -R <.bed> -a 2000 -b 2000 -out <matrix.ma.gz> --skipZeros -p max` and `plotHeatmap -m <matrix.ma.gz> -out <heatmap.pdf> --colorMap YlGnBu --heatmapHeight 25 --missingDataColor '#FEFED7'`.

Representations of genomic regions as a dense plot of the ChIP-Seq reads were designed using fluff (Georgiou and Heeringen, 2016): `fluff profile -i <genomic interval> -d <.bam> <> -o <profile.pdf> -n -S <#> -c <hex code>`.

The RNA polymerase II ChIP-Seq was not processed for peak calling, instead, reads mapped to gene bodies were counted with Homer `annotatePeaks.pl genebody.gtf xenTro7 -size given -norm 1e7 -normLength 175 -hist 11 -ghist -noann -nogene -fragLength 175 -cpu 8 -d TagDirectories`. 'TagDirectories' are directories that summarise SAM files and used instead of these by the software Homer; such directories are created with the command: `makeTagDirectory TagDir/ .sam -unique -single`. Identification of differentially active genes following the requisites defined in Chapter 3, was done using R code provided by George Gentsch.

Identification of differentially bound sites by comparing the Brachyury ChIP-Seq of the different conditions was done using the R package 'DiffBind' (Ross-Innes et al., 2012). For such anlaysis, the input was a table containing the names and paths to the each of the replicates mapped read files (sorted BAM files with marked duplicates) and to the peak files containing peaks called in all conditions. 'DiffBind' first counts and

normalised the reads (total mapped reads) and then uses DESeq2 algorithm to identify differentially bound sizes, as explained above. The output was a table with adjusted p-values and fold changes for each peak, which was filtered to select only peaks with a FDR equal or less than 0.05 (5% change of a false positive). The PCA plot on Figure 4.13A was designed using DiffBind.

De novo motif discovery and motif enrichment in peaks was done using Homer with the commands: (`findMotifsGenome.pl <.bed> xenTro7 <outputfile> -size 400 -len 8/12`) and `annotatePeaks.pl <.bed> xenTro7 -m <.motif> <> -size 600 -noann -nogene`, respectively.

Image design was processing was done using Ipython ('seaborn'), Microsoft® Excel for Mac OS X, GraphPad Prism 7 for Mac OS X, Adobe Photoshop CC and Adobe Illustrator CC.

Chapter 3

Transcriptome comparison of dorsalised and ventralised *Xenopus tropicalis* embryos

In Chapter 1, I refered to the process of the dorso-ventral (DV) axis determination, the first break in symmetry of the amphibian egg. DV determination occurs as early as fertilisation; the sperm entry point (SEP) acts as a reference to the prospective dorsal side of the embryo. This process is accompained by the formation of the grey crescent.

Historically, the grey crescent was first described as the initial break in the symmetry of the amphibian egg and was later associated with the DV axis determination. During the decades of the 1970s and 1980s many researchers were interested in understanding how the grey crescent was formed. There were two theories: the contraction and the rotation hypothesis. The first stated that upon fertilisation the egg cortex would contract radially towards the SEP (Rzehak, 1972; Palecek, Ubbels, and Rzehak, 1978; Ubbels et al., 1983) leading to the formation of the grey crescent on the opposite side. The rotation hypothesis, developed from observations in *Rana pipiens*, stated that the cortical layer of the egg shifted 30° relative to the cytoplasmic core in a direction related to the SEP (Elinson, 1975; Elinson and Manes, 1978; Elinson, 1980). The latter theory is the one accepted today and much owed to the 1986's experiments from Vincent *et al.*. In that work, the authors used *Xenopus laevis* eggs in which they injected two distinct fluorescent dyes, one in the subcortical cytoplasm and another in the egg surface. They observed two movements of the subcortical cytoplasm: an initial convergence of the animal subcortical hemisphere towards the entry point and a second overall rotation of the subcortical cytoplasm that superimposes to the first.

They confirmed that it was the 30° rotation or displacement of the cortical cytoplasm that marks the prospective dorsal midline of the embryo (Vincent, Oster, and Gerhart, 1986). Two years later, in 1988, Elinson and Rowning observed for the first time in eggs undergoing cortical rotation an array of parallel microtubules forming in the vegetal hemisphere. These microtubules were parallel to the direction of the rotation and disappeared at the end of cortex displacement. The authors suggested that the microtubules would serve as tracks for the cytoplasmic rotation that ultimately would be involved in the DV determination (Elinson and Rowning, 1988). Furthermore, the authors showed that UV irradiation of the vegetal pole of the eggs, shortly after fertilisation, lead to the disruption of the microtubule array which in turn resulted in an embryo without dorsal structures.

The role of UV irradiation in early development had been tested and described many years before. In 1972 it had been shown in *Rana pipens* that UV treatment affected neural induction (Grant and Wacaster, 1972), in 1980 Scharf and Gerhart described that embryos treated with UV irradiation developed without any dorsal structures (Scharf and Gerhart, 1980) and Manes and Elinson showed that UV disrupted cortical rotation and the formation of the grey crescent (Manes and Elinson, 1980; Vincent and Gerhart, 1987). It was only in 1988, the work described above, that the authors made the connection between the disruption of microtubule and consequently the absence of a dorsal structures in these embryos. We now know, as described in Chapter 1, that the microtubules are essential for dorsal determination, they transport Wnt/β-catenin components to the prospective dorsal side resulting in an asymmetrical nuclear enrichment of β-catenin that triggers the formation of the dorsal centre.

For many years, researchers have tested the effects of drugs or other perturbations, such as UV irradiation, during early development in order to better understand the process. An example is the treatment of amphibian eggs and embryos with lithium, specifically lithium chloride (LiCl). During the decades of 1940s and 1950s researchers have described different effects of LiCl treatment in amphibian embryos treated with different doses and at different developmental stages (Pasteels, 1945; Hall, 1942; Backstrom, 1954). By the late 1980s Kao *et al.* showed that by exposing 32-cell^{+} *Xenopus leavis* embryos to 0.3M LiCl for 6 minutes, these embryos would develop exaggerated

dorso-anterior structures, like the head and cement gland (Kao, Masui, and Elinson, 1986). The authors described this phenotype to be similar to the one obtained by exposing the embryos to deuterium oxide (D_2O), a drug that when used prior to cortical rotation caused the development of hyper-dorsalised embryos (Scharf et al., 1989). Furthermore, the authors used UV irradiation, a known ventralising treatment, to efficiently rescue the embryos treated with LiCl (Kao, Masui, and Elinson, 1986). In the same work, LiCl was introduced as an efficient drug to dorsalise embryos and as a tool to study DV patterning. Two years later, Kao and Elinson further described the 'LiCl phenotype' as an over commitment of cells to a dorsal and anterior fate as the whole marginal zone becomes dorsalised (Kao and Elinson, 1988). Furthermore, the authors introduce a scale of dorsalisation development, the dorsoanterior index (DAI) (Figure 3.1). This index was constructed by adding the phenotypes of LiCl-treated embryos to the index of axis deficiency (IAD) that described phenotypes of ventralised embryos. The IAD in turn was adapted from the 'UV syndrome' (Malacinski, Allis, and Chung, 1974) or 'Dorsal reduction' (Scharf and Gerhart, 1980) in which 0 described a normal embryo and 5 described an 'aneural' embryo, without neural or dorsal tissue. The IAD had a similar scale where 0 was normal and 5 was an embryo without somites or any tail mesenchyme. Finally, the DAI introduced in 1988, inverted the scale and 5 represented a normal embryo, absence of dorsal structures was classified with a DAI of 0 (5-0 would be a gradual loss of dorsal structures) and DAI of 10 represented the hyperdorsalised embryo (DAI 6-10 are increasingly LiCl treatment effects) (Figure 3.1).

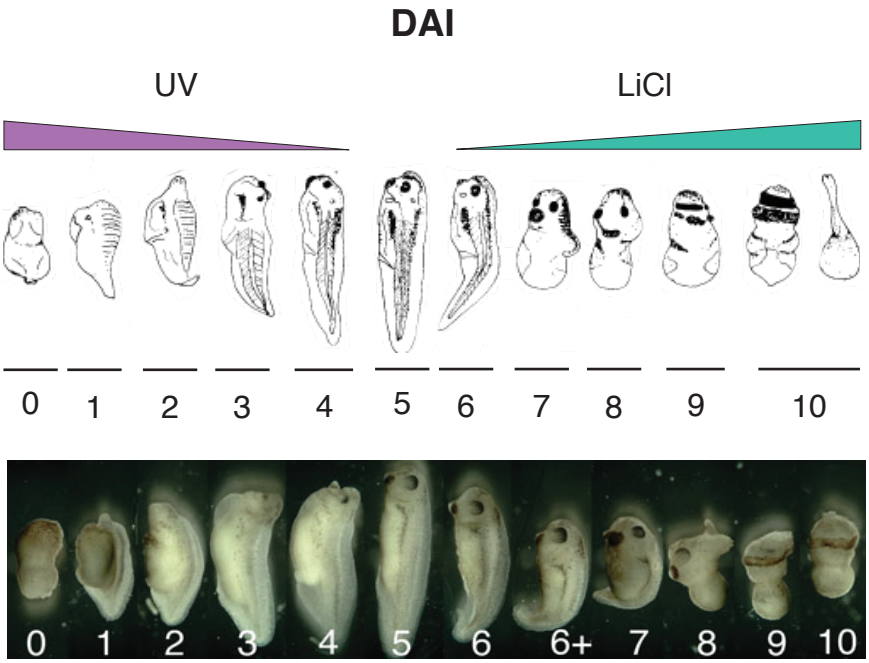

Figure 3.1: **Tailbud *Xenopus laevis* embryos drawing and pictures representing the different degrees of the dorsaoanterior index (DAI)**

Drawings and pictures of *Xenopus laevis* embryos, either irradiated with UV for an increasing time (DAI 0-4) or an increasing concentration of LiCl (DAI 6-10). DAI of 5 is an untreated embryo that represents the wild-type phenotype. Increasing the exposure time to UV leads to embryos with increasingly less dorso-anterior structures, to the extreme phenotype representing a 'belly'-like structure (DAI of 0). Increasing the concentration of LiCl leads to embryos with increasingly exaggerated dorso-anterior structures, like the eyes and the cement gland. At the highest dorsalisation phenotype the embryo resembles a cylinder of radially formed dorso-anterior structures or the formation of a *proboscis*-like structure of chordo-mesoderm (DAI of 10). Figure adapted from (Danilchik, 2011) and (Kao and Elinson, 1988).

While the effect of UV was understood in the 1980s, it was only in 1996 that LiCl was described to act specifically as a GSK-3β inhibitor (Klein and Melton, 1996; Stambolic, Ruel, and Woodgett, 1996). This inhibition explains the dorsalisation phenotype, since that at 32-cell stage, GSK-3β is highly enriched on the ventral side of the embryo, maintaining β-catenin only on the dorsal side. Inhibition of GSK-3β, leads to the ventral expansion of active (nuclear) β-catenin inducing these cells to become dorsal.

Since the end of the 1980s these two treatments, LiCl and UV have been used by scientists as tools to study the determination of the dorso-ventral axis. In the late 1980s the laboratory of Jonathan Cooke focused on analysing and describing the phenotypic effects of these treatments during development, specifically the effect on mesoderm. They showed that UV treatments has no effect on the midblastula transition, embryos

have no developmental retardation, and have the same number of cells as untreated embryos. In UV-treated embryos the mesoderm developed radially symmetrically and as a tubular monolayer of the trunk lateral plate type. Moreover they showed that embryos formed no prechordal mesoderm, formed 25% less of somite muscle and its blood forming capacity was enhanced (Cooke and Smith, 1987). On the other hand, LiCl-treated embryos, although also radially symmetric, develop a massive notochord (prechordal mesoderm), smaller somites and blood tissue. Overall, these embryos gastrulate normally but only dorsal mesoderm ingresses, the kind that would in a normal embryo only ingress through the blastopore (Cooke and Smith, 1988). Given the dorsalising effect of lithium, and since mesoderm is first induced dorsally, researchers were interested in testing the effect of LiCl in inducing this germ layer. While LiCl was not capable of inducing mesoderm by itself, it enhanced the response to the mesoderm-inducing factor, Activin (Cooke, Symes, and Smith, 1989; Kinoshita and Asashima, 1995; Smith, 1987).

These treatments have been widely described and scientists have confidently used them as tools to generate dorsalised and ventralised embryos for decades. Given the new 'omics' tools that allow us to study the whole proteome, transcriptome or epigenome, we can now better understand the effects of these treatments. In this project, I set out to analyse and compare the whole poly(A) transcriptome of LiCl- and UV-treated embryos. The goal was to create a dataset of genes differentially expressed in each condition that would allow to better understand the effect of the treatments. In addition, by comparing to dissected dorsal and ventral sections of a developing embryo I was able to assess the similarity of a whole dorsalised/ventralised embryo to its 'real' cell type in the untreated embryo. And finally, identify and characterise genes which have not been described before. Throughout the duration of this project, some publications have referred to the analyses of the whole poly-(A) transcriptome of LiCl-treated *Xenopus laevis* embryos (Ding et al., 2016; Ding et al., 2017). My work differentiates from these as I described the treatments in *Xenopus tropicalis* for the first time, focusing the comparison on LiCl- and UV-treated embryos and the genes differentially expressed between each condition.

3.1 UV and LiCl treatments efficiently ventralise and dorsalise *Xenopus tropicalis* embryos

3.1.1 Phenotypic analysis

Although LiCl and UV manipulations have been well described and widely used for many years in *Xenopus laevis*, I could not find an example applied to *Xenopus tropicalis* in the literature. Given this, I first tested the conditions that led to the most extreme phenotypes (DAI of 0 for UV and of 10 for LiCl) in the highest number of embryos. Figure 3.2 shows a scheme representing the treatments and conditions that led to these results: LiCl; 32-64-cell embryos submerged in 0.3M LiCl/MMR for 5 minutes followed by three washes in 0.05x MMR; UV, 20-40min post fertilisation embryos were irradiated with a UV short wave (254nm) at a distance of 2 cm from the source for 2'-2'10"; WT, untreated embryos (siblings) used as a control for staging and transcriptome analysis (Fig. 3.2). For more details see Chapter 2.

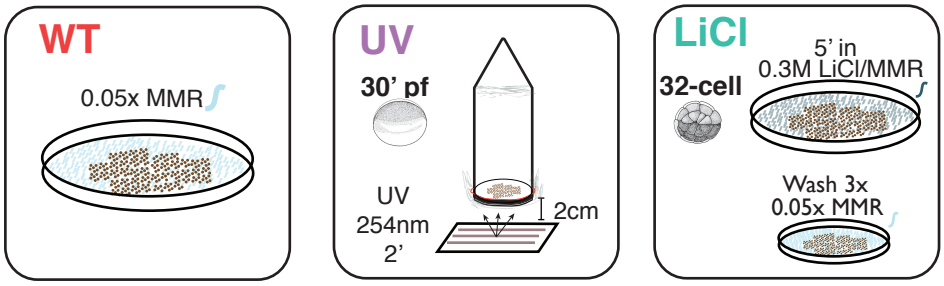

Figure 3.2: **Diagram showing procedures to generate dorsalised (LiCl) and vetralised (UV) embryos and the control (WT)**

The three conditions studied in this work. Wild-type embryos were untreated *Xenopus tropicalis* embryos cultured in 0.05X MMR until harvested at stage Nieuwkoop and Faber (NF) stage 11.5. UV-treated embryos were placed in a 50 ml falcon conical tube closed with saran wrap and inverted, allowing the embryos to be placed in the centre of the tube opening. Embryos were placed at 2 cm from the UV source and irradiated for 2 minutes with a short-wave (254nm), within the first 30 minutes after fertilisation. To dorsalise, 32-cell stage embryos were exposed to 0.3M LiCl for 5 minutes and then gently washed in 0.05x MMR. Please refer to Methods (Chapter 2) for more details on the treatments and embryo handling.' - minutes

Both UV and LiCl treatments resulted in previously described abnormal formations of the blastopore lip; in UV-treated embryos the appearance of the blastopore lip was delayed, and it formed circumferentially rather than on the dorsal side while in LiCl treatment caused blastopore lip formation to be initiated on time but circumferentially

(Fig. 3.3). Given the differences in developmental speed between embryos, the formation of the blastopore lip could not be used to assess the efficiency of the treatments. Hence, embryos were kept until tailbud stages and scored for its DAI at this stage (Fig. 3.3). Only treatments that resulted in embryos with an average DAI score of 0.5-0.8, in the case of UV; and 9.4-10 in the case of LiCl were considered for further analyses. UV irradiation was less penetrant than LiCl treatment given the lack of absolute control of the irradiated area.

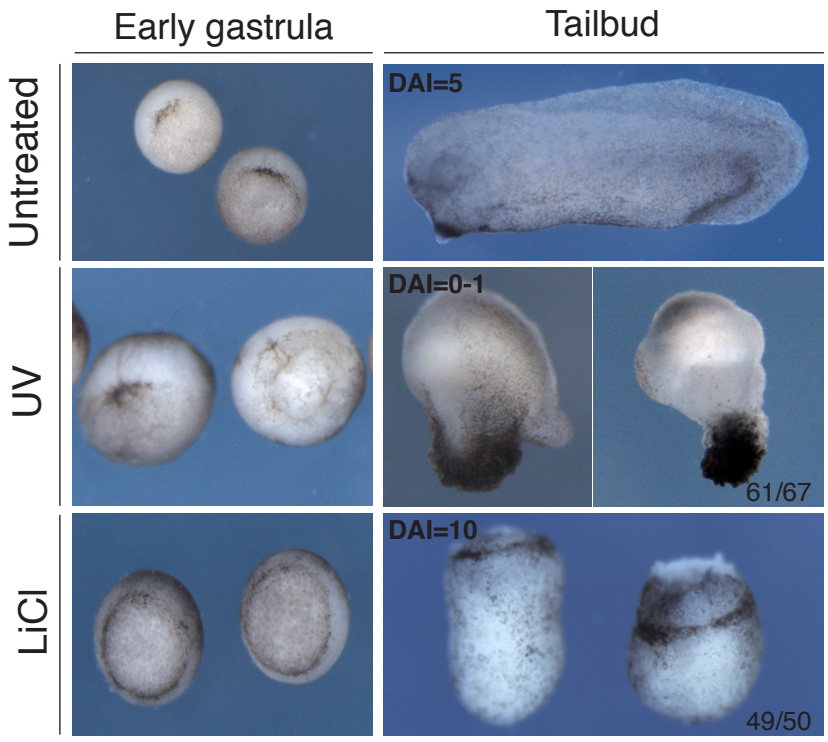

Figure 3.3: **LiCl and UV treatments efficiently dorsalised and ventralised *Xenopus tropicalis* embryos**

Control/untreated embryos (WT) at early gastrula (Nieuwkoop and Faber (NF) stage 10.5) and tailbud stages (NF26). UV-treated embryos show little phenotypic differences at early gastrula stage, comparing to WT embryos. Tailbud UV-treated embryos show a clear ventralisation with complete loss of dorso-anterior structures, representing an embryo with DAI=0. Dorsalisation is visible in LiCl-treated early gastrula embryos, as the blastopore lip forms synchronously around the embryo. By stage 26 the shows a clear dorsalised phenotype, DAI of 10, with exaggeration of anterior structures like a circular cement gland. Number in picture: number of embryos with respective phenotype/total number of treated embryos.

3.1.2 Expression of known ventral and dorsal markers

The next step was to verify if the LiCl- and UV-treated embryos, which by stage 11 were phenotypically similar, had changed its cell fate and become enriched for dorsal and ventral cells, respectively. I analysed the expression pattern by whole mount *in situ* hybridisation (WMISH) and transcript level by q-RT-PCR (quantitative real-time PCR, qPCR) of known ventral and dorsal gene markers (Fig. 3.4A). The expression pattern of *goosecoid* and *noggin* by gastrula stage, as seen in WT (Fig. 3.4), was very similar and marked the dorsal area of the embryo, the Spemann organizer (SO) which will give rise to the dorsal- and anterior-most tissues of the embryo. The LiCl treatment efficiently dorsalised the embryo, as seen by the expansion of these markers to the ventral side and around the blastopore (Fig. 3.4A), suggesting a change in fate of these cells. Although with less penetrance, for reasons explained above, the UV treatment had the opposite effect, as it led to the loss (or reduction) of the expression domain of dorsal markers. These results were further verified by quantitative comparison of transcripts by qPCR between treated and untreated embryos (Fig. 3.4C). The graph shows, by absolute quantification, that *noggin* and *gsc* were more expressed in LiCl-treated and less in UV-treated embryos compared to WT (Fig. 3.4C). Since treated and untreated embryos had the same number of cells, the qPCR analysis indicated that more cells are expressing dorsal markers in LiCl-treated embryos.

The ventral markers *bmp4* and *wnt8a* were expressed in the same cells of the gastrula in a broader area of the embryo, compared to the dorsal cells on the opposite side (Fig. 3.4A). Dorsalised embryos had reduced or lost expression of these markers in accordance with the expansion of Wnt and BMP antagonists such as *noggin*. Although not very clear by WMISH, the expression pattern, of both ventral marker expanded dorsally in UV-treated embryos (Fig. 3.4A). Similarly, the quantitative analysis of the transcripts indicated a significant increase in UV-treated compared to WT and decrease in dorsalised embryos (Fig. 3.4C). Another ventral marker *sizzled* (*szl*) also showed a significant increase in expression levels in UV-treated embryos (Fig. 3.4C). In addition to ventral and dorsal marker genes I analysed the expression of markers of posterior and axial/dorsal mesoderm. The notochord is the dorsal-most mesodermal structure of the embryo and it has been described to be 'overdeveloped' in dorsalised embryos. In

dorsalised gastrula embryos the expression pattern of notochord marker *not* expanded ventrally (Fig. 3.4B) and the transcript levels were significantly higher when compared to untreated embryos (Fig. 3.4C). The caudal homeobox gene *xcad3* was expressed ventrally in cells that will form posterior mesoderm and, upon UV-treatment its expression pattern expanded dorsally (Fig. 3.4B) and overall transcript levels increased (Fig. 3.4C). The levels of posterior mesoderm markers, *msgn1*, *mespA* and *tbx6* were down in dorsalised embryos compare to untreated (Fig. 3.4C).

Together, these results indicated that the treatments were effectively altering the cell fate during development; LiCl-treatment resulted in embryos enriched for dorsal cells while UV irradiation led to embryos enriched for ventral cells.

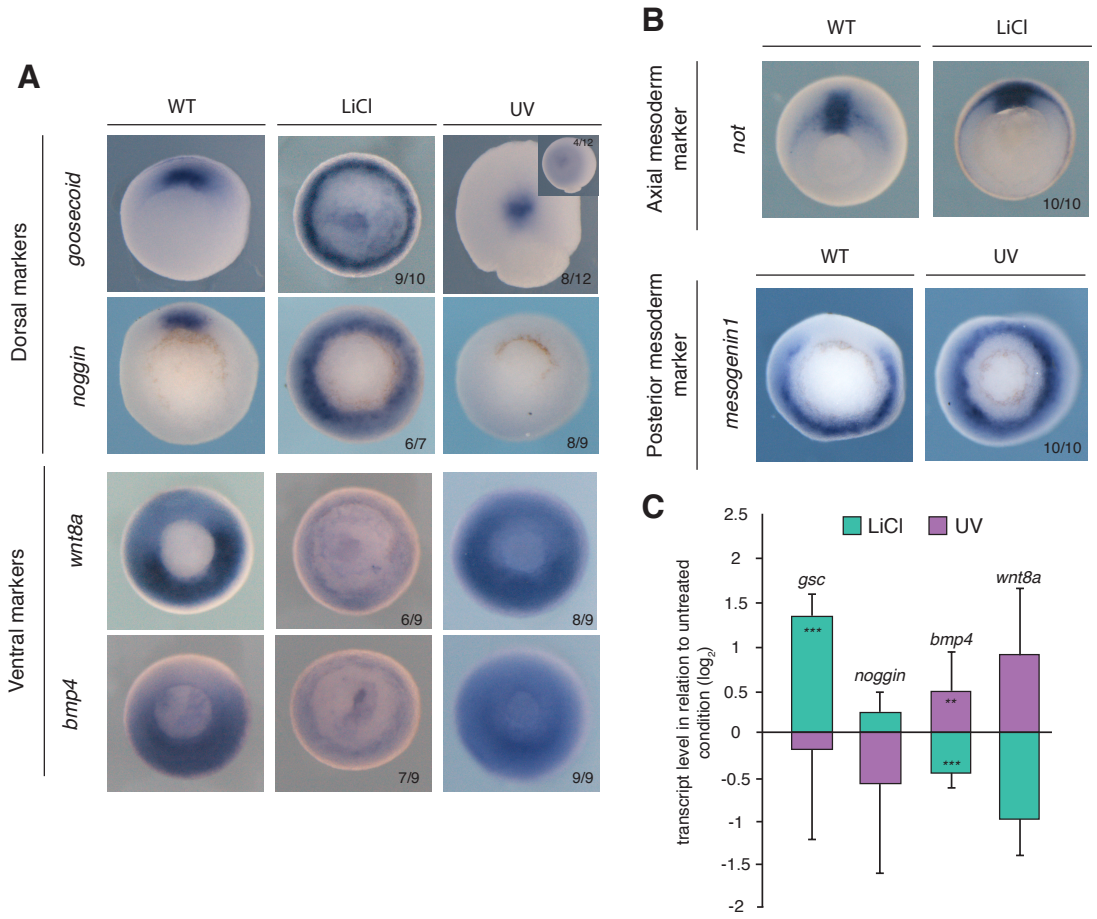

Figure 3.4: **Expression of ventral and dorsal markers quantified by qPCR and analysed by WMISH**

A) Expression pattern of the dorsal markers, *noggin* and *goosecoid* and the ventral markers *wnt8a* and *bmp4* in untreated (WT), LiCl- and UV-treated gastrula stage (NF11.5) embryos. The expression domain of dorsal markers expanded ventrally in LiCl-treated embryos and was lost or reduced in UV-treated embryos. The expression domain of ventral markers expanded dorsally in UV-treated embryos and the expression was loss in LiCl-treated embryos. **B)** Expression pattern of the axial mesoderm marker *not* in WT and LiCl-treated embryos and the posterior mesoderm marker *mesogenin 1* in WT and UV-treated embryos. The expression of *not* expanded ventrally in LiCl-treated embryos and the expression of *mesogenin 1* expanded dorsally in UV-treated embryos, while it was only ventral in WT embryos. **C)**Transcript fold changes (log2 scale) of dorsal (gsc and noggin) and ventral (bmp4 and wnt8a) markers following LiCl or UV treatment as measured by RT-qPCR in mid-gastrula embryos (n=3). Student's two-tailed t test: *, p-value ¡0.1; **, p-value ¡0.05; ***, p-value ¡0.01. Error bars represent the standard error of the mean (s.e.m.) of biological triplicates. Student's-two-tailed t test: ** p-value<0.05; ***p-value<0.01. Error bars represent the standard error of the mean (s.e.m) of biological triplicates.

3.2 Whole poly(A) comparison

To further characterise these embryos and have a better understanding of the transcriptomic changes occurring in both treatments, I studied the whole poly(A) transcriptome of gastrula stage (NF11-11.5) treated and untreated embryos. For this purpose, I col-

lected 5 biological replicates of five to ten treated embryos for each condition, extracted total RNA and prepared poly(A) libraries of the coding transcriptome (Fig. 3.5) followed by paired-end sequencing. The resulting reads were aligned to the transcriptome of the *Xenopus tropicalis* (assembly 7.1) and all further analysis is described in Methods and Materials.

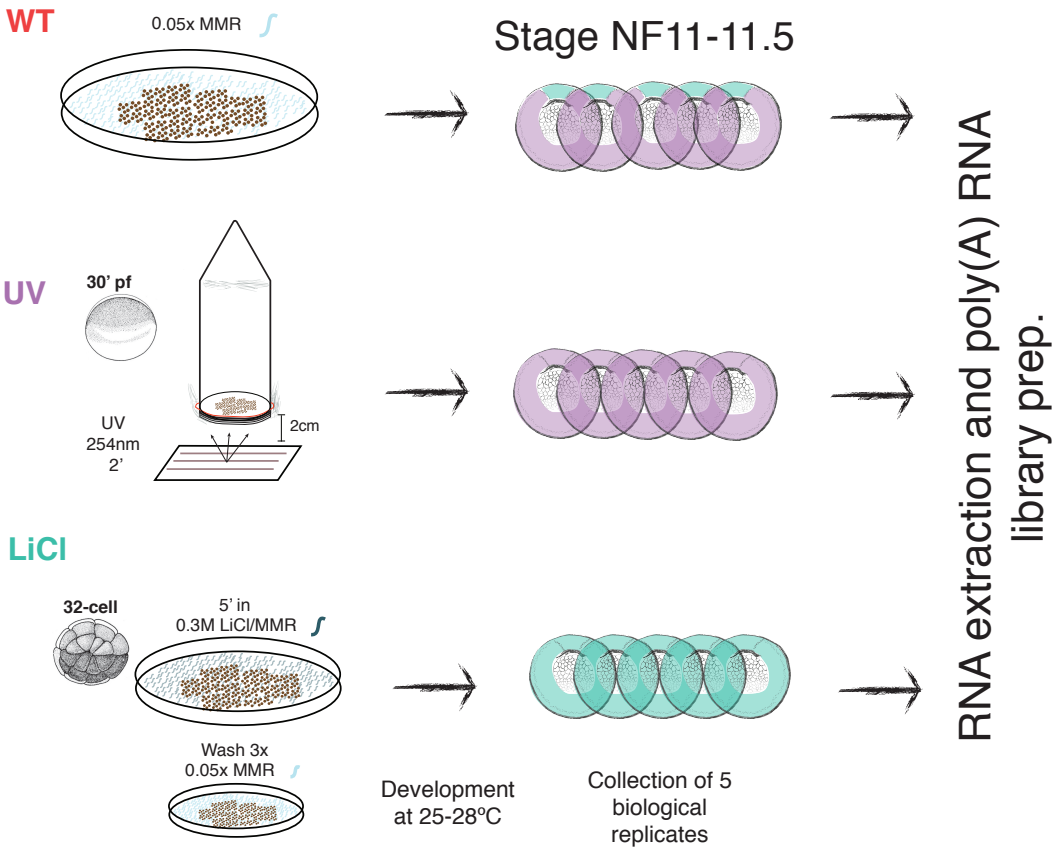

Figure 3.5: **Diagram of procedure for embryo collection for preparation of poly(A) library followed by deep-sequencing**

Embryos from 5 different crosses (biological replicates) were treated as shown in Figure 3.2, incubated at 25-28°C and harvested at late gastrula stage (NF11.5 or NF11^{+}). Total RNA was extracted from 5-8 pooled embryos and poly(A) paired-end libraries were generated and sequenced (see Chapter 2 for details).

In order to understand the similarities between the treatments I compared the distribution of the transcripts for the three conditions. The principal component analysis (PCA) (Fig. 3.6A) revealed that most variance was explained by PC1 (48%) which clearly separated the two treatment conditions, LiCl and UV. This was quite striking given that by this stage the embryos were phenotypically undistinguishable, however

their transcriptome was very different. Biological variance (embryos from different crosses) also played a role in separating the samples (PC2, 22%), a characteristic which has been described in studies of absolute quantification of RNA in frog embryos (Owens et al., 2016). The PCA analysis also indicated that, while WT embryos were located in between the two other conditions, they were much more similar to UV-treated embryos. The higher similarity between ventralised and untreated embryos was not unexpected, as by this stage the ventral side represents most of the embryo (see Figure 3.4A, the expression of ventral markers (*bmp4*, *wnt8a*, *msgn1*, *xcad3*) in untreated embryos). The similarities between UV and WT replicates may also be explained by the lower penetrance of the UV irradiation, as mentioned above.

These trends were confirmed when identifying differentially expressed (DE) genes by pairwise comparison using DESeq2. I used 5 biological replicates, which were more than what is generally used in similar experiments, which made the comparison more robust and provided higher confidence in the identification of differentially expressed (DE) genes. I identified genes DE in LiCl- or UV-treated embryos when compared to untreated embryos (the upregulated genes are represented in red and the downregulated in blue) (Fig. 3.6B-D). The criteria to identify these genes was based on a false discovery rate (FDR) smaller than 0.01 and a fold change equal or bigger than 2. The analysis revealed that only 0.6% of the active transcriptome is different between UV and WT while it is around 10 times more different (6.57%) when comparing LiCl to untreated (Fig. 3.6B-D). The DE genes in UV were mostly downregulated (79%, 93 genes) in relation to WT (Fig. 3.6B,C) while the opposite occurs in dorsalised embryos, 74% (914 genes) of the DE genes were upregulated (Fig. 3.6B,D).

These analyses revealed that at the transcript level ventralised embryos were very similar to whole untreated embryos while dorsalised embryos had undergone more transcriptomic changes and thus were more different from the control. As referred above, these results were not unexpected as ventral markers are overepresented in the embryo at this stage compared to the small domain of dorsal markers. The expansion of the small dorsal domain to the whole embryo has a higher impact than the expansion of an already dominating ventral domain.

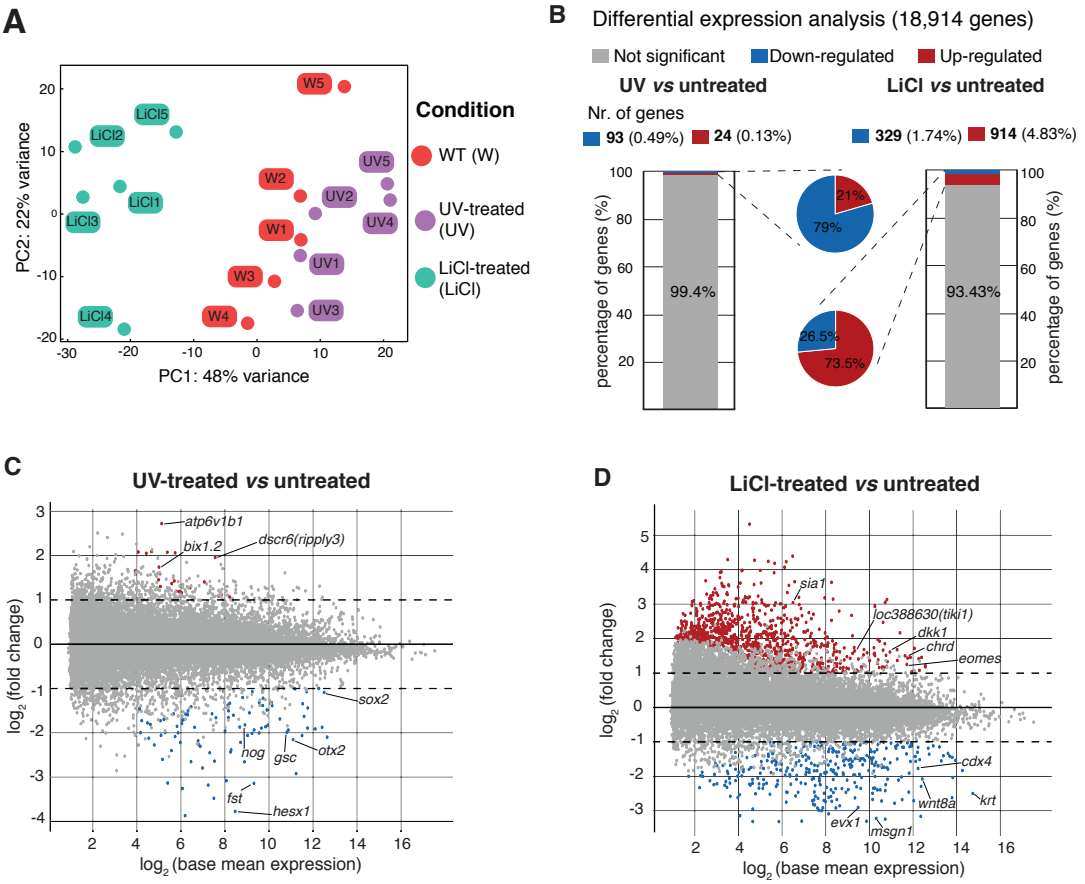

Figure 3.6: **Ventralised embryos are transcriptionally more similar to whole embryos than dorsalised embryos**

A) Principal component analysis (PCA) of untreated, LiCl- and UV-treated embryos represented by five biological replicates for each condition. **B-D**. Identification of affected genes upon UV or LiCl treatment. **C** and **D**. MA plots showing the transcript fold change against read coverage between the indicated conditions using the log2 scale for both fold change and mean of normalised read counts among samples. Differentially expressed genes were classified (B) and highlighted (C,D) as such if fold change ¿2 and FDR ?1%.

3.2.1 Identification of differentially expressed genes between dorsalised and ventralised embryos

The main goal of this project was to understand the transcriptional effect of LiCl and UV treatments, techniques that have historically been used to dorsalise and ventralise frog embryos, respectively. With this in mind, I focused on comparing the transcriptomes of both conditions to first confirm the effect of the treatments and second to identify genes with unknown roles in early development. I compared the 5 replicates of each condition and identified the differentially expressed genes (Appendix II and III). The comparison was made in relation to dorsalised embryos, meaning that positive values correspond to genes that are upregulated in dorsalised and downregulated

in ventralised embryos, and vice-versa. As the PCA plot in Fig. 3.6 indicates, LiCl- and UV-treated embryos are transcriptionally very different, 8.6% of the genes were differentially expressed. Similar to the comparison to untreated embryos, most of the differences were due to increase in expression, as 70% of the 8.6% are upregulated in LiCl-treated embryos (fold change >2) (Fig. 3.7).

The Figure 3.7 denotes some of the most differentially expressed genes and with the highest fold change. Among the upregulated genes in dorsalised embryos there were known dorsal markers such as *sia1*, *gsc*, *noggin chordin* and *admp*. Other genes involved in dorsal development, specifically in Wnt signalling included *fzd8* (Itoh, Jacob, and S, 1998) and *loc388630* (*Tiki1*)(Zhang et al., 2012b; Reis et al., 2014; Zhang et al., 2016). Within the group of upregulated genes I also found *pkdcc.1*, which has been recently identified in RNA-Seq experiments done in dissected gastrula stage embryos, as a gene dorsally enriched (Popov et al., 2016; Ding et al., 2016; Vitorino et al., 2015). The neural marker *zic2* known to be expressed in dorsal ectoderm and involved in anterior-posterior (AP) patterning of the neural tube has a 2 fold increase in expression while *sarcalumenin* (*srl*), a somite marker, has a 13 fold increase, compared to ventralised embryos. Another example of a gene expressed in the chordo-mesoderm is *foxa4*, which was also upregulated in LiCl-treated embryos. The examples given here are of genes already identified as dorsal markers and others that are involved in the regulation of anterior and dorsal/axial tissues.

I refer to the 485 genes downregulated in LiCl as the genes upregulated in UV. In this group I found the ventral markers tested before (Fig. 3.4), *bmp4*, *wnt8a* and the posterior mesoderm marker *msgn1*. The list of genes upregulated in ventralised included genes involved in posterior development such as *evx1*, *msx1* and *mespb* and members of the ventx family of transcription factors (TFs), *ventx1.1* and *ventx1.2*, regulators of ventral fate. Furthermore there were genes involved in ectoderm development, such as *tfap2a* and *olfm4*. The former is expressed in the neural crest and head and the latter is secreted by non-neural head ectoderm (Tsuda et al., 2002; Luo et al., 2003; Luo et al., 2002).

For both lists (upregulated in LiCl and in UV) it was reassuring to have identified dorsal and ventral markers together with genes expressed in tissues that derive

from these cell types: neural tube and axial mesoderm in the case of dorsal cells and epidermis, neural crest and posterior mesoderm in the case of ventral cells.

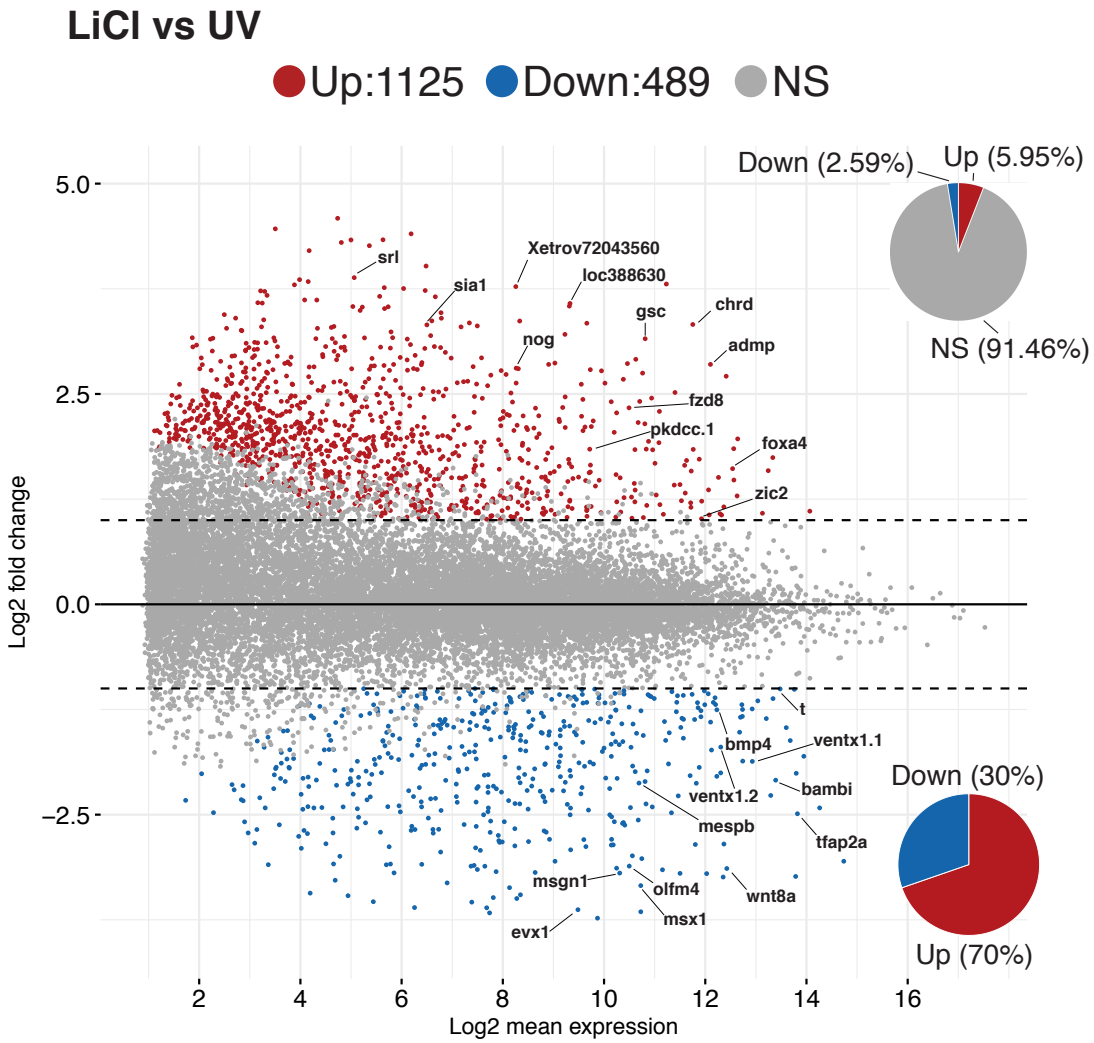

Figure 3.7: **Transcriptome of LiCl- and UV-treated embryos is highly distinct at gastrula stage**

MA plot showing the transcriptome differences between LiCl- and UV-treated embryos using transformed ($\log_2$) fold change and the transformed ($\log_2$) mean average of each transcript. Differentially expressed genes are represented as red and blue dots if upregulated or downregulated in LiCl, respectively. Genes downregulated in LiCl are upregulated in the UV condition. The pie-chart on the top right indicates the universe of active transcripts and the percentage of upregulated genes (red, 5.95%), downregulated genes (blue, 2.59%) and unchanged genes (grey, NS, 91.46%) in LiCl-treated embryos. This chart shows that 8.54% of the whole active poly(A) transcriptome is different between dorsalised and ventralised embryos. The pie-chart on the lower right indicates that of these 8.54%, 70% of the genes (1125 genes) are upregulated in LiCl-treated embryos while 30% (489 genes) are downregulated (or upregulated in UV). *srl-sarcalumenin*; *sia1-siamois 1*; *nog-noggin*; *gsc-goosecoid*; *chrd-chordin*; *fzd8-frizzled 8*; *pkdcc.1-protein kinase domain containing, cytoplasmic homolog, gene 1*; *admp-anti-dorsalising morphogen protein*; *foxa4-forkhead box A4*; *ventx-vent homeobox*; *bambi-bmp and activin membrane-bound inhibitor*; *msgn1-mesogenin 1*; *msx1-msh homeobox 1*; *mespb-mesoderm posterior homolog B*; *evx1-even-skipped homeobox 1*; *olfm4-olfactomedin 4*; *tfap2a-tto transcription factor AP-2 alpha*.

Given the extent of the list of DE genes and that many genes were not classified with a common name due to lack of annotation, to better understand the nature of the transcriptome of each condition I proceeded to do a gene ontology (GO) analysis. I focused on comparing the enrichment of terms associated with biological processes (BP) using a previously generated list of gene-specific BP term associations (Owens et al., 2016; Gentsch, Patrushev, and Smith, 2015). The most relevant GO terms and the corresponding enrichment (represented by -log10(p-value) and number of genes in each category) for each condition are represented in Figure 3.8.

Genes associated with both gastrulation (GO:0007369) and primitive streak formation (GO:0090009) GO terms were enriched in LiCl compared to UV: although both embryos go through gastrulation, the process starts on the dorsal side of the embryo and this category was populated by genes expressed in this region, thus the higher enrichment in LiCl-treated embryos. The genes found in this category, that were overexpressed in dorsalised embryos, included *gsc* and *cer1*. Even though amphibian embryos do not form a primitive streak they have an analagous structure, the blastopore,where the same genes are expressed, resulting in the enrichment of this GO term in dorsalised embryos (Fig. 3.8A). The 9 genes in this category overexpressed in LiCl-treated embryos included *nodal*, *otx2* and *otx1*, *lhx1* and *hhex*.

Transcripts associated with somitogenesis (GO:0001756) were overrepresented in ventralised embryos, this was related to the overall enrichment for posterior tissues; e.g genes involved in paraxial mesoderm, such as *msgn1*, *mesp2*, *mespA*, *cdx4* and *t*. As expected, the enrichment of genes associated with dorsal/ventral specification was similar between the two conditions (Fig. 3.8A).

When analysing signalling pathways, ventralised embryos were enriched for genes involved in the positive regulation of BMP signalling (GO:00030509) which substantiates what is known of the 'ventral center' as a source of active BMP signalling (Fig.3.8B). Such genes included *bmp4*, *msx1*, *foxj1* and members of the helix-loop-helix family of transcription factors hes (*hes3.3, hes5.1, hes6.1, hes8*). Genes associated with overall BMP signalling pathway (GO:0030509) were found in similar numbers in both conditions, however, with higher significance in ventralised embryos (Fig. 3.8B). Among the 23 genes of this category overexpressed in UV, there was *ventx1.1*, *ventx1.2*, *ventx3.2*

and *bmp7.1* while genes of the same category enriched in dorsalised embryos, included *admp* and *bmp5*.

When comparing genes associated with Wnt Signalling, the enrichment was not so straight forward: genes associated with overall Wnt signalling (GO:0016055) were represented in both conditions, while genes associated with positive regulation of the pathway (GO:0030177) were enriched in dorsalised embryos (*admp*, *zic1-4*, *hhex*), while genes associated with canonical Wnt signalling (GO:0060070) were enriched in UV-treated embryos (*t*, *myc*, *xarp*) (Fig. 3.8B). These discrepancies could be explained by poor annotation of GO terms in relation to amphibian development as there are two waves of Wnt signalling, maternal and zygotic. Maternal Wnt signalling is mostly associated with dorsal enrichment of β-catenin on the dorsal side of the embryo that triggers the cascade in these cells. After the midblastula transition (MBT), zygotic Wnt signalling, mostly via Wnt8a, is high on the ventral cells of the embryo leading to the formation of posteriorised tissues.

The comparison of genes associated with distinct tissue types is represented in Figure 3.8C. Genes associated with mesoderm development (GO:0007498) were equally represented in both conditions, however lateral (GO:0048368) (and its derivative blood vessel (GO:0001568)) and paraxial mesoderm (GO:0048339) were more associated with ventralised embryos. Transcripts associated with the GO term for heart development (GO:0007507) was equally enriched in both conditions, probably due to the distinct ancestries of its cells. LiCl-treated embryos were enriched for genes associated with endoderm (GO:0007492) which affirmed the enrichment for dorso-anterior cells, that will give rise to mesoderm and endoderm (mesendoderm). Genes associated with this GO term that were overexpressed in LiCl-treated embryos included *nodal*, *hhex*, *otx1-2*, *foxa2* and *nkx2-1*. These results were in conformity with the morphology description of LiCl- and UV-treated embryos and the quantification of the distinct mesodermal derivatives (Cooke and Smith, 1987; Cooke, Symes, and Smith, 1989).

Regarding the ectoderm, there was a clear distinction between the different kinds of derivatives of this germ layer: epidermis and neural tissue. Genes associated with neurogenesis (GO:0022008), head development (GO:0060322) and central nervous system development (GO:0007417) were enriched in LiCl-treated embryos, as its ancestry

are the cells that first ingress during gastrulation, the dorsal-most cells in the embryo. The genes that caused this enrichment included *zic1-4*, *sia1*, *chd6*, *lama5* the blimp-associated transcription factor *prdm12* and the homeodomain transcription factor *prdm16*. On the contrary, terms associated with epidermis (GO:0008544) were highly enriched in UV-treated embryo, these are the cells of the animal cap that do not ingress and are formed in response to high levels of BMP and Wnt signalling. The enriched genes in ventralised embryo that populate this GO-term category included *krt12*, *krt5.7* and *grhl3*.

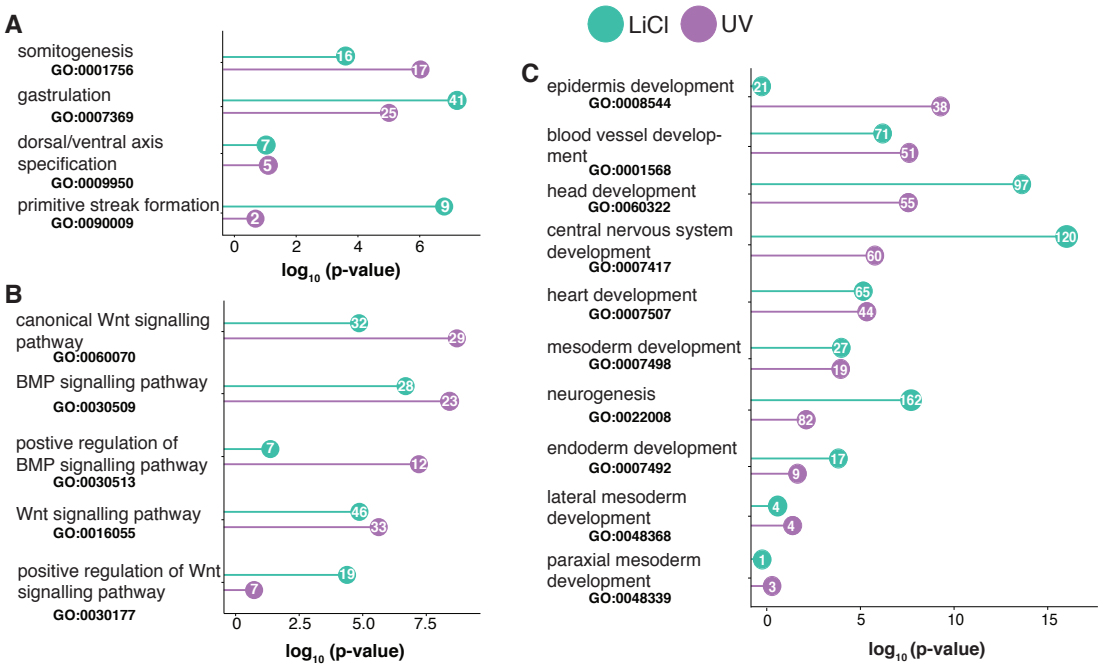

Figure 3.8: **GO term enrichment comparison between dorsalised and ventralised embryos**

Bar plots show the -log10 of the p-value of a statistical hypergeometric test between selected genes of each condition (upregulated) and the whole universe of transcribed genes in relation to Gene ontolgy (GO) terms associated with biological function (BP). This analysis allows the understanding of the nature of each condition's transcriptome by comparing the enrichment of genes for each GO term. The GO terms shown were selected based on the relevance to this study. The numbers in each bar represent the number of upregulated genes in each condition associated with the specific GO term. **A)** Comparison of the enrichment of genes associated with early developmental processes in both conditions. Genes associated with gastrulation and the primitive streak formation are enriched in dorsalised compared to ventralised embryos. Genes upregulated in UV-treated embryos are more associated with somitogenesis than in dorsalised embryos, while there is no significant difference in genes associated with dorsal/ventral axis specification. **B)** Analysis of enrichment of genes associated with Wnt and Bmp signalling pathways. **C)** GO terms associated with the regulation and development of different embryonic tissues are differentially enriched in the two conditions. LiCl-treated embryos overexpress genes associated with head and neural tube development while UV-treated embryos are enriched for genes associated with posterior and epidermis development.

Although the use of GO terms allowed for the better understanding of the nature of each condition's transcriptome, it also revealed some limitations of such analysis in the context of early *Xenopus* development. An example of such limitation was referred above, when analysing genes involved in different waves of Wnt signalling that occur in the embryo at gastrula stages.

Overall, these results reaffirmed that the treatments were correctly transforming the whole embryo into a representation of either dorsal or ventral cells. Furthermore, the transcriptome analysis not only captured the DV positioning of the cells but also its downstream derivatives; e.g anterior mesoderm and head/neural tube in the case of LiCl-treated and posterior mesoderm and epidermis in the case of UV-treated embryos.

3.3 Comparison with published transcriptomic data of dissected embryos

This study has so far indicated that LiCl and UV treatments resulted in embryos that represented dorsal and ventral cells (and its derivatives), however, to further confirm these results I compared the transcriptomic data from this work to published data of untreated dissected embryos. In recent years, the use of highthroughput sequencing has become more widespread in the field of developmental biology and with it, the number of whole-genome/transcriptome data available has increased. Many publications have analysed and compared the transcriptome of dissected frog embryos using both *Xenopus laevis* (Popov et al., 2016; Ding et al., 2016; Ding et al., 2017) and *Xenopus tropicalis* (Blitz et al., 2017). For ease of comparison, in terms of annotation, I compared the LiCl/UV data to the data of Blitz *et al.* in which they dissected *Xenopus tropicalis* stage NF10.5 embryos into 5 pieces: animal cap (AC), ventral marginal zone (VMZ, or VM in this study), lateral marginal zone (LMZ), dorsal marginal zone (DMZ or DM in this study) and the vegetal mass (VEG) (Fig.3.9A) (Blitz et al., 2017). For the purpose of this work I only compared the DM and VM datasets with each other, and with the LiCl/UV datasets. It is important to point out that this was not the ideal way of

comparing treatments with dissected halves, first these were independent experiments executed by different researchers using different lines of frogs; second, the stage at which the transcriptome was studied was not the same (their study was stage NF10.5 this study was stage NF11-11.5) and third, for statistical significance purposes, their study used only two biological replicates while I used 5. In that study the researchers focused their analysis in identifying different transcription factors represented in each dissected half, and I was interested in the whole poly-A transcriptome and so, I analysed their raw data.

Figure 3.9: **Comparison and correlation of DE genes in dorsalised *vs* ventralised with DE genes in DM *VM* halves**

A) On left is a diagram representing dissections done in early gastrula embryo from Blitz *et. al.*, 2017, of which I used the data derived from the DMZ (DM) and VMZ(VM) (Blitz et al., 2017). The Venn diagram represents the overlap between differentially expressed (DE) genes identified when comparing DM with VM (DM*vs*VM) and LiCl with UV (LiCl*vs*UV). **B)** Heatmap representing the $\log_2$ of the fold change between UV and LiCl conditions of the 121 DE genes between DM and VM halves. Positive fold changes are associated with genes upregulated in dorsalised and represented in red, and in blue are negative fold changes, which are genes upregulated in ventralised embryos. For each gene there is white or black box on the left-hand side of the heatmap representing whether the gene is upregulated in DM or VM, respectively. Genes underlines in red (22) are not DE (p-value<0.01, fold change>2) between LiCl- and UV-treated embryos. **C)** Regression plot of the fold changes in the four conditions (LiCl, UV, DM and VM) of the genes identified in VM and DM. The plot is green if the correlation between the two conditions is positive (pearsonr>0) and red is the correlation is negative (pearsonr<0). **D)** Heatmap of the $\log_2$ of the fold change between LiCl and UV (LiCl vs UV) and between DM and VM (DM vs VM) of the DE genes identified between dorsalised and ventralised embryos. In red are positive fold changes and in blue negative fold changes (pairwise comparisons were made in relation to UV and VM, which means that positive fold changes are associated with genes upregulated in LiCl and DM). The regression plot on the right-hand side shows a positive correlation (pearsonr>0) between the fold changes represented on the heatmap. DE - differentially expressed; DMZ - dorsal marginal zone; VMZ - ventral marginal zone; AC - animal cap; LMZ - lateral marginal zone; VEG - vegetal mass; fc -fold change; padj - p-value adjusted; pearsonr - Pearson correlation coefficient; p - p-value; vs - *versus*; padj - adjusted p-value.

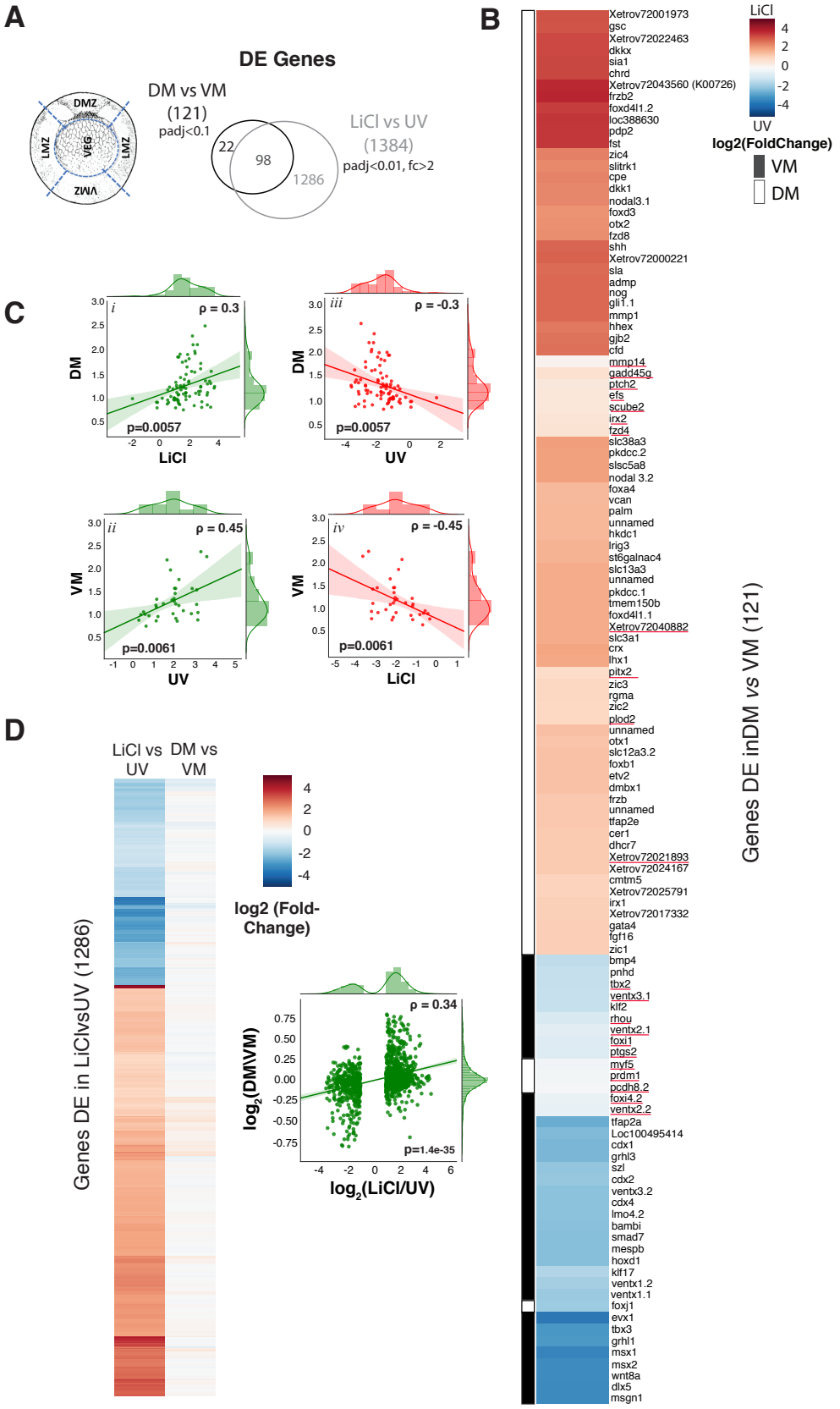
A
DE Genes
DM vs VM
(121)
padj<0.1
22
98
1286
LiCl vs UV
(1384)
padj<0.01, fc>2
DMZ
LMZ
VEG
LMZ
VMZ
B
LiCl
4
2
0
-2
-4
UV
log2(FoldChange)
VM
DM
Genes DE inDM vs VM (121)
Xetrov72001973
gsc
Xetrov72022463
dkkx
sia1
chrd
Xetrov72043560 (K00726)
frzb2
foxd4l1.2
loc388630
pdp2
fst
zic4
slitrk1
cpe
dkk1
nodal3.1
foxd3
otx2
fzd8
shh
Xetrov72000221
sla
admp
nog
gli1.1
mmp1
hhex
gjb2
cfd
mmp14
gadd45g
ptch2
efs
scube2
irx2
fzd4
slc38a3
pkdcc.2
slsc5a8
nodal 3.2
foxa4
vcan
palm
unnamed
hkdc1
lrig3
st6galnac4
slc13a3
unnamed
pkdcc.1
tmem150b
foxd4l1.1
Xetrov72040882
slc3a1
crx
lhx1
pitx2
zic3
rgma
zic2
plod2
unnamed
otx1
slc12a3.2
foxb1
etv2
dmbx1
frzb
unnamed
tfap2e
cer1
dhcr7
Xetrov72021893
Xetrov72024167
cmtm5
Xetrov72025791
irx1
Xetrov72017332
gata4
fgf16
zic1
bmp4
pnhd
tbx2
ventx3.1
klf2
rhou
ventx2.1
foxi1
ptgs2
myf5
prdm1
pcdh8.2
foxi4.2
ventx2.2
tfap2a
Loc100495414
cdx1
grhl3
szl
cdx2
ventx3.2
cdx4
lmo4.2
bambi
smad7
mespb
hoxd1
klf17
ventx1.2
ventx1.1
foxj1
evx1
tbx3
grhl1
msx1
msx2
wnt8a
dlx5
msgn1
C
i
ρ = 0.3
p=0.0057
DM
LiCl
iii
ρ = -0.3
p=0.0057
DM
UV
ii
ρ = 0.45
p=0.0061
VM
UV
iv
ρ = -0.45
p=0.0061
VM
LiCl
D
LiCl vs UV
DM vs VM
Genes DE in LiClvsUV (1286)
4
2
0
-2
-4
log2 (Fold-Change)
ρ = 0.34
p=1.4e-35
log2(DM\VM)
log2(LiCl/UV)

Figure 3.9

The RNA-Seq reads from DM and VM were downloaded from the publicly available databases and analysed the same way as the LiCl and UV data: aligned to the *Xenopus tropicalis* transcriptome, reads on exons counted and I used DESeq2 to identify DE genes between the two conditions. This analysis resulted in the identification of 121 genes DE when comparing DM vs VM (86 upregulated in DM and 35 in VM), a much lower number than the LiCl/UV comparison but with the same proportion of upregulated genes (71% up in DM, 29% down in VM (Fig. 3.9), similar to LiCl *vs* UV, 70% up and 30% down (Fig. 3.7)). The heatmap in Figure 3.9B shows the fold change (log2) (positive values are in red and represent genes upregulated in LiCl and negative values in blue, upregulated in UV) between LiCl- and UV-treated embryos of these 121 genes; black or white bar next to each genes represents whether it was overexpressed in VM or DM, respectively. The majority of the genes clustered as expected, LiCl with DM (red and white) and UV with VM (blue and black). The graphs in the Figure 3.9C reflect this observation as they show the correlation between the fold changes of the genes upregulated in each condition. There was a positive correlation between DM/LiCl (Fig. 3.9C,i) and VM/UV (Fig.3.9C,ii) and negative correlation between DM/UV (Fig. 3.9C,iii) and VM/LiCl (Fig. 3.9C,iv). From the 121 DE genes of the Blitz *et al.* experiment, there were 4 which did not follow the correlation stated above: *myf5*, *prdm1*, *pcdh8.2* and *foxj1.* Of these, *myf5*, *prdm1*, *pcdh8.2* were not differentially expressed between LiCl- and UV-treated embryos based on an adjusted p-value smaller than 0.01 or a fold change higher than 2. On the other hand, *foxj1* was overexpressed in dorsal cells of the early gastrula embryo (in DM and in expression profile in Xenbase) but the gene was upregulated in UV-treated embryos. *Foxj1* is a known marker of multiciliated cells and later in development is expressed throughout the epidermis a multiciliated tissue. This characteristic justified the overexpression of the gene in ventralised embryos, as these embryos were enriched for an epidermal cell fate.

While the majority of the DE genes between DM and VM were represented in the LiCl/UV comparison, there were 1286 that were only differentially expressed in the latter group. Despite the fact that these genes were not differentially expressed in the dissection experiments, the fold change of the transcripts still correlated positively with

LiCl/UV (Fig.3.9D).

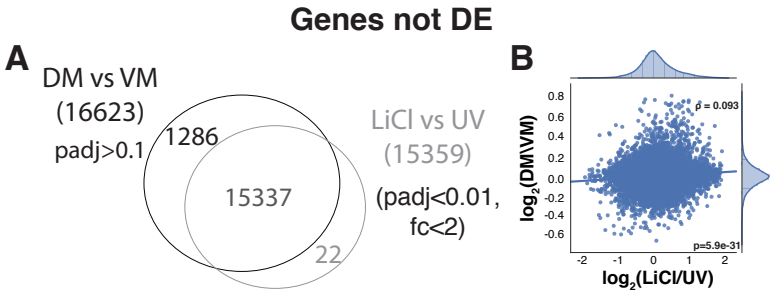

Figure 3.10: **Comparison and correlation of unchanged genes in both experiments**

A Venn diagram representing the overlap between genes not differentially expressed (unchanged genes) in both comparisons: LiCl*vs*UV and DM*vs*VM. **B)** Regression plot of the fold changes of LiCl*vs*UV and of DM*vs*VM of the genes identified in VM and DM. As expected, the plot indicates low, but positive correlation between the fold changes of unchanged genes. DE - differentially expressed; vs -*versus*; padj - adjusted p-value.

In addition, when comparing the whole transcriptome, the majority of the transcripts were not differentially expressed in both experiments (Fig.3.10A) and the fold changes in both experiments correlated positively (Fig.3.10B).

So far, I showed that LiCl and UV treatments successfully dorsalised and ventralised *Xenopus tropicalis* embryos, respectively, and that these embryos represented enriched forms of each cell type and its derivatives. LiCl-treated embryos were a result of an expansion of the early maternal Wnt Signalling into the whole embryo, resulting in an enrichment for dorso-anterior structures such as head and neural tube. On the other hand, UV-treated embryos were not exposed to this early maternal Wnt signalling, resulting in the absence of Wnt and BMP antagonists and the expansion of the BMP and zygotic Wnt domain into the whole embryo. This led to an embryo with posteriorised mesoderm and neural tissue, together with an enrichment for epidermal fate cells. I also showed that a LiCl-treated an UV-treated embryo was transcriptionally comparable to a dorsal (DMZ) and ventral (VMZ) cells of the embryo.

Gene	Name	Condition	Expression	Function/Information
cpe	*CarboxypeptidaseE*	LiCl	Small peak of expression just before stage 12 and increases at later stages.	Function: Zinc carboxypeptidase: Catalysis the release of C-terminal arginine or lysine from polypeptides. Part of the dorsal signature identified in (Ding et al., 2016). It has no expression data.
c8orf4	*Chromosome 8 open reading frame 4*	UV	Starts at MBT increasing during gastrulation and peaks at stage 14, increasing again at stage 32.	Also known as TC-1, a transposable element associated with neural tissue (Faunes et al., 2011).
72022004	N/A	UV	Expression starts at stage 10 and peaks just after stage 12, decreasing during tailbud stages.	N/A
K00726	N/A	LiCl	Starts to be expressed at the start of gastrulation, peaks around stage 15 and decreases from then on.	There is no data published data about the gene. Contains an E3 ubiquitin-ligase RNF220 domain, giving it high homology to the protein rnf220, a postive regulator of Wnt signalling.

Table 3.1: Differentially expressed genes selected for spatial expression analysis

The four genes selected based on the successful generation of WMISH probes. The table includes information derived from **Xenbase** (http://www.xenbase.org) (Karpinka et al., 2015) and the temporal expression details were derived from **Searchable Database of *Xenopus tropicalis* Gene Expression Profiles** (http://genomics.crick.ac.uk/apps/profiles/) (Collart et al., 2014; Owens et al., 2016).

3.4 Identification and validation of novel genes

The comparison of dorsalised and ventralised embryos yielded a high number of differentially expressed genes, and although a lot of them were known genes, others were only classified based on the homology to other genes, but its expression pattern or function had not been studied. A third group included genes which, using the most recent annotation for gene models, had not been named yet. By inquiring the top genes (lowest adjusted p-value and highest fold change) I selected genes that could have a new or unknown role in early development.

First, I used BLAST to search for the sequences in the frog genome to ensure the gene was not wrongly annotated, second I used published data of temporal expression of early *Xenopus tropicalis* embryo (Owens et al., 2016; Collart et al., 2014) to select genes expressed during gastrula stages. Once the genes were selected, the ones with annotated names were searched on Xenbase (Karpinka et al., 2015) for expression and publication data. For genes without annotation, the sequence was used to BLAST in other genomes to find homologies. Of the full list of selected genes (Appendix I), Table 3.1 shows the ones chosen for further investigation.

My goal was to study the expression profile of these genes, in wild-type embryos, and further explore any gene with a potential relevant role in early development. The genes

were cloned from *Xenopus tropicalis* cDNA and sense and anti-sense mRNA probes were made to study the spatial expression pattern by WMISH. I successfully generated probes for 4 genes which gave conclusive expression patterns as shown in Figure 3.11. From the four genes, two were detected as upregulated in UV-treated embryos, *c8orf4*, and *72022004* and the other two in LiCl, *K00726* and *cpe*. As summarised in Table 3.1, *c8orf4* also known as *tc1* and it has been identified as a transposable element that acts on the neural tissue. By gastrula stage, the expression of the gene was barely detectable in wild-type embryos although it seemed to be downregulated in LiCl-treated embryos and upregulated in the prospective epidermis of UV-treated embryos (Fig. 3.11B). At tailbud stage, the gene was expressed in the head, but not the neural tube (Fig. 3.11B). Interestingly, *72022004* had a similar expression pattern: low levels at gastrula stage although higher in UV-treated embryos and by tailbud stage the gene was expressed in the head, showing higher expression in the branchial arches, which are populated by neural crest cells (Fig.3.11B). The other two genes, *cpe* and *K00726*, were upregulated in LiCl-treated genes, as seen by qPCR analysis (Fig.3.11A), although it was not clear by WMISH (Fig. 3.11B). *cpe* had been identified as enriched in the dorsal half of dissected *Xenopus laevis* gastrula stage embryos (Ding et al., 2016), although its expression pattern had not been described. I showed that the gene was faintly expressed in the blastopore region of wild-type stage 10.5 embryos and by tailbud stage it was expressed dorsally and in the anterior most area of the neural tube (Fig1.10B). Lastly, *K00726*, showed a characteristic dorsal expression on the blastopore at gastrula stage and by tailbud the gene was only present in the neural tube, similarly to *cpe* (Fig. 3.11B). At gastrula stage it was noticeable the expansion of the expression of *K00726* in dorsalised embryos and the loss in UV-treated embryos (Fig. 3.11B).

As a result of the transcriptomic analysis I was able to identify and characterise the expression pattern of genes with potential roles in dorsal/ventral tissues and its derivatives, for the first time. From the spatial expression data it seemed clear that genes enriched ventrally, as a result of high BMP and Wnt signals, were involved in the regulation of tissues such as epidermis and neural crest cells, while genes discovered in LiCl-treated embryos were expressed in the dorsal most structures, specifically of the neural tube.

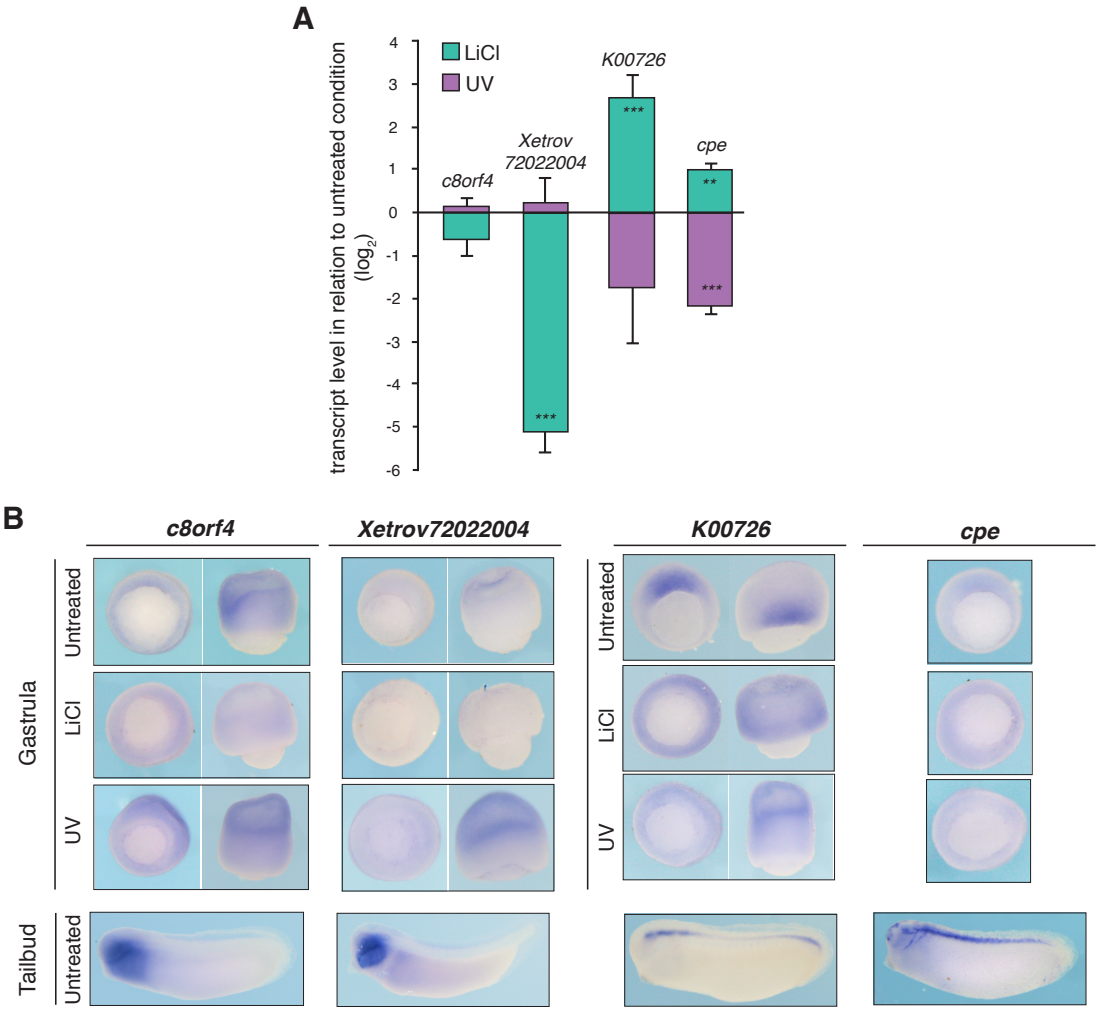

Figure 3.11: **Expression pattern analysis by WMISH and quantified by qPCR of uncharacterised genes identified by RNA-Seq analysis**

A) Transcript fold changes (log2 scale; RT-qPCR) inflicted on c8orf4, Xetrov72022004, K00726 and cpe upon LiCl or UV treatment as measured by RT-qPCR in mid-gastrula embryos (n=3). **B)** Spatial expression patterns of c8orf4, Xetrov72022004, K00726 and cpe as visualised by WMISH on untreated, LiCl- and UV-treated embryos of gastrula (vegetal and lateral view except for cpe with vegetal view only) and mid-tailbud stage (unperturbed condition only, lateral view). textitcpe-*carboxipeptidase E*; *c8orf4-chromosome 8 open reading frame 4*; *odc-ornithine decarboxylase*.

3.5 Characterisation of K00726, a rnf220-like ubiquitin ligase

Of the four genes described above, *K00726* seemed to be an interesting gene to study further: first, the gene had an expression pattern similar to a typical dorsal marker and second contained a partial E3 ubiquitin-protein ligase RNF220 middle domain (Fig1.12B). The domain is specific to the members of the Ring finger protein 220 (Rnf220) family of genes, of which there are two genes in *Xenopus*, *rnf220.1* and

renf220.2. To guarantee that *K00726* was an unique gene and not a product of poor annotation I aligned the two protein sequences found in *Xenopus tropicalis* and *Xenopus laevis* (Fig1.12A), which showed that Rnf220.1 was more closely related to K00726 than was with Rnf220.2, a much smaller protein. For the purpose of this study I did not include Rnf220.2 in the analysis and I referred to Rnf220.1 simply as Rnf220.

Rnf220 is a RING domain E3 ubiquitin ligase that had been shown to positively regulate Wnt signalling (Ma et al., 2014). While small quantities of β-catenin (5pg) injected into the ventral blastomere of a 4-cell stage embryo did not induce a secondary axis, when co-injected with mouse *Rnf220* a proportion of the embryos developed a partial or secondary axis (Ma et al., 2014). Despite its ubiquitin domain, Rnf220 stabilised β-catenin via its C-terminal RING domain in an interaction mediated by the ubiquitin-specific protease 7 (USP7) (Ma et al., 2014). Furthermore, a construct lacking the N-terminus (ΔN) portion, including part of the E3 ubiquitin domain, was still capable of stimulating Wnt reporter expression in the presence of β-catenin, while removing both the N-terminus and the RING domain (ΔNΔR) had the opposite effect, inhibiting Wnt signalling (Ma et al., 2014). All of the experiments referred to in Ma *et al.* were performed using the mouse *Rnf220*, however the *Xenopus laevis Rnf220* had a similar Wnt enhancement activity in luciferase reporter assays in HEK293 cells (*personal communication*).

I compared the protein sequences of the frog K00726 and Rnf220 (Fig.1.12B). As referred above, K00726 contains the Rnf220 E3 ubiquitin specific domain (179-271aa) and, similarly, the RING domain on the C-terminus of the protein. Although K00726 is bigger than Rnf220, 419 amino acids (aa) and 301aa, respectively, its ubiquitin domain was smaller. However, no other domains were identified in the K00726 protein sequence. Given the importance of the RING domain and, potentially, of the E3 ubiquitin-protein ligase domain I compared the domains of Rnf220 and K00726 (Fig1.12C, D). The RING domain was very similar between the two protein, both with 40aa and only two of the aminoacides were not conserved, overall they were 75% identical (using Clustal 2.1) (Fig.1.12C). On the other hand, the E3 ubiquitin protein ligase domain was very distinct, only 35% identity (Clustal2.1) between the two proteins (Fig. 1.12D).

I was interested in understanding the role of K00726, specifically in enhancing Wnt

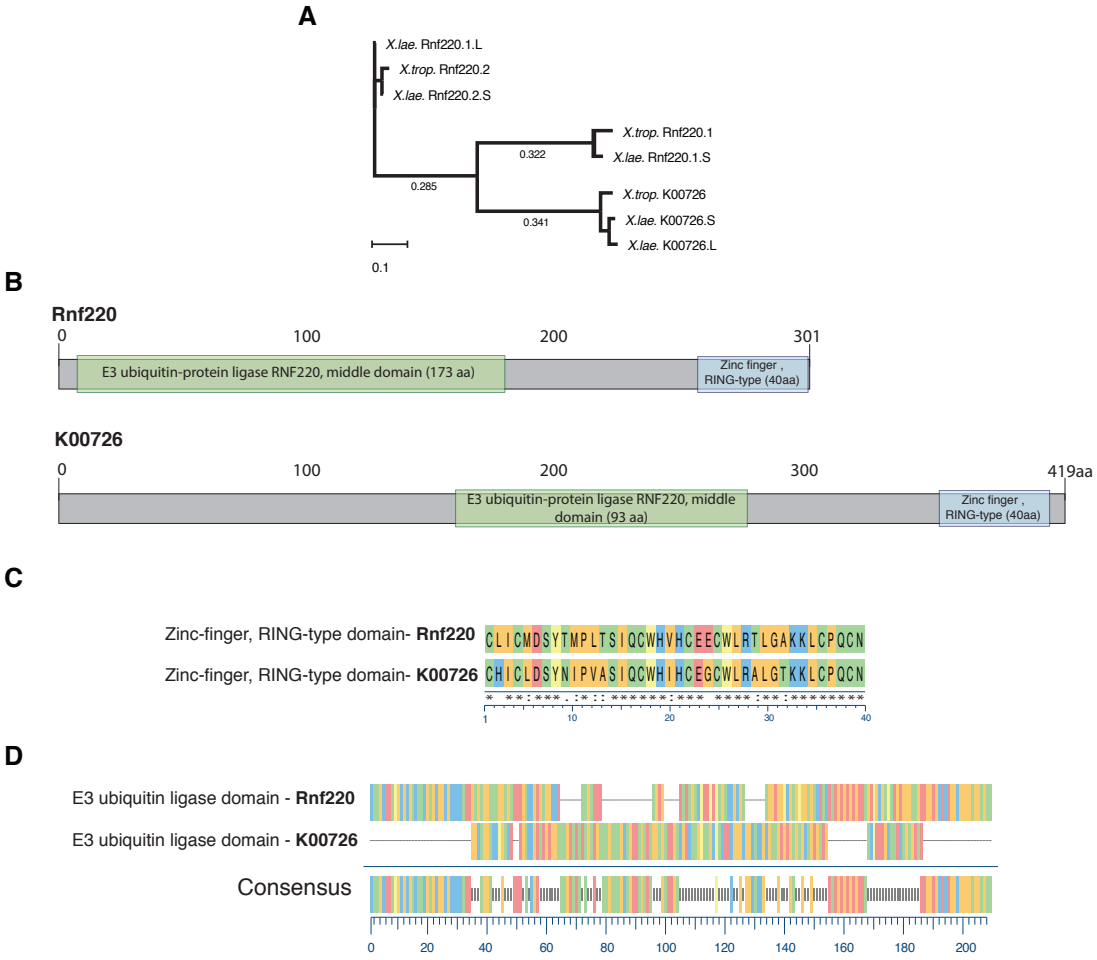

Figure 3.12: **K00726 and Rnf220 protein sequence analysis**

A) Phylogenetic tree based on the protein sequence similarity of *Xenopus laevis* Rnf220.1.L , Rnf220.1.S, Rnf220.2.S, Rnf220.2.L, K00726 and the *Xenopus tropicalis* Rnf220.1, Rnf220.2 and K00726. The .L and .S versions of each *Xenopus laevis* protein refers to the chromosome from which it derived, the 'long' (L), or the 'short' (S), since *Xenopus laevis* is an allotetraploid species. The tree was constructed by the MegaAlign Pro™software using Clustal Omega alignment with the default parameters. **B)** Representation of the proteins Rnf220 and K00726 and the position of the E3 ubiquitin-protein ligase and the RING domains. The domains were identified using the **InterPro** tool from EMBL-EBI (https://www.ebi.ac.uk/interpro/) (Jones et al., 2014). **C)** Comparison of the Zinc-finger, RING-type domain sequences of Rnf220 and K00726 by alignment. **(*)** - fully conserved aminoacid; **(:)** - conservative mutation; **(.)** - semi-conservative mutation; **( )** - non-conservative mutation. **D)** Comparison of the E3 ubiquitin ligase domain sequences of Rnf220 and K00726 by alignment. In both **C)** and **D)** the alignment was done using the Clustal Omega in MegaAlign Pro™software with the default parameters. rnf220-ring finger protein 220, RING-really interesting new gene.

signalling similarly to Rnf220. As reported by Ma et *al.* (Ma et al., 2014), the RING domain is essential for promoting Wnt signalling, and since the domain was highly conserved with K00726 (Fig. 3.12C) it was a plausible hypothesis. To test this I used *Xenopus laevis* embryos and injected one of the ventral blastomeres at the 4-

cell stage with *K00726* mRNA or co-injected with 5pg of β-catenin and assessed the formation of a secondary axis. This experiment was analogous to the one described in Ma et. *al* and aimed to show whether K00726 was involved in stabilising β-catenin and therefore would induce a partial or full secondary axis. As a control for the induction of a double axis, embryos were injected with 250pg β-catenin (Fig. 3.13). Similarly to *Rnf220*, *K00726* by itself was not capable of inducing a secondary axis but, it did not contribute to β-catenin stabilisation as co-injection of 5/10/20pg of *β-catenin* and 1000pg of *K00726* did not lead to the induction of a secondary axis (Fig. 3.13). However, when an amount of *β-catenin* capable of inducing a secondary axis was co-injected with *K00726* there was a reduction in the number of full double axis formed and an increase in embryos without a secondary axis (Fig. 3.13).

In summary, K00726, a newly identified dorsally expressed gene in early *Xenopus* embryos, shares a partial E3 ubiquitin-ligase protein domain and a almost fully conserved C-terminus RING domain with Rnf220. While Rnf220 has been shown to enhance Wnt signalling by stabilising β-catenin, K00726 did not show the same effect, despite the conservation of the RING domain. Given that Rnf220 mediated the stabilisation via USP7 it can be the case that K00726 was not capable of this interaction. The main differences between the two proteins resided on the less conserved E3 ubiquitin-ligase domain, which, although not necessary for interaction with β-catenin, when removed with the RING domain led to a repression of Wnt signalling. Further experiments will be necessary to conclude on the role of K00726 in early development.

3.5.1 K00726 is a Wnt/β-catenin target gene

In addition to studying the protein sequences I investigated the genomic region of *K00726* and whether the gene was bound by relevant TFs. Since *k00726* was expressed dorsally and at the start of gastrulation, I searched for binding of β-catenin in the promoter and cis-regulatory regions. For this purposed I used publicly available ChIP-Seq data on the binding profile of β-catenin at NF10.5 (Nakamura et al., 2016). Although β-catenin did not bind to the promoter of the gene, it did bind to three other regions within intron 1 (e1, e2 and e3) (Fig. 3.14A), which given the proximity were potential regulatory regions of the gene. To test whether these regions were capable

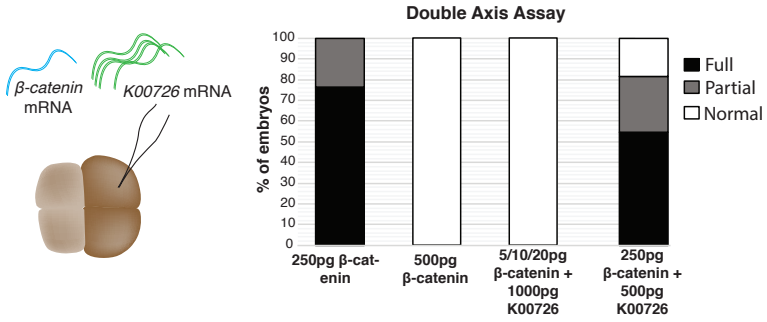

Figure 3.13: **K00726 acts distinctly from Rnf220 in stabilising β-catenin**

On the left-hand side is a diagram representing the injection strategy for the double axis assay: inject one of the ventral cells (larger and darker) of the 4-cell stage *Xenopus laevis* embryo with *K00726* mRNA and/or *β-catenin*mRNA. On the right-hand side is a plot showing the quantification, in percentage (%) of the embryos that formed a secondary axis. Normal embryos did not form any secondary axis, partial refers to embryos that formed a secondary axis wihtout a cement gland (the most anterior structure) and full refers to embryos that formed a secondary axis containing a cement gland.

of driving expression I cloned them into a vector containing *firefly* luciferase, together with the gene promoter sequence, to assess its transcription driver capacity. The plasmids were co-injected, into the 2 cells of the 2-cell stage embryo, with *Renilla* mRNA as a control for a dual-luciferase assay (see Methods). A plasmid containing the *Xenopus* cytoskeleton actin promoter (CSKA) was used as positive control (data not shown) and the pGl3-Basic vector without any promoter or enhancer (empty vector) as the negative control (Fig. 3.14C). Embryos were collected at gastrula stage and processed for luminescence readings. The luciferase assay indicated that the promoter by itself was capable of driving expression; 6 fold increased compared to empty vector. When combined with regulatory region e2 and e3 the transcription levels increased substantially, specifically with e2 (Fig. 3.14C), which had the highest β-catenin binding (Fig. 3.14A). Interestingly, the data indicated that e1 could represent an inhibitory regulatory region given that its luciferase activity was reduced to levels similar to the negative control, empty vector (Fig. 3.14C). In addition to the luciferase assay, I investigated whether β-catenin induced expression of *K00726*. I injected *β-catenin* into the animal pole of 2-cell stage embryo and analysed the induction of *K00726* in animal caps cultured until the start of gastrulation. The levels of *K00726* were measured by qPCR and normalised to the house-keeping gene *odc*, and indicated that β-catenin induced the expression of *K00726* (Fig. 3.14D). Although I did not show directly that the binding of β-catenin to the regulatory regions e2 and e3 led to the expression of *K00726*, I did

show that β-catenin binds these regions prior to activation of the gene (Fig. 3.14A), these regions were capable of driving transcription via the *K00726* promoter and that expression of β-catenin in naïve cells led to the overexpression of *K00726* (Fig. 3.14C). Overall, I was confident that *K00726* was a target gene of Wnt/β-catenin signalling.

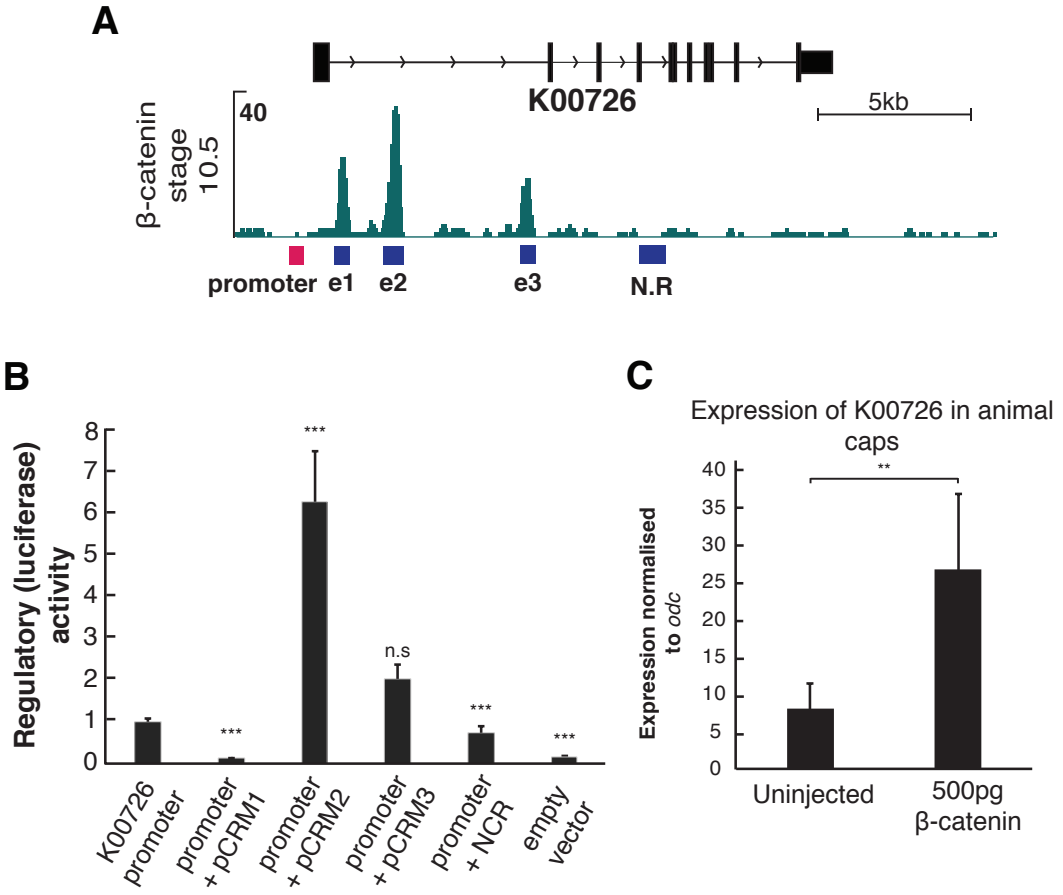

Figure 3.14: ***K00726* is activated by β-catenin**

A) Genomic snapshot of DNA occupancy of ?-catenin near the K00726 locus in early gastrula embryos (Nakamura and Hoppler, 2017). **B)** Promoter, putative cis-regulatory modules (e) 1 to 3 and negative control region (N.R) of K00726 were explored for their regulatory capacity in a dual luciferase assay. Reporter activity was normalised to basal activity of the endogenous promoter. Student's two-tailed t test: ***, p-value ¡0.01; n.s, not significant. Error bars represent the standard error of the mean (s.e.m.) of biological duplicates. **C)** Transcript levels (normalised to odc) of K00726 in animal caps derived from embryos injected with and without 500pg of ?-catenin as measured by RT-qPCR (n=3). Student's two-tailed t test: **, p-value ¡0.05. Error bars represent the standard error of the mean (s.e.m.) of biological triplicates. *odc-ornithine decarboxylase.*

3.6 Summary

- I described the conditions to successfully dorsalise and ventralise *Xenopus tropicalis* embryos with UV and LiCl treatments, respectively.

- I compared the whole poly-(A) transcriptome of the dorsalised and ventralised embryos that revealed that the latter were transcriptionally more similar to whole-embryos while the former had a substantially higher number of up-regulated genes.

- The analysis of genes overrepresented in each condition indicated that dorsalised embryos were enriched for genes associated with anterior mesoderm and head/neural tube, while ventralised embryos were enriched for genes that regulate posterior mesoderm and epidermis.

- The comparison of LiCl/UV datasets with published transcriptome of dissected dorsal and ventral halves of gastrula stage embryos indicated that LiCl and UV treatments accurately represented dorsal and ventral regions, respectively.

- By WMISH I uncovered the spatial expression pattern of uncharacterised genes that were differentially expressed in dorsalised and ventralised embryos.

- I further characterised *K00726*, a dorsally expressed gene, similar to the Wnt-enhancing Rnf220. Although I did not identify a similar role for *K00726* in improving Wnt signalling I was able to show that β-catenin binds active regulatory regions near *K00726* and induces its expression.

Chapter 4

Differential binding of *Brachyury* in dorsalised and ventralised *Xenopus tropicalis* embryos

In the previous chapter I showed how the perturbation of the dorsal-ventral axis determination can alter the embryonic transcriptome. *Xenopus* has been used as animal model for early development for its ease of manipulation and as a good provider of biological material: one fertilisation can yield thousands of embryos. Together with zebrafish and *Drosophila*, *Xenopus* has also become a good model to study early chromatin regulation. Such studies rely on chromatin immunoprecipitation to identify genomic regions to which modified histones, components of the transcriptional machinery and transcription factors bind. In Chapter 1, I referred to examples of studies that allowed the construction of gene regulatory networks of early vertebrate development using ChIP-Seq. However, most of these studies use whole embryos, and although they have provided detailed information of dynamics based on time-series experiments, there is a lack of information on spatial regulation. To this end, one of the goals of this project was to understand spatial regulation during early development.

As described in Chapter 3, dorsalised and ventralised embryos can be used as a proxy for dorsal and ventral cells and its derivatives. With this in mind, I used the same embryos to study regulation at the chromatin level. In this Chapter, I will describe my attempts to understand the differences in the chromatin landscape between distinct cell types in the early embryo.

The initial analyses focused on active transcription and regulatory regions by comparing the DNA binding of RNA polymerase II (RNAPII) and the co-activator protein

p300. However, my main focus was to compare the binding of Brachyury, a developmentally relevant transcription factor (TF), that is zygotically activated and expressed in dorsal and ventral cells. Such comparison would allowed me to understand whether early developmental events, such as dorsal-ventral determination, affect chromatin and the binding of transcription factors.

4.1 Identification of actively transcribed genes in dorsalised and ventralised embryos by profiling RNAPII

As a proof-of-principle experiment to test ChIP-Seq on LiCl and UV-treated embryos, I decided to do a ChIP-Seq experiment using a DNA-binding protein whose binding associates with active transcription: RNA polymerase II (RNAPII). Such experiment allowed me to test the ChIP-Seq protocol using treated embryos and I could access its efficiency by comparing to transcriptome data generated in the previous Chapter. The whole-genome profile of RNAPII binding has already been described for several developmental stages in untreated *Xenopus tropicalis* embryos (Hontelez et al., 2015; Charney et al., 2017). Although these data provide temporal information on gene activation during development it fails to provide spatial information. Given this, by profiling RNAPII occupancy in dorsalised and ventralised embryos I was able to identify differentially active genes in the two conditions and validate the use of the technique in these embryos.

Profiling of RNAPII was done by chromatin immunoprecipitation followed by high-throughput sequencing (ChIP-Seq) using a ChIP-grade antibody previously used in frog embryos (Hontelez et al., 2015). I analysed the binding of RNAPII in gastrula stage embryos, the same stage used in RNA-Seq, described in the previous chapter, Nieuwkoop-Faber stage 11 (NF11). Embryos were treated with UV irradiation or LiCl as described in Chapters 2 and 3, harvested at stage NF11 and crosslinked with formaldehyde for 20 minutes at room temperature. These conditions for crosslinking were determined *a priori* by ChIP-qPCR (data not shown) and used for all ChIP-Seq experiments described in this chapter. The number of harvested embryos depended on the abundance of the protein to be precipitated. More details of the ChIP-Seq protocol are described in Chapter 2. For each ChIP experiment prior to immunoprecipitation, 2-5% of sonicated chromatin was collected and used as an input control. DNA from both the input and ChIP were used to create paired-end libraries containing adapter sequences compatible with the Illumina® sequencing platform. Sequenced data were assessed for quality of the ChIP, and if satisfactory were used for subsequent bioinformatic analyses. All of the sequencing reads were mapped to the *Xenopus tropicalis* genome assembly JGI 7.1 using Bowtie1 (Langmead, 2010) allowing only 1 reported

alignment per read and duplicate reads were suppressed from subsequent analysis.

For each condition, dorsalised (LiCl) and ventralised (UV) embryos, two biological replicates were merged, as well as all the input samples, and all were normalised per 1 million mapped reads. To identify active transcription of genes I counted the reads that mapped to gene bodies (Fig.4.1A). Annotated gene bodies were binned into 10 regions and uniquely mapped reads were counted in each bin. Active transcription is associated with transcript elongation and binning the gene body allowed to distinguish between a localised enrichment of RNAPII or a continuous enrichment along the gene body. Genes with less than 40% mappability were removed (based on the high complexity input sample) before determining RNAPII enrichment over input (RNAPII/Input).

For each condition, genes were considered to be actively transcribed if at least 80% of the gene body had an enrichment of 2.6 fold over the input sample. This allowed me to identify 1468 genes actively transcribed in LiCl-treated and 1011 genes in UV-treated embryos. Genes were specified as differentially active between LiCl- and UV-treated embryos if there was >1.5 fold difference of continuous enrichment along the gene body between these conditions. I identified 679 preferentially active genes in dorsalised embryos and only 105 in UV. Figure 4.1B and C shows the average binding (coverage) of RNAPII over gene bodies of each identified category of differentially active genes. This approach allowed to confidently identify genes whose transcription levels were higher in one condition compared to the other.

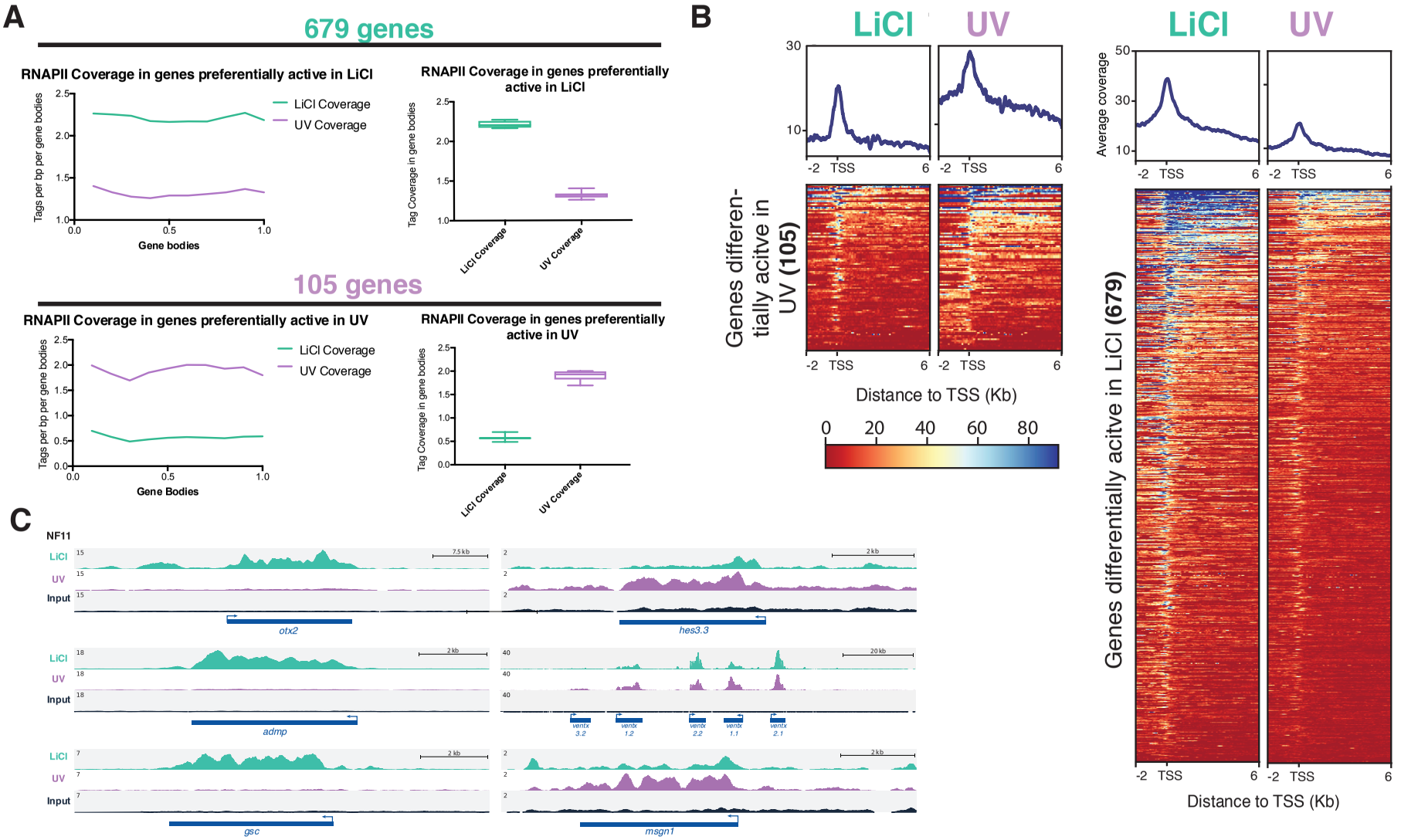

Figure 4.1: **RNAPII profiling in dorsalised and ventralised embryos**

A) Average DNA occupancy of RNAPII in genes identified as preferentially active in LiCl- and UV-treated embryos. **B)** Heatmap of RNAPII binding in genes differentially active in dorsalised (LiCl) and ventralised (UV) embryos. Plot on top of the heatmap represents the average DNA occupancy around the transcription start site (TSS).**C)** Genomic snapshot of RNAPII binding in genes differentially activated: *otx2*, *admp* and *gsc* in dorsalised embryos and *hes3.3*, *ventx* family members and *msgn1* in ventralised embryos. LiCl - Lithium chloride; UV - Ultra-violet; TSS - transcription start site; msgn - mesogenin; otx - orthodenticle homeobox; admp - anti dorsalising morphogenic protein; ventx - vent homeobox; gsc - goosecoid; hes - hairy and enhancer of split.

4.1.1 Preferentially active transcription positively correlates with transcriptome output

Reassuringly, the preferentially active genes in dorsalised embryos included dorsal markers such as *otx2*, *admp*, *gsc*, *nog* and *not* while ventral markers were preferentially transcribed in ventralised embryos, such as *msgn1*, *ventx1.1*, *ventx1.2*, *evx1*, *bambi* (Fig.4.1C). In addition to the known markers, other genes identified in the transcriptome comparison also showed increased RNAPII enrichment, such as *pkdcc.1* and *loc388630* in LiCl-treated embryos and *hes3.3*, *foxj1* and *72022004* (*Xetro.A01563*) in UV-treated embryos.

A more general comparison between RNAPII binding and the transcript level, revealed that genes with higher transcript levels in LiCl (Chapter 3) had, on average, an higher binding of RNAPII to its gene body in dorsalised than in ventralised embryos (Fig.4.2A,B). Similarly, the coverage of RNAPII on genes with higher transcript levels in ventralised embryos was higher compared to dorsalised embryos. Another common feature to the RNAPII and transcriptome analyses was that higher numbers of differentially active and upregulated genes were found in dorsalised embryos compared to ventralised embryos. Moreover, Figure 4.2B indicates that even in genes downregulated in LiCl-treated embryos, there was some binding of RNAPII to the TSS, but less elongation, while the binding of RNAPII to genes downregulated in UV-treated embryos was generally lower.

In summary, RNAPII binding differed between dorsalised and ventralised embryos, which allowed the identification of differentially transcribed genes. Furthermore, active transcription correlated positively with the transcriptome data. The data also indicated that dorsal cells were transcriptionally more active than ventral cells, as detected at the chromatin and transcriptome levels.

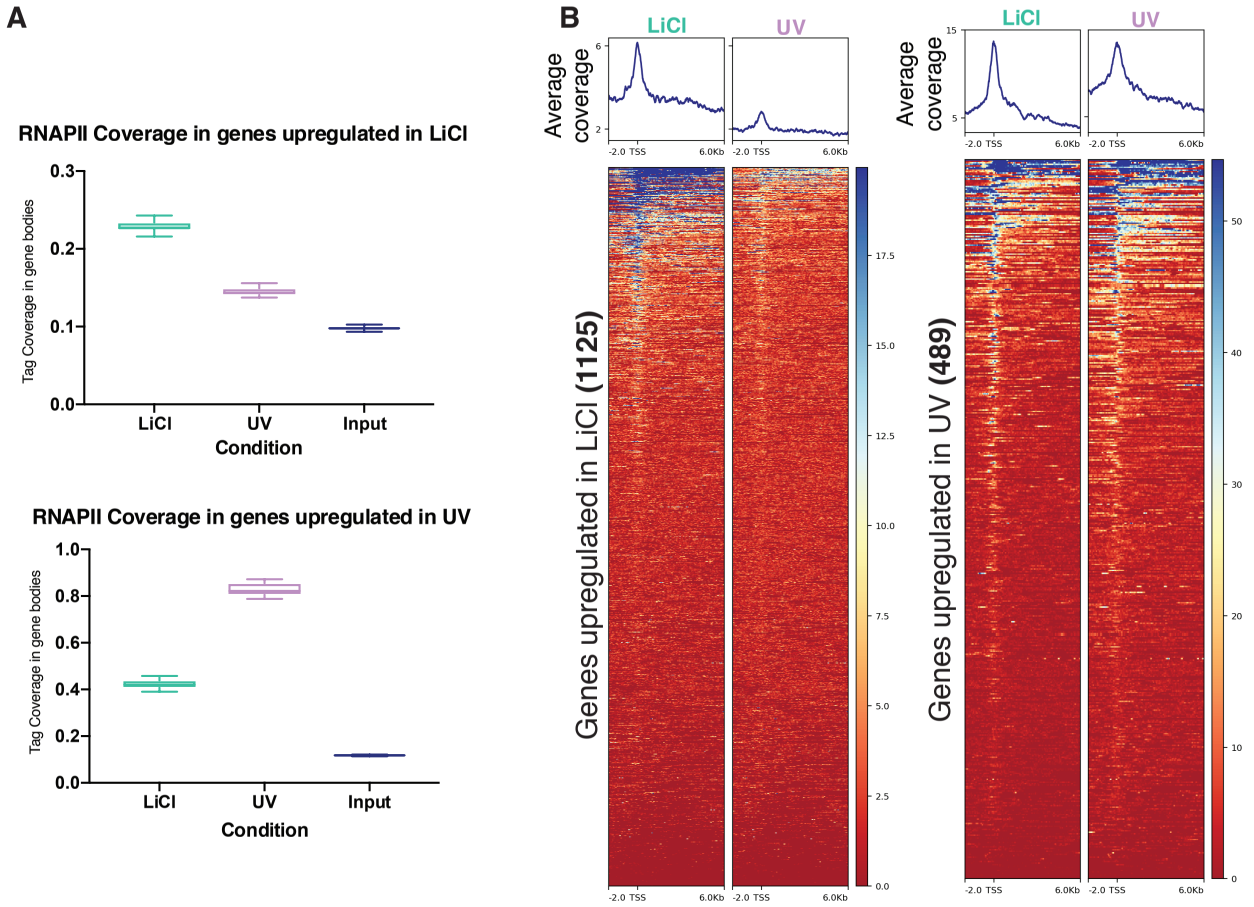

Figure 4.2: **Correlation between gene RNAPII binding and transcript level**

A) Average DNA occupancy of RNAPII in gene bodies of upregulated genes in LiCl- and UV-treated embryos. **B)** Hierarchical heatmap of RNAPII ChIP-Seq in gene bodies upregulated in dorsalised and ventralised embryos.

4.2 Binding of the enhancer protein p300 correlates positively with active transcription

Following the identification of transcriptional differences at the chromatin levels I was interested in investigating regulation at the enhancer level. For this I opted to perform ChIP-seq of the transcription co-activator protein p300, commonly used as a marker for active enhancers (Heintzman et al., 2007; Visel et al., 2009). Like the RNAPII ChIP, gastrula stage LiCl- and UV-treated embryos (NF11) were used to detect p300 binding. For this experiment I only had one sample per condition and because of this I adopted a distinct approach to study active enhancers in dorsalised and ventralised embryos. Instead of comparing the two samples I characterised the binding for each cell type separately. p300 ChIP-Seq profile is similar to that of a transcription factor, and so, unlike RNAPII, genomic profiling of p300 binding resulted in the identification of peaks. These are regions with high focal enrichment compared to the input sample. These peaks or genomic intervals represent putative regulatory regions. Like RNAPII, the binding of p300 has also been described in early development of *Xenopus tropicalis* across different developmental stages (Hontelez et al., 2015).

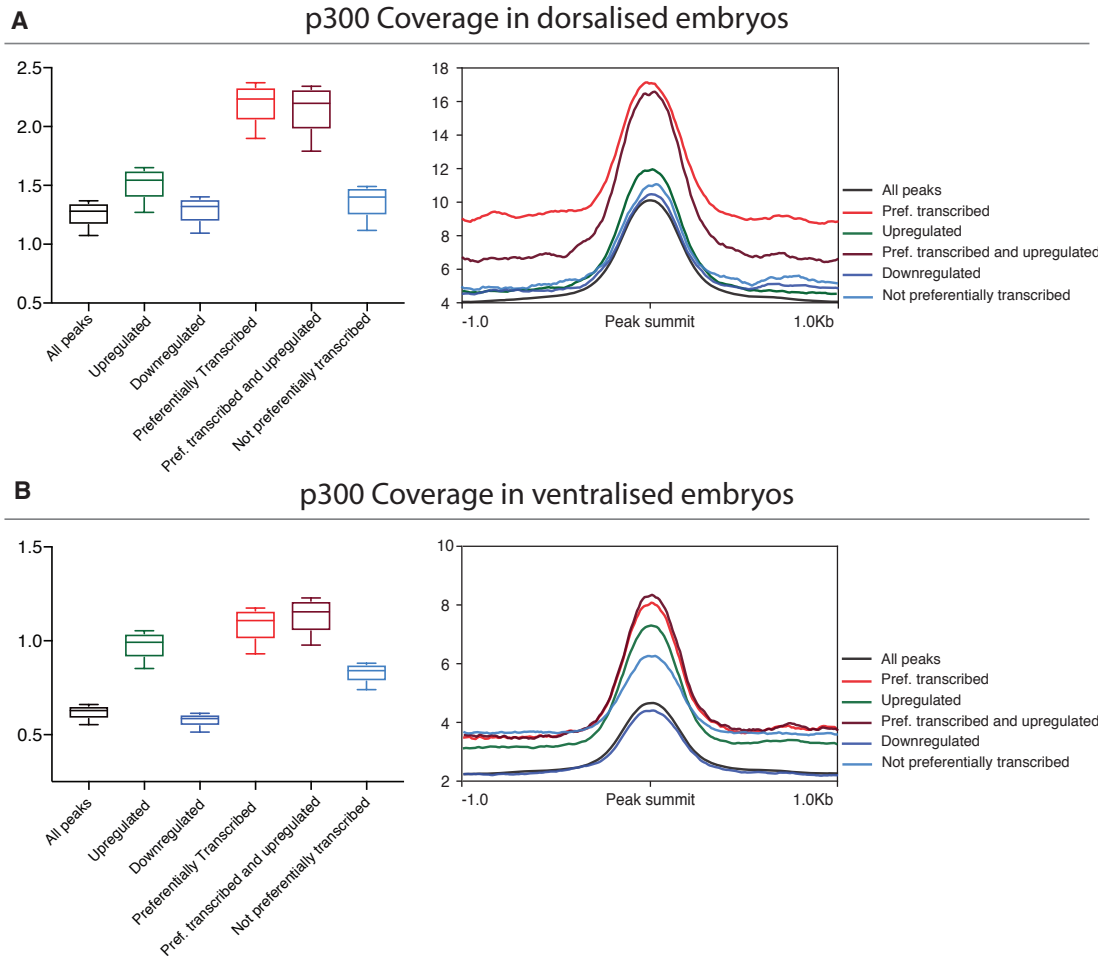

Figure 4.3: **p300 coverage in dorsalised and ventralised embryos**

A) DNA occupancy of p300 near different genes, grouped by expression levels or RNAPII binding, in dorsalised embryos. Genes upregulated and downregulated refer to the RNA-Seq comparison between LiCl- and UV-treated embryos. Genes preferentially transcribed refer to genes with higher RNAPII binding when compared to the other condition. Genes not preferentially transcribed are genes with an RNAPII enrichment >2.6 over the input but <1.5 over the other condition. For each condition, the plots on the left and right-hand side represent the same data, box-plot of the read distribution and an average profile of the binding around the peak summit, respectively. **B)** Same as **A)** , but related to p300 binding in ventralised embryos.

I used published data of p300 binding at gastrula stages (NF10.5 and NF12.5) (Hontelez et al., 2015) to identify p300 binding sites (putative enhancers), in the whole untreated embryo, by peak calling. Since there was no data to represent the exact developmental stage at which I analysed the binding of p300 (NF11) I merged the peaksets of the the time points immediately before and after, which should cover all of the active enhancers during gastrulation. My approach was to count the number of reads (normalised to 1 million mapped reads) from my p300 ChIP-Seq on dorsalised and ventralised embryos, that covered distinct sets of these enhancers. Since there

was no genome-wide data on chromosome conformation in early frog development that would allow enhancers to be mapped to their genes, I used the closest gene approach. For each condition I identified the p300 binding sites closest to genes with differential transcript and RNAPII binding levels between UV- and LiCl-treated embryos. Figure 4.3 shows that, in both conditions, p300 DNA occupancy was higher near genes that were upregulated and were preferentially transcribed compared to the other p300 peaks. Figure 4.4, shows an example of the binding of RNAPII and p300 near the *msgn1* and *gsc* loci. It showed that *gsc* was highly transcribed in LiCl, seen by RNAPII track, which was accompanied by DNA occupancy levels of p300 (peak height) when compared to *msgn1*, a gene downregulated in dorsalised embryos. Vice-versa when analysing the same genes in ventralised embryos, *msgn1* was highly transcribed and had robust binding of p300 while *gsc* showed almost no binding of RNAPII and p300.

The positive correlation between RNAPII and p300 was expected since both proteins mark positive transcription, and my analysis reinforced the cell-type specific behaviour of both. Unfortunately, I did not manage to generate genome-wide tracks of chromatin accessibility, either by assaying for transposase accessible chromatin with high-throughput sequencing (ATAC-Seq) or by mapping DNAse I hypersensitive sites across the genome (DNase-Seq). This was due to technical complications of applying either protocol in gastrula stage embryos derived from the high yolk content. However, p300 binding has been associated with DNaseI hypersensitive sites (Heintzman et al., 2007), indicating that the binding of this protein could be used as a proxy for open chromatin. Given this, the data suggested that regions near active genes in dorsal and ventral cells were more accessible than regions that are not active (Fig. 4.3).

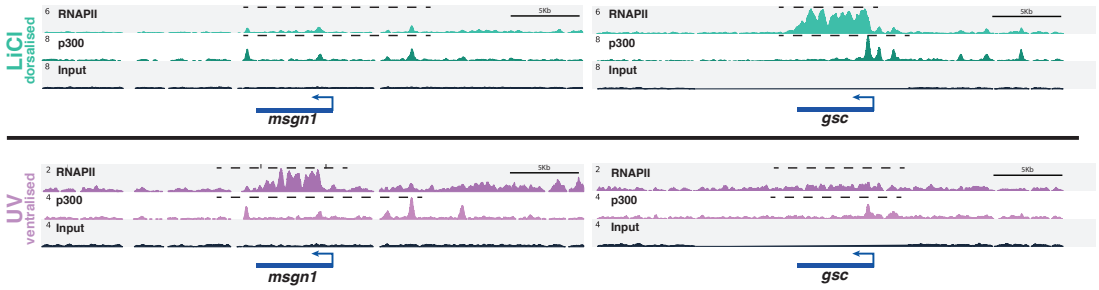

Figure 4.4: **Binding profile of RNAPII and p300 in genomic regions near *gsc* and *msgn1* in dorsalised and ventralised embryos**

Genomic snapshot around *goosecoid* (*gsc*) and *mesogenin 1* (*msgn1*) loci in dorsalised and ventralised embryos with the tracks for RNAPII and p300 ChIP-Seq. (*msgn1*) is upregulated and differentially transcribed in ventralised embryos and *gsc* in dorsalised embryos. Higher RNAPII binding to gene bodies correlates with higher p300 binding in the proximal regulatory regions.

4.3 Brachyury binding in dorsalised and ventralised embryos

Since I detect cell type specific differences in active chromatin I was interested in understanding if this would influence the behaviour of other transcription factors. For the rest of this Chapter, I tackle this question by studying the binding of a zygotic transcription factor present in dorsal and ventral cells. I hoped to explore whether and how cell type specific recruitment behaviour of a transcription factor (TF) occurs *in vivo*. I chose to study Brachyury (or t) binding because it is a well studied TF, whose binding profile has been thoroughly analysed in early frog development (Gentsch et al., 2013) and, furthermore, it has been described to bind different genomic targets in distinct mesodermal derivatives from human embryonic stem cells (hESCs) (Faial et al., 2015).

4.3.1 Validation of ChIP-grade antibody

To perform ChIP-Seq, I used two different antibodies against *Xenopus* Brachyury, one, previously used and validated for the same purpose (Gentsch et al., 2013) and a second antibody generated during this project (see Materials and Methods for details). The second antibody, referred here as the new antibody (nAb) was generated as a result of reduced stock of the original one. For validation of the new antibody I fol-

lowed the ENCODE ChIP-Seq guidelines for antibody validation (Landt et al., 2012), that includes primary and secondary characterisation. Before antibody purification, the rabbits' bleeds were tested in a dotblot assay (data not shown), using purified Brachyury protein, and upon purification the antibody was tested by Western Blot (WB), immunoprecipitation (IP) and whole-mount immunohistochemistry (WMIHC) in gastrula stage embryos (Fig. 4.5). The antibody was used to immunoprecipitate endogenous and exogenous Brachyury protein by WB using anti-Brachyury serum (Cunliffe and Smith, 1994) or an anti-HA antibody, which were detected as bands of the correct size (50 kDA) (Fig. 4.5A). However, the antibody did not recognise the denatured form of the protein in a WB (Fig. 4.5B). I reasoned that this happened because the antibody was purified using the native full length protein. Furthermore, the antibody was also validated for spatial expression of the protein as seen by WMIHC, marking the mesodermal involuting sheet of cells of the late gastrula stage embryo (Fig. 4.5C).Furthermore the antibody was successfully used for ChIP. This means that this antibody was of ChIP-grade quality that preferentially recognised the native form of Brachyury.

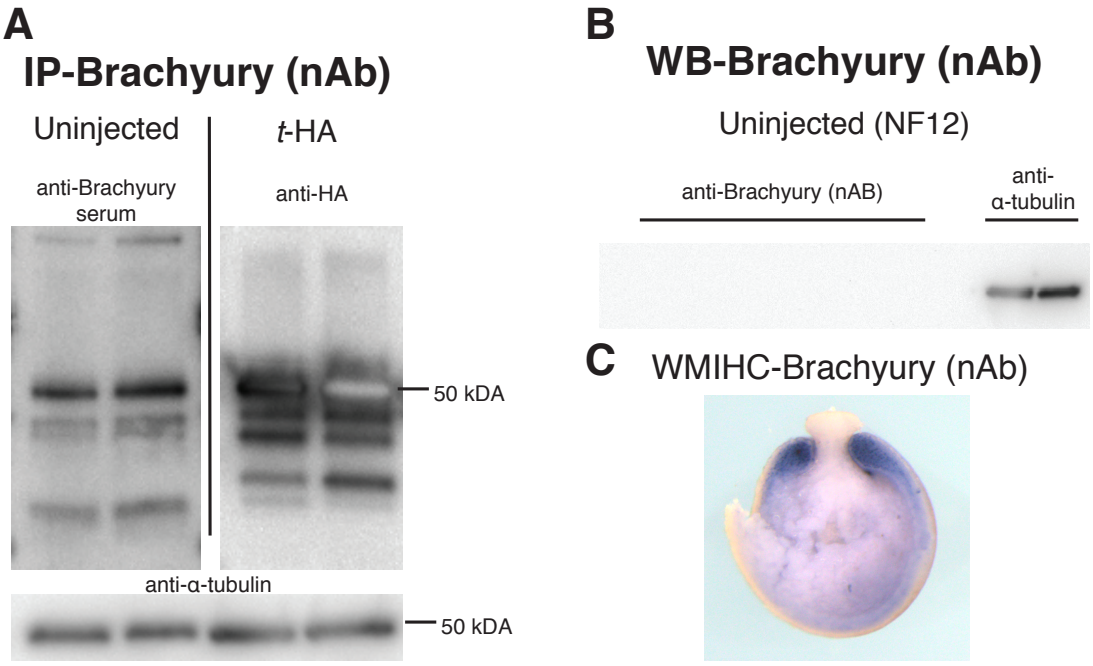

Figure 4.5: **Validation of anti-Brachyury antibody for ChIP-Seq**

Three assays were used to validate the new antibody against Brachyury; immunoprecipitation (IP), Western Blot (WB) and whole embryo immunohistochemistry. **A)** Embryonic extract of uninjected and embryos injected with *t*-HA mRNA were immunoprecipitated with the new antibody and loaded into a polyacrylamide gel for WB. For blotting I used anti-Brachyury serum and anti-HA antibody to detect endogenous Brachyury and HA-*t*, respectively. **B)** Western Blot of whole embryos extract and the new anti-Brachyury antibody was used to blot. No signal was detected, indicating that this antibody does recognise the denatured form of the protein. **B)** WMIHC on bissected stage NF12 *Xenopus tropicalis* embryo using the new Brachyury antibody.

4.3.2 Comparison of the binding of Brachyury in dorsalised and ventralised embryos

I performed several ChIP-Seq on stage NF11 *Xenopus tropicalis* LiCl- and UV-treated embryos using different antibodies against Brachyury. For each condition I performed the experiment three times, representing three biological replicates, replicate 1 (rep.1) and 2 were performed using the antibody described before (Gentsch et al., 2013) while replicate 3 corresponds to the ChIP experiment using the antibody generated during this project. Figure 4.6 shows the correlation between the different replicates based on normalised read coverage on peaks identified in any ChIP sample. The input profile was the result of merging all the inputs libraries sequenced during the project in order to obtain a high complexity control. The replicates of each condition clustered

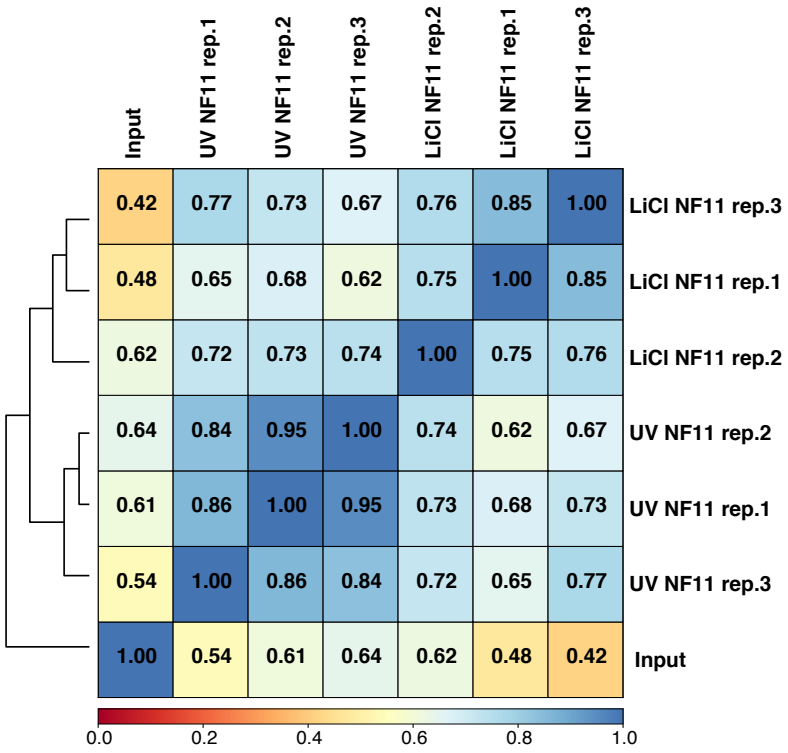

Figure 4.6: **Correlation between Brachyury ChIP replicates in dorsalised and ventralised embryos**

The correlation was calculated based on the number of reads in peaks and the values represent the Pearson correlation coefficient.

together, but UV replicates were more similar amongst each other than were LiCl replicates; the average Pearson correlation factor was 0.9 and 0.8, respectively. This clustering indicated that the Brachyury binding was distinct in ventralised and dorsalised embryos, but most of the binding was probably similar, specially as seen by the correlation between conditions.

The genomic targets of Brachyury have previously been identified for stage NF12 embryos, so in order to accuretely compare to my dataset I also performed ChIP-Seq on untreated stage NF11 embryos (WT). The Brachyury genomic targets identified in this sample are represented in the heatmap on Figure 4.7A, together with the read coverage from Brachyury ChIP-Seq on LiCl- and UV-treated embryos. There were four distinct clusters characterised by the Brachyury coverage which was seemingly higher in UV compared to LiCl in the top two clusters (Fig. 4.7, dark blue and light blue), but similar on the other two clusters (Fig. 4.7, lime green and orange).

To explore the differences between the two conditions I did peak calling on each

replicate separately using the same high complexity input and a more stringent q-value cutoff ($5e^{-4}$), using the software MACS2 (Feng, Liu, and Zhang, 2002; Zhang et al., 2008). Each peakset was further filtered based on the fold enrichment of each peak (minimum of 5 fold). The exact fold change threshold was set based on the visual inspection of called peaks. MACS2 is an excellent tool to identify binding events based on sequencing reads. However, peak calling success is largely dependant on the signal-to-noise ratio of the binding profile and complexity of the ChIP-Seq library. For this reason, it was necessary to evaluate the quality of the peak calling individually and set different thresholds for each replicate. Each peakset, a list of genomic coordinates, was extended by 150 basepairs (bp) up- and downstream from the peak summit. Every ChIP-Seq experiment has regions with high artificial signal known as 'blacklisted' regions, which I identified by performing peak calling on the input sample using no control. These regions were then subtracted from the LiCl and UV peaksets. Next, I defined a set of genomic regions that represented Brachyury binding events in dorsalised and ventralised embryos. This list was constructed by finding peaks that were shared by at least two of three biological replicates. Using this strategy I identified 627 peaks in dorsalised embryos and 1108 peaks in ventralised embryos (Fig. 4.7B).

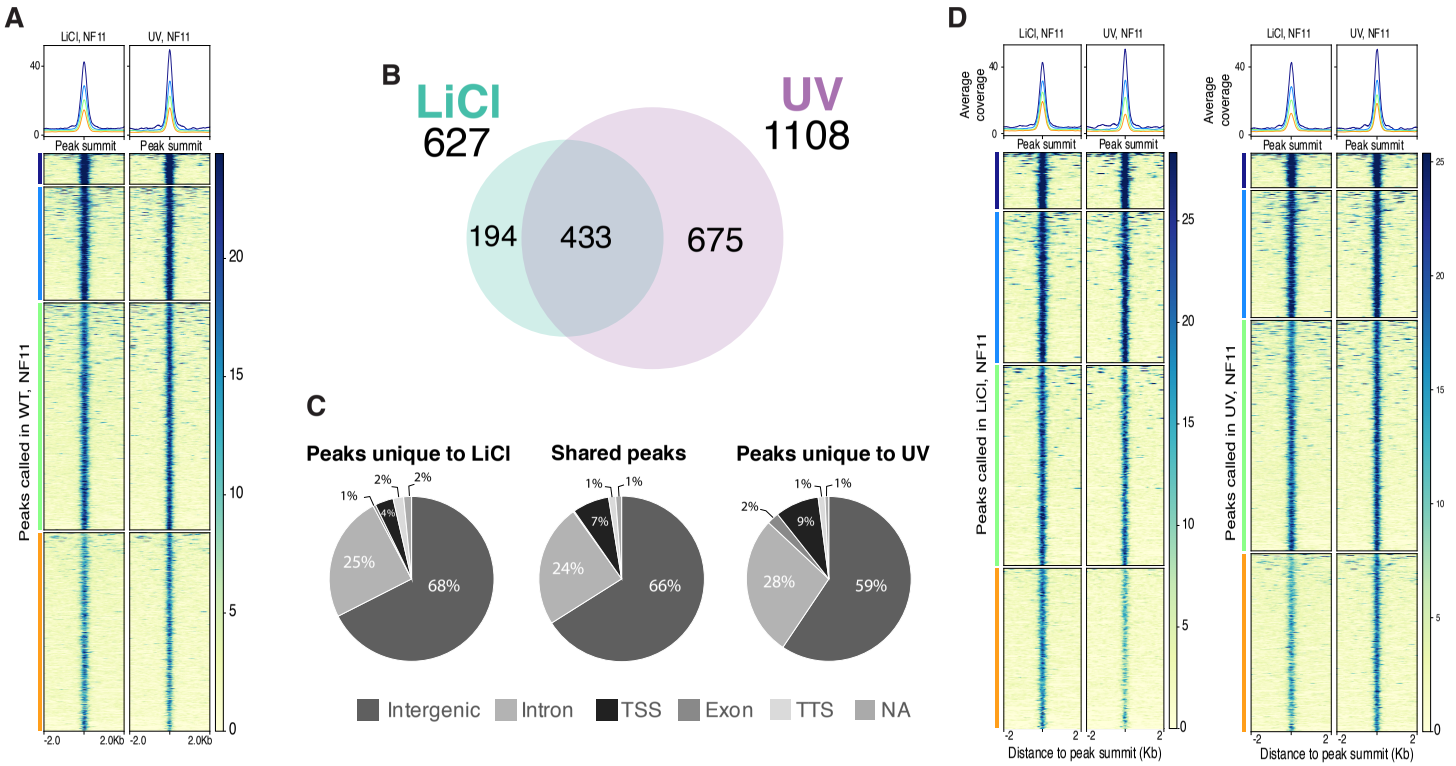

Figure 4.7: **Characterisation and comparison of Brachyury ChIP-Seq in dorsalised and ventralised embryos**

A) Clustered heatmap of DNA occupancy of Brachyury in LiCl- and UV-treated embryos. **B)** Venn diagram of the comparison of peaks called by MACS2 in each condition. Each peakset is a consensus of the three replicates of each condition. **C)** Pie-chart of genomic localisation of peaks uniquely and shared Brachyury binding. **D)** Clustered heatmaps showing the read density of the merged ChIP-Seq experiments of each condition in peaks called in dorsalised or in ventralised embryos. TSS - transcription start site, TTS - transcription termination site; NA - not applicable; Kb - kilobases.

The first observation was that the number of peaks called in ventralised embryos was almost twice the number of binding events that were detected in dorsalised embryos. Secondly, when comparing the peaksets, the majority of the LiCl peaks were shared with UV (433, 69%) (Fig. 4.7B). Comparison to the genomic targets identified in WT NF11 embryos indicated that there was no extraordinary new binding events occurring in any of the conditions (1185 of the total 1302 peaks, 91% are shared).

The genomic localisation of these peaks revealed little difference between the unique (not shared) and shared peaks (Fig. 4.7C). The majority of the binding events was found in intergenic and intronic regions, peaks unique to ventralised embryos were detected more frequently in the promoter (transcription start site (TSS)) and exon regions at the expense of intergenic regions (Fig. 4.7C).

The comparison of the read distribution between LiCl and UV conditions for these peaksets revealed that DNA occupancy of Brachyury is higher in UV-treated embryos (Fig. 4.7D, darker blue cluster); except for one cluster of peaks found in the LiCl condition (Fig. 4.7D, orange cluster).

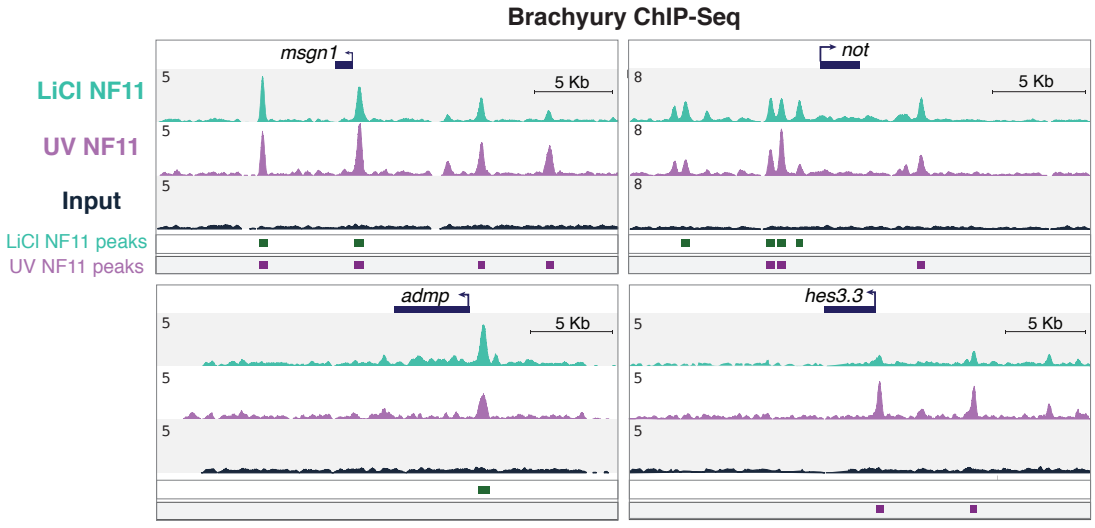

Figure 4.8: **Condition-dependent DNA occupancy of Brachyury at called peaks**

The peakset comparison revealed sites that are bound in both conditions (shared) or only in one of the conditions (unique). The figures shows examples of genomic regions where the three kinds of peaks are found; near the locus of *msgn1*,*admp*, *not* and *hes3.3*.

Despite the fact that the overall enrichment of Brachyury in dorsalised embryos was lower than in ventralised embryos, there was still a set of peaks called only in one condition (unique). The classification of unique peaks was based on the peak calling done for each condition as described above. In some cases, the unique peaks might have Brachyury binding in the other condition, however, given the criteria defined for peak calling, it was not considered a peak in that condition. Figure 4.8 shows four genomic locations near four developmentally relevant genes, the binding profile of Brachyury and the peaks called for each condition. The top two examples show binding near *msgn1* and *not*, two known Brachyury targets, and a set of shared and unique peaks (Fig. 4.8). The two bottom genomic snapshots are regions near the genes *admp* and *hes3.3* and show peaks unique to LiCl and UV, respectively. Interestingly, both *admp* and *hes3.3* are differentially transcribed in dorsalised and ventralised embryos, respectively, which could indicate that Brachyury occupancy is higher near genes transcriptionally active. However, I did not find any correlation between sites uniquely bound in each condition and gene transcription.

In summary, the data indicated that DNA occupancy by Brachyury was higher in ventralised embryos compared to dorsalised embryos. These differences resulted in the identification of more binding sites in UV- than in LiCl-treated embryos. The comparison of the binding sites revealed that most of the identified sites in dorsalised embryos were shared with the other condition, and only a small subset of sites were uniquely bound. Furthermore, I did not find any correlation between unique sites and tissue-specific active transcription or enhancers. Moreover, visual inspection of the DNA occupancy of Brachyury in the sites identified as uniquely bound in one condition, indicated that peak calling was not reliable in identifying differential binding.

4.3.3 Comparison of the binding of Brachyury in dorsalised and ventralised embryos

Similarly to the analyses done for RNAPII, I calculated the ratio of normalised read counts in peaks, between LiCl and UV (LiCl/UV, positive is high in LiCl). As expected the ratio was positive for the sites identified as unique in LiCl and negative

in UV unique sites and the fold change of shared peaks is close to 1, with a similar distribution of positive and negative ratios (Fig. 4.9). This indicated that most of the peakset comparison reflected some of the quantitative differences of Brachyury binding in between conditions.

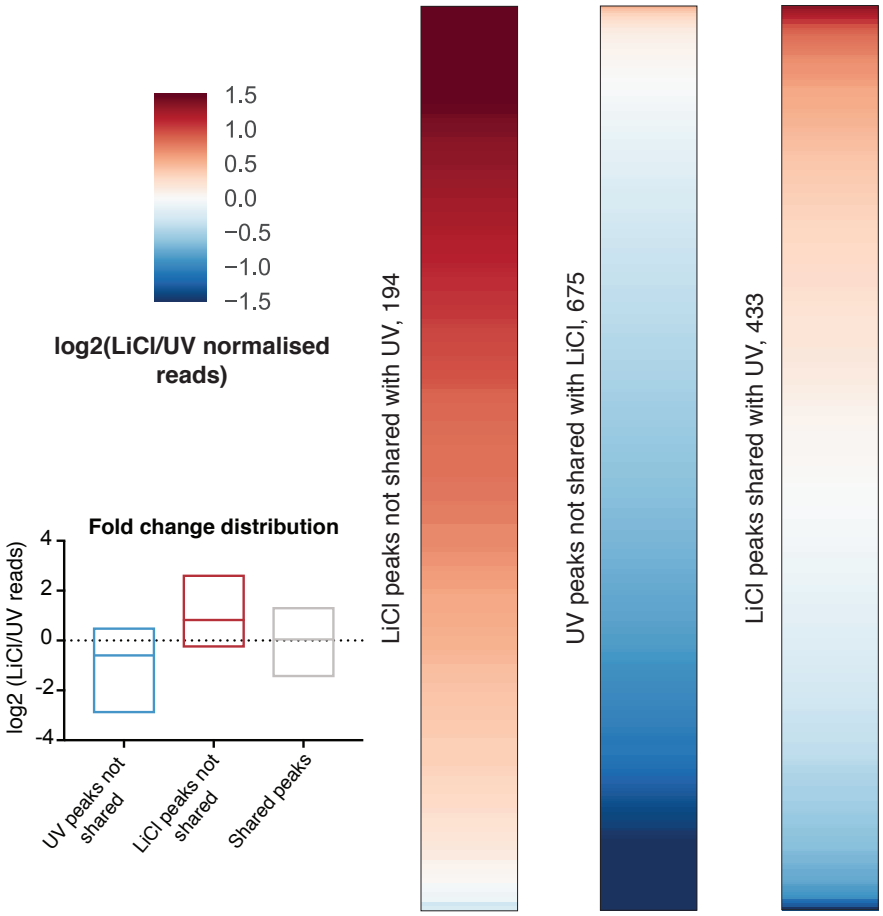

Figure 4.9: **Peak calling reflected quantitative differences in Brachyury binding**

Reads from dorsalised and ventralised Brachyury ChIP-Seq were counted in the three peaksets; unique to LiCl or UV and shared peaks. For each condition the LiCl/UV ratio was calculated and $\log_2$ transformed. The boxplot shows the distribution of these ratios and the heatmap shows the ratio of each peak. Red means that the binding is higher in dorsalised and blue in ventralised embryos.

4.4 Quantification of Brachyury in dorsalised and ventralised embryos during gastrula stages

The main observation from the Brachyury ChIP-Seq experiment on dorsalised and ventralised stage NF11 embryos was that the former had less binding events with less DNA occupancy. This led me to question whether there were differences in Brachyury

protein levels between the two conditions: less protein in LiCl-treated embryos. The transcriptome comparison by RNA-Seq (Chapter 3) revealed that *Brachyury* had higher transcript levels in ventralised embryos with a fold change of around 2. In whole embryos the expression of Brachyury is seemingly constant around the blastopore, similar in ventral and dorsal cells, at gastrula stage. However, it has been described that dorsally, the expression is lower due to the presence of *goosecoid*, a *Brachyury* repressor (Boucher et al., 2000). Given that dorsalised embryos have an expanded expression domain of *goosecoid*, it is expected that dorsalised embryos have lower levels of Brachyury.

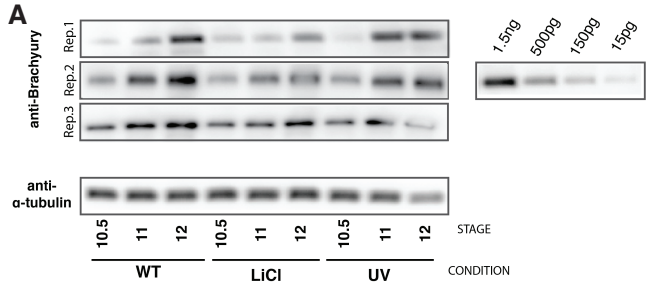

B

Stage/ Condition	LiCl/WT	LiCl/UV	UV/WT
10.5	0.77	0.63	1.20
11	0.84	0.63	2.04
12	0.69	1.66	0.54

LiCl NF12/WT NF11	LiCl NF12/UV NF11
1.28	0.93

Figure 4.10: **Semi-quantitative IP/WB of Brachyury in three gastrula stage untreated (WT), LiCl- and UV-treated embryos**

A) For each stage 10 *Xenopus tropicalis* embryos were collected and embryonic extract was immunoprecipitated using the same antibody used for ChIP-Seq. The IP samples were loaded into a polyacrylamide gel, together with Brachyury purified protein of known concentration. The experiment was done three times which are represented as replicate 1-3. **B)** Using the chemiluminescence from the protein dilution series, a standard curve was designed and a concentration was assigned to each experimental band. The tables show the ratio, averaged from the three experiments, between the conditions at each stage. The second table shows that the ratio between LiCl NF12 and LiCl NF11 is around 1.

To investigate this, I designed a short time-series experiment to quantify Brachyury levels in LiCl-, UV-treated and WT embryos. The time series included the stage I used for ChIP (NF11) plus the stage before (NF10.5) and after (NF12). This way, I was able to detect the dynamics of Brachyury during gastrula stages, compare the conditions and identify stages where the amount of protein was similar. Embryos were cultured at 25°C and embryos of the three stages were collected around 60-75min apart. For each stage, 15 embryos were harvested and the embryonic extract was used to precipitate Brachyury, using the old ChIP-grade antibody. The IP was visualised by Western Blot and quantified by running a known amount of purified Brachyury protein on the

same polyacrylamide gel (Fig. 4.10). The experiment was done three times and the average ratio of protein quantification between the conditions is shown in Figure 4.10. The expected dynamic of Brachyury expression was observed in untreated embryos; increased during gastrulation reaching high levels at stage 12. Interestingly, on the one hand UV-treated embryos reached similar levels of Brachyury, earlier, at stage NF11.5, which were maintained during stage NF12. On the other hand, LiCl-treated embryos had lower levels of Brachyury throughout the first two stages analysed, but by stage NF12 the levels were similar to those in stage NF11 UV-treated embryos (Fig. 4.10, ratio LiCl NF12/UV NF11.5 of 0.98). Neither dorsalised nor ventralised embryos had differences in developing speed, as described before (Cooke and Smith, 1987; Cooke and Smith, 1988) and observed in this work, which indicated that the differences in Brachyury levels were specific to its regulation. I did not explore what led to these differences, however I hypothesise, that in dorsalised embryos Brachyury expression is reduced due to the high levels of *goosecoid* and *otx2* (Latinkic et al., 1997; Latinkic and Smith, 1999; Lerchner et al., 2000) while in ventralised embryos high zygotic Wnt signalling, via xWnt8, maintains high levels of Brachyury (Vonica and Gumbiner, 2002; Sokol, 1993).

The time-series experiment confirmed the hypothesis that the levels of Brachyury are lower in dorsalised embryos which could explain the differences seen in the binding of the transcription factor. This indicated that, in addition to the cell type specific conditions that Brachyury encounters in the nucleus, the amount of available protein may also influence its binding to the DNA. Given this, I decided to study the binding profile of Brachyury in stage NF12 dorsalised embryos in which the levels of the TF were similar to those of the ventralised embryos. This comparison allowed me to first understand whether the increase in protein concentration leads to more binding of Brachyury and, secondly, I could more accurately compare it to ventralised embryos. However, this comparison was not ideal since I was comparing two different developmental stages, but given the circumstances of working with an *in vivo* model this was the most reasonable strategy. Furthermore, the binding profile of Brachyury had been shown to be reasonbly constant between developmental stages even further apart, gastrula and tailbud (Gentsch et al., 2013), and so I assumed that one hour of

development would not cause drastic changes.

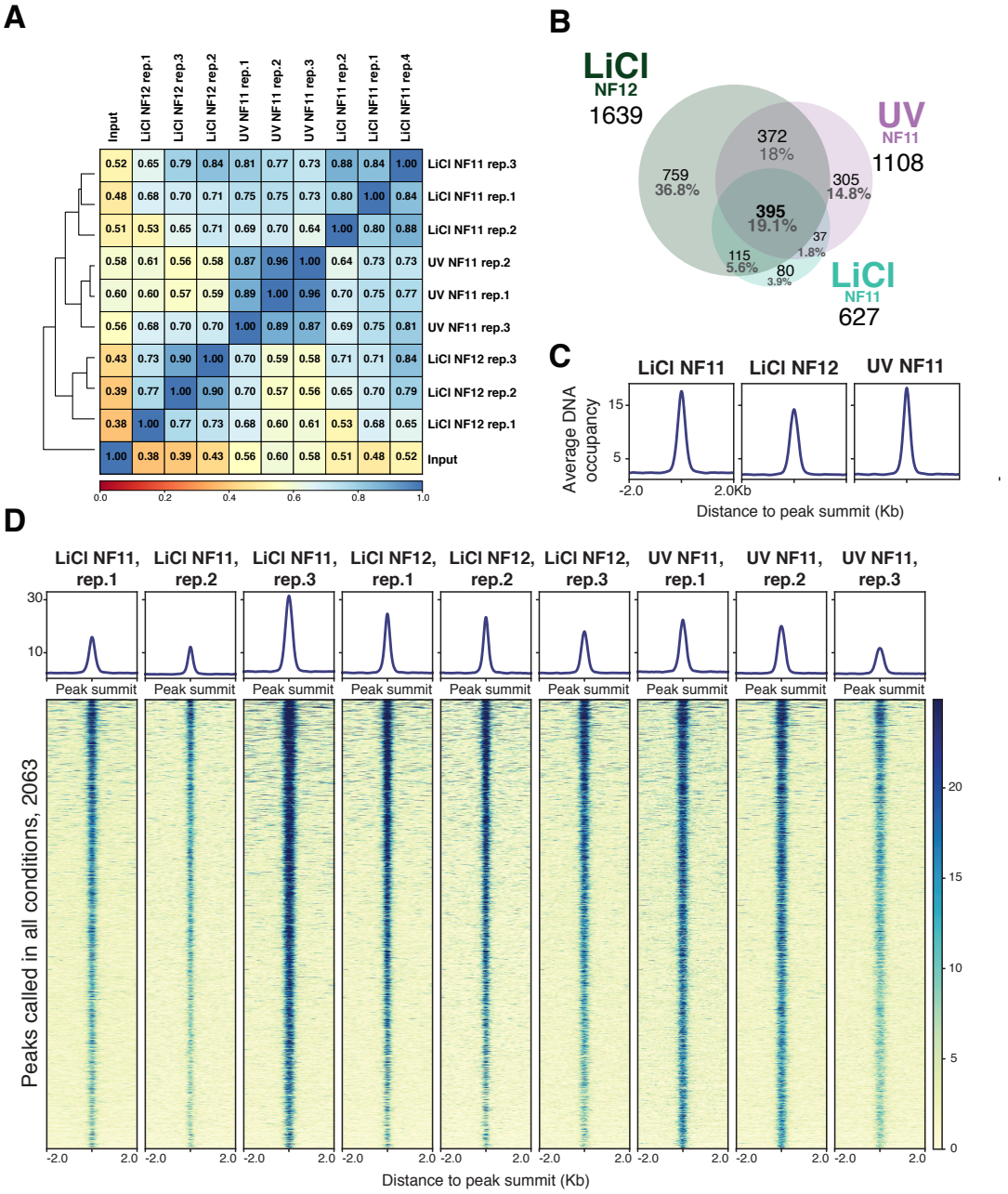

Figure 4.11: **Brachyury ChIP-Seq on Stage NF12 dorsalised embryos and comparison to the other two conditions**

A) Pearson correlation between all replicates based on reads in peaks called in all conditions. Replicates of each condition cluster together. **B)** Venn diagram of the comparison of peaksets identified in each condition. Percentages are related to peaks called in all conditions, 2063. **C)** Average DNA occupancy in all peaks, of the merged reads of the three replicates, of each condition. **D)** Heatmap showing hierarchical distribution of Brachyury DNA occupancy of each replicate, within 2kb of the Brachyury peaks summits.

4.5 Higher levels of Brachyury lead to more binding events in dorsalised embryos

Similarly to the experiments described above on stage NF11 embryos, I performed ChIP-Seq on LiCl-treated embryos harvested at stage NF12 in biological triplicates, using two different Brachyury antibodies; replicate 1 with the previously published antibody (Gentsch et al., 2013) and replicates 2 and 3 with the antibody produced during this project. The sequencing data was processed for quality control as previously described and the for each replicate, peaks were called and subsequently filtered as described above. A Brachyury peakset for LiCl NF12 was made from the comparison of the three replicates; only peaks found in at least two of the replicates were considered. This peakset contained 1639 peaks, which were almost three times the number of peaks called in stage NF11 dorsalised embryos (Fig. 4.11B). This observation indicated that the increase in the amount of Brachyury led to more binding events and even more than the number observed in ventralised embryos with similar Brachyury expression levels (Fig. 4.10).

The comparison of the peaksets of all conditions resulted in the identification of 2063 binding sites: 36.7% were unique to stage NF12 dorsalised embryos, while a similar number of peaks were shared between LiCl NF12 and the other two conditions (395, 19.1%) or shared only with UV NF11 (373, 18%) (Fig. 4.11B). Ventralised embryos yielded 305 uniquely called Brachyury binding sites, while dorsalised embryos of stage NF11 shared most of their peaks with the other two conditions (Fig. 4.11B).

Interestingly, when comparing the overall DNA occupancy across all peaks, the average in LiCl NF12 was marginally lower than the other two conditions which had comparable DNA occupancies (Fig. 4.11C). The profiles shown in Figure 4.11 were based on merging the reads from the three replicates of each condition. However, when plotting the profile of each replicate a considerable variation among them was clear. The most striking difference from other replicates was seen in replicate 3 of LiCl-treated NF11 embryos which could be explained by the use of a different antibody. However, I do not observe this trend in the other conditions e.g, UV NF11 rep.3 was done using the same antibody, and this was the replicate with the lowest overall occupancy. Nevertheless, the comparison of DNA occupancy across all peaks revealed

that the replicates of each condition clustered together, the Pearson correlation between replicates for each condition ranged from 0.8 - 0.9 (Fig. 4.11A). However, LiCl NF11 replicate 3 had a correlation of 0.84 and 0.79 with LiCl NF12 replicate 2 and LiCl NF12 replicate 3, respectively. These differences reinforced the importance of biological replicates in ChIP-Seq experiments, specially when comparing different conditions and dissecting quantitative differences.

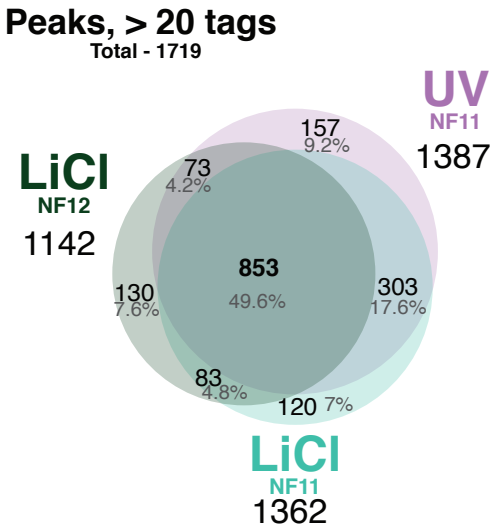

Figure 4.12: **Venn diagram of peaks called based on tag/read count**

Reads of each condition were counted in the 2063 peaks and regions with more than 20 tags (normalised mapped reads) were considered a peak of that condition. The threshold was set on 20 tags based in the maximum number of tags counted in the input sample. The percentages are related to total number of peaks with more than 20 tags, 1719.

The analysis of stage NF11 LiCl- and UV-treated embryos revealed that peak calling was not the most reliable tool to identify small differences in the binding profile of a transcription factor. While peak calling algorithms are good at identifying higher DNA occupancy peaks, the identification of smaller peaks is less reliable. A way of dissecting the quantitative aspect of the binding was by counting the reads of each condition in all 2063 peaks called previously. Thus, peaks were re-called if the condition yielded more than twice the maximum of input tags (mapped reads) recorded within genomic regions of the peakset. Figure 4.12 shows a Venn diagram that resulted from such an approach and based on a threshold of 20 tags per peak. With this approach, around 300 peaks were discarded from all the conditions for the low number of reads, and the

majority of peaks were shared between the conditions (853, 49.6%) (Fig. 4.12). This led to an increase of 30% in the number of the shared peaks (Fig. 4.11B, 19.1%), mostly at the expense of LiCl NF12 peaks. This approach also indicated that the majority of the binding sites are shared between all the conditions; e.g, majority of sites have more than 20 reads in the three conditions. This indicated that if there were differences in the binding of Brachyury, these would be quantitative. In order to identify these differences I would have to use a bioinformatic tool that allowed to me identify which sites are consistently, within replicates, and significant, between conditions, differentially bound.

So far, I have shown that the detection of Brachyury binding was affected by the expression level. Stage NF11 dorsalised embryos yielded a low number of detectable binding events which increased substantially by stage NF12, when protein levels were similar to those observed in ventralised NF11 embryos. In dorsalised stage NF12 embryos more Brachyury binding events were identified by peak calling. As a result of analysing the data by counting mapped reads in peaks, I decided to dismiss the peak calling as a tool to identify the differences between dorsalised and ventralised embryos, since these were mostly quantitative.

4.6 Qualitative comparison of Brachyury binding in dorsalised and ventralised embryos

The previous analysis that identified peaks by setting a threshold for the number of reads allowed me to compare the conditions, however, it did not take into account the variation among replicates, since the tags used were the average of the triplicates. Furthermore, the analysis did not discriminate between peaks with more than 20 tags. My goal was to identify genomic sites that were, consistently and significantly, differentially bound in each condition. To identify these sites I used an approach similar to that used for RNA-Seq analysis, in which a quantitative readout (reads in peaks) was used to calculate the probability of a site being differentially bound in one condition compared to another. For such analysis I used the R package 'DiffBind' to calculate differentially bound peaks. I counted the aligned reads of the three replicates of each condition on peaks identified in all conditions, 2063. Similarly to RNA-Seq analysis,

the software permits an unbiased comparison of the samples, by principal component analysis (PCA) (Fig. 4.13A), before the identification of differentially bound (DB) sites. The PCA plot showed that most of the variance was explained by principal component (PC) 1 (65%) separates stage NF12 dorsalised embryos from ventralised embryos, while one of the ventralised samples was more similar to stage NF11 dorsalised embryos. The second component, PC2, represented only 14% of the variance and separated dorsalised from ventralised embryos.

Figure 4.13: **Identification of differentially bound sites in dorsalised and ventralised embryos**

A) Principal component analysis (PCA) using normalised reads in peaks from three replicates of each condition (LiCl NF11, LiCl NF12, UV NF11). The principal component 1 (PC1) explains most of the variance between samples and separates LiCl NF12 from UV NF11. PC2 explains only 14% of the variance and separates dorsal from ventral conditions.**B)** Clustered heatmap of Brachyury ChIP-Seq signal centred in sites identified as differentially bound (DB). The plot on top represents the average coverage of each cluster. identifiable by the coloured bar next to the heatmap. Coverage if Brachyury in dorsalised stage NF12 does not vary in the two clusters while in ventralised embryos it is higher in the smaller cluster (cluster 1). **C)** Following previous representations of peaksets, here, the Venn diagram shows the positively DB sites of each condition. Comparison between LiCl NF11 and UV NF11 or LiCl NF11 and LiCl NF12 did not yield any significant DB sites. Of the 2063 peaks,1595 peaks that are similarly bound in the two conditions while 95 have significantly more binding in ventralised embryos and 373 in dorsalised embryos. The sites preferentially bound in each condition are represented in hierarchical heatmaps of Brachyury binding. The heatmap and plot of DNA occupancy are in accordance with the identification of the DB sites.

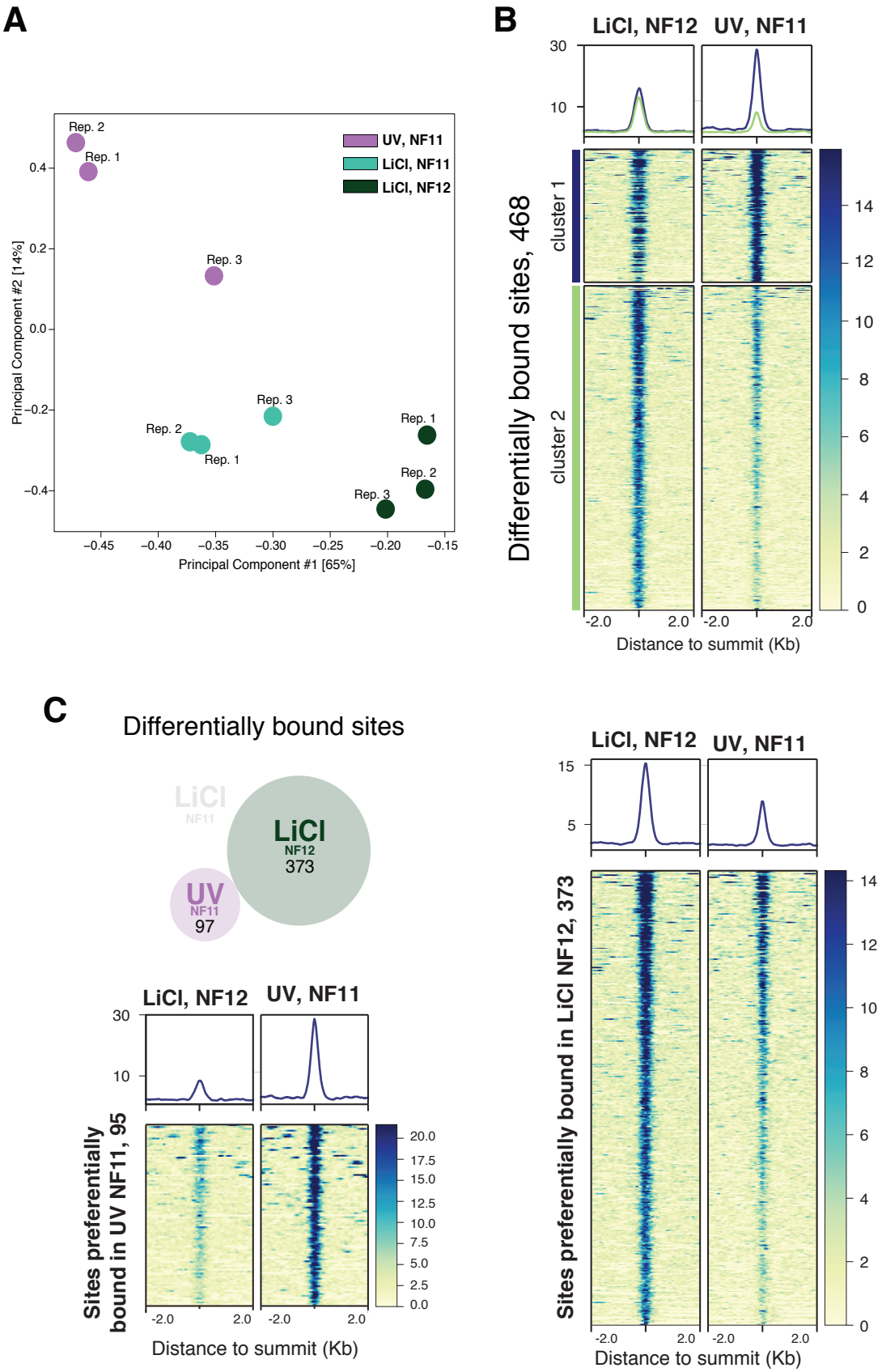
A
Rep. 2
Rep. 1
Rep. 3
Rep. 3
Rep. 2
Rep. 1
Rep. 1
Rep. 2
Rep. 3
UV, NF11
LiCl, NF11
LiCl, NF12
Principal Component #2 [14%]
Principal Component #1 [65%]
B
LiCl, NF12
UV, NF11
Differentially bound sites, 468
cluster 1
cluster 2
Distance to summit (Kb)
C
Differentially bound sites
LiCl
NF11
LiCl
NF12
373
UV
NF11
97
LiCl, NF12
UV, NF11
Sites preferentially bound in UV NF11, 95
Distance to summit (Kb)
LiCl, NF12
UV, NF11
Sites preferentially bound in LiCl NF12, 373
Distance to summit (Kb)

Figure 4.13

Differentially bound (DB) sites were identified based on a false discovery rate smaller than 0.05. Of the 2063 peaks, 468 sites were found to be DB between stage NF11 ventralised embryos and NF12 dorsalised embryos (Fig. 4.13C). None of the peaks was found to be differentially bound between stage NF11 dorsalised embryos and any of the other two conditions (Fig. 4.13C). For this reason, for all the subsequent analyses LiCl NF11 data was not included. The majority of the sites were bound similarly in all the conditions, indicating that Brachyury binding was mostly unchanged in dorsal and ventral cells (1595 peaks not differentially bound).

Read coverage in the 468 DB sites revealed two clusters, one where the binding of Brachyury is higher in ventralised embryos (Fig. 4.13B, cluster 1) and the larger cluster in which the binding was higher in dorsalised embryos (Fig. 4.13B, cluster 2). Interestingly, the DNA occupancy in dorsalised embryos did not change in both clusters (cluster 1 and cluster 2 have a similar enrichment), while cluster 1 showed a higher DNA occupancy in ventralised when compared to cluster 2.

Each of the identified DB sites had a fold change associated with it, which allowed me to identify which peaks were preferentially bound in which condition: 378 sites in LiCl NF12 and only 95 sites DB in UV NF11 (Fig. 4.13C,D). Figure 4.13C reveals that while LiCl NF12 preferentially bound sites have higher occupancy in dorsalised embryos than in ventralised embryos, the difference between the two conditions is more predominant in UV NF11 preferentially bound sites (Fig. 4.13C).

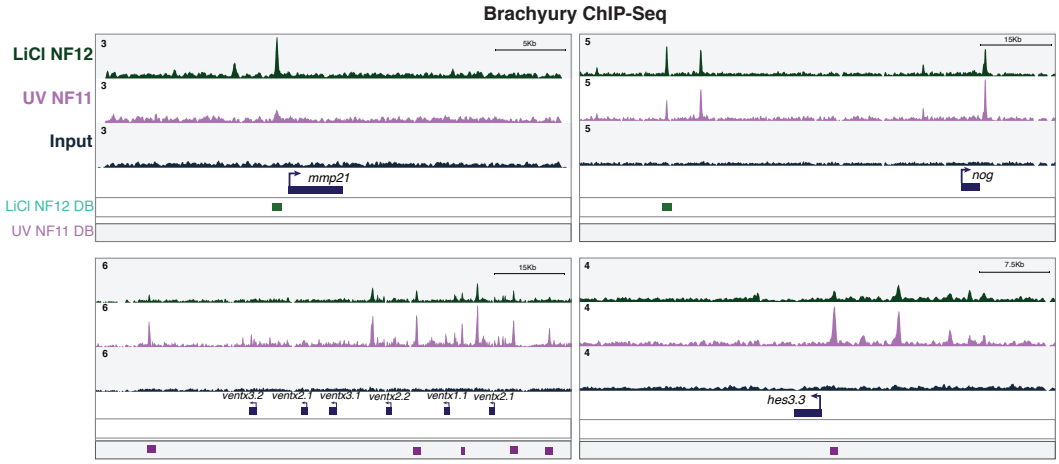

Figure 4.14: **Differential Brachyury binding in dorsalised and ventralised embryos**

The figure shows four genomic regions around the *mmp21*, *nog*, *ventx* and *hes3.3* loci. LiCl NF12 DB refers to peaks identified as preferentially bound in dorsalised embryos and UV NF11 DB refers to peaks identified as preferentially bound in ventralised The first two show sites with higher binding in dorsalised embryos and the last two in ventralised embryos. mmp - matrix metallopeptidase; nog - noggin.

Sites with higher DNA occupancy of Brachyury in dorsalised embryo include the promoter region of the *matrix metallopeptidase 21* (*mmp21*) and a regulatory region upstream of *noggin* (*nog*) (Fig. 4.14). The genomic regions around the *ventx* genes include a few DB sites with higher occupancy in ventralised embryo as well as the region of the promoter of *hes3.3*. Despite the examples given in Figure 4.14, I did not find any correlation between Brachyury binding and active transcription or transcript levels.

4.6.1 Differential binding near Brachyury gene targets

The list of true Brachyury direct gene targets is short and difficult to dissect due to gene cross regulation (Gentsch et al., 2013), indicating that most of Brachyury binding is opportunistic. When comparing Brachyury binding in ventralised and dorsalised embryos, true gene targets were bound similarly in both conditions, e.g; *msgn1*, *mespb*, *mespa*, *myf5*, *sox2* with the exception of four genes: *hes7.2*, *foxb1*, *pax3* and *t2*. These genes had near their locus one or more DB sites in either or both conditions (Fig. 4.15). Of the four, two are repressed by Brachyury and expressed in neural tissue,

foxb1 and *pax3* while *hes7.2* and *t2* are expressed in posterior mesoderm and activated by Brachyury (Gentsch et al., 2013). *Foxb1* was the only of these genes that was differentially transcribed in dorsalised embryos, the same condition where DNA occupancy of Brachyury is higher. Furthermore, *hes7.2* a gene involved in posterior mesoderm, more precisely in somitogenesis, had three sites with higher Brachyury binding in ventralised embryos, including one near the promoter region (Fig. 4.14). The neural development regulator *pax3* is repressed by Brachyury (Gentsch et al., 2013) and had one site preferentially bound in dorsalised NF12 embryos and two in ventralised NF11 embryos, that could represent cell type specific regulatory regions. Finally, the other Brachyury gene, *t2* was bound similarly in the promoter region, however there were two regulatory regions upstream that were predominantly bound in dorsalised or in ventralised embryos (Fig. 4.15). Similarly to the *pax3* gene, this could represent cell-type specific regulatory regions.

Figure 4.15: **Brachyury binding near true gene targets in dorsalised and ventralised embryos**

Six genomic snapshots of Brachyury binding in LiCl- and UV-treated embryos. LiCl NF12 DB refers to peaks identified as preferentially bound in dorsalised embryos and UV NF11 DB refers to peaks identified as preferentially bound in ventralised. The first two panels on the left-hand side show the occupancy pattern near *hes7.2* and *foxb1*; the former only has Brachyury preferential binding in ventralised embryos and the latter in dorsalised embryos. The next two panels, show binding near *tt2* and *pax3*, in both cases there are peaks preferentially bound in LiCl- and UV-treated embryos. Finally, the last two panels show ChIP-Seq profile of Brachyury near *msgn1*, *mespa* and *mespb*, and in all cases DNA occupancy is similar in both conditions.

The data indicated that most sites were bound similarly by Brachyury in both cell types with a small subset of sites with higher occupancy in one condition than in the other. As most of Brachyury binding is opportunistic and only 4 of its true targets were differentially bound, the preferentially bound sites could be explained by differences in chromatin accessibility in each dorsal and ventral cells. Unfortunately, I was unable to generate data of chromatin accessibility in dorsalised and ventralised embryos, which stopped me from exploring this hypothesis. In addition to chromatin accessibility, the binding to DNA can be regulated by the presence of other TFs, co-factors. In the next section I refer to my attempt to identify cell type specific co-factors that may influence the binding of Brachyury to differentially bound sites.

4.6.2 *de novo* motif analysis and enrichment comparison

Transcription factors are recruited to the DNA based on the presence of short sequences recognisable by the DNA-binding domain of a protein, known as transcription factor motifs. Different families of transcription factors, with homology within its DNA-binding domain, will recognise variants of the same motif and bind the same genomic sites. Data from a ChIP-Seq experiment can be used to identify the motifs bound by the immunoprecipitated transcription factor, and, potentially identify co-factors if other motifs are found enriched in the vicinity of the peak. For the purpose of identifying potential co-factors I did *de novo* motif discovery on the peaksets identified before. Such analysis resulted in the identification of short sequences enriched in the peaks, which when compared to known motifs can suggest which family of factors could bind these genomic regions.

Brachyury contains a T-box domain within its DNA-binding domain which recognises a specific motif sequence, shared among T-box transcription factors. Furthermore, Brachyury can bind as a dimer and there are variants of the motif that accommodate for this, palindromic sequences. With this in mind, the *de novo* motif analysis for each dataset was done twice, one searching for 8bp and the other for 12bp motifs. The analysis was done in different peaksets; all the peaks, peaks not differentially bound and peaks preferentially bound in each condition. This allowed me to investigate if the nature of the bound regions influenced the binding of Brachyury.

The results of the analysis are in Figure 4.16 that shows the most enriched motifs in both analysis, the predicted domain, the how many peaks had the motif (% targets) and the motif frequency in random sequences (% background). In the peaks called in all conditions, the T-box domain, the monomeric and partial palindromic motif were the most commonly found, in 60% of the peaks. The other more commonly found motifs included the Homeodomain and the Forkhead motifs (Fig. 4.16). The same motifs were found enriched in peaks that were not differentially bound, in addition to the high mobility group (HMG) domain, which is recognised by Sox proteins. Another distinction between the two datasets was that the Homeodomain identified in the latter was associated with the POU proteins. Given that the motifs were found at similar percentages to that of Brachyury, indicated that transcription factors containing a

Homeodomain, Forkhead or HMG domains could bind the same sites. These peaks were not differentially bound which means that this data did not inform on what leads to the differences in binding between dorsalised and ventralised embryos. For that, I did a similar *de novo* motif analysis on peaks preferentially bound in dorsalised or ventralised embryos. Interestingly, in both cases, the most enriched motif was no longer the T-box, but the Forkhead or the Homeodomain in LiCl- and UV-treated embryos, respectively. The T-box motif was found in around 48% of the peaks in both peaksets, while two distinct versions of the Forkhead motif was found in 64% of the sites preferentially bound in LiCl-treated embryos and the Homeodomain was found in 52% of the sites preferentially bound in UV-treated embryos (Fig. 4.16). This indicated that sites where Brachyury binds distinctly in the two cell types are inherently different in sequence and consequently in terms of the distinct transcription factors could bind.

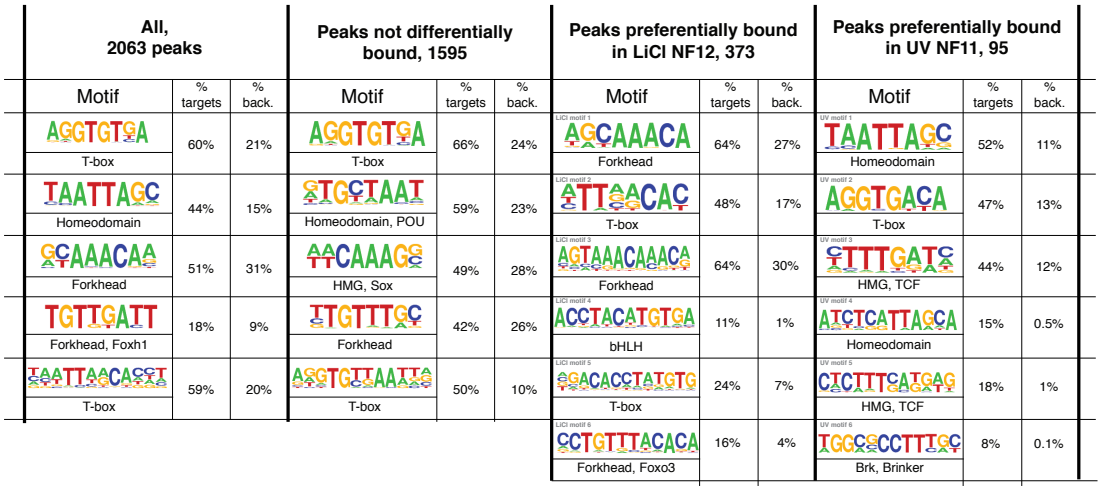

Figure 4.16: ***de novo* motif discovery in differentially or similarly bound sites**

The image shows the top motif sequences (based on p-value and percentage of occurrences) in distinct peaksets: peaks called in all conditions, peaks not differentially bound and peaks preferentially bound in dorsalised or in ventralised embryos. The *de novo* motif discovery was done within 300bp of the peak summit and with instructions to find 8bp and 12bp sequence motifs. The % in targets represents the percentage of peaks that contains the motif and the % of background is the proportion found in randomly selected genomic regions.

4.6.3 Identification of cell type specific co-factors based on transcriptome data

In dorsalised embryos, the sites with higher Brachyury binding are enriched for the Forkhead domain and many proteins containing this DNA binding domain were up-

regulated in these embryos: Fox genes involved in axial mesoderm regulation, such as *foxa1*, *foxa2* and *foxa4*. Other Fox proteins expressed in dorsalised embryos at this stage included *foxd4l1.1* and *foxd4l1.2*, involved in gastrulation and *foxd3* and *foxb1* which were associated with neural development. The basic helix-loop-helix (bHLH) motif was also found in 11% of these sites and bHLH transcription factors upregulated in this condition included *neurogenin 3*, *myf6* and *mycn*. On the other hand, genomic sites with higher DNA occupancy of Brachyury in ventralised embryos were enriched for the Homeodomain and HMG/TCF domains (Fig. 4.16). There are very distinct Homeodomain-containing TFs expressed in distinct tissues of the embryo and unfortunately it was not possible to identify which specific family of proteins the domain was related to. However, ventralised embryos upregulate homeodomain-containing genes including: 7 members of the Hox family (*hoxb1*, *hoxb5*,*hoxa1*, *hoxd1*, *hoxb1*, *hoxb4*, *phox2a*), all three members of the Cdx family (*cdx1*, *cdx2*, *cdx4*), members of the Dlx family involved in epidermis and neurogenesis development (*dlx2*, *dlx3*, *dlx5*, *dlx6*), *gbx2.1*/*gbx2.2* which repress anterior structures and the ventral factors of the Ventx family (*ventx1.1*, *ventx1.2*, *ventx3.2*). Ventralised embryos have high levels of Wnt zygotic activity, as seen in Chapter 3, which could explain the enrichment of the HMG/TCF domain, indicating that these sites could be bound by both Brachyury and the Wnt effectors, TCFs. Furthermore, the data indicated that in 8% of the sites there was a motif that resembled the one that is recognised by the Brinker DNA-binding domain. *Brinker* is gene discovered in *Drosophila*, a target of Bmp4 and acts as a repressor downstream of BMP signalling. However, there is no ortholog described in *Xenopus* to which I could infer the TF that binds this motif. It could indicate that if these sequence motifs are conserved, the sites preferentially bound in ventralised embryos were enriched for targets of BMP signalling, that similar to Wnt signalling is highly activated in these embryos.

To confirm that these motifs were enriched in the peaksets where they were found, I analysed the distribution of all these motifs in sites preferentially bound in LiCl- or in UV-treated embryos. The analysis indicated that, the motifs found at high percentages in each condition were enriched on those peaks and not on the others (Fig.4.17). The UV motifs were enriched in peaks preferentially bound in ventralised embryos and not

in the peaks preferentially bound in the LiCl condition, and vice-versa for LiCl motifs (Fig. 4.17).

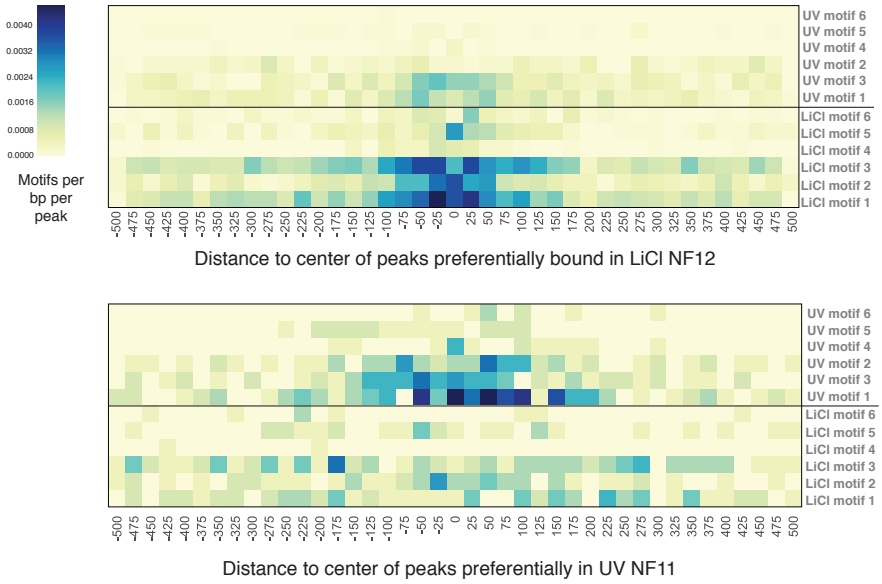

Figure 4.17: **Enrichment of motifs found in sites preferentially bound in LiCl- and UV-treated embryos**

Heatmaps show motif enrichment within 500bp of the DB peak summit. Enrichment is calculated as the number of motifs found per bp per peaks calculated in bins of 25bp. The figure confirms that the motifs more commonly found in cell-type specific peaks (DB sites) are more enriched in that condition.

The *de novo* motif discovery indicated that for genomic regions bound similarly in dorsal and ventral cells the most enriched motif was the T-box and similar occurrences of Forkhead and Homeodoamain motifs. However, when analysing cell type specific preferential binding events, the T-box domain was no longer the predominant motif, instead the Forkhead and the Homeodomain occupied most of these sites in dorsalised and ventralised embryos, respectively. This indicated that these sites could rely on other co-factors of these families for effective binding of Brachyury. This hypothesis was supported by the transcriptome data, that revealed that TFs containing Forkhead and Homeodomain binding domains were upregulated in dorsalised and ventralised embryos, respectively.

4.7 Summary

- I described the cell type specific recruitment of RNAPII and transcription, with more genes actively transcribed in dorsalised embryos.

- Genes upregulated in each condition showed higher RNAPII binding to its gene body, indicating that upregulated genes were actively transcribed in each cell type.

- There is a positive correlation between RNAPII occupancy and p300 binding in regulatory regions near active genes, revealing tissue specific regulation of transcription.

- I described the validation of a new antibody against *Xenopus* Brachyury for ChIP-Seq experiments.

- I studied Brachyury binding in stage NF11 dorsalised and ventralised embryos. The experiment revealed differences in the DNA occupancy pattern of Brachyury between LiCl- and UV-treated embryos. Peak calling and read quantification revealed that dorsalised embryos have substantially less binding events and lower overall DNA occupancy by Brachyury in these sites.

- The investigation of the levels of Brachyury protein during gastrulation in dorsalised and ventralised embryos revealed that dorsalised embryos have lower levels at the stage I performed the ChIP, however by stage NF12 the levels are similar to those of stage NF11 ventralised embryos.

- I analysed the binding profile of Brachyury on stage NF12 dorsalised embryos which allowed to accurately compare the DNA occupancy pattern in dorsal and ventral cells. The increase in protein level led to the identification of more binding events in LiCl-treated embryo, although the overall occupancy did not increase.

- I showed that the use of peak calling is not a good tool to identify differences in DNA occupancy between two conditions. By counting reads in peaks and comparing them, I identified genomic regions that are differentially bound by Brachyury in dorsal and ventral cells: 468 sites, most of them with higher binding in dorsalised embryos. However, the majority of the sites are bound similarly in the two conditions (1595 peaks).

- Data mining on peak sequences revealed that different motifs are enriched in sites predominantly bound in one condition; Forkhead motif in dorsalised and Home-

odomain in ventralised embryos. These sites might be differentially bound due to the presence or absence of specific co-factors, since Forkhead- and Homeodomain-containing TFs are differentially expressed in dorsalised and ventralised embryos, respectively.

Chapter 5

Implications of knockout versus knockdown in *Xenopus* embryos

In the previous chapter, I reported on the differential binding of Brachyury in dorsal and ventral mesodermal cells. Brachyury is an essential gene for mesodermal development, which was shown in different animal models (Stott, Kispert, and Herrmann, 1993; Gentsch et al., 2013; Beddington, Rashbass, and Wilson, 1992; Schulte-Merker et al., 1994). Downregulation or abrogation of its expression leads to a striking phenotype of axial truncation, characterised by the loss of most axial mesoderm. In frog embryos, the phenotype has been generated by morpholino oligomers (MOs) mediated knockdown (KD) and thoroughly characterised (Gentsch et al., 2013).

Since the mid-1990s, a few years after their discovery, MOs have been an essential tool for developmental biologists working with zebrafish and *Xenopus* to study gene function. This KD approach is based on the use of antisense oligos complementary to either translation or splicing sites of transcripts (mRNA) leading to perturbations and ultimately downregulation of the gene. The advantage of MOs compared to other antisense techniques is the use of a backbone of morpholine instead of ribose, as a nucleic acid analogue. This transformation grants morpholinos, among another things, a higher resistance to nucleases, making it an easy-to-use tool for gene function (Summerton, 2017; Summerton and Weller, 1997).

More recently, genome editing tools such as TALEN and type II CRISPR system made it possible to knock out (KO), rather than only transiently knocking down genes. Recent studies in zebrafish showed low concordance between mutant (KO) and mor-

phant phenotypes, either because mutants are not null or the MO generated off-target defects (Kok et al., 2015). Given this disagreement, in this chapter I report on the implications of knocking out *versus* knocking down *Brachyury* in *Xenopus tropicalis*. This work is part of a collaborative project where we compared the previously described *Brachyury* morphant (Gentsch et al., 2013) with a newly TALEN-generated *Brachyury* KO embryo both morphologically and transcriptionally and explore further the unknown effects of MOs.

The experiments described in this Chapter were done in collaboration with George Gentsch, Thomas Spruce and Nick Owens.

5.1 Generation of TALEN-mediated KO of Brachyury Paralogues

The TALEN-mediated mutagenesis that led to the generation of mutant frog lines was done by Thomas Spruce which I will described here. In order to generate the Brachyury KO (knock-out) mutant the coding regions of the two *Xenopus* paralogues,*Xbra*(t) and *Xbra3*(*t2*) were targeted using TALENs (Fig. 5.1). Targeting the two genes was essential for the functional study of Brachyury, as they are expressed synergistically and have redundant roles (Gentsch et al., 2013; Hayata et al., 1999). Furthermore, the mutant embryos were compared with previously generated double morphants, embryos generated with MOs against both genes, t and *t2*, which reproduced the classical Brachyury null mouse phenotype (Chesley, 1935; Gentsch et al., 2013). The two genes are present in tandem in the *Xenopus* genome and, given the short distance between them (within 30kb) were likely to co-segregate during meiosis. Two rounds of TALEN-mediated mutagenesis were carried-out to generate the double mutants (Fig. 5.1). In the first round, wild-type (WT) 1-cell stage embryos were injected with a TALEN pair targeting a *SacI* restriction site in exon 1 of *t*. This proved to be successful, with both vegetal and animal injections, in ˜90% of the injections. This approach resulted in a series of indels (insertions and deletions) ranging from 1-6bp in exon 1, identified in PCR clones by Sanger sequencing.

The mutations were present in the germ line of 80% of F0 females raised to sexual maturity, which were crossed with WT frogs to generate the F1 line of t with a 2bp deletion ($t^{\mathrm{e1.2D}}$) (Fig. 5.1). This deletion was expected to produce a truncated protein lacking the critical T-box domain (Fig. 5.2). Furthermore, the short-tail phenotype was observed, as previously described in t morphants (Gentsch et al., 2013), in homozygous offspring of a F0 t (t^{TAL}) mutant intracross (data not shown). Offspring of the F1 t mutants ($t^{\mathrm{e1.2D/+}}$) crossed with WT was used for the second round of mutagenesis targeting *t2* (Fig. 5.1). Heterozygous embryos of this F2 line ($t^{\mathrm{e1.2D/+}}$) were injected with a TALEN pair targeting a *EcoRI* restriction site in exon 3 of *t2*. The second round was less efficient. Only 30% (6/21) of the embryos carried a mutation in the *t2* locus. Tadpoles identified by genotyping as carrying the *t2* mutations were raised to sexual maturity and 3 out of 15 frogs were found to have the mutation present in

the germline. Embryos from one of these frogs carried a 7bp deletion in the exon 3 of *t2* ($t2^{e3.7D}$) and on the same chromosome as the 2bp deletion of *t* ($t^{e1.2D}$) (Fig. 5.1). Similarly, the 7bp deletion in *t2* locus affected the T-box domain by shifting stop codons into the reading frame prematurely (Fig. 5.2). This strategy allowed us to establish a heterozygous $t/t2$ frog line containing mutations ($t^{e1.2D}$ and $t2^{e3.7D}$) on the same allele which were used for all the subsequent experiments (Fig. 5.1).

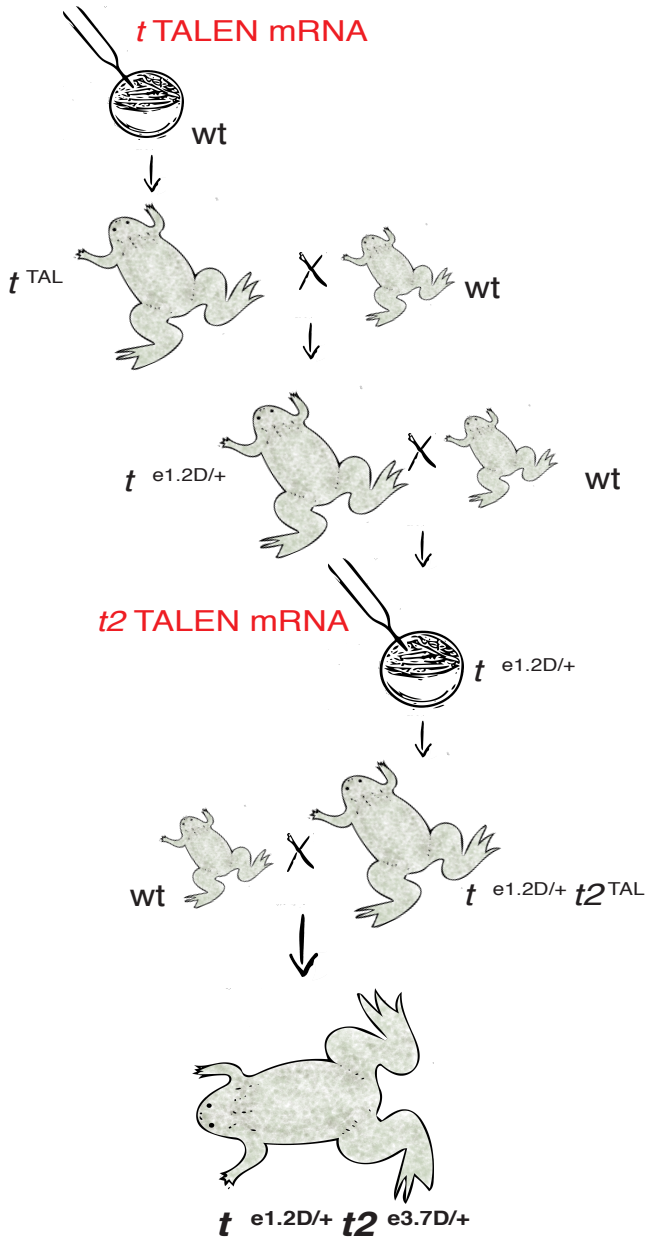

Figure 5.1: **Diagram showing procedure to generate the heterozygous frogs $t^{\mathbf{e1.2D/+}}/t2^{\mathbf{e3.7D/+}}$**

$t^{\mathrm{e1.2D/+}}/t2^{\mathrm{e3.7D/+}}$ frogs were generated from two rounds of TALEN-mediated mutagenesis. In the first round a TALEN targeting exon 1 of *t* was injected into wild-type (WT) *Xenopus tropicalis* 1-cell stage embryos. Frogs containing the mutation in the germline were crossed with WT and the resulting embryos were injected with the second TALEN targeting exon 3 of *t2*. $t^{\mathrm{e1.2D/+}}$ frogs with this mutation were crossed with WT to generate the heterozygous frogs with mutations in both embryos ($t^{\mathrm{e1.2D/+}}/t2^{\mathrm{e3.7D/+}}$, or $t^{+/-}/t2^{+/-}$), used in the subsequent experiments. wt-wild-type, e-exon, D-deletion.

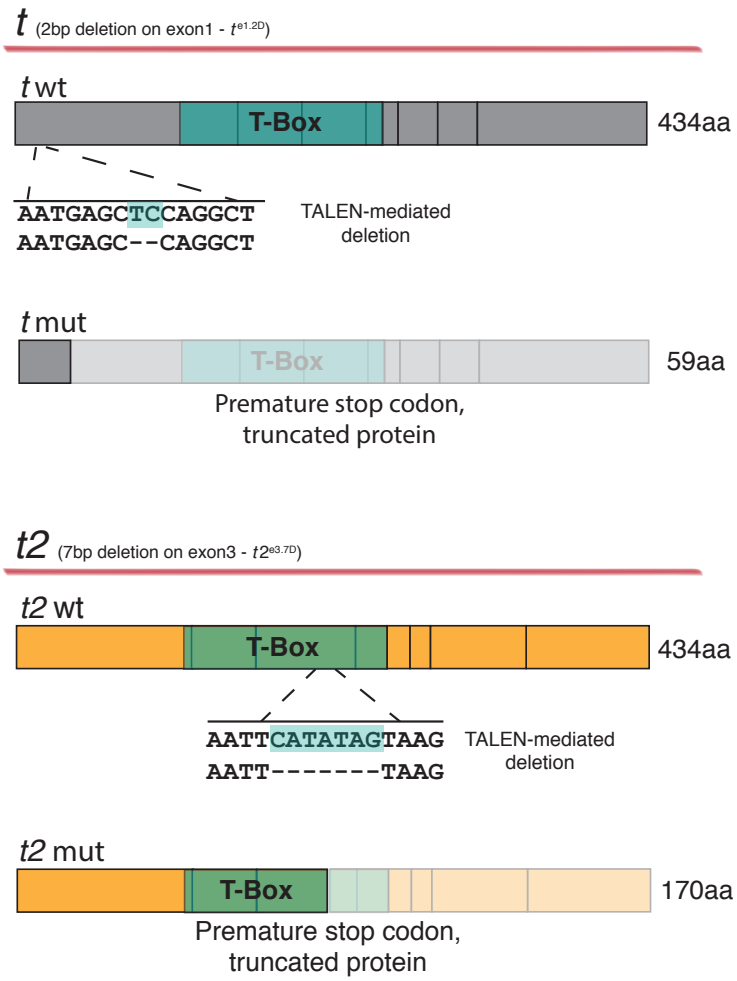

Figure 5.2: **Localisation of TALEN-mediated mutations and predicted mutated protein product**

The diagrams represent the two mutations generated by TALENs: 2bp deletion in exon 1 of *t* and 7bp deletion in exon 3 of *t2*. These are frameshift mutations that result in premature a STOP codons in frame which leads to the prediction of synthesis of truncated proteins: a 59aa t protein and 170aa t2 protein.

5.2 Deletions nullify Brachyury Function

In order to confirm that the genomic mutations were actually nullifying both loci, I cloned $t^{e1.2D}$, $t2^{e3.7D}$ and the corresponding WT mRNAs into N- and C-terminally HA-tagged expression vectors. The strategy was to express the constructs in *Xenopus laevis* and confirm the presence of a premature stop codon and production of shorter proteins. The 8 constructs were individually injected into 1-cell stage *Xenopus laevis* together with mRNA encoding for fam83g-myc to be used as control for translation efficiency. Embryos were collected for protein extraction at mid-gastrula stage and processed for Western Blot analysis (Fig. 5.3).

This experiment revealed the expected protein size for the endogenous expressed mRNAs: WT *t* and *t2* were fully transcribed as both N- and C-terminally HA-tagged versions were present at the correct size, about 50 kDa (Fig. 5.3). The detection of a single product for all translation products indicated that neither one of them contains internal translational start sites. The absence of any C-terminally tagged mutant protein suggests the premature end of translation. Analysis of the HA-$t^{e1.2D}$ clearly showed the production of a shorter protein of around 20 kDa, however I was unable to detect the predicted 6kA product of HA-$t2^{e3.7D}$, possibly due to its poor stability or technical issues in plotting such short proteins.

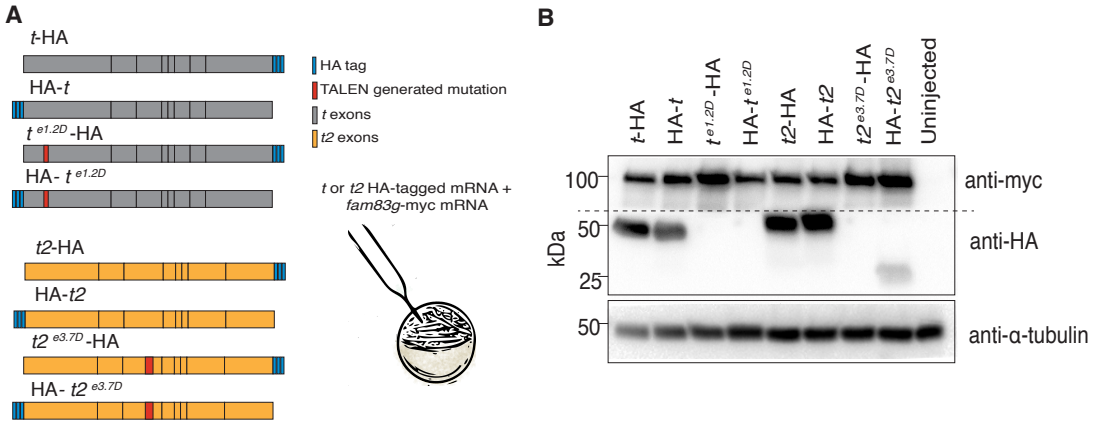

Figure 5.3: **Truncated mutant product confirmed by Western Blot**

A) Diagram showing the mRNA constructs *t/t2* wild-type and mutant tagged with HA either C- or N-terminally. *Xenopus laevis* were co-injected at 1-cell stage with *fam83g-myc* mRNA as a control for translation efficiency. **B)** Western Blot of embryonic extract of *X.laevis* embryos injected with *t* and *t2* wild-type and mutant HA-tagged constructs. Detection of myc shows the protein fam83g as a translation efficiency control and endogenous α-tubulin was used as a gel electrophoresis loading control. Blot using anti-HA antibody shows the t and t2 proteins. Both N- and C-terminal tagged wild-type proteins (t-HA, t2-HA, HA-t and HA-t2) are present and at the right size, 50 kDa. As expected, the C-terminally tagged mutant sequences ($t^{\mathrm{e1.2D}}$-HA and $t2^{\mathrm{e3.7D}}$-HA) do not show any product using the HA antibody, indicating the production of a truncated protein. Of the N-terminally tagged mutant proteins ($\mathrm{t^{e1.2D}}$-HA and $\mathrm{t2^{e3.7D}}$-HA) only the 20 kDa from the mutant sequence is detected. The absence of a band for HA-$\mathrm{t^{e1.7D}}$ is probably due to the size of the protein and its stability making it difficult to blot.

Furthermore, the injection of the mutant mRNAs did not result in the typical phenotype of overexpression of Brachyury. The phenotype is characterised by morphogenetic movements defects during gastrulation, which was absent in embryos injected with $t^{\mathrm{e1.2D}}$ and $t2^{\mathrm{e3.7D}}$ mRNAs (Fig. 5.4). Both experiments led to conclude that the TALEN-meditated mutations resulted in a null Brachyury. From here in I'll refer to the $^{\mathrm{e1.2D}}$ as t^{-} and $t2^{\mathrm{e3.7D}}$ as $t2^{-}$.

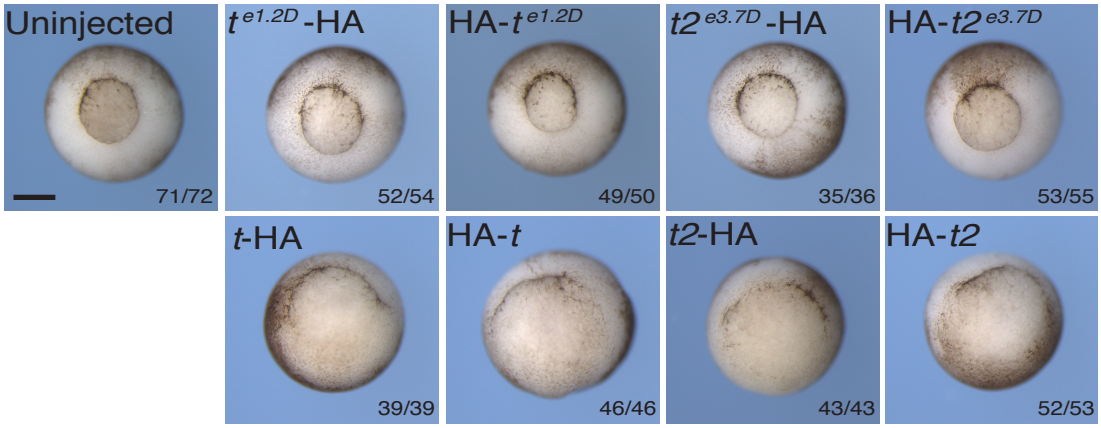

Figure 5.4: **Embryos injected with mutant *Brachyury* mRNA do not show gastrulation defects**

Phenotypes of embryos injected with constructs containing the mutant sequences for *t* and *t2* (upper row) and embryos injected with wild-type sequences (lower row). As expected, overexpression of *Brachyury* leads to developmental defects associated with gastrulation movements. Embryos injected with the mutant sequences do not show any developmental defects, similar to control embryos (uninjected), indicating that the mutation leads to a null allele.

The expression levels of *t* and *t2* in *t*/*t2* heterozygous and homozygous mutants neurula stage embryos were analysed by quantitative real-time PCR (RT-qPCR). *t* transcripts increased 1.5-2-fold in mutants compared to WT, suggesting an increased stability of the transcript or transcription compensation for reduced *Brachyury* levels (Fig5.5). This means that the generated mutations did not lead to non-sense mediated decay, which is similar to what it has been reported for *vegfaa* mutants in zebrafish (Rossi et al., 2015). Since *t2* induction is directly dependant on *t*, its expression was reduced by about 5-fold in mutants compared to WT. Heterozygous embryos did not show the same reduction in *t2*, suggesting that half the amount of *t* was sufficient to maintain expression of *t2*. This was in accordance with the lack of axial truncation phenotype in heterozygous embryos. However, an increase in *t* levels could still be detected in heterozygous embryos, similar to homozygous mutants.

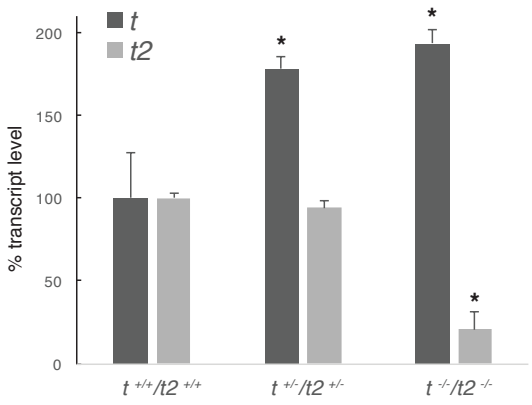

Figure 5.5: **Quantification of *t* and *t2* transcripts in wild-type, heterozygous and mutant embryos**

Transcript levels of *t* and *t2* measured by RT-qPCR in heterozygous and homozygous early neurula stage embryos. The expression is represented in percentage in relation to control levels ($t^{+/+}/t2^{+/+}$). Each bar represents the average measure from biological triplicates and the error bar are the standard error of the mean (SEM). Two-tailed t-test: *, $p<0.05$.

5.3 Brachyury KO and KD are phenotypically undistinguishable

After confirming that the mutations resulted in the nullification of Brachyury function I proceeded to compare the mutants with the morphants. Natural mating of *Brachyury* heterozygous ($t^{+/-}/t2^{+/-}$) frogs resulted in the expected three types of genotypes: wild-type ($t^{+/+}/t2^{+/+}$) (WT), heterozygous ($t^{+/-}/t2^{+/-}$) ($t/t2$ het) and homozygous ($t^{-/-}/t2^{-/-}$ ($t/t2$ KO). For the analyses I used the three kinds of embryos and compared them with the three conditions from the morpholino experiments: uninjected embryos and embryos injected with either a control MO (cMO) or MO against *t* and *t2* (a total of 4 MOs were injected, for each gene a combination of translation start site- and a splice-blocking MOs). These 4 morpholinos and the resulting phenotype had been previously tested and validated (Gentsch et al., 2013).

The initial comparison was phenotypical, as the *Brachyury* lack of function phenotype is well described. The expectation was to observe a shortened antero-posterior (AP) axis from tailbud-stage onwards. Figure 5.6 shows the comparison at tailbud stages NF26 and NF30 for all the 6 different conditions. The control conditions (Uninjected, cMO, WT) and the heterozygous embryos showed no deviant phenotype while $t/t2$ MO and $t/t2$ KO show a similar axis truncation with no distinguishable feature

between both. I did not proceed to further investigate each phenotype; i.e., measure AP axis length or other organs; so I did not exclude the existence of other morphological differences. Additionally, the previously described morphology and timing of developmental defects in *t/t2* MO (Gentsch et al., 2013) were confirmed. Together, I concluded that the knockdown of Brachyury phenocopied the loss of function of the same genes to the point that the embryos were undistinguishable. Moreover, half the amount of Brachyury (*t/t2* het) was sufficient for proper axial extension and resulted in a wild-type-like phenotype.

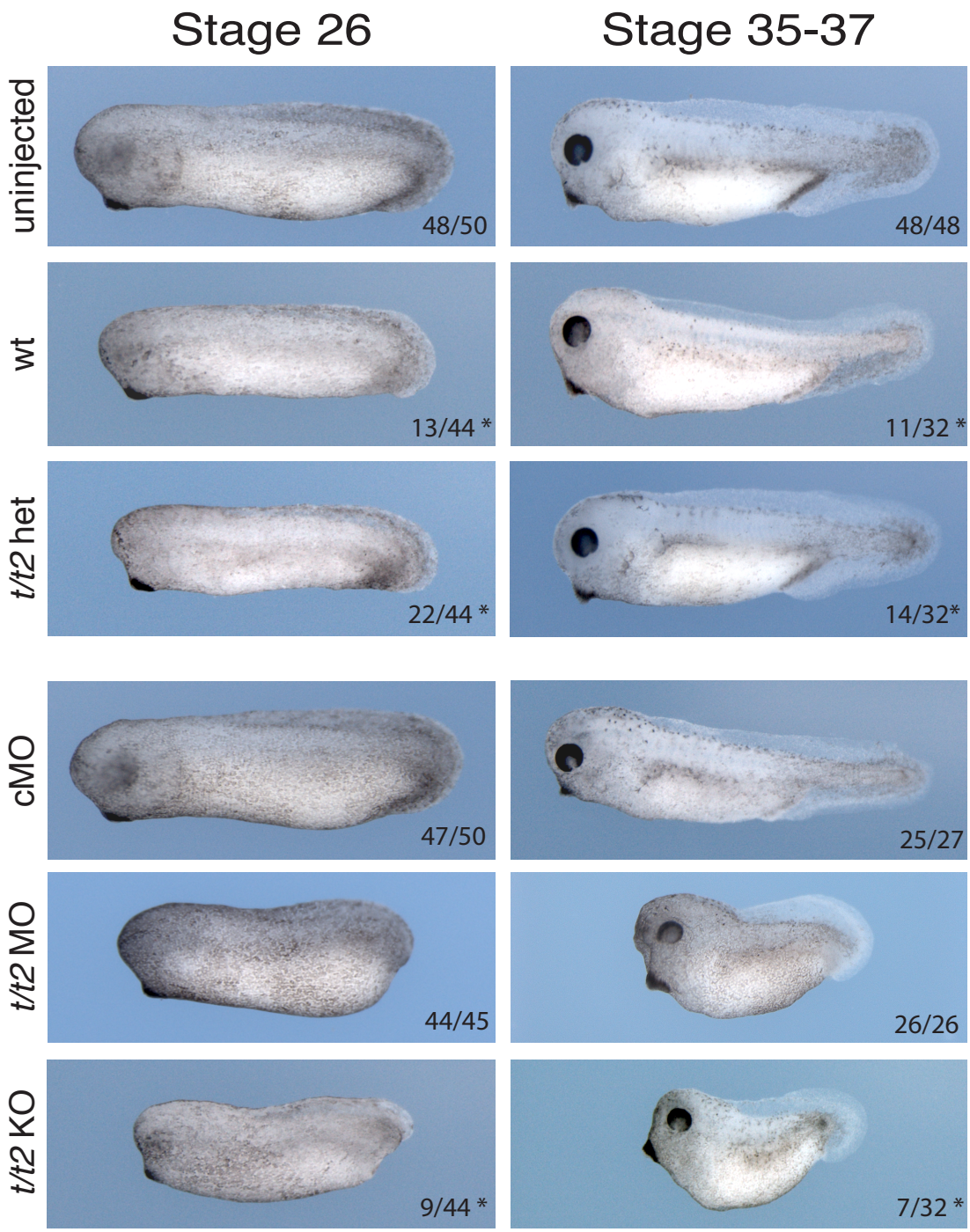

Figure 5.6: **Mutant and morphants embryos are indistinguishable at tailbud stages**

Phenotypical comparison of between the different genotypes and conditions generated for the experiment, at two tailbud stages, NF26 and NF38. The control embryos for both experiments, uninjected, wild-type (wt), *t/t2* heterozygous (*t/t2* het) and embryos injected with control morpholino (cMO) share the same phenotypic characteristics of a normal developing embryo. The KO and MO embryos are undistinguishable, as both present the *Brachyury* null phenotype of axial truncation. *Numbers refer to genotyping results. Scale bar, 0.25 mm.

5.3.1 Posterior mesoderm the notochord are consistently affected in Brachyury KO and KD

The genes *t* and *t2* are master regulators of mesoderm development and known to particularly regulate dorsal and posterior mesoderm. To investigate whether KO and MOs similarly affected mesoderm development, I analysed the expression of several mesodermal and mesodermal derivative markers by multi-probe WMISH (Fig.5.7). I used a multi-probe approach, since the expression pattern of these genes is well characterised and do not overlap spatially. Embryos injected with cMO had unaffected mesoderm as seen by the expression pattern of markers of paraxial mesoderm (*tbx6, T-box 6*) its derivatives , the somites (*actc1, cardiac actin 1*), notochord (*cav1, caveolin 1*), intermediate and ventral mesoderm subtypes such as heart (*myh6, myosin heavy chain 6*), pronepheros (*hoxd8*) and blood (*tal1,T-cell acute lymphocytic leukemia 1*). However, both mutants (*t/t2* KO) and morphants (*t/t2* MO) had defects in paraxial and dorsal mesoderm as seen by the loss of *tbx6* expression in the paraxial mesoderm which results in the loss of posterior somites and malformation of more anterior ones, seen by expression of *actc1* (Fig. 5.6). The notochord, a derivative of the dorsal mesoderm, was completely absent in embryos lacking Brachyury, shown by the (lack of) expression of *cav*. However, despite a delay in the formation of some of these tissues, derivatives of intermediate and ventral mesoderm were not affected in *t/t2* KO nor MO.

TALEN-mediated mutagenesis of *t* and *t2* led to the loss of function of both alleles resulting in a phenotype of axial truncation and disruption of posterior mesoderm undistinguishable from the MO-mediated knockdown of the same genes.

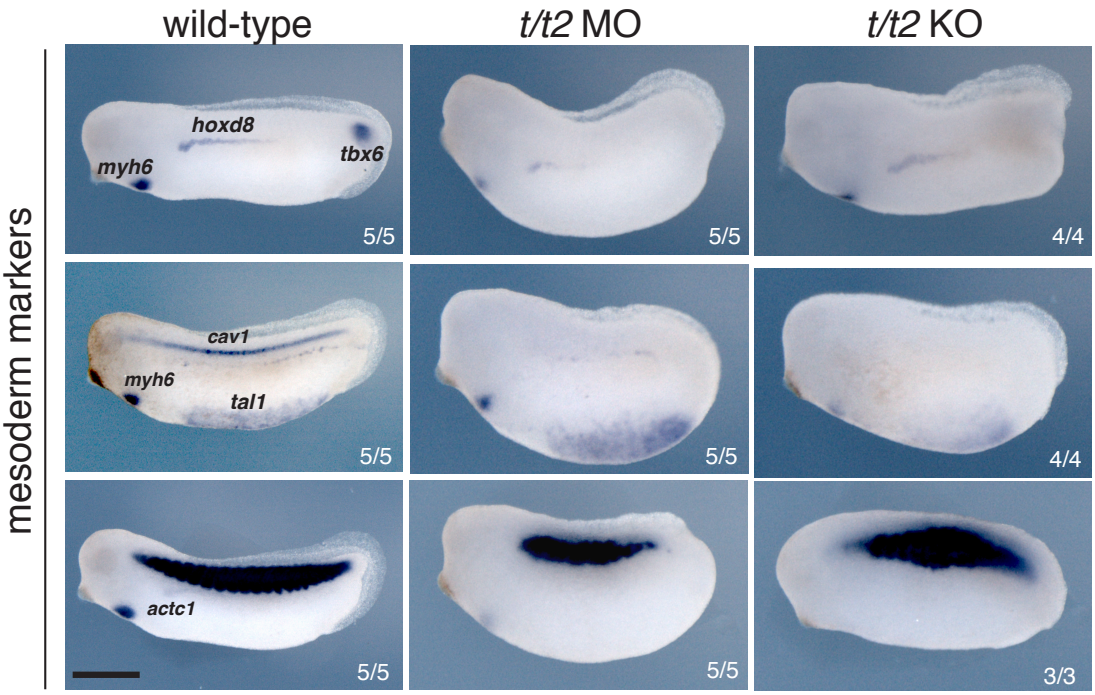

Figure 5.7: **Posterior mesoderm is affected in both KD and KO embryos**

Combinatorial whole-mount in situ hybridisations at mid-tailbud stage showed that only posterior mesoderm (paraxial mesoderm: *tbx6, T-box 6*) including its derivatives notochord (*cav1, caveolin 1*) and somites (*actc1, actin, alpha, cardiac muscle 1*) are consistently absent or malformed in Brachyury KO and KD embryos. In contrast, anterior (cardiac: *myh6, myosin heavy chain 6*, *actc1, actin, alpha, cardiac muscle 1*), intermediate (pronephros: *hoxd8*) and ventral (blood: *tal1, T-cell acute lymphocytic leukemia 1*) mesoderm were largely intact. Scale bar, 0.5 mm.

5.4 Transcriptome-wide comparison of Brachyury KO and KD embryos

I was able to confirm that the TALEN-mediated mutation led to a null phenotype that was morphologically undistinguishable from the MO-generated knockdown embryos. Given this, we further investigated whether these two kinds of embryos, KO and KD, were also transcriptionally similar, by comparing the whole poly-A transcriptome.

In order to do such analysis I collected embryos from a natural mating cross between two *t/t2* heterozygous frogs and processed them individually for DNA extraction and genotyping. Single embryos were genotyped for both *t* and *t2* (Fig. 5.8). Embryos were collected at two developmental stages, stage NF26 and NF34, both tailbud stages in which the effects of the absence of *Brachyury* take place. The RNA (see Chapter 3 for details) from 5 to 10 sibling embryos with the same genotype was combined and processed together in order to obtain 3 biological replicates of each genotype: wild-

type ($t^{+/+}/t2^{+/+}$), heteroxygous ($t^{+/-}/t2^{+/-}$) and mutant or KO ($t^{-/-}/t2^{-/-}$). Embryos from three different crosses were injected with *t* and *t2* splice- and translation-blocking morpholinos (total of 4 morpholinos, 4.5ng each) and standard control morpholino (cMO) from GeneTools (18ng) plus uninjected embryos were collected at the same stages and processed for RNA extraction, similarly.

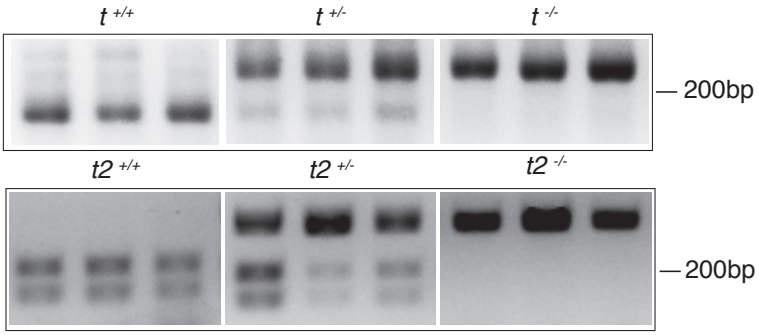

Figure 5.8: **Example of genotyping of single embryos prior to poly-A library preparation**

Single embryos were processed for DNA and RNA extraction. DNA was used for genotyping prior to poly-A library preparation. Upon extraction, DNA was amplified for the *t* and *t2 locus*, as described in Chapter 2, and subsequently digested with either *SacI* (*t*) or *EcoRI* (*t2* and fragments separated by gel electrophoresis in order to identify the mutations. The figure shows examples of 3 embryos representative of each genotype. The TALEN-induced mutation masks the restriction site resulting in a single band in the gel, while wild-type embryos present two bands as a result of the digestion by the restriction enzyme and, finally, heterozygous embryos have the three bands.

Of the work described from here on, I only contributed to the discussion of results and suggestions of further analyses. The libraries were prepared by Thomas Spruce and computational analysis was done mostly by George Gentsch with contributions from Nick Owens. Furthermore, the work described here forms part of a article submitted for publication in Developmental Cell, currently under review.

The RNA-Seq poly-A(+) libraries consisted of the 6 conditions described above at two developmental stages and biologial triplicates: a total of 36 libraries were made and sequenced to produce paired-end reads that were aligned to *Xenopus tropicalis* gene models. Reads were counted per gene model (except ribosomal and mitochondrial RNA) and raw counts were used for differential expression analysis using DESeq2. Furthermore, in order to identify genes differentially expressed with consistent fold changes, both developmental stages were considered, meaning that a gene would have to be differentially expressed (DE) at both time points to be considered.

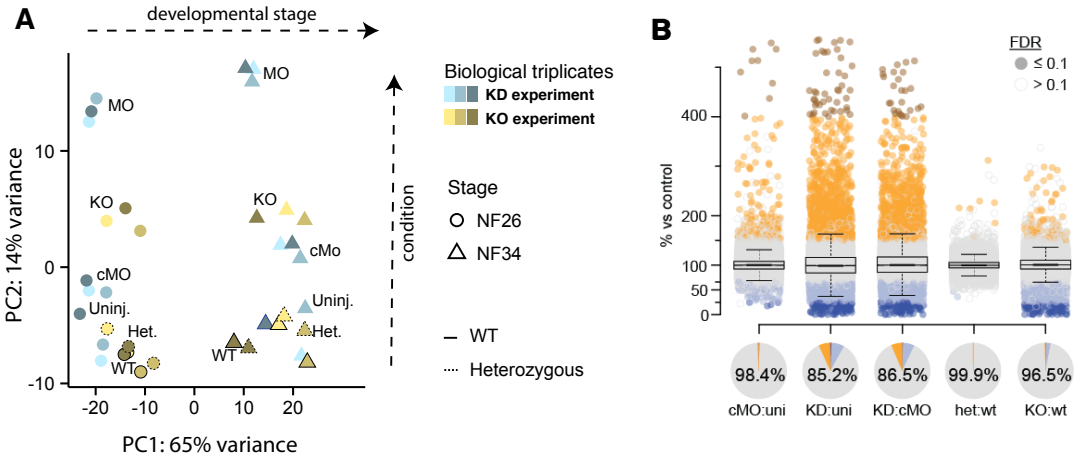

Figure 5.9: **Morpholino-injected embryos show higher transcriptional variances than KO embryos**

A) Principal component analysis (PCA) of the RNA-Seq data generated from biological triplicates of each condition. The KO experiment comprises the control wild-type embryos (WT, yellow grade with stroke around), heterozygous (Het., yellow with dashed stroke) and the homozygous mutants (KO, yellow). The KD experiments includes uninjected embryos (Uninj., in blue), embryos injected with a control morpholino (cMO, blue) and embryos injected with the 4 morpholinos targeting *t* and *t2*, the morphants (MO, blue). Most of the variance between samples is explained by the developmental stage (PC1 = 65%) and PC2 accounts for the differences seen between the conditions (PC2 = 14%). **B)** Jitter plot showing the differences in the transcriptome (pairwise comparison with the appropriate control) in percentage, of each condition. Genes with FDR 10% were coloured: navy blue <25%, sky blue 25-67%, orange 150-400% and brown >400%. The piecharts represent the whole universe of transcripts analysed, in grey are the unchanged gene, in orange the upregulated portion and in blue the downregulated portion (based on a fold change ≥1.5 or FDR ≤10%).The percentage in each piechart refers to the proportion of unchanged transcripts between the condition and the relative control.

Before the identification of DE genes, the principal component analysis (PCA), shown in Figure 5.9A, indicated that most of the variance seen in the transcriptome of the embryos was explained by the developmental stage (Fig.5.9A, PC1:65%). Principal component 2, explained most of the remaining variance which was associated with the condition. The PCA revealed that, at both stages, the control conditions, wild-type (WT) and uninjected, clustered together (very similar transcriptionally), as well as heterozygous (Het.) embryos (Fig.5.9A, yellow circles and triangles with dashed stroke around). Interestingly, embryos injected with the control morpholino (cMO) did not cluster as well with the other control conditions and the variance increased with time. As expected, KO embryos were transcriptionally distinct from the control conditions and these differences do not seem to increase over developmental time. However, embryos injected with morpholinos against *t* and *t2* had the most distinct transcriptome and like cMO, the separation to the control conditions increased with time (Fig. 5.9A).

To better understand the consistent transcriptional differences between conditions,

the transcript levels of annotated and expressed genes (genes with 7 or less fragments in the control were disregarded) were analysed by pairwise comparison. As referred above, for this analysis both developmental stages were considered and misregulated genes were identified by a FDR $\leq$10% and a fold change $\geq$1.5. Figure 5.9B shows the results of the pairwise comparison and reveals the same trend as the PCA. The transcriptome of heterozygous and wild-type siblings were only 0.1% different, while KO embryos showed 3.5% of misregulated genes, with most being downregulated (Fig. 5.9B). Comparison of the MO experiment conditions revealed that cMO-injected embryos have 1.6% of its genes misregulated when compared to uninjected embryos. While KO embryos displayed 96.5% of unchanged transcripts, KD (*t* and *t2* MO-injected) embryos have 85.2%-86.5% when compared to uninjected and cMO, respectively. This means that embryos injected with *t* and *t2* MOs had a 4-fold increase in misregulated genes in comparison to KO embryos (˜14% *versus* 3.5%, respectively).

In summary, KO and KD embryos were transcriptionally distinct from the correspondent control embryos, however KD embryos showed a higher number of misregulated genes. Furthermore, embryos injected with a cMO also showed a significant percentage of misregulated genes, unexpected for a control condition.

5.4.1 Activation of immune response genes in morpholino-injected embryos

In order to understand which genes were causing the transcriptomic differences between conditions, gene ontology (GO) analysis for terms associated with biological function (BP) was used. First, the affected genes identified above where grouped in Venn diagrams, for up and down regulated genes. Five of the most populated categories were analysed: (A) genes affected only by cMO, (B) genes affected by both the cMO and the *t/t2* MO, (C) genes affected only by *t/t2* MO, (D) genes affected by both the *t/t2* MO and in the KO and finally (E) genes affected only in KO embryos (Fig.5.10). The Venn diagrams showed that most of the genes affected by the KO alone (E) and in the KO and *t/t2* MO (D) were downregulated and, more interestingly, that the number of misregulated genes in MO alone (C) were almost five times the number of genes affected in both KO and KD embryos (D). GO term analysis in each of these Venn

fields was revealing on the nature of the genes affected in each condition. Genes downregulated in both KD and KO embryos (D) were highly enriched for terms associated with muscle system process, cardiovasculogenesis and somitogenesis. These processes are associated with mesoderm regulation and differentiation, the formation of somites that will form muscle and in heart formation, known to be regulated by *Brachyury*. Upregulated genes of the same group (D), showed enrichment for terms associated with spinal cord development, which is also known to be a consequence of loss of *Brachyury*, as neuromesodermal progenitors switch from a mesodermal to a neural fate under this conditions (Gentsch et al., 2013). Hence, the genes misregulated in both KO and KD embryos represented the regulatory core affected by the loss *Brachyury* and responsible for the axial truncation phenotype observed in both conditions.

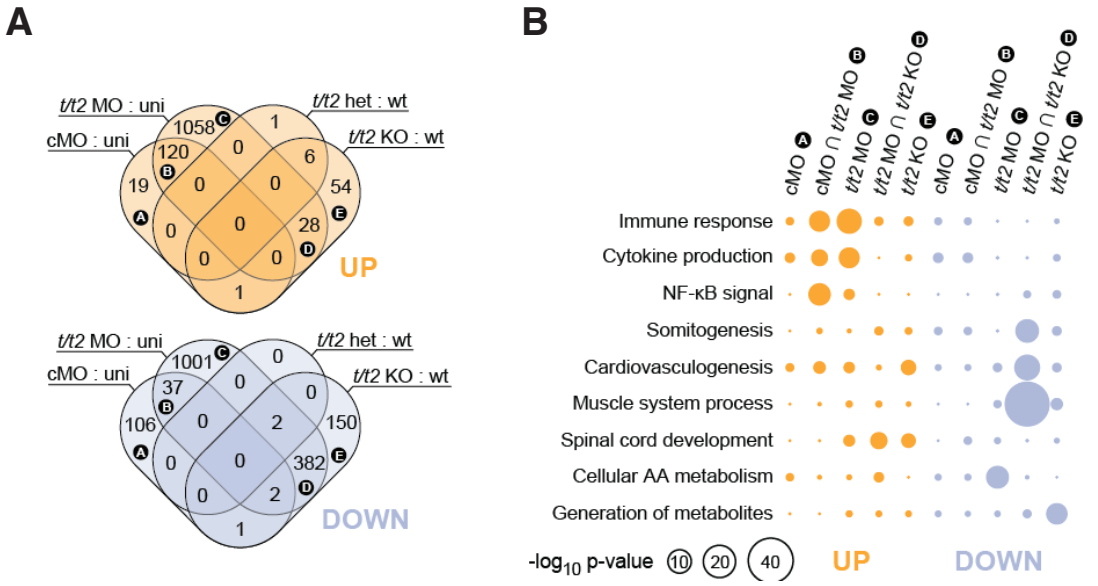

Figure 5.10: **Transcriptional differences between KO and KD embryos are related to innate immune response**

A) Venn diagrams of positive(orange) and negative (blue) transcript fold changes (≥1.5-fold and FDR ≤10%). Main categories are represented by letter A-D, see text for more details. **B)** Representation of the statistical significance (hypergeometric p-value) of enrichment for selected biological processes among the indicated Venn fields.

The other group that showed significant association with GO terms were genes upregulated only in KD (B, 120 genes) and in both KD and cMO (C, 1058 genes) (Fig. 5.10B). In these groups there were genes associated with immune response, cytokine production and NF-κB signalling pathways, such as Toll-like supressors, complement components, cytokines, caspases and tumour suppressors. This overall immune re-

sponse was a side effect of injecting control or *t/t2* MO since these genes were only misregulated in these two conditions. Furthermore, investigation of the binding of *t* at tailbud stages, by ChiP-Seq (Gentsch et al., 2013), showed no binding events near these genes, in contrast to genes affected in both morphants and mutant embryos (data not shown).

The transcriptome comparison allowed the identification of the gene-regulatory core affected by the loss of *Brachyury* by the overlap of genes affected in both KD and KO embryos. This group of genes, although not extensive, was responsible for the phenotype that makes morphants and mutants undistinguishable. The experiment also indicated that the use of morpholinos caused a large misregulation of genes associated with immune response. This observation was very pertinent, specially in that, since its conception, morpholinos have never been described to cause such an immune response. Although not shown here, the reduction of the morpholino dose, to concentrations that still cause a phenotype, showed a reduction in the overexpression of genes associated with the immune response (data not shown).

5.4.2 Off-target mis-splicing caused by morpholino

In the previous section I described that embryos injected with morpholinos showed an increase in expression of genes associated with innate immune response, described as a MO-side effect. However, when investigating the GO terms associated with genes downregulated in KD alone (C) or KD and cMO (D) there was no significant enrichment for a GO term. This indicated that this group of genes was not associated with any biological function and its misregulation was not explained by the effect on any specific pathway or cellular process. The 'randomness' of genes downregulated in MO-injected embryos led to investigate the off-target effects of MOs, such as mis-splicing, which in turn can affect transcript stability. An initial hint of off-target hybridisation by MOs resulted from 'BLASTing' the cMO, *t* splice MO (MOsplice) and the *t2* sequences; the three morpholinos contained at least 8 consecutive bases that matched the most frequently encountered canonical splice site in *Xenopus* (Fig. 5.11A).

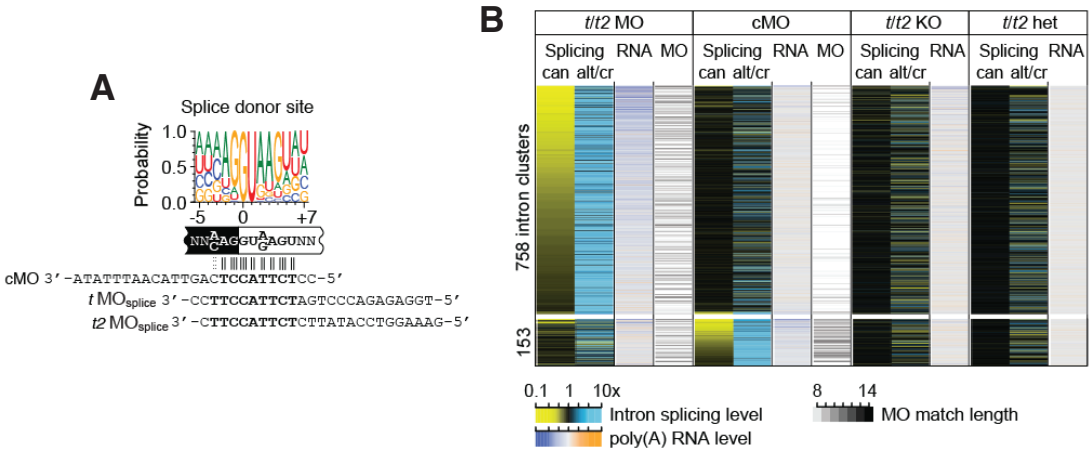

Figure 5.11: **Morpholino-injected embryos have more events of mis-splicing compared to control**

A) Consensus sequence of of the most commonly found splice donour sequence in *Xenopus* embryos at tailbud stage and the best alignment to cMO, *t* MO_{splice} and *t2* MO_{splice}. **B)** Hierarchical heatmap of differential splicing (alt, alternative; can, canonical, cr, cryptic) between *t/t2* MO, cMO, *t/t2* homo- and heterozygotes. 758 and 153 blocked splice junctions were identified in *t/t2* MO and cMO, respectively. These mis-splicing events are positively correlated with decreased transcripts (RNA) and more consecutive MO (10) base pairing (MO).

This observation strengthen the hypothesis that MO could hybridise to 'off-target' mRNAs causing events of mis-splicing and consequently affect stability and expression of transcripts. The hypothesis was tested by analysing the RNA-Seq data in search for differential splicing in the different conditions. The software Leafcutter (Li, Knowles, and Pritchard, 2016), an annotation-free method, that allows the identification of alternative splicing events by focusing on intron excision events was used. The analysis resulted in the identification of 758 and 153 intron clusters (blocked splice junctions) that were differentially spliced in *t/t2* and cMO morphant embryos, respectively (Fig. 5.11B). Figure 5.11B shows a heatmap of differential splicing and indicates that, for the identified clusters, in embryos injected with MOs, canonical (can) splicing decreased at the expense of alternative(alt) or cryptic (cr) splicing. Furthermore, the identified sites showed more consecutive base pairing with the corresponding injected MO (cMO; 49:2 (nobs:nexp), Mann-Whitney U p<2.2e-16, *t/t2* MOs; 92:26, p<7.8e-15). Likewise, the blocked spliced junctions correlated positively with decreased transcript levels (more than 1.5 fold change) compared to randomly selected active splice sites (cMO; 19:1(nobs:nexp), cMO; 42:2, in both cases, Mann-Whitney U p<2.2e-16). The number of alternative splicing events observed in embryos injected with *t/t2* MOs is

around 5 times more than the events detected in embryos injected with the cMO, probably explained by the number of MO sequences injected; 4:1 (*t/t2* MO: cMO).

Some of these mis-splicing events were validated by RT-qPCR using primers that spanned an alternative/cryptic splice junction and for the gene *dtymk*, which showed 10-100 times increase of the spliced alternative while the whole transcript (measured in exon1) expression level decreases (data not shown). Similar to the reduction of immune response, mis-splicing decreased when reducing the MO dose to a level that still produced a phenotype (data not shown), however, none of the side effects was completely abrogated.

5.5 Summary

- I described how to successfully create and validate a *Xenopus tropicalis t/t2* KO embryo using TALENs.
- The morphological comparison of *t/t2* MO-generated KD to TALEN-generated KO tailbud embryos revealed that they were undistinguishable.
- Comparison of the whole poly(A) transcriptome of wild-type, KO, heterozygous siblings and embryos injected with *t/t2* MOs, cMO or uninjected revealed that cMO embryos had significant transcript mis-regulation compared to other control conditions, and similarly, *t/t2* morphants had a bulk of mis-regulated genes not shared with KO embryos.
- The transcriptome data also revealed a group of DE genes in both KO and KD embryos as the core regulatory network responsible for the loss of Brachyury phenotype, mostly associated with mesoderm regulation and differentiation.
- The majority of genes upregulated only in MO-injected embryos were associated with immune response while downregulated genes were not associated with any biological process.
- MO-injected embryos showed an increased level of cryptic or alternative splicing and such events were associated with more than 10 consecutive base-pairing with the corresponding MO sequence.

- Two side effects were identified as a result of injecting MOs; immune response and off-target mis-splicing, that could be mitigated but not abolished by reducing the morpholino dose.

Chapter 6

Discussion

During this project I have used tools of a modern embryologist to analyse early vertebrate development through multi-'omics' data integration, and genome editing. Although developmental biology has embraced the use of *in vitro* stem-cell cultures, *in vivo* studies are essential to understand biological processes in context. In the last decade, highthroughput sequencing technologies have evolved at great speed which allowed, at increasingly lower costs, to investigate many thousands of nuclei acid sequences at once, rather than single genomic loci or gene transcripts. The integration of these big datasets has allowed the construction and understanding of gene regulatory networks involved in distinct developmental processes. In Chapter 3 and 4 I refer to the use of RNA-Seq and ChIP-Seq, two sequencing applications, first to compare the whole poly-(A) transcriptome of dorsalised and ventralised embryos, and second, to investigate the *in vivo* cell type specific regulation at the chromatin level. Recent developments in the field of genome editing yielded molecular tools to sequence-specifically introduce mutations. In Chapter 5, I refer to a collaboration project where we used engineered nucleases to generate null mutants to compare their transcriptomes to that of Brachyury morphants, revealing the implications of gene knockdown *versus* knockout.

My main projects are described in Chapter 3 and 4 which have in common the study of cell type specific gene regulation during early development. Our animal model of choice is the *Xenopus* embryo, which offers many advantages when studying early development. The *Xenopus* embryo develops externally with simple culture requirements, relatively fast, and its size is ideal for manipulation and nucleic acid injection. In the advent of modern developmental biology, *Xenopus* is particularly useful for its

abundance in source material for high-throughput studies exploring the whole transcriptome, proteome or genome. The genomes of the two *Xenopus* species, *tropicalis* and *laevis*, have been sequenced in the last decade which has allowed, for example, the generation of genomic maps of histone marks, transcriptional machinery proteins and transcription factors for the first hours of development (Bogdanović et al., 2016; Hontelez et al., 2015; Paranjpe et al., 2013; Heeringen et al., 2014; Gentsch et al., 2013). *Xenopus* embryos are also ideal for single-cell transcriptome or proteome studies due to their cell size, amenability for manual dissection, and their known cell fate (Onjiko, Moody, and Nemes, 2015; De Domenico et al., 2015; Wühr et al., 2014; Smits et al., 2014; Flachsova, Sindelka, and Kubista, 2013). However, as the embryo develops, manipulation of single cells becomes less viable and, so far, there has not been single-cell studies that span the developmental studies beyond the mid-blastula transition. Although technologies such as Fluidigm for single-cell mRNA quantification have been developed in recent years, these are not compatible with the cell size and the yolk content of *Xenopus* embryos.

Thus, single-cell studies might not be feasible yet during certain stages in *Xenopus* development. However, other technologies allow investigating cell type specific features, based on the bulk analyses of cells (McClure and Southall, 2015). Some of them rely on transgenic lines expressing a cell type specific promoter driving expression of fluorescent nuclear proteins, such as isolation of nuclei tagged in specific cell types (INTACT) (Deal and Henikoff, 2010a; Deal and Henikoff, 2010b) and batch isolation of tissue-specific for chromatin immunoprecipitation (BiTS-ChIP) (Bonn et al., 2012a; Seyres et al., 2016). The application of INTACT, yields a cell type specific analysis of chromatin and nuclear RNA studies. This technique was first described in *Arabidopsis thaliana* (Deal and Henikoff, 2010b) and has since then been applied to *Drosophila melanogaster* embryos and a derivative of this concept to zebrafish embryos (Henry et al., 2012; Ma and Weake, 2014; Steiner et al., 2012; Trinh et al., 2017). There is one published example of INTACT applied to *Xenopus laevis* tailbud stage embryos to study the proteome of cardiac and skeletal muscle cells (Amin et al., 2014). Commonly, nuclei are extracted before selecting a specific cell type. This is particularly challenging with early stage *Xenopus* embryos due to their high yolk content. Isolating nuclei from late blastula

stage embryos has been achieved by running a sucrose gradient (Finkielstein, Lewellyn, and Maller, 2001). However, there are no examples in the literature of successfully isolating fluorescently labelled nuclei from early stage embryos, to be processed for studying the transcriptome or chromatin.

I considered developing the tools described above, for *Xenopus* embryos, but reasoned that such an approach was too risky in producing timely results. The number of cells needed for chromatin extraction was another limiting factor. Thus, I changed strategy to study cell type specific regulation during early development by taking advantage of the easy manipulation of cell fate determination in early *Xenopus* embryos. I have enriched the whole embryo for dorsal or ventral cells by dorsalisation or ventralisation, which provided sufficient embryonic cell material to study cell type specific gene regulatory networks.

In the next sections, I will discuss the results of Chapter 3 to 5.

6.1 Dorsal and ventral cells have a very distinct transcriptome

I decided to use dorsalised and ventralised embryos as a proxy to study cell type specific gene regulation *in vivo* across the dorso-ventral axis of gastrula stage embryos. Ultraviolet (UV) irradiation shortly after fertilisation and treatment with lithium chloride (LiCl) at 32-cell stage, are the most reported methods for high efficient ventralisation and dorsalisation, respectively. At the start of this project neither LiCl- or UV-treated embryos had been transcriptionally profiled and I reasoned this would be an useful dataset, given the historical importance of the methods and the potential to identify new genes involved in setting up the dorso-ventral axis. Furthermore, since I intended to use these embryos for ChIP-Seq, these transcriptional profiles would complement the analysis of the chromatin landscapes. The comparison revealed that dorsalised embryos have more differentially expressed genes compared to ventralised embryos. My goals were to report on these differences, evaluate whether these embryos really adopt the transcriptomic signature of dorsal and ventral cells of the unperturbed embryo and identify new genes differentially expressed along the dorso- ventral axis.

By the end of this project Ding *et al.* generated a RNA-Seq dataset from *Xenopus*

laevis LiCl-treated embryos (Ding et al., 2017). Nevertheless, my comparison remains relevant since I focus on comparing UV- and LiCl-treated embryos in order to identify the genes that make dorsal and ventral cell different. In addition, whole transcriptome datasets of dissected gastrula embryos have been released (Ding et al., 2016; Popov et al., 2016; Blitz et al., 2017) which were useful to verify my experimental conditions. This verification revealed that LiCl- and UV-treated embryos were truly enriched for dorsal and ventral regions of the untreated embryo. Although the analysis of dissected parts of the embryo might be better at averaging the expression of single cells in space and time, it has the disadvantage of depending on visual cues, such as the emerging dorsal blastopore, to identify these anatomical domains. In addition, the dissection process could activate stress-responding pathways that introduce experimental artefacts. Furthermore, I have shown, that dorsalised and ventralised embryos not only represent dorsal/ventral cells at a specific developmental time but also the cell type progeny. For example, the over-representation of ectodermal markers in UV-treated embryos. These markers are not ventrally enriched at gastrula stage, but ventral cells are exposed to high levels of BMP and Wnt signalling and will become ectodermal. In a way, these treated embryos resemble stem cell cultures in that an initial cue of a signalling pathway, canonical Wnt in this case, alters the fate of the cells towards dorsal or ventral. Although enriched for a cell type, similar to stem cell cultures under differentiation, it represents an heterogeneous group of cells, but in an *in vivo* context.

One advantage of my experimental design over embryo dissections is that it leads to the overexpression of genes that may be expressed at low levels and would not be identified otherwise. I observed this when analysing the expression pattern of non-annotated and uncategorised genes whose transcript levels are normally very low during gastrulation (Fig. 3.11). Among these genes I chose to further study *K00726*, because of its similarity to the Wnt enhancing protein Rnf220. In Chapter 3, I presented preliminary results that indicate the gene does not have the same capacity of stabilising β-catenin as Rnf220 (Ma et al., 2014), moreover, it might have the opposite effect. Further experiments are required to test the function of *K00726* in the same developmental context and confirm the role of *Rnf220* in stabilising β-catenin when injecting their mRNA in ventral blastomers. Moreover, I could test the role of K00726 in activating or repressing

Wnt signalling by performing a TOPflash assay in HEK293 cells. In order to understand the functional differences between K00726 and RNF220, I could express variants of the protein in which either the E3 ubiquitin ligase and/or the zinc-finger domains are removed (Fig. 3.12) and see how Wnt activation is affected. Although I still do not know how K00726 acts upstream of Wnt signalling I have strong evidence that it is Wnt-activated. I have shown that β-catenin binds some cis-regulatory regions and that the gene is induced in animal cap cells upon β-catenin mRNA injection. To further corroborate its regulation, one could repeat the luciferase assays in the absence of any β-catenin-associated TCF binding motifs. These experiments would substantiate an action model by which Wnt signalling regulates K00726 in dorsal cells.

6.2 Cell type specific chromatin regulation *in vivo*

Transcriptome analysis of UV- and LiCl-treated embryos indicated that these embryos accurately represent ventral and dorsal cells, respectively and thus they were appropriate to investigate cell type specific chromatin regulation. My approach avoided any nuclei isolation followed by FACS sorting and lowered the number of embryos required for chromatin profiling. Both UV and LiCl treatments allow for many embryos to be manipulated at once and the whole embryo can subsequently be used for chromatin extraction. The cell type specific chromatin landscape analysis included the profiling of RNAPII, the active enhancer marker protein p300 and the T-box transcription factor Brachyury.

Profiling of RNAPII allowed to corroborate whether the differences observed in the transcriptome were reflected on the chromatin level. I showed that genes positively differentially expressed have, comparatively, higher RNAPII occupancy within its gene body. Furthermore, I was able to identify differentially transcribed genes in the two cell types, that although the RNAPII levels might be heightened by the experimental context, they should represent the differences seen in dorsal and ventral cells. Further validation could have been achieved by RNAPII ChIP-qPCR on dorsal and ventral dissected halves.

The profiling of p300 is used as a good indicator for enhancer activation in the distinct cells (Heintzman et al., 2007; Visel et al., 2009). However, in my experiment

I lacked biological replicates required to reliably identify cell type specific regulatory regions, alternatively I compared regions within the same condition. Furthermore, this study could have been complemented with ChIP-Seq for Groucho/transducin-like enhancer of split (Gro/TLE) protein, a co-repressor shown to be a better predictor of tissue-specific regulatory regions in early *Xenopus* development (Yasuoka et al., 2014).

Another aspect of cell type specific chromatin regulation was the recruitment of sequence-specific transcription factors in different cell types. I chose Brachyury for several reasons: (1) it is expressed in both cell types, (2) its binding profile had been determined in *Xenopus tropicalis* at the developmental stage of interest (Gentsch et al., 2013) and (3) the human ortholog had been shown to bind in a cell type-specific manner in different mesodermal derivatives of human embryonic stem cells (hESCs) (Faial et al., 2015). In *Xenopus*, Brachyury binds thousands of sites at gastrula stage but, the majority at lower rather than higher levels indicating that these sites are unlikely regulated by the TF (Gentsch et al., 2013). Knocking down *Xbra* and *Xbra3*, indicated that only a very small subset of putative Brachyury targets were affected transcriptionally (Gentsch et al., 2013). Gentsch *et. al,* also studied the binding profile of Xbra in early tailbud embryos and the comparison of the two datasets revealed that at least 94% of the binding sites were maintained at later stages. These experiments revealed that, in the whole embryo, Brachyury binds thousands of sites in a sequence-specific manner (sites were enriched for the T-box motif), however, only a small proportion are biologically relevant and, most of these binding events are maintained post gastrulation.

Brachyury binding profile is overall temporally unchanged when comparing gastrula and tailbud embryos (Gentsch et al., 2013). Although I have identified a subset of genomic regions where Brachyury was differentially bound, the majority of the binding events are similar in dorsalised and ventralised embryos. This indicates, that both temporally and spatially, Brachyury binding during early *Xenopus* development is mostly constant.

Different aspects can, independently or collectively, influence the differential binding of sequence-specific transcription factors, such as chromatin accessibility, histone modifications and the presence or absence of co-factors (Biggin, 2011; Voss and Hager, 2014; Spitz and Furlong, 2012). I did not manage to generate reliable data for chro-

matin accessibility or nucleosome positioning, but I did identify potential co-factors based on the *de novo* motif analysis. I found differential enrichment for DNA motifs of the Homeodomain and Forkhead family which suggest that TFs containing corresponding DNA binding domains could act as co-factors required for Brachyury binding. It has been shown that the Homeodomain protein Xom (Ventx 2.2), which is activated by BMP signalling, mediates crosstalk between Wnt and BMP signalling by interacting with LEF1/TCF, which is essential for ventral fate adoption (Gao et al., 2007). Furthermore, Ventx2.1 has been shown to interact with Smad1 (Henningfeld et al., 2002) which in turn interacts with Brachyury (Messenger et al., 2005). Both the Homeodomain and the TCF motifs were enriched in ventralised embryos, suggesting that in dorsal cells, in the absence of Ventx and zygotic Wnt, Brachyury was not capable of binding these sites as efficiently. I could test this hypothesis by determining Brachyury binding in embryos overexpressing, separately, dorso-ventral fate opposing homeobox genes *gsc* and *Ventx1/2* (Sander, Reversade, and Robertis, 2007), respectively, and test the binding of Brachyury under these conditions.

The results described are complementary to those of Faial *et al.* in which human embryonic stem cells had been differentiated into anterior mesendoderm and posterior mesoderm by subjecting them to Activin-A (FlyA) or BMP (FlyB), respectively (Faial et al., 2015). In both cell cultures BRACHYURY is expressed, but at lower levels in FlyA . These culture conditions resemble our *in vivo* condition in that there are higher levels of Nodal (Activin) signalling, in dorsalised and higher levels of BMP in ventralised embryos. Furthermore, we also observed lower levels of Brachyury and higher *Eomes* in dorsalised compared to ventralised embryos, similarly to FlyA. The authors identified cell type specific genomic landscape for Brachyury binding in the two cell types that correlated positively with gene expression. For example, in FlyA, BRACHYURY occupies genomic regions near genes associated with anterior primitive streak and endoderm, while in FlyB, binds regions near genes related to mid/posterior primitive streak and its derivatives (Faial et al., 2015). The number of differentially bound sites that I identified was smaller, and, although I find some examples of these sites being associated with gene expression, I was not able to establish a similar correlation. The 95 peaks preferentially bound in UV are near 82 genes and of these, 12/1125

(1125 genes are overexpressed in LiCl) are downregulated and 15/489 (489 genes are overexpressed in UV) are upregulated. The 373 peaks preferentially bound in LiCl are near 349 genes, of which, 31/1125 are upregulated and 7/349 are downregulated. Although there is some indication that DNA occupancy of Brachyury was stronger near genes that are preferentially expressed in one condition over the other, this was not significant.

On one hand, FlyA-treated cells differentiate into endoderm and many of the genomic sites that are preferentially bound by BRACHYURY in FlyA over FlyB are near genes associated with endoderm. Furthermore, these sites are co-bound by SMAD2/3 and EOMES, both key regulators of endoderm, while BRACHYURY is not necessary for the expression of endodermal markers. On the other hand, FlyB generates cells expressing BRACHYURY-dependant mesodermal markers and, in these cells, BRACHYURY sites are co-bound by EOMES and SMAD1. However, overexpression of BRACHYURY leads to upregulation of both mesodermal and endodermal markers, indicating its capacity in regulating both cell types (Faial et al., 2015).

In *Xenopus*, Brachyury is not involved in endoderm formation: in animal cap assays it is not capable of robustly inducing *gsc* nor *Sox17*, while *VegT* and *Eomes* can induce both endodermal makers (Conlon et al., 2001). However, it has been shown that the *Drosphila* ortholog of Brachyury promotes differentiation of endoderm, when overexpressed in animal caps (Marcellini, 2006). The difference in Brachyury structure between *Drosophila* and *Xenopus* reside in the N-terminal domain, which is essential for the interaction with Smad1. Messenger *et al.* showed that an N-terminally truncated Xbra is still capable of binding DNA but not Smad1, was capable of activating endodermal genes, such as *goosecoid* (Messenger et al., 2005).

These observations suggest that the Brachyury-Smad1 interaction has allowed the cell-type specific Brachyury-dependent gene regulation: in the presence of Smad1 Brachyury induces mesoderm and in the absence induces endoderm (Marcellini, 2006). BRACHYURY and Xbra are different in that the former interacts with both SMAD2/3 and SMAD1, while the latter does only so with Smad1 (Messenger et al., 2005; Faial et al., 2015). This suggests, that the capacity of BRACHYURY to bind SMAD2/3 has improved its cell type specific capacity of either promoting expression of posterior or

anterior mesendoderm markers. Since Xbra does not interact with Smad2/3, the same cell-type specific regulation does not take place. In turn, I suggest that in dorsal cells, with low Smad1 and high Smad2/3, VegT and Eomes take over in activating and regulating endodermal genes. Although *Eomes* and *Xbra* have a similar expression pattern during gastrulation (Gentsch et al., 2013) (Fig. 1.6), we have shown that the former has higher expression in dorsalised and the later in ventralised embryos. It would be interesting to test the binding profile of Eomes in dorsalised and ventralised embryos and investigate the differences of gene targets. My hypothesis is that Eomes would show a more cell type specific binding profile than Xbra does since dorsalised embryos are enriched for mesendoderm cells, which are mostly regulated by Eomes.

Improvements in the ChIP-Seq and sequencing library preparation protocols have allowed the investigation of chromatin landscape regulators from a small numbers of cells (Gentsch and Smith, 2017; Gentsch, Patrushev, and Smith, 2015; Gentsch and Smith, 2014). Given this, I would suggest a complementary experiment using *Xenopus* animal cap cells and induce, with increasing levels of Activin, different mesodermal types, and study the binding profile of T-box transcription factors in this context. Higher levels of Activin generates mesodermal cells with dorso-anterior identity and low Activin would lead to ventral and posterior identity, both expressing distinct levels of *Brachyury* (Green and Smith, 1990; Green, New, and Smith, 1992; Green, Smith, and Gerhart, 1994; Gurdon, Mitchell, and Mahony, 1995; Symes, Yordán, and Mercola, 1994; Gurdon et al., 1994; Wilson and Melton, 1994). This experiment would better resemble the FlyA/FlyB comparison and could help dissect the differences in cell type specific gene and chromatin regulation by Brachyury.

6.3 Off-target effects and immune response caused by morpholinos

Antisense morpholino oligomers (MO) have been used for the past two decades by developmental biologist as an indispensable tool to study gene function. With the recent emergence of genome editing tools, such as TALEN and CRISPR, morphant phenotypes have been revisited. This led to the discovery, mainly in zebrafish, that phenotypes previously associated with a morpholino knockdown, a morphant phenotype, did not

resemble the null mutant generated by CRISPR (or TALENs). This discrepancy could be because mutations were not null or morpholinos were causing side effects. To this end, we investigated the differences between embryos injected with a MO mix that inhibit Brachyury expression and TALEN-generated Brachyury mutants and focused on a whole poly-A transcriptome comparison, since, phenotypically, they are indistinguishable. We have found that while a regulatory core of Brachyury dependant genes is affected similarly in morphants and mutants, there is a subset of genes that are only affected in morphants. Furthermore, we observed that embryos injected with a standard control morpholino also have this misregulation. Further investigation identified two distinct side effects of the morpholino injection on the transcriptome: a cell-intrinsic immune response and an increase of cryptic or alternative splicing associated with regions partially complementary to the MO sequence.

These discoveries are relevant since morpholinos are widely used tools, and investigators should be aware of its possible side effects. This is particularly true if analysing later developmental stages with weak phenotypes. We advise that when studying gene function by knockdown with morpholinos, dose optimisation is essential to mitigate the side effects and the preferential use of translation- rather than splice-blocking morpholinos, since the latter have a higher probability of binding to off-target splicing junctions.

In this work we refer only to the side effects of Brachyury and control MOs, we plan to analyse publicly available data of morphant transcriptomes to search for similar side effects. Furthermore, we have plans to study each morpholino individually and its effect in causing the same side effects as well as study the effect of culture temperature, since it could affect MO hybridisation.

Appendices

Appendix I

Gene	Name	Condition	Expression	Function/Information
LOC398630	*N/A*	LiCl	Expression starts before NF12	Blasting the mRNA indicates it its the gene *tiki1*. Gene was described in *Xenopus* (Zhang et al., 2012b) and is associated with Wnt signalling and head formation.
srl	*sarcalumenin*	LiCl	Expressed after stage NF14, in the somites	No literature referring specifically to the gene. Interacts with apobec2 .
ned49	*neural precursor cell expressed developmentally down-regulated 9*	LiCl	Expression starts at MBT	Signal transducing adaptor protein
Xetrov7202751	*unnamed*	LiCl	Expression peaks at stage NF10 and at stage NF15	Predicted to be insulin-2 like LOC100494294.
ptpru	*protein tyrosinase phosphatase, receptor u*	LiCl	Expression starts at stage NF10 dorsally. Later it is expressed in the floorplate, brain and pronopheric kidney	Ectopic expression prevents the Wnt-mediated posteriorisation of the neural plate (Morgan, El-Kadi, and Theokli, 2003).
mmp17	*matrix metallopeptidase 17*	LiCl	Expression peaks at stage NF10 dorsally.	N/A
Xetrov72018683	*LOC100124853*	LiCl	Starts to be expressed at stage NF10.	Predicted to be FRAS1 related extracellular matrix 1 (*frem1*), transcript variant X3. However the gene *frem1* is annotated elsewhere in the genome.
Xetrov72037173	N/A	LiCl	Expressed at low levels high variability between clutches.	Contains a EGF-like module containing, mucin-like, hormone receptor-like sequence. Similar to emr-1, a adhesion G-protein coupled receptor.
pgm2l1	*phosphoglucomutase 2-like 1*	LiCl	Maternal transcript whose levels peak at stage NF9. Reaches lowest level at stage NF12.	N/A
tdgf1p2	*teratocarcinoma-derived growth factor 1, member 2 AKA: zcr2*	LiCl	Expressed at stage NF10 and peaks at stage NF16.	Involved in left-right patterning (Onuma, Yeo, and Whitman, 2006) and other members of the family are associated with Nodal signalling
Xetrov72021302	*N/A*	LiCl	Maternally expressed, peaks at stage NF10.	Predicted to be hematopoietic SH2 domain containing
f3	*coagulation factor III*	LiCl	Maternally expressed, peaks at stage NF10	N/A
tmem150b	*transmembrane protein 150B*	LiCl	Transcription starts at stage NF9, peaking at NF12. Expressed in the endoderm and mesendoderm.	Identified as part of the dorsal signature in *Xenopus* embryos (Ding et al., 2016).
styk1	*serine/threonine/tyrosine kinase 1*	UV	Transcribed at stage NF10 and peaks at stage NF12.	Known to activate MAP kinase and PI3k
bspry	*B-box and SPRY domain containing*	UV	Highly expressed during gastrula stages.	N/A
Xetrov72003455	N/A	UV	Highly expressed during gastrula stages.	N/A
Xetrov72003454	*unnamed*	UV	Expressed during gastrula stages.	N/A
ptger4	*prostaglandin E receptor 4*	UV	Highly expressed during gastrula stages, peaking at stage NF12.	N/A

Gene	Name	Condition	Expression	Function/Information
sh3d21	*SH3 domain containing 21*	UV	Expressed during gastrulation	Adaptor protein CMS/SETA.
Xetrov72002596	*N/A*	UV	Expressed during gastrulation	BLAST resulting in one hit - serine/threonine protein kinase N2-like (LOC105948381).
vgll1	*N/A*	UV	Expressed after gastrulation	N/A.
slc35d2	*solute carrier family 35 (UDP-GlcNAc/UDP-glucose transporter), member D2*	UV	Maternally expressed and peaks at stage NF9 and then decreases during gastrulation	In *Drosophila* has been suggested to be involved in the regulation of nucleotide?sugar levels that can differently affect Wingless and two distinct aspects of Notch signalling (Goto et al., 2001).
dip2a	*disco interacting protein 2 homolog A*	UV	Maternally expressed and peaks at stage NF9 and then decreases during gastrulation, recovering the levels at stage NF15	In humans has been shown to bind to FSTL1 (follistatin like 1) and in the mouse it is expressed in the visceral mesoderm (Ouchi et al., 2010; Tanaka et al., 2010).
fam83a	*family with sequence similarity 83 member A*	UV	Expression starts during gastrulation at low levels	Predicted to be Hes-5-like (LOC100495414).
Xetrov72027348	*LOC100495414*	UV	Highly expressed during gastrula stages, peaking at stage NF12.	N/A

Genes were selected based on the adjusted p-value from the DESeq2 analysis. The table includes information derived from **Xenbase** (http://www.xenbase.org) (Karpinka et al., 2015) and the temporal expression details were derived from **Searchable Database of *Xenopus tropicalis* Gene Expression Profiles** (http://genomics.crick.ac.uk/apps/profiles/) (Collart et al., 2014; Owens et al., 2016).

Appendix II

Differential expression analysis of LiCl- and UV-treated embryos at gastrula stage (NF11.5)

Genes up-regulated in LiCl-treated embryos
Differential analysis using DESeq2
fc> 2, padj. <0.01

Gene	baseMean	log2FoldChange	lfcSE	stat	pvalue	padj
Xetrov72020486|Xetrov72020486|loc388630	641.423026	3.57642447	0.220930949	16.18797408	6.13E-59	1.15E-54
Xetrov72010022|Xetrov72010022|foxa4	5956.26946	1.61247093	0.133258953	12.10028218	1.05E-33	4.96E-30
Xetrov72030083|Xetrov72030083|mmp1	1410.07294	2.861498166	0.23616695	12.11642087	8.65E-34	4.96E-30
Xetrov72020478|Xetrov72020478|pm20d1	988.31045	2.774833745	0.243566411	11.39251397	4.56E-30	1.72E-26
Xetrov72033932|Xetrov72033932|fzd8	1440.88332	2.335087186	0.206532863	11.30612897	1.22E-29	3.29E-26
Xetrov72026575|Xetrov72026575|ppp1r3c.1	87.4201578	3.72992693	0.329796525	11.30978238	1.17E-29	3.29E-26
Xetrov72038527|Xetrov72038527|foxp2	100.577318	3.655346949	0.327388647	11.16516098	6.04E-29	1.26E-25
Xetrov72035990|Xetrov72035990|slc38a3	600.571736	2.101630869	0.196701093	10.68438837	1.20E-26	2.09E-23
Xetrov72005175|Xetrov72005175|srl	64.7584169	3.753328947	0.351716977	10.67144662	1.38E-26	2.17E-23
Xetrov72035278|Xetrov72035278	1632.69393	2.161124319	0.20972785	10.30442225	6.73E-25	9.05E-22
Xetrov72043560|Xetrov72043560 (**K00726)**	304.815714	3.776461936	0.367036389	10.28906683	7.89E-25	9.29E-22
Xetrov72014334|Xetrov72014334|pou4f1.2	76.035226	2.959439327	0.291450636	10.15417008	3.17E-24	2.60E-21
Xetrov72027551|Xetrov72027551|unnamed	1129.33058	2.407690305	0.237451592	10.13971008	3.68E-24	2.77E-21
Xetrov72026895|Xetrov72026895|unnamed	21.7486552	5.135245931	0.531410476	9.663426231	4.31E-22	2.80E-19
Xetrov72033588|Xetrov72033588|nedd9	600.291917	2.465059179	0.256255921	9.61952088	6.61E-22	4.15E-19
Xetrov72017783|Xetrov72017783|nog	478.797227	2.851782694	0.297430763	9.588055606	8.98E-22	5.45E-19
Xetrov72000768|Xetrov72000768|zic4	285.12217	2.5121135	0.26669608	9.419386683	4.54E-21	2.51E-18
Xetrov72016719|Xetrov72016719|cntnap1	169.452844	2.824716594	0.300148064	9.411077167	4.91E-21	2.57E-18
Xetrov72031314|Xetrov72031314|tspan7	197.268364	1.928856518	0.204926151	9.412446933	4.85E-21	2.57E-18
Xetrov72037173|Xetrov72037173	53.2129068	2.780640762	0.300910928	9.240743712	2.45E-20	1.12E-17
Xetrov72042969|Xetrov72042969	391.124768	2.094766616	0.228482513	9.168170433	4.81E-20	2.11E-17
Xetrov72017906|Xetrov72017906	49.679391	3.515090291	0.385844776	9.110115022	8.23E-20	3.37E-17
Xetrov72000221|Xetrov72000221	61.8204369	2.934841559	0.324015873	9.057709211	1.33E-19	5.23E-17
Xetrov72018683|Xetrov72018683	70.5610887	2.45208082	0.271828354	9.020695521	1.87E-19	7.18E-17
Xetrov72020695|Xetrov72020695|cpe	112.381395	2.477701753	0.276523237	8.960193648	3.24E-19	1.17E-16
Xetrov72021302|Xetrov72021302	48.6050449	4.332685893	0.488662073	8.866425548	7.55E-19	2.63E-16
Xetrov72032574|Xetrov72032574	108.202772	3.051889	0.345526309	8.832580676	1.02E-18	3.50E-16
Xetrov72002782|Xetrov72002782|pat	333.552463	1.888929198	0.214921074	8.788943616	1.51E-18	4.90E-16
Xetrov72021605|Xetrov72021605|fst	636.106348	3.545037588	0.409564009	8.65563749	4.90E-18	1.54E-15
Xetrov72000357|Xetrov72000357|chrd	3452.20507	3.326367304	0.386312628	8.61055804	7.27E-18	2.24E-15
Xetrov72026912|Xetrov72026912|sftpa	30.9970894	4.330721596	0.504608001	8.582348261	9.30E-18	2.82E-15
Xetrov72033032|Xetrov72033032	136.213555	2.633300436	0.309925456	8.49656067	1.95E-17	5.84E-15
Xetrov72021492|Xetrov72021492|foxd4l1.2	108.819124	3.465889199	0.409586591	8.46192057	2.63E-17	7.62E-15
Xetrov72003610|Xetrov72003610	71.883348	4.403552346	0.521523532	8.443631165	3.08E-17	8.78E-15
Xetrov72026864|Xetrov72026864|dkk1	1964.2233	2.451396192	0.291611285	8.406383136	4.23E-17	1.17E-14
Xetrov72013989|Xetrov72013989|dpf1	95.8225206	3.369221366	0.402554466	8.369603736	5.78E-17	1.56E-14
Xetrov72042269|Xetrov72042269	105.292894	2.524510136	0.303679828	8.313064954	9.33E-17	2.42E-14
Xetrov72024775|Xetrov72024775	25.6554835	4.588455136	0.552201093	8.309391622	9.62E-17	2.45E-14
Xetrov72030447|Xetrov72030447|il1r2	598.640418	3.208862033	0.389217187	8.244399629	1.66E-16	4.11E-14
Xetrov72014354|Xetrov72014354	552.717133	1.640801105	0.199075715	8.242095761	1.69E-16	4.14E-14
Xetrov72016834|Xetrov72016834|slc4a1	306.298524	2.807186934	0.343278103	8.177588119	2.90E-16	6.65E-14
Xetrov72006278|Xetrov72006278	2705.29004	2.517841089	0.312162256	8.065808866	7.28E-16	1.59E-13
Xetrov72009195|Xetrov72009195	362.732799	1.839246084	0.229264227	8.022385813	1.04E-15	2.25E-13
Xetrov72023130|Xetrov72023130	249.386979	2.778036006	0.34767869	7.990239501	1.35E-15	2.88E-13
Xetrov72020537|Xetrov72020537|unnamed	20.7707223	2.942927327	0.368429306	7.987766652	1.37E-15	2.91E-13
Xetrov72032369|Xetrov72032369	78.3303253	2.791043239	0.349886699	7.976991543	1.50E-15	3.14E-13
Xetrov72001973|Xetrov72001973	28.2639528	3.184238749	0.400255741	7.955510488	1.78E-15	3.61E-13
Xetrov72007519|Xetrov72007519	1580.83157	2.912458611	0.366539759	7.94581908	1.93E-15	3.87E-13
Xetrov72014053|Xetrov72014053|smoc1	161.029422	3.344590569	0.421777754	7.92974627	2.20E-15	4.35E-13
Xetrov72007533|Xetrov72007533	32.4474528	3.882858809	0.490613876	7.914286567	2.49E-15	4.88E-13
Xetrov72022463|Xetrov72022463	23.4537156	3.290877815	0.417448561	7.883313346	3.19E-15	6.13E-13
Xetrov72014980|Xetrov72014980|nkx2-8	55.6158214	3.169279717	0.402354243	7.876839316	3.36E-15	6.24E-13
Xetrov72004745|Xetrov72004745|fap	40.1574704	4.262599477	0.545789569	7.809968755	5.72E-15	9.98E-13
Xetrov72010166|Xetrov72010166|foxd3	751.891534	2.235472612	0.286342597	7.806985889	5.86E-15	1.01E-12
Xetrov72001653|Xetrov72001653|veph1	17.0381081	4.203636697	0.540526481	7.776930162	7.43E-15	1.26E-12
Xetrov72b000019|Xetrov72b000019|loc644100	10.3495156	4.462766825	0.574875405	7.763015752	8.29E-15	1.38E-12
Xetrov72011406|Xetrov72011406	27.0468143	4.300683009	0.554010526	7.762818231	8.31E-15	1.38E-12
Xetrov72020468|Xetrov72020468|mmp17	788.07947	2.108120772	0.272562654	7.734444696	1.04E-14	1.70E-12
Xetrov72005350|Xetrov72005350|cdk15	64.4012241	2.493475836	0.3229405	7.721161753	1.15E-14	1.86E-12
Xetrov72030361|Xetrov72030361|lhx1	2170.62922	1.921123201	0.250135928	7.68031691	1.59E-14	2.53E-12
Xetrov72013654|Xetrov72013654|unnamed	321.72706	3.367779592	0.439170653	7.668498724	1.74E-14	2.75E-12
Xetrov72019088|Xetrov72019088|slc12a3.2	6062.69761	1.477847129	0.193496408	7.63759464	2.21E-14	3.36E-12
Xetrov72010511|Xetrov72010511|frzb2	2403.84876	3.807537306	0.499309425	7.625606711	2.43E-14	3.63E-12
Xetrov72032712|Xetrov72032712|scn8a	123.48734	1.973712755	0.259414845	7.608326167	2.78E-14	4.09E-12
Xetrov72037692|Xetrov72037692|fbn1	109.402923	3.400639929	0.448281294	7.585950999	3.30E-14	4.75E-12
Xetrov72021109|Xetrov72021109|admp	4397.42161	2.852089404	0.37770419	7.551119317	4.32E-14	6.16E-12
Xetrov72000087|Xetrov72000087|lama4	143.525368	3.297307609	0.437608863	7.534828219	4.89E-14	6.87E-12
Xetrov72016923|Xetrov72016923|ppp1r9b	36.3983061	3.533130526	0.469615112	7.52346003	5.33E-14	7.44E-12
Xetrov72005652|Xetrov72005652	1669.04927	2.41204796	0.320720935	7.520706313	5.45E-14	7.49E-12
Xetrov72023862|Xetrov72023862|ntrk2	16.8060013	3.836041824	0.510416172	7.515517801	5.67E-14	7.74E-12

Xetrov72028660|Xetrov72028660|lrp1	1286.60541	1.097356003	0.147237463	7.452967328	9.13E-14	1.21E-11
Xetrov72014322|Xetrov72014322	46.4195197	3.660744242	0.492504534	7.43291481	1.06E-13	1.39E-11
Xetrov72021397|Xetrov72021397|foxd4l1.1	3473.98249	1.84178813	0.247800742	7.432536784	1.07E-13	1.39E-11
Xetrov72022530|Xetrov72022530|tdgf1p2	278.894557	2.245111314	0.30233621	7.425876348	1.12E-13	1.45E-11
Xetrov72027037|Xetrov72027037|zc4h2	551.810408	2.200267109	0.296725942	7.415149123	1.21E-13	1.55E-11
Xetrov72033827|Xetrov72033827|cdh12	53.8983579	3.045957199	0.412172077	7.390013464	1.47E-13	1.82E-11
Xetrov72020291|Xetrov72020291|plbd2	456.028585	1.515875986	0.205105854	7.390700732	1.46E-13	1.82E-11
Xetrov72024253|Xetrov72024253|slc24a6	472.407663	1.34545408	0.182635761	7.366870917	1.75E-13	2.10E-11
Xetrov72024950|Xetrov72024950|usp28	639.020682	1.226036104	0.166640299	7.35738059	1.88E-13	2.22E-11
Xetrov72012417|Xetrov72012417|unnamed	857.468313	1.163098986	0.158210744	7.351580275	1.96E-13	2.31E-11
Xetrov72001239|Xetrov72001239|unnamed	14.8251512	3.859331036	0.525119451	7.349434546	1.99E-13	2.33E-11
Xetrov72000247|Xetrov72000247|fam184a	71.2677389	3.087403046	0.420778869	7.33735288	2.18E-13	2.53E-11
Xetrov72038648|Xetrov72038648|n4bp3	406.295228	1.62672629	0.221863125	7.332116538	2.27E-13	2.62E-11
Xetrov72009496|Xetrov72009496|slc29a2	1837.15644	1.176082177	0.160430588	7.33078519	2.29E-13	2.63E-11
Xetrov72018038|Xetrov72018038	555.203367	2.172074247	0.296433604	7.327354989	2.35E-13	2.68E-11
Xetrov72009360|Xetrov72009360|pdp2	52.2705078	3.536459216	0.484010329	7.306577986	2.74E-13	3.11E-11
Xetrov72010379|Xetrov72010379|akr1c1	88.4984187	4.021182397	0.553483487	7.265225598	3.72E-13	4.12E-11
Xetrov72037469|Xetrov72037469|ccdc77	1333.93229	2.675309275	0.36827337	7.264465732	3.75E-13	4.12E-11
Xetrov72009344|Xetrov72009344|znf565	48.8002259	2.679930141	0.369564775	7.251584356	4.12E-13	4.48E-11
Xetrov72007305|Xetrov72007305|acvr1	445.24808	1.142782707	0.157610561	7.25067345	4.15E-13	4.49E-11
Xetrov72038905|Xetrov72038905|pfkfb3	2201.06574	1.184957666	0.163537602	7.245781098	4.30E-13	4.63E-11
Xetrov72011327|Xetrov72011327	86.9549836	3.04160725	0.420009788	7.241753263	4.43E-13	4.74E-11
Xetrov72020194|Xetrov72020194|ndnf	192.424467	2.449071509	0.339359244	7.216752019	5.32E-13	5.63E-11
Xetrov72040518|Xetrov72040518	306.293095	2.630422201	0.365238786	7.201924616	5.94E-13	6.25E-11
Xetrov72020198|Xetrov72020198|frmd3	35.2692314	3.493329915	0.485131525	7.20078934	5.99E-13	6.26E-11
Xetrov72017851|Xetrov72017851|dkkx	179.591651	3.309234767	0.459794572	7.197202762	6.15E-13	6.40E-11
Xetrov72032672|Xetrov72032672|unnamed	15.9685699	3.617771743	0.503559347	7.184399937	6.75E-13	6.95E-11
Xetrov72034856|Xetrov72034856|sla	43.1015412	2.834837367	0.396820099	7.143885537	9.07E-13	9.19E-11
Xetrov72028840|Xetrov72028840|ptpru	337.156661	2.239553747	0.313548712	7.14260228	9.16E-13	9.22E-11
Xetrov72008861|Xetrov72008861|pcsk9	74.0990557	2.014114658	0.282266971	7.135495352	9.64E-13	9.63E-11
Xetrov72016999|Xetrov72016999|dhx58	83.5599549	2.873836072	0.402994749	7.131199802	9.95E-13	9.86E-11
Xetrov72026767|Xetrov72026767|hhex	1036.29611	2.629793847	0.369153043	7.123857976	1.05E-12	1.03E-10
Xetrov72042081|Xetrov72042081	190.253189	2.92934564	0.411752819	7.114330496	1.12E-12	1.10E-10
Xetrov72034880|Xetrov72034880|scgn	13.748937	3.797616132	0.533786041	7.11449128	1.12E-12	1.10E-10
Xetrov72031321|Xetrov72031321|gjb2	5454.23487	2.711715978	0.38121013	7.113441558	1.13E-12	1.10E-10
Xetrov72023107|Xetrov72023107	68.3774272	2.783217188	0.392413086	7.092569767	1.32E-12	1.26E-10
Xetrov72004111|Xetrov72004111	31.8247651	3.539818091	0.500553146	7.071812694	1.53E-12	1.45E-10
Xetrov72016524|Xetrov72016524	129.75793	2.07092726	0.293036203	7.06713792	1.58E-12	1.50E-10
Xetrov72006643|Xetrov72006643	171.912338	2.282161649	0.323098362	7.063364956	1.63E-12	1.52E-10
Xetrov72000023|Xetrov72000023|ush2a	86.1353566	2.223265147	0.314860738	7.061106325	1.65E-12	1.54E-10
Xetrov72042259|Xetrov72042259|hes7.1	266.652691	2.732497035	0.387521808	7.051208419	1.77E-12	1.64E-10
Xetrov72034822|Xetrov72034822|march11	37.4892545	3.166761696	0.449150018	7.05056567	1.78E-12	1.64E-10
Xetrov72039624|Xetrov72039624|epyc	26.6389025	2.652068018	0.37740155	7.027178394	2.11E-12	1.92E-10
Xetrov72013775|Xetrov72013775|pkdcc.1	840.97476	1.844506562	0.263206238	7.007837573	2.42E-12	2.16E-10
Xetrov72040358|Xetrov72040358	177.788542	2.618621723	0.37547972	6.974069666	3.08E-12	2.68E-10
Xetrov72003550|Xetrov72003550|npdc1.1	270.773162	1.256019258	0.180256119	6.967970143	3.22E-12	2.79E-10
Xetrov72002339|Xetrov72002339|kng1	807.871946	3.341370761	0.480893474	6.94825558	3.70E-12	3.18E-10
Xetrov72029992|Xetrov72029992|amhr2	41.6924201	2.923181134	0.420848155	6.945928351	3.76E-12	3.22E-10
Xetrov72000346|Xetrov72000346|gpr126	18.2792158	2.823021438	0.406568677	6.943529102	3.82E-12	3.26E-10
Xetrov72009273|Xetrov72009273|ces3	68.1856975	3.153092912	0.454425942	6.93862877	3.96E-12	3.34E-10
Xetrov72022000|Xetrov72022000|cfd	1735.81303	2.748610294	0.396427387	6.933452081	4.11E-12	3.45E-10
Xetrov72037991|Xetrov72037991|lrig3	10330.4583	1.744293333	0.251796374	6.927396543	4.29E-12	3.59E-10
Xetrov72000051|Xetrov72000051|hivep2	68.0483949	2.904800452	0.420429989	6.909118108	4.88E-12	4.06E-10
Xetrov72028857|Xetrov72028857|gli1.1	521.330224	2.868051257	0.415406514	6.904203864	5.05E-12	4.19E-10
Xetrov72006792|Xetrov72006792	46.2059033	2.397665767	0.34838095	6.882310203	5.89E-12	4.84E-10
Xetrov72016738|Xetrov72016738|grin2c	331.406375	1.711346802	0.249847507	6.84956525	7.41E-12	5.89E-10
Xetrov72006804|Xetrov72006804	24.8386081	3.109538011	0.456886398	6.805932555	1.00E-11	7.85E-10
Xetrov72042553|Xetrov72042553|mdga1	21.6317423	3.064404962	0.450355143	6.804418706	1.01E-11	7.90E-10
Xetrov72009386|Xetrov72009386|fmo2	49.4827174	3.763913787	0.555331024	6.777784103	1.22E-11	9.42E-10
Xetrov72025680|Xetrov72025680|bcl2l12	623.983332	1.159896637	0.171171598	6.776221364	1.23E-11	9.48E-10
Xetrov72038999|Xetrov72038999|il17ra	60.0748848	1.783061731	0.264192415	6.74910266	1.49E-11	1.13E-09
Xetrov72010533|Xetrov72010533|cebpa	16.9392375	2.705246029	0.403279688	6.708113765	1.97E-11	1.48E-09
Xetrov72038987|Xetrov72038987	721.359095	1.512469153	0.22548391	6.707658885	1.98E-11	1.48E-09
Xetrov72008248|Xetrov72008248|rasal2	522.33061	1.070773043	0.159723567	6.703913904	2.03E-11	1.50E-09
Xetrov72b000107|Xetrov72b000107|fam134b	52.5150577	2.096913535	0.313424965	6.690320702	2.23E-11	1.64E-09
Xetrov72009821|Xetrov72009821|fads1	165.206741	1.139676158	0.170513609	6.683784143	2.33E-11	1.71E-09
Xetrov72042967|Xetrov72042967	51.0426014	2.038162845	0.30530119	6.675908621	2.46E-11	1.79E-09
Xetrov72024866|Xetrov72024866	1218.0153	1.218005341	0.182986594	6.656254503	2.81E-11	2.02E-09
Xetrov72041348|Xetrov72041348|ces1	848.883529	1.655570416	0.249127476	6.645475012	3.02E-11	2.14E-09
Xetrov72017793|Xetrov72017793	7.92794489	3.584560945	0.539855677	6.639850416	3.14E-11	2.21E-09
Xetrov72018648|Xetrov72018648|tep1	31.2926198	2.799483892	0.422478021	6.62634209	3.44E-11	2.42E-09
Xetrov72041710|Xetrov72041710	24.327813	3.303177829	0.500358029	6.601628507	4.07E-11	2.83E-09
Xetrov72012470|Xetrov72012470	8.81429577	3.719143393	0.56461181	6.587080415	4.49E-11	3.11E-09
Xetrov72013833|Xetrov72013833|zic3	5123.11576	1.062058904	0.16130465	6.584180322	4.57E-11	3.16E-09
Xetrov72010596|Xetrov72010596|f3	82.9258306	2.84790698	0.43694151	6.517821986	7.13E-11	4.83E-09
Xetrov72043417|Xetrov72043417|sia1	89.4833114	3.321417557	0.510003937	6.512533168	7.39E-11	4.97E-09

Xetrov72025882|Xetrov72025882|ddx25	848.25292	1.573329315	0.241619832	6.511590145	7.44E-11	4.98E-09
Xetrov72026786|Xetrov72026786|unnamed	4909.44468	1.508985207	0.2324073	6.492847727	8.42E-11	5.59E-09
Xetrov72007880|Xetrov72007880	24.4023002	3.007999309	0.464215301	6.47975045	9.19E-11	6.07E-09
Xetrov72042258|Xetrov72042258|per1	94.3124586	3.193757283	0.492948254	6.478889534	9.24E-11	6.08E-09
Xetrov72017405|Xetrov72017405|crtap	78.4356168	2.116812668	0.326804639	6.477303003	9.34E-11	6.13E-09
Xetrov72021204|Xetrov72021204|adh7	19.0290906	3.617300577	0.562435525	6.431493777	1.26E-10	8.04E-09
Xetrov72038083|Xetrov72038083|slc12a1	315.640421	2.800715244	0.435654041	6.428759939	1.29E-10	8.11E-09
Xetrov72029873|Xetrov72029873|b4galnt1	358.173319	2.07689573	0.323065906	6.428706007	1.29E-10	8.11E-09
Xetrov72008010|Xetrov72008010	580.318982	2.339831832	0.364115579	6.426069	1.31E-10	8.22E-09
Xetrov72024464|Xetrov72024464|cib3	8.4903905	3.581085339	0.559096784	6.405125982	1.50E-10	9.34E-09
Xetrov72014590|Xetrov72014590|gsc	1797.39966	3.156953015	0.493160961	6.401465783	1.54E-10	9.53E-09
Xetrov72030237|Xetrov72030237|tfap2e	143.624714	1.357461804	0.212117617	6.399571261	1.56E-10	9.62E-09
Xetrov72032656|Xetrov72032656|il1rapl1	6.17679681	3.251838669	0.508217433	6.398518547	1.57E-10	9.66E-09
Xetrov72037973|Xetrov72037973|pcdh12	19.3794457	2.543685624	0.398422525	6.384392101	1.72E-10	1.05E-08
Xetrov72030452|Xetrov72030452|ift57	459.942816	1.485996016	0.233303276	6.369374844	1.90E-10	1.16E-08
Xetrov72043015|Xetrov72043015	269.718721	2.257393807	0.354795644	6.36251838	1.98E-10	1.21E-08
Xetrov72040828|Xetrov72040828	246.498208	2.199710416	0.345878994	6.359768752	2.02E-10	1.22E-08
Xetrov72028195|Xetrov72028195	148.497571	2.646165486	0.416151208	6.358663479	2.04E-10	1.23E-08
Xetrov72002663|Xetrov72002663|bmp5	8.28193125	3.725441663	0.586721126	6.349595232	2.16E-10	1.29E-08
Xetrov72030239|Xetrov72030239|arl13b	99.1416357	1.410916197	0.223006859	6.32678387	2.50E-10	1.48E-08
Xetrov72009929|Xetrov72009929	3772.55431	1.725839526	0.274424108	6.288950129	3.20E-10	1.86E-08
Xetrov72041883|Xetrov72041883	70.4330676	2.358447075	0.375334943	6.283579818	3.31E-10	1.91E-08
Xetrov72032425|Xetrov72032425	21.0191029	2.587703665	0.411826731	6.283476687	3.31E-10	1.91E-08
Xetrov72038081|Xetrov72038081|anpep	859.729862	2.113346768	0.336598172	6.278544998	3.42E-10	1.96E-08
Xetrov72014618|Xetrov72014618|st6galnac4	459.815056	1.721960529	0.274474869	6.273654613	3.53E-10	2.01E-08
Xetrov72023462|Xetrov72023462|tdgf1p3	98.4724429	2.438551143	0.388970274	6.269248083	3.63E-10	2.06E-08
Xetrov72022088|Xetrov72022088|ngf	6.61253742	3.103480241	0.495314344	6.265678108	3.71E-10	2.11E-08
Xetrov72034574|Xetrov72034574|ccr2	9.13507969	3.672428364	0.586707829	6.2593819	3.87E-10	2.19E-08
Xetrov72043017|Xetrov72043017	18.4737167	2.113268946	0.338098358	6.250456107	4.09E-10	2.29E-08
Xetrov72041732|Xetrov72041732	54.3898645	3.238091525	0.518358775	6.246815301	4.19E-10	2.34E-08
Xetrov72030475|Xetrov72030475|slc35f2	1498.97223	1.024700194	0.164286719	6.237267385	4.45E-10	2.47E-08
Xetrov72036594|Xetrov72036594|gata4	3901.42723	1.22646839	0.196831458	6.231058814	4.63E-10	2.55E-08
Xetrov72034159|Xetrov72034159|darmin	9702.65989	1.588833506	0.255241765	6.2248179	4.82E-10	2.64E-08
Xetrov72002785|Xetrov72002785	38.7440049	2.348030667	0.379055707	6.194421086	5.85E-10	3.17E-08
Xetrov72017332|Xetrov72017332	153.545414	1.207612622	0.194967491	6.193917848	5.87E-10	3.17E-08
Xetrov72000644|Xetrov72000644	13.9028007	2.474400359	0.400586743	6.176940205	6.54E-10	3.50E-08
Xetrov72032793|Xetrov72032793|zbed1	489.133493	1.559144871	0.252829981	6.166772094	6.97E-10	3.70E-08
Xetrov72001076|Xetrov72001076|pkdcc.2	766.529183	2.064485721	0.335117546	6.160482337	7.25E-10	3.82E-08
Xetrov72037162|Xetrov72037162	28.4912426	3.018649719	0.491596328	6.140505014	8.23E-10	4.27E-08
Xetrov72042832|Xetrov72042832	172.562069	2.471132804	0.403880712	6.118471934	9.45E-10	4.86E-08
Xetrov72000486|Xetrov72000486|plg	25.2604054	2.907042798	0.475418575	6.114701758	9.67E-10	4.96E-08
Xetrov72019326|Xetrov72019326|c6.2	749.193482	2.616581149	0.43049495	6.078076295	1.22E-09	6.17E-08
Xetrov72006126|Xetrov72006126	50.2803604	1.991355222	0.327885941	6.073316887	1.25E-09	6.34E-08
Xetrov72000849|Xetrov72000849|slc3a1	1562.53291	1.839257055	0.30297017	6.070752966	1.27E-09	6.43E-08
Xetrov72020499|Xetrov72020499	81.9576373	2.491661326	0.410517042	6.069568544	1.28E-09	6.46E-08
Xetrov72002617|Xetrov72002617|txlnb	80.0943596	1.797542102	0.296342525	6.065758195	1.31E-09	6.58E-08
Xetrov72027003|Xetrov72027003|tmem150b	1992.61642	1.836888511	0.30281719	6.065998137	1.31E-09	6.58E-08
Xetrov72031241|Xetrov72031241|rab34	622.637967	1.460391388	0.241268395	6.052974263	1.42E-09	7.08E-08
Xetrov72029639|Xetrov72029639|pgm2l1	297.02007	2.066835371	0.34149726	6.052275126	1.43E-09	7.10E-08
Xetrov72030901|Xetrov72030901	20.6463634	2.287629322	0.378499455	6.043943502	1.50E-09	7.43E-08
Xetrov72031924|Xetrov72031924	1789.65121	2.145817084	0.355433967	6.03717507	1.57E-09	7.71E-08
Xetrov72008730|Xetrov72008730|cdh11	765.231966	2.436094647	0.404614683	6.020776677	1.74E-09	8.45E-08
Xetrov72014962|Xetrov72014962|chac1	240.647484	1.956524225	0.325106394	6.018104414	1.76E-09	8.54E-08
Xetrov72017675|Xetrov72017675|cd40	49.3123552	2.839093396	0.471942309	6.015763671	1.79E-09	8.65E-08
Xetrov72012345|Xetrov72012345	21.7052662	2.191377376	0.364691985	6.008844363	1.87E-09	9.00E-08
Xetrov72040709|Xetrov72040709	216.255516	2.724527465	0.453546959	6.007156283	1.89E-09	9.05E-08
Xetrov72008216|Xetrov72008216|pappa2	12.3729758	2.87227417	0.478905805	5.997576429	2.00E-09	9.55E-08
Xetrov72030939|Xetrov72030939|igsf3	847.648718	2.789471907	0.465359941	5.994224389	2.04E-09	9.70E-08
Xetrov72000300|Xetrov72000300|mecom	46.9294823	2.576142339	0.430880087	5.978791822	2.25E-09	1.06E-07
Xetrov72018587|Xetrov72018587|vcan	242.925608	1.606278078	0.269638748	5.957148555	2.57E-09	1.20E-07
Xetrov72035925|Xetrov72035925|ropn1l	54.8031745	2.392104841	0.402181915	5.947818014	2.72E-09	1.27E-07
Xetrov72028995|Xetrov72028995|bbx	60.497558	2.097007238	0.353263158	5.936105106	2.92E-09	1.35E-07
Xetrov72020356|Xetrov72020356|slco4c1	399.668691	2.33224432	0.393640243	5.924811701	3.13E-09	1.44E-07
Xetrov72010464|Xetrov72010464	23.7565025	3.158775932	0.533208315	5.924093534	3.14E-09	1.44E-07
Xetrov72041440|Xetrov72041440	4.64507192	3.443390395	0.58159003	5.92064894	3.21E-09	1.46E-07
Xetrov72018944|Xetrov72018944|dgkb	9.99599326	2.788587902	0.473095695	5.89434216	3.76E-09	1.70E-07
Xetrov72006322|Xetrov72006322	206.926452	2.598529101	0.441096177	5.891071465	3.84E-09	1.73E-07
Xetrov72041203|Xetrov72041203	115.590222	2.995196884	0.508602534	5.889071885	3.88E-09	1.75E-07
Xetrov72043461|Xetrov72043461	32.5191647	2.422035567	0.411549782	5.885158182	3.98E-09	1.78E-07
Xetrov72016275|Xetrov72016275|lgals9	47.0137804	3.0577544	0.519611778	5.884690317	3.99E-09	1.78E-07
Xetrov72026165|Xetrov72026165|nodal	276.584298	1.73195218	0.296249955	5.846252969	5.03E-09	2.22E-07
Xetrov72026826|Xetrov72026826|neurog3	97.6593725	2.528983817	0.432786388	5.843492054	5.11E-09	2.25E-07
Xetrov72014636|Xetrov72014636|six1	255.6886	2.217812454	0.37983325	5.838910773	5.25E-09	2.30E-07
Xetrov72020722|Xetrov72020722|bmp3	111.135853	2.005801716	0.344497148	5.822404423	5.80E-09	2.53E-07
Xetrov72004128|Xetrov72004128	19.2133035	3.280869556	0.563470593	5.822610085	5.79E-09	2.53E-07
Xetrov72024633|Xetrov72024633	5.59312298	3.402046519	0.584808845	5.817365025	5.98E-09	2.59E-07

Xetrov72026317|Xetrov72026317|c17orf42	125.761964	1.178820169	0.202912439	5.809501737	6.27E-09	2.71E-07
Xetrov72012642|Xetrov72012642|fmn1	27.3232907	2.37883774	0.409852361	5.804133304	6.47E-09	2.78E-07
Xetrov72030483|Xetrov72030483|nck2	72.1469037	1.179120572	0.203132536	5.804685918	6.45E-09	2.78E-07
Xetrov72026086|Xetrov72026086|kcnj9	8.39752689	3.297908054	0.568711704	5.79891012	6.67E-09	2.86E-07
Xetrov72024727|Xetrov72024727|tecta.1	30.8133235	2.485436532	0.429240679	5.790309855	7.03E-09	2.99E-07
Xetrov72029971|Xetrov72029971|zic2	3891.90972	1.016963997	0.175644502	5.789899385	7.04E-09	2.99E-07
Xetrov72001095|Xetrov72001095|mycn	252.52484	1.113270334	0.193388425	5.756654433	8.58E-09	3.62E-07
Xetrov72030200|Xetrov72030200|znf205	181.533148	1.105264233	0.192280313	5.748192405	9.02E-09	3.79E-07
Xetrov72013259|Xetrov72013259|unnamed	6050.39148	1.849957654	0.32186646	5.747593758	9.05E-09	3.80E-07
Xetrov72025247|Xetrov72025247	29.3047897	2.530770545	0.440485161	5.745416128	9.17E-09	3.84E-07
Xetrov72009666|Xetrov72009666|cdh8	6.56300995	3.022583014	0.527220422	5.733053744	9.86E-09	4.09E-07
Xetrov72026667|Xetrov72026667	8.68410578	3.381671322	0.590432905	5.727443868	1.02E-08	4.21E-07
Xetrov72038683|Xetrov72038683|plat	99.3181239	3.064074371	0.535060522	5.726593989	1.02E-08	4.22E-07
Xetrov72009370|Xetrov72009370|fmo3	40.2439529	2.793255467	0.488269061	5.720730001	1.06E-08	4.34E-07
Xetrov72028461|Xetrov72028461|pex14	354.608375	1.36188369	0.238648871	5.706642084	1.15E-08	4.68E-07
Xetrov72014609|Xetrov72014609|crx	6389.28	1.966435848	0.344653724	5.705540701	1.16E-08	4.69E-07
Xetrov72001391|Xetrov72001391|agtr1	17.6354356	2.636590308	0.462284802	5.703389546	1.17E-08	4.73E-07
Xetrov72026491|Xetrov72026491|nkx2-3	36.1893034	2.346304862	0.411735932	5.698567161	1.21E-08	4.84E-07
Xetrov72024986|Xetrov72024986|ret	8.09283644	2.85355434	0.50082689	5.697685962	1.21E-08	4.85E-07
Xetrov72019277|Xetrov72019277|aqpep	13.0911412	2.938914971	0.516217307	5.693174043	1.25E-08	4.95E-07
Xetrov72034556|Xetrov72034556|shh	125.188605	2.92730824	0.515626294	5.677189617	1.37E-08	5.40E-07
Xetrov72006449|Xetrov72006449|LOC101732582	50.3434825	2.271008818	0.400124986	5.675748571	1.38E-08	5.43E-07
Xetrov72006076|Xetrov72006076	86.16561	2.102566068	0.372652227	5.642166916	1.68E-08	6.53E-07
Xetrov72023986|Xetrov72023986	6.53317005	2.75957911	0.489909262	5.632837182	1.77E-08	6.88E-07
Xetrov72000046|Xetrov72000046|utrn	37.8481749	1.387841649	0.246646811	5.626837997	1.84E-08	7.10E-07
Xetrov72002088|Xetrov72002088	36.6872001	2.579501378	0.459762336	5.610510425	2.02E-08	7.77E-07
Xetrov72040122|Xetrov72040122	1215.95942	2.275675773	0.406239124	5.601813411	2.12E-08	8.15E-07
Xetrov72014282|Xetrov72014282|dnase1	4.82273301	3.281172566	0.587239143	5.587455481	2.30E-08	8.82E-07
Xetrov72001996|Xetrov72001996|ripply2.1	406.561994	1.983092837	0.355149945	5.583818516	2.35E-08	8.95E-07
Xetrov72004182|Xetrov72004182|cacna1h	16.9202873	2.463738969	0.441270297	5.583287576	2.36E-08	8.96E-07
Xetrov72040807|Xetrov72040807	119.396936	1.995682168	0.357767596	5.578152389	2.43E-08	9.19E-07
Xetrov72013810|Xetrov72013810|tc2n	6.9079264	3.052548379	0.547365971	5.576796037	2.45E-08	9.25E-07
Xetrov72020827|Xetrov72020827|ifngr1	205.256557	1.18391841	0.21242328	5.573392938	2.50E-08	9.41E-07
Xetrov72034224|Xetrov72034224|adhfe1	116.522683	2.558785689	0.45927135	5.57140281	2.53E-08	9.48E-07
Xetrov72011678|Xetrov72011678	92.6758795	1.874229814	0.336486914	5.569993173	2.55E-08	9.54E-07
Xetrov72037148|Xetrov72037148|gmip	10.1248271	3.16711114	0.568778146	5.568271503	2.57E-08	9.61E-07
Xetrov72042029|Xetrov72042029	26.9490635	3.053572551	0.548468563	5.567452284	2.58E-08	9.64E-07
Xetrov72025838|Xetrov72025838|slc16a9	11.1818491	2.245945421	0.405033304	5.545088265	2.94E-08	1.09E-06
Xetrov72035977|Xetrov72035977	74.3871586	2.802721234	0.50556918	5.543694797	2.96E-08	1.10E-06
Xetrov72026572|Xetrov72026572|rassf4	55.4676267	2.324757911	0.419558688	5.540960001	3.01E-08	1.11E-06
Xetrov72003242|Xetrov72003242|hsd3b1	12.9040765	2.455987564	0.443615212	5.536301505	3.09E-08	1.14E-06
Xetrov72014511|Xetrov72014511|otx2	2185.72174	2.29355012	0.41535477	5.521906302	3.35E-08	1.23E-06
Xetrov72017121|Xetrov72017121|slc13a3	500.402898	1.861388292	0.337800984	5.510310457	3.58E-08	1.30E-06
Xetrov72029751|Xetrov72029751|slc43a2	127.978148	1.788057649	0.324638915	5.507835212	3.63E-08	1.31E-06
Xetrov72018271|Xetrov72018271	219.789057	1.053438717	0.191571994	5.498918173	3.82E-08	1.37E-06
Xetrov72033755|Xetrov72033755	31.5042533	2.459793857	0.447321997	5.498933376	3.82E-08	1.37E-06
Xetrov72027170|Xetrov72027170|fgf16	46.1475538	1.233296231	0.224266524	5.499243534	3.81E-08	1.37E-06
Xetrov72000127|Xetrov72000127|plekhg1	656.491554	1.633952881	0.297865769	5.48553427	4.12E-08	1.47E-06
Xetrov72042970|Xetrov72042970	51.2237501	1.907488858	0.347843204	5.483760601	4.16E-08	1.48E-06
Xetrov72034558|Xetrov72034558|gpr20	18.7814723	3.157396043	0.576233267	5.47937133	4.27E-08	1.52E-06
Xetrov72001394|Xetrov72001394|fam43a	333.264802	1.502676105	0.274373421	5.476755365	4.33E-08	1.53E-06
Xetrov72043407|Xetrov72043407|mogat2.1	6.11991041	3.257475417	0.595884592	5.466621324	4.59E-08	1.62E-06
Xetrov72039918|Xetrov72039918|myf6	7.90896553	3.108037762	0.569455957	5.457907193	4.82E-08	1.69E-06
Xetrov72002512|Xetrov72002512|tmem200a	3.67009774	3.152189449	0.57884619	5.445642561	5.16E-08	1.81E-06
Xetrov72039461|Xetrov72039461|ccr4	12.4920492	2.88109334	0.529101762	5.445253729	5.17E-08	1.81E-06
Xetrov72038497|Xetrov72038497|slc5a8	1176.4959	2.044616423	0.375781616	5.440969794	5.30E-08	1.85E-06
Xetrov72010279|Xetrov72010279|fut6	3.82592241	3.163263653	0.581788753	5.43713442	5.41E-08	1.88E-06
Xetrov72002854|Xetrov72002854	161.039805	2.102841287	0.386887295	5.435281322	5.47E-08	1.89E-06
Xetrov72013866|Xetrov72013866|ednrb2	21.6328953	1.514013852	0.279055245	5.425498631	5.78E-08	1.98E-06
Xetrov72043544|Xetrov72043544	157.371439	2.652451955	0.489818907	5.415168584	6.12E-08	2.07E-06
Xetrov72035518|Xetrov72035518|cmtm7	332.402395	1.17323532	0.216623354	5.416014934	6.09E-08	2.07E-06
Xetrov72021080|Xetrov72021080|fgfrl1	15.9813345	2.403710215	0.44416684	5.411728208	6.24E-08	2.11E-06
Xetrov72038488|Xetrov72038488|iqch	85.6602834	1.825768494	0.337922268	5.402924476	6.56E-08	2.20E-06
Xetrov72023270|Xetrov72023270	2.64104817	3.1684159	0.588408308	5.384723254	7.26E-08	2.41E-06
Xetrov72021263|Xetrov72021263|psat1	121.213133	1.719703836	0.319488173	5.38268388	7.34E-08	2.43E-06
Xetrov72021774|Xetrov72021774|pnp	53.2970261	2.473786991	0.459634179	5.382077972	7.36E-08	2.44E-06
Xetrov72026741|Xetrov72026741|unnamed	1566.37763	1.358648002	0.252595109	5.37875815	7.50E-08	2.48E-06
Xetrov72020580|Xetrov72020580|celf5	17.6250553	2.21480222	0.41201086	5.375591852	7.63E-08	2.52E-06
Xetrov72002857|Xetrov72002857	60.9027252	2.162549258	0.403539007	5.358959654	8.37E-08	2.73E-06
Xetrov72018552|Xetrov72018552	7.49399152	3.028301545	0.565470505	5.355366055	8.54E-08	2.78E-06
Xetrov72013050|Xetrov72013050|exoc3l2	73.4471401	1.938192977	0.362150134	5.351904621	8.70E-08	2.83E-06
Xetrov72003895|Xetrov72003895|dlg4	28.174036	3.058055654	0.571575595	5.350220824	8.78E-08	2.85E-06
Xetrov72002056|Xetrov72002056	16.410129	1.900510916	0.355819572	5.341220852	9.23E-08	2.99E-06
Xetrov72002106|Xetrov72002106	273.292416	1.145864884	0.214685377	5.337414697	9.43E-08	3.05E-06
Xetrov72001251|Xetrov72001251|fetub	57.9388723	2.6623001	0.498920254	5.336123515	9.50E-08	3.06E-06
Xetrov72009790|Xetrov72009790|chka	323.522063	1.376723718	0.258164689	5.332734394	9.67E-08	3.11E-06

Xetrov72004164|Xetrov72004164|unc80	22.1141382	1.943384995	0.365114544	5.322672097	1.02E-07	3.27E-06
Xetrov72036759|Xetrov72036759	31.2608623	2.252450198	0.423370801	5.32027762	1.04E-07	3.30E-06
Xetrov72035966|Xetrov72035966	20.6900307	2.969331712	0.558445909	5.317133971	1.05E-07	3.35E-06
Xetrov72001465|Xetrov72001465|ostalpha	10.82163	2.06259585	0.387926079	5.316981663	1.06E-07	3.35E-06
Xetrov72032993|Xetrov72032993	24.694986	2.169974319	0.408229906	5.315569204	1.06E-07	3.37E-06
Xetrov72028498|Xetrov72028498	17.0522787	2.821179076	0.531007699	5.312877915	1.08E-07	3.42E-06
Xetrov72023742|Xetrov72023742|st3gal5	14.3027564	2.169240162	0.408851897	5.305686921	1.12E-07	3.53E-06
Xetrov72002841|Xetrov72002841	834.077361	1.563797818	0.294823676	5.304179905	1.13E-07	3.55E-06
Xetrov72016594|Xetrov72016594	17.323816	2.058116007	0.388800394	5.29350288	1.20E-07	3.75E-06
Xetrov72042510|Xetrov72042510	62.2054561	2.572679727	0.486344022	5.289835203	1.22E-07	3.82E-06
Xetrov72041037|Xetrov72041037|wdr93	16.1045662	2.035470816	0.384940143	5.287759289	1.24E-07	3.85E-06
Xetrov72015819|Xetrov72015819|loc402377	25.7300136	2.957824148	0.55941395	5.287362154	1.24E-07	3.86E-06
Xetrov72002758|Xetrov72002758|tube1	312.527674	1.432068598	0.271008177	5.28422652	1.26E-07	3.91E-06
Xetrov72021099|Xetrov72021099|pacsin1	80.7901054	1.427991839	0.270235313	5.284253282	1.26E-07	3.91E-06
Xetrov72016987|Xetrov72016987|tgm2	33.1095794	2.469843718	0.467799822	5.279702129	1.29E-07	4.00E-06
Xetrov72035832|Xetrov72035832	10.658158	2.950034622	0.558951646	5.277799329	1.31E-07	4.04E-06
Xetrov72033686|Xetrov72033686	79.2927454	1.100544263	0.209262872	5.259147288	1.45E-07	4.43E-06
Xetrov72038602|Xetrov72038602|plekho2	7.88655335	3.03294243	0.576747777	5.258698082	1.45E-07	4.44E-06
Xetrov72034914|Xetrov72034914|penk	12.2348467	2.714295265	0.516270085	5.257510257	1.46E-07	4.46E-06
Xetrov72026014|Xetrov72026014|crlf3	640.395223	1.23871203	0.235983108	5.249155512	1.53E-07	4.65E-06
Xetrov72007363|Xetrov72007363	10.2924932	3.130573508	0.596694227	5.246528899	1.55E-07	4.71E-06
Xetrov72035589|Xetrov72035589|slc6a3	7.54947004	3.114208968	0.594899937	5.234845012	1.65E-07	4.99E-06
Xetrov72030020|Xetrov72030020|erg	9.00736769	3.110402012	0.595354099	5.224457203	1.75E-07	5.26E-06
Xetrov72030823|Xetrov72030823	322.363442	1.736582819	0.332907024	5.216419887	1.82E-07	5.48E-06
Xetrov72027900|Xetrov72027900	22.0717116	2.375212206	0.456019279	5.208578483	1.90E-07	5.70E-06
Xetrov72029482|Xetrov72029482	62.4229921	1.534612107	0.294676017	5.20779439	1.91E-07	5.71E-06
Xetrov72043460|Xetrov72043460	90.0772767	2.03318738	0.390588537	5.205445593	1.94E-07	5.78E-06
Xetrov72021409|Xetrov72021409	88.2160026	1.797821681	0.345634475	5.201511456	1.98E-07	5.89E-06
Xetrov72017725|Xetrov72017725	138.30339	2.134407135	0.410741722	5.196470237	2.03E-07	6.02E-06
Xetrov72038020|Xetrov72038020|rasgrf1	13.2800685	2.619164119	0.504367395	5.19296875	2.07E-07	6.12E-06
Xetrov72031929|Xetrov72031929	2.85831283	3.081993884	0.593484254	5.193050804	2.07E-07	6.12E-06
Xetrov72019238|Xetrov72019238|nfasc	19.9508	2.180782086	0.420033242	5.191927371	2.08E-07	6.14E-06
Xetrov72038319|Xetrov72038319|plekhg7	248.123129	2.122788936	0.409832551	5.179649419	2.22E-07	6.53E-06
Xetrov72033604|Xetrov72033604|cdh6	15.1178872	2.399487964	0.463902172	5.172400797	2.31E-07	6.78E-06
Xetrov72032262|Xetrov72032262|myo16	7.54246637	2.955198761	0.572003838	5.166396735	2.39E-07	6.97E-06
Xetrov72028325|Xetrov72028325	2.66713087	3.059786335	0.593184096	5.158240683	2.49E-07	7.23E-06
Xetrov72022736|Xetrov72022736	10.6947747	3.061298716	0.594094514	5.152881642	2.57E-07	7.42E-06
Xetrov72008206|Xetrov72008206	73.5724578	1.998819988	0.388001136	5.151582828	2.58E-07	7.46E-06
Xetrov72036450|Xetrov72036450	216.267187	1.050783615	0.204207846	5.145657412	2.67E-07	7.69E-06
Xetrov72038390|Xetrov72038390|rhobtb2	42.1517442	1.900440714	0.37041845	5.130523913	2.89E-07	8.31E-06
Xetrov72042108|Xetrov72042108	5.50229005	2.954295707	0.576293893	5.126369965	2.95E-07	8.48E-06
Xetrov72035475|Xetrov72035475	44.7059752	2.497188945	0.487180346	5.125799854	2.96E-07	8.49E-06
Xetrov72023106|Xetrov72023106	9.29968224	2.090414137	0.409155277	5.109097336	3.24E-07	9.21E-06
Xetrov72034665|Xetrov72034665|ube2ql1	94.193338	1.216738798	0.238351176	5.104815582	3.31E-07	9.39E-06
Xetrov72041758|Xetrov72041758	61.8502354	2.264528456	0.444313138	5.096694793	3.46E-07	9.79E-06
Xetrov72008035|Xetrov72008035|slc39a4	6.54999056	3.012971071	0.591874764	5.090555058	3.57E-07	1.01E-05
Xetrov72038358|Xetrov72038358|abcd2	6.62521878	2.697504227	0.530207925	5.087634685	3.63E-07	1.02E-05
Xetrov72039736|Xetrov72039736|cd74	11.5994812	1.964924967	0.386232382	5.087416436	3.63E-07	1.02E-05
Xetrov72034033|Xetrov72034033|hdac9	83.1069189	2.017562038	0.39748102	5.07587013	3.86E-07	1.08E-05
Xetrov72007524|Xetrov72007524	14.345094	2.366160367	0.466555636	5.071550277	3.95E-07	1.10E-05
Xetrov72042107|Xetrov72042107	25.8082337	2.012934437	0.397176098	5.068115754	4.02E-07	1.12E-05
Xetrov72035399|Xetrov72035399|cck	3.79034987	3.011263585	0.595025928	5.060726677	4.18E-07	1.16E-05
Xetrov72031618|Xetrov72031618|kcne1	9.05969842	2.761221422	0.545996632	5.057213283	4.25E-07	1.18E-05
Xetrov72033662|Xetrov72033662|tgfbr2	62.0836568	1.721026584	0.340276538	5.0577292	4.24E-07	1.18E-05
PAC:20699956	50.7548235	2.506928452	0.497314384	5.040932926	4.63E-07	1.28E-05
Xetrov72002057|Xetrov72002057	48.8892223	1.306695442	0.259401067	5.037355689	4.72E-07	1.30E-05
Xetrov72013923|Xetrov72013923|nova1	56.3480245	2.851562201	0.566797265	5.031009103	4.88E-07	1.34E-05
Xetrov72033388|Xetrov72033388|nek10	42.5120733	1.995012655	0.396778032	5.028032037	4.96E-07	1.36E-05
Xetrov72032095|Xetrov72032095	3.11580042	2.928612426	0.582948255	5.023794826	5.07E-07	1.39E-05
Xetrov72020479|Xetrov72020479|gabra2	12.8984323	2.853075976	0.568175288	5.021471428	5.13E-07	1.41E-05
Xetrov72028979|Xetrov72028979|mcf2l	78.4607543	1.340206104	0.266956241	5.02032131	5.16E-07	1.41E-05
Xetrov72011581|Xetrov72011581|lrrc8c	310.069233	1.399431769	0.27924679	5.011451587	5.40E-07	1.47E-05
Xetrov72005441|Xetrov72005441|march4	4.37053556	2.889034015	0.577485754	5.002779715	5.65E-07	1.53E-05
Xetrov72041731|Xetrov72041731	6.3283106	2.762841637	0.552567406	5.00000834	5.73E-07	1.55E-05
Xetrov72013377|Xetrov72013377|numbl	795.235956	1.47115505	0.294293794	4.998933307	5.76E-07	1.56E-05
Xetrov72024086|Xetrov72024086	3.17486728	2.848790575	0.57057429	4.99284778	5.95E-07	1.61E-05
Xetrov72013979|Xetrov72013979|mamld1	9.33633553	2.88306708	0.577543898	4.991944492	5.98E-07	1.61E-05
Xetrov72028702|Xetrov72028702|c2cd3	222.075026	1.255825039	0.252106645	4.981324619	6.32E-07	1.69E-05
Xetrov72016194|Xetrov72016194	10.62754	2.241759081	0.449963656	4.982089226	6.29E-07	1.69E-05
Xetrov72020107|Xetrov72020107|tmem132b	28.6540916	2.616839127	0.525206829	4.982492574	6.28E-07	1.69E-05
Xetrov72037752|Xetrov72037752|mical3	245.197612	1.295958736	0.260624148	4.972519795	6.61E-07	1.76E-05
Xetrov72042087|Xetrov72042087|bai2	39.8408634	2.681836777	0.539422633	4.971680111	6.64E-07	1.77E-05
Xetrov72026735|Xetrov72026735|nkx6-2	310.231199	2.128491236	0.428335911	4.969210338	6.72E-07	1.79E-05
Xetrov72019393|Xetrov72019393|LOC100495742	314.659213	1.216103081	0.245053995	4.962592345	6.96E-07	1.84E-05
Xetrov72023152|Xetrov72023152|avd	129.408247	1.168214633	0.235643804	4.957544443	7.14E-07	1.88E-05
Xetrov72042977|Xetrov72042977	41.815315	2.186962313	0.441103855	4.957930625	7.12E-07	1.88E-05

Xetrov72005969|Xetrov72005969	5.2714991	2.950373493	0.595847884	4.951554875	7.36E-07	1.93E-05
Xetrov72009217|Xetrov72009217|cdc14a	57.8945859	1.98895534	0.402154398	4.945750561	7.59E-07	1.98E-05
Xetrov72018695|Xetrov72018695|trpm6	91.1955953	1.604507995	0.325023127	4.93659639	7.95E-07	2.08E-05
Xetrov72015830|Xetrov72015830	59.0418895	2.157865697	0.437670272	4.93034559	8.21E-07	2.14E-05
Xetrov72008313|Xetrov72008313|adamts18	57.7907873	1.735445763	0.352080031	4.929122953	8.26E-07	2.15E-05
Xetrov72023173|Xetrov72023173	17.2840128	2.272952972	0.461127651	4.929118799	8.26E-07	2.15E-05
Xetrov72014803|Xetrov72014803	30.3869102	1.973984993	0.40072036	4.92609109	8.39E-07	2.18E-05
Xetrov72006084|Xetrov72006084|fev	7.30987464	2.933136487	0.596386065	4.918184142	8.74E-07	2.26E-05
Xetrov72041526|Xetrov72041526	7.47604204	2.796849346	0.568815636	4.916969872	8.79E-07	2.27E-05
Xetrov72021859|Xetrov72021859|dazl	810.754348	1.126846195	0.229277285	4.914774673	8.89E-07	2.28E-05
Xetrov72019099|Xetrov72019099|lifr	50.6389355	1.126922783	0.229257999	4.915522192	8.85E-07	2.28E-05
Xetrov72040572|Xetrov72040572|kcp	41.1896132	2.83207975	0.576800732	4.909979464	9.11E-07	2.32E-05
Xetrov72038392|Xetrov72038392|prkcq	3.03626255	2.799995461	0.571815502	4.896676381	9.75E-07	2.46E-05
Xetrov72034491|Xetrov72034491|tmeff1	248.535058	1.337848435	0.273924252	4.884008718	1.04E-06	2.62E-05
Xetrov72036219|Xetrov72036219|aqp4	4.9210607	2.659597095	0.544643862	4.883185661	1.04E-06	2.63E-05
Xetrov72040137|Xetrov72040137|kcnip1	40.74819	2.252011029	0.462182571	4.872557231	1.10E-06	2.76E-05
Xetrov72043101|Xetrov72043101|hsd3b7	37.8690327	2.641789266	0.542484674	4.869795209	1.12E-06	2.80E-05
Xetrov72035600|Xetrov72035600|znf527	5011.55683	1.076731501	0.221112535	4.869608595	1.12E-06	2.80E-05
Xetrov72003106|Xetrov72003106|rasal3	84.9902302	2.565489873	0.527297203	4.865358393	1.14E-06	2.85E-05
Xetrov72023442|Xetrov72023442	28.261162	2.12226959	0.43636587	4.863509586	1.15E-06	2.87E-05
Xetrov72023220|Xetrov72023220	39.6460559	1.296005811	0.266466537	4.863671915	1.15E-06	2.87E-05
Xetrov72035237|Xetrov72035237	9.20411278	2.747147339	0.565657775	4.856553666	1.19E-06	2.96E-05
Xetrov72042209|Xetrov72042209	39.8531369	1.833339224	0.377561957	4.855730799	1.20E-06	2.97E-05
Xetrov72007570|Xetrov72007570|gabra3	12.3883295	2.413151763	0.497074368	4.854709717	1.21E-06	2.98E-05
Xetrov72034689|Xetrov72034689|unnamed	2057.04488	1.676672064	0.345516896	4.852648544	1.22E-06	3.01E-05
Xetrov72004534|Xetrov72004534|grid2ip	42.5271541	1.946438571	0.401314846	4.850153417	1.23E-06	3.03E-05
Xetrov72036358|Xetrov72036358|klhl10	8.80162118	2.685546263	0.554138757	4.846342597	1.26E-06	3.08E-05
Xetrov72001014|Xetrov72001014|hrg	38.0888885	2.435843122	0.502976295	4.842858695	1.28E-06	3.13E-05
Xetrov72009368|Xetrov72009368	6.13789745	2.869860954	0.592855527	4.840742513	1.29E-06	3.16E-05
Xetrov72003911|Xetrov72003911	5.25467663	2.730997485	0.564417252	4.838614477	1.31E-06	3.19E-05
Xetrov72008182|Xetrov72008182	63.6467418	1.710583582	0.354531837	4.824908244	1.40E-06	3.41E-05
Xetrov72023223|Xetrov72023223	12.1593141	2.292060052	0.475582921	4.819475116	1.44E-06	3.50E-05
Xetrov72029758|Xetrov72029758	11.9146839	2.863312521	0.594452795	4.816719753	1.46E-06	3.54E-05
Xetrov72034161|Xetrov72034161|steap2	3.71442824	2.78151004	0.578006558	4.812246507	1.49E-06	3.62E-05
Xetrov72034496|Xetrov72034496|slc30a8	45.013217	2.489430427	0.517735403	4.808306351	1.52E-06	3.68E-05
Xetrov72010919|Xetrov72010919|rgs2	24.3062343	2.642182762	0.54966685	4.806880319	1.53E-06	3.69E-05
Xetrov72028506|Xetrov72028506	103.974665	1.992124313	0.415325511	4.796537316	1.61E-06	3.87E-05
Xetrov72009218|Xetrov72009218|rspry1	82.511054	1.109639029	0.231417752	4.794960718	1.63E-06	3.89E-05
Xetrov72012225|Xetrov72012225	352.644093	1.327526454	0.277382559	4.785904561	1.70E-06	4.06E-05
Xetrov72007904|Xetrov72007904|nlgn4x	6.57623175	2.809792068	0.58839172	4.775376628	1.79E-06	4.27E-05
Xetrov72024979|Xetrov72024979|mms19	616.152564	1.034526049	0.216779697	4.772246024	1.82E-06	4.32E-05
Xetrov72016513|Xetrov72016513	64.4683185	1.798578347	0.376876022	4.77233425	1.82E-06	4.32E-05
Xetrov72016946|Xetrov72016946|srms	5.08866763	2.820381872	0.591308279	4.769731746	1.84E-06	4.36E-05
Xetrov72001716|Xetrov72001716|cdc42ep3	48.7043625	2.005248015	0.421456817	4.757896739	1.96E-06	4.59E-05
Xetrov72011380|Xetrov72011380	53.8393176	1.214651548	0.255403226	4.755819126	1.98E-06	4.64E-05
Xetrov72028323|Xetrov72028323	58.0001996	1.965708424	0.414807888	4.738840515	2.15E-06	5.00E-05
Xetrov72010990|Xetrov72010990	8.23903446	2.229157407	0.470489283	4.737955763	2.16E-06	5.01E-05
Xetrov72005308|Xetrov72005308|unnamed	20.0905001	2.150701834	0.453987127	4.737363041	2.17E-06	5.02E-05
Xetrov72025791|Xetrov72025791	5281.04841	1.158466464	0.244680366	4.734611452	2.19E-06	5.08E-05
Xetrov72020466|Xetrov72020466|agxt2l1	12.0866638	1.779424766	0.376034346	4.732080423	2.22E-06	5.10E-05
Xetrov72028317|Xetrov72028317|htr3b	39.6698623	1.756190038	0.371120649	4.732126986	2.22E-06	5.10E-05
Xetrov72022766|Xetrov72022766|mef2bnb	89.8385016	1.240531479	0.262120093	4.732683642	2.22E-06	5.10E-05
Xetrov72010354|Xetrov72010354|gipc2	47.9237909	2.171195977	0.45878714	4.732469128	2.22E-06	5.10E-05
Xetrov72038048|Xetrov72038048|sh3tc2	8.05028119	2.33052468	0.492671546	4.730382135	2.24E-06	5.14E-05
Xetrov72029685|Xetrov72029685|sim2	10.9446437	1.935432132	0.40967822	4.724273924	2.31E-06	5.29E-05
Xetrov72020339|Xetrov72020339|prdm5	17.8258234	2.258679201	0.478251409	4.722786299	2.33E-06	5.32E-05
Xetrov72024277|Xetrov72024277	32.5806663	2.42255585	0.51315113	4.720940304	2.35E-06	5.37E-05
Xetrov72000070|Xetrov72000070|kif26b	147.030934	1.403954975	0.297667738	4.716517098	2.40E-06	5.47E-05
Xetrov72008518|Xetrov72008518|lrp3	67.9166697	1.03820692	0.220368391	4.711233393	2.46E-06	5.60E-05
Xetrov72008443|Xetrov72008443|adcy7	106.31542	1.528059772	0.324760168	4.705194554	2.54E-06	5.76E-05
Xetrov72001099|Xetrov72001099|zic1	2954.95603	1.231148187	0.261831009	4.702071744	2.58E-06	5.84E-05
Xetrov72026396|Xetrov72026396|b3galt6	284.802823	1.045123265	0.222459566	4.698036961	2.63E-06	5.94E-05
Xetrov72028416|Xetrov72028416|unnamed	342.769691	1.288419278	0.274310678	4.696934469	2.64E-06	5.96E-05
Xetrov72034208|Xetrov72034208|irx1	3353.47567	1.206901238	0.257061107	4.694997444	2.67E-06	6.01E-05
Xetrov72024793|Xetrov72024793|usp54	422.508553	1.255069796	0.267957712	4.683835325	2.82E-06	6.30E-05
Xetrov72005050|Xetrov72005050|nostrin	13.3868239	2.612080847	0.557804857	4.682786128	2.83E-06	6.32E-05
Xetrov72037879|Xetrov72037879|met	43.5684365	1.834597862	0.392004962	4.680037347	2.87E-06	6.39E-05
Xetrov72020186|Xetrov72020186|cdh24	4.87339454	2.682137239	0.573158393	4.679574216	2.87E-06	6.40E-05
Xetrov72016008|Xetrov72016008	48.3119635	1.980587804	0.423613746	4.675456885	2.93E-06	6.52E-05
Xetrov72023086|Xetrov72023086	22.6448062	1.421436186	0.304069466	4.674708728	2.94E-06	6.54E-05
Xetrov72015367|Xetrov72015367	8.10387297	2.605233046	0.557458038	4.673415518	2.96E-06	6.57E-05
Xetrov72036591|Xetrov72036591	13.2524594	2.356576589	0.504284037	4.673113591	2.97E-06	6.57E-05
Xetrov72032217|Xetrov72032217	20.5713981	2.064179054	0.441861341	4.671553864	2.99E-06	6.61E-05
Xetrov72037852|Xetrov72037852	9.02453384	2.516211425	0.538781639	4.670187774	3.01E-06	6.64E-05
Xetrov72007234|Xetrov72007234	11.4985677	2.262295908	0.484527108	4.669080159	3.03E-06	6.66E-05
Xetrov72035650|Xetrov72035650	9.75329728	2.063394611	0.442089234	4.66737132	3.05E-06	6.70E-05

Xetrov72043651|Xetrov72043651	6.06821365	2.625256641	0.562862456	4.664117516	3.10E-06	6.79E-05
Xetrov72014648|Xetrov72014648|fam181a	4.09167974	2.672992616	0.573575197	4.660230482	3.16E-06	6.90E-05
Xetrov72015602|Xetrov72015602	27.3085119	1.961817486	0.421697237	4.652194314	3.28E-06	7.15E-05
Xetrov72004150|Xetrov72004150|lrp2	291.257716	2.405033919	0.517179872	4.650285232	3.31E-06	7.21E-05
Xetrov72028961|Xetrov72028961|atp11a	11.0055734	2.084136981	0.448367794	4.648275382	3.35E-06	7.27E-05
Xetrov72040731|Xetrov72040731|osbpl8	125.912303	1.505468653	0.324242981	4.64302619	3.43E-06	7.44E-05
Xetrov72012285|Xetrov72012285	136.479174	1.879565123	0.404987776	4.641041619	3.47E-06	7.50E-05
Xetrov72004352|Xetrov72004352|sned1	72.8730011	2.077635393	0.448270967	4.634775723	3.57E-06	7.71E-05
Xetrov72003118|Xetrov72003118	83.878707	1.871364464	0.40377946	4.634620255	3.58E-06	7.71E-05
Xetrov72036022|Xetrov72036022	52.7701834	1.496368947	0.32325623	4.629049062	3.67E-06	7.91E-05
Xetrov72030134|Xetrov72030134|adc	3169.63955	1.710393587	0.369659386	4.626944833	3.71E-06	7.97E-05
Xetrov72019786|Xetrov72019786|gria2	5.17177367	2.386552139	0.516365588	4.621826467	3.80E-06	8.12E-05
Xetrov72001672|Xetrov72001672|nkx2-2	6.60227712	2.392497225	0.517847918	4.620076945	3.84E-06	8.17E-05
Xetrov72024903|Xetrov72024903|tnks2	495.280753	1.119819777	0.242709126	4.613834656	3.95E-06	8.41E-05
Xetrov72006911|Xetrov72006911	9.22531987	2.580151072	0.559377621	4.612538967	3.98E-06	8.46E-05
Xetrov72021782|Xetrov72021782|sfrp2	283.921713	1.278523213	0.277407366	4.608829368	4.05E-06	8.60E-05
Xetrov72015725|Xetrov72015725	6.98234302	2.397876449	0.520907211	4.603269834	4.16E-06	8.81E-05
Xetrov72020764|Xetrov72020764|dmrta1	7.43363702	2.501623686	0.543639807	4.601619773	4.19E-06	8.87E-05
Xetrov72036451|Xetrov72036451	40.2734736	1.791944038	0.390391758	4.590117492	4.43E-06	9.33E-05
Xetrov72025201|Xetrov72025201|tmprss4	155.083297	1.254373608	0.273874167	4.580109261	4.65E-06	9.77E-05
Xetrov72031785|Xetrov72031785	5.16045622	2.623411018	0.573295951	4.576015258	4.74E-06	9.95E-05
Xetrov72031081|Xetrov72031081|shox	4.76459684	2.600510523	0.569050174	4.569914287	4.88E-06	0.000101993
Xetrov72014818|Xetrov72014818|mettl11a	15.0365272	2.153113684	0.471208733	4.569341636	4.89E-06	0.000102159
Xetrov72000697|Xetrov72000697|capn10	107.967374	1.729187046	0.379017874	4.562283636	5.06E-06	0.000105188
Xetrov72020039|Xetrov72020039|zap70	6.39705644	2.315284592	0.508193432	4.555912071	5.22E-06	0.000107833
Xetrov72022753|Xetrov72022753	5.29794369	2.71684335	0.596552691	4.5542387	5.26E-06	0.000108502
Xetrov72014683|Xetrov72014683	475.631895	1.462804779	0.321537975	4.54939974	5.38E-06	0.000110738
Xetrov72029172|Xetrov72029172|tubgcp3	352.814364	2.10280755	0.462268362	4.548889174	5.39E-06	0.000110886
Xetrov72002033|Xetrov72002033|c1orf95	5.24113288	2.628428092	0.577963979	4.54773686	5.42E-06	0.000111373
Xetrov72002128|Xetrov72002128|ripply2.2	1883.22157	1.937347233	0.426422375	4.543258854	5.54E-06	0.000113395
Xetrov72024878|Xetrov72024878|igsf9b	9.91931824	2.158888364	0.475363878	4.54154904	5.58E-06	0.000114195
Xetrov72035614|Xetrov72035614|pkhd1l1	3.82200328	2.499022557	0.550973437	4.535649795	5.74E-06	0.000117225
Xetrov72042101|Xetrov72042101	13.1392512	2.479348011	0.54687909	4.533631027	5.80E-06	0.00011805
Xetrov72002377|Xetrov72002377	36.9706204	1.510353279	0.33316269	4.533380608	5.80E-06	0.000118063
Xetrov72029477|Xetrov72029477|slitrk1	11.3186199	2.413149901	0.532644782	4.530505101	5.88E-06	0.000119552
Xetrov72019558|Xetrov72019558	7.48447618	2.681572483	0.593455691	4.518572362	6.23E-06	0.000126218
Xetrov72008811|Xetrov72008811|pde3b	214.152063	1.009884393	0.223639853	4.515672773	6.31E-06	0.00012782
Xetrov72042387|Xetrov72042387	47.6967041	1.297834154	0.287535954	4.513641293	6.37E-06	0.000128774
Xetrov72034472|Xetrov72034472|serpinb5	24.4792166	1.877875638	0.416892063	4.504464837	6.65E-06	0.000134322
Xetrov72009224|Xetrov72009224|c8b	417.941694	2.240690127	0.497502489	4.503877225	6.67E-06	0.00013455
Xetrov72024798|Xetrov72024798|abca5	12.8644104	2.293684262	0.509296701	4.50363071	6.68E-06	0.000134562
Xetrov72011426|Xetrov72011426	34.5649751	2.287481941	0.50813489	4.501721857	6.74E-06	0.000135631
Xetrov72021412|Xetrov72021412|klhdc8a	14.4972779	1.766643459	0.392538943	4.50055591	6.78E-06	0.000136159
Xetrov72015771|Xetrov72015771	8.44166105	2.650189361	0.588872911	4.500443664	6.78E-06	0.000136159
Xetrov72003893|Xetrov72003893	6.20806692	2.649928713	0.589264037	4.497014151	6.89E-06	0.000138225
Xetrov72016819|Xetrov72016819|mllt6	246.529536	1.00888294	0.224385808	4.496197643	6.92E-06	0.000138609
Xetrov72036170|Xetrov72036170	62.057361	1.96399351	0.437221139	4.491991199	7.06E-06	0.000141076
Xetrov72036310|Xetrov72036310	10.4385493	2.643818924	0.589438407	4.485318388	7.28E-06	0.000145102
Xetrov72003088|Xetrov72003088|pnpla7	31.4016376	2.117216712	0.472480798	4.481064037	7.43E-06	0.000147318
Xetrov72011874|Xetrov72011874	111.865761	1.567683756	0.349836286	4.481192539	7.42E-06	0.000147318
Xetrov72018777|Xetrov72018777|nwd1	15.2965374	2.115114524	0.472081706	4.480399256	7.45E-06	0.00014755
Xetrov72019772|Xetrov72019772|gucy1a3	5.58110608	2.199742585	0.491099305	4.479221537	7.49E-06	0.000148055
Xetrov72012129|Xetrov72012129	44.7123678	2.4944912	0.557288815	4.476119263	7.60E-06	0.000149907
Xetrov72028146|Xetrov72028146	9.19147662	2.084108688	0.465756996	4.474669636	7.65E-06	0.000150612
Xetrov72015759|Xetrov72015759	154.502022	1.141995935	0.255286459	4.473390171	7.70E-06	0.000151317
Xetrov72035591|Xetrov72035591	177.56798	1.924638924	0.430281068	4.472980723	7.71E-06	0.000151333
Xetrov72007571|Xetrov72007571|gabra1	5.36968057	2.467192748	0.551890814	4.470436337	7.81E-06	0.000152985
Xetrov72034753|Xetrov72034753|obscn	17.0839204	2.457744182	0.550138795	4.467498392	7.91E-06	0.000154778
Xetrov72016631|Xetrov72016631|dnah9	197.51792	1.403502338	0.314218574	4.466643458	7.95E-06	0.000155237
Xetrov72014232|Xetrov72014232	20.1807518	1.878864647	0.421300036	4.459683092	8.21E-06	0.000159862
Xetrov72028701|Xetrov72028701|myo7a	5.3418545	2.445441148	0.548370587	4.459468111	8.22E-06	0.000159862
Xetrov72000396|Xetrov72000396	18.1694441	1.602244419	0.35951004	4.456744575	8.32E-06	0.000161572
Xetrov72000426|Xetrov72000426|pygm	8966.13688	1.083105697	0.243244351	4.452747583	8.48E-06	0.000164271
Xetrov72038769|Xetrov72038769|spam1	256.795531	2.29291582	0.515351516	4.449226885	8.62E-06	0.000166815
Xetrov72009828|Xetrov72009828|il5ra	3.45115763	2.375128481	0.533884098	4.44877173	8.64E-06	0.000166998
Xetrov72002526|Xetrov72002526	16.1904468	1.872580184	0.421302057	4.444744935	8.80E-06	0.000169807
Xetrov72003786|Xetrov72003786	27.0601861	1.727777618	0.389392947	4.437105579	9.12E-06	0.000175227
Xetrov72020694|Xetrov72020694|tbx1	420.251065	2.026379162	0.456831556	4.435725018	9.18E-06	0.000176174
Xetrov72004358|Xetrov72004358|pfas	194.419194	1.474721886	0.332490932	4.435374751	9.19E-06	0.000176281
Xetrov72031082|Xetrov72031082|tnfsf11	77.8646714	1.391829353	0.31391207	4.433819171	9.26E-06	0.000177377
Xetrov72001676|Xetrov72001676	83.2549203	1.617000466	0.364717217	4.433573164	9.27E-06	0.0001774
Xetrov72000863|Xetrov72000863|fyn	47.4702834	1.050920458	0.23719222	4.430670022	9.39E-06	0.000179622
Xetrov72041992|Xetrov72041992	6.92666459	2.230291882	0.503756798	4.427318679	9.54E-06	0.000182065
Xetrov72027695|Xetrov72027695|gramd1a	218.610787	1.23067014	0.278153724	4.424424455	9.67E-06	0.000183815
Xetrov72004413|Xetrov72004413|zeb2	1561.12758	1.217832634	0.275544861	4.419725454	9.88E-06	0.000187416
Xetrov72030214|Xetrov72030214	8.11459745	2.113235368	0.478132004	4.419773937	9.88E-06	0.000187416

Xetrov72026520|Xetrov72026520|gsg1l	6.68724661	2.559566914	0.579284201	4.418499434	9.94E-06	0.000188129
Xetrov72021265|Xetrov72021265|palm	635.261588	1.674801693	0.379355116	4.414865176	1.01E-05	0.000190742
Xetrov72005601|Xetrov72005601	35.1386787	1.415673903	0.321056564	4.409422088	1.04E-05	0.000195208
Xetrov72025566|Xetrov72025566|ptpn6	7.95214816	2.363919521	0.536321226	4.407656093	1.04E-05	0.000196218
Xetrov72018189|Xetrov72018189	13.1987016	1.757514636	0.398778607	4.407244038	1.05E-05	0.000196395
Xetrov72032584|Xetrov72032584	32.5373934	1.734245056	0.393580605	4.406327533	1.05E-05	0.000197032
Xetrov72016985|Xetrov72016985|epb42	2.05755183	2.6147381	0.593829104	4.403182804	1.07E-05	0.000199514
Xetrov72034450|Xetrov72034450	189.316897	1.873186368	0.425513715	4.402176244	1.07E-05	0.000200044
Xetrov72027264|Xetrov72027264|cd3e	7.57683593	2.386130251	0.542881775	4.39530366	1.11E-05	0.000205868
Xetrov72034882|Xetrov72034882|pqlc1.1	65.8958566	1.419074382	0.322900899	4.39476752	1.11E-05	0.000205969
Xetrov72024201|Xetrov72024201	55.081263	1.527254267	0.347970282	4.389036494	1.14E-05	0.000211056
Xetrov72011346|Xetrov72011346	7.17426511	2.072759026	0.472462394	4.387140758	1.15E-05	0.000212619
Xetrov72023839|Xetrov72023839	8.92755043	2.182306621	0.497496244	4.386579091	1.15E-05	0.000212825
Xetrov72036032|Xetrov72036032	17.3639625	2.042618036	0.465732294	4.385820058	1.16E-05	0.00021315
Xetrov72b000050|Xetrov72b000050	9.97817464	2.271889818	0.518168741	4.384459421	1.16E-05	0.000214067
Xetrov72042142|Xetrov72042142|cad	4325.91186	1.062736772	0.242428423	4.38371359	1.17E-05	0.000214592
Xetrov72009377|Xetrov72009377|rpe65	171.128437	1.570905983	0.358389957	4.383231041	1.17E-05	0.000214858
Xetrov72015346|Xetrov72015346|efcab11	70.5378819	1.412492253	0.322944443	4.373793335	1.22E-05	0.000223711
Xetrov72041585|Xetrov72041585|dgat1	44.3481594	1.210693562	0.27710996	4.369000527	1.25E-05	0.00022779
Xetrov72028673|Xetrov72028673|mxra5	13.8382227	2.001678191	0.45882551	4.362613125	1.29E-05	0.000234318
Xetrov72037920|Xetrov72037920|cyfip2	81.8481488	1.926810094	0.442588802	4.353499417	1.34E-05	0.000243572
Xetrov72009469|Xetrov72009469|slc7a6	203.820493	1.013074885	0.232766374	4.35232489	1.35E-05	0.000244409
Xetrov72039699|Xetrov72039699|sparc	189.206628	1.816322286	0.417359582	4.351936227	1.35E-05	0.000244607
Xetrov72031688|Xetrov72031688|rcan1	248.764563	1.897160143	0.436014456	4.351140465	1.35E-05	0.000245261
Xetrov72009557|Xetrov72009557|unnamed	45.7665349	1.358793837	0.313232175	4.337976571	1.44E-05	0.000259171
Xetrov72010441|Xetrov72010441|lrrn4cl	34.9453319	1.782816539	0.41224229	4.324681342	1.53E-05	0.000273734
Xetrov72040315|Xetrov72040315	6.14824749	2.276344373	0.526512812	4.323435863	1.54E-05	0.000274761
Xetrov72034251|Xetrov72034251|prkag1	16.8032989	1.964426737	0.454389771	4.323219541	1.54E-05	0.00027477
Xetrov72028785|Xetrov72028785|col4a2	43.0043846	1.631959674	0.377530828	4.322718977	1.54E-05	0.000275133
Xetrov72031578|Xetrov72031578|rab30	77.871819	1.092692143	0.252927089	4.320186298	1.56E-05	0.000277784
Xetrov72032963|Xetrov72032963	6.62336161	2.458184546	0.5697168	4.314748218	1.60E-05	0.00028337
Xetrov72014674|Xetrov72014674|prdm12	50.4037979	1.295187876	0.300533392	4.309630513	1.64E-05	0.000288919
Xetrov72042450|Xetrov72042450	14.8210186	2.034034204	0.472023606	4.309178987	1.64E-05	0.000289238
Xetrov72039634|Xetrov72039634|unnamed	47.2024049	2.228453312	0.517913114	4.302755137	1.69E-05	0.000296921
Xetrov72037656|Xetrov72037656	26.6395283	2.507981832	0.583032003	4.301619499	1.70E-05	0.000297613
Xetrov72027183|Xetrov72027183	7.84017573	2.567720613	0.596894387	4.301800568	1.69E-05	0.000297613
Xetrov72012002|Xetrov72012002	10.5490811	2.527585579	0.587640683	4.301243348	1.70E-05	0.000297841
Xetrov72025436|Xetrov72025436|slc23a2	56.6908731	1.617968561	0.376238711	4.300377693	1.71E-05	0.000298729
Xetrov72032985|Xetrov72032985	228.26687	1.212827424	0.28212269	4.298936119	1.72E-05	0.000300399
Xetrov72016635|Xetrov72016635|chd6	58.4996039	1.531778071	0.356426933	4.297593503	1.73E-05	0.000301943
Xetrov72033042|Xetrov72033042|lama1	882.310988	2.180090373	0.50769	4.294136924	1.75E-05	0.000306291
Xetrov72003103|Xetrov72003103	3.24670855	2.529148438	0.588994452	4.294010628	1.75E-05	0.000306291
Xetrov72033156|Xetrov72033156|ccdc165	19.7061407	1.860318013	0.4332717	4.293652259	1.76E-05	0.000306502
Xetrov72038018|Xetrov72038018|ppfia2	8.25412882	2.480906775	0.578416736	4.289133803	1.79E-05	0.000311937
Xetrov72033043|Xetrov72033043|lama3	4.06461001	2.46538697	0.574977106	4.287800232	1.80E-05	0.000313526
Xetrov72021174|Xetrov72021174|nfib	3.95879731	2.38882889	0.557351769	4.286034464	1.82E-05	0.000315736
Xetrov72018134|Xetrov72018134	3.52327841	2.395614631	0.559414636	4.28235959	1.85E-05	0.000320233
Xetrov72042247|Xetrov72042247	9.16599742	1.902510614	0.444408246	4.280997559	1.86E-05	0.000321782
Xetrov72012284|Xetrov72012284|aldh5a1	152.912018	1.519539662	0.354979112	4.280645283	1.86E-05	0.000321996
Xetrov72032860|Xetrov72032860	3.21257395	2.548090648	0.595569908	4.278407312	1.88E-05	0.000324952
Xetrov72007864|Xetrov72007864|pnliprp2	20.5168638	2.540799996	0.594550932	4.273477442	1.92E-05	0.000331616
Xetrov72042958|Xetrov72042958|arhgef10l	37.7800698	1.951072045	0.456638839	4.272680896	1.93E-05	0.000332499
Xetrov72016335|Xetrov72016335|sspo	5.67280374	2.343858833	0.548814797	4.270764651	1.95E-05	0.000335063
Xetrov72029767|Xetrov72029767|reps2	69.3716342	1.667129438	0.390683205	4.267215522	1.98E-05	0.000340125
Xetrov72036131|Xetrov72036131	49.1724818	2.007398753	0.470549627	4.266072351	1.99E-05	0.000341249
Xetrov72029144|Xetrov72029144|hip1	52.7001777	1.955327397	0.458858873	4.261282744	2.03E-05	0.000347697
Xetrov72014829|Xetrov72014829|lrrc57	96.5167766	1.011727831	0.237516835	4.259604721	2.05E-05	0.000349682
Xetrov72041445|Xetrov72041445	17.4715249	1.434111524	0.336806952	4.257962953	2.06E-05	0.00035194
Xetrov72002176|Xetrov72002176|otx1	2899.36577	1.42368357	0.334523466	4.255855615	2.08E-05	0.00035495
Xetrov72041578|Xetrov72041578	3.42486793	2.532565716	0.59514764	4.255357069	2.09E-05	0.000355421
Xetrov72007796|Xetrov72007796	34.7061551	1.14070258	0.268098998	4.25478121	2.09E-05	0.000356015
Xetrov72024990|Xetrov72024990|robo4	3.76873007	2.477287004	0.582437131	4.253312281	2.11E-05	0.000357713
Xetrov72035840|Xetrov72035840	9.69959069	1.80106054	0.424083199	4.246950935	2.17E-05	0.000367686
Xetrov72025171|Xetrov72025171|acap3	64.5215885	1.63956	0.386105165	4.24640784	2.17E-05	0.000368246
Xetrov72003636|Xetrov72003636	6.19998175	2.290546994	0.539905238	4.242498192	2.21E-05	0.000374049
Xetrov72002873|Xetrov72002873	17.2210608	1.364359209	0.321649302	4.241760205	2.22E-05	0.000374945
Xetrov72027962|Xetrov72027962	24.9095319	1.881142702	0.443790657	4.238806455	2.25E-05	0.000379571
Xetrov72005381|Xetrov72005381|pdk1	2309.14445	1.070604791	0.252995399	4.231716443	2.32E-05	0.000390687
Xetrov72004946|Xetrov72004946|ntn3	517.483899	1.578272081	0.373109436	4.230051368	2.34E-05	0.000392887
Xetrov72021577|Xetrov72021577	51.3265514	1.883971764	0.44587376	4.225347919	2.39E-05	0.000400469
Xetrov72038145|Xetrov72038145|hkdc1	361.40282	1.67691274	0.397415063	4.219550031	2.45E-05	0.000410542
Xetrov72002699|Xetrov72002699	20.4003656	1.785923431	0.423469234	4.217362891	2.47E-05	0.000413974
Xetrov72033420|Xetrov72033420|nrp1	55.3730002	1.511125115	0.358660558	4.213245868	2.52E-05	0.000420676
Xetrov72027320|Xetrov72027320	33.287345	1.717629108	0.407703561	4.212936245	2.52E-05	0.00042088
Xetrov72026175|Xetrov72026175	106.072317	1.835019734	0.435872606	4.209990969	2.55E-05	0.000426027
Xetrov72035427|Xetrov72035427|nrn1	7.80896846	2.339605965	0.555768827	4.209674691	2.56E-05	0.000426246

Xetrov72022251|Xetrov72022251|spef1	60.056347	1.557781225	0.370223251	4.207680695	2.58E-05	0.000429576
Xetrov72027025|Xetrov72027025	5.61480777	2.50508128	0.595592234	4.206034154	2.60E-05	0.00043202
Xetrov72000021|Xetrov72000021|col12a1	4.12338037	2.49292046	0.592738668	4.205766546	2.60E-05	0.00043215
Xetrov72005226|Xetrov72005226	8.25624788	2.427500369	0.578457641	4.196504975	2.71E-05	0.000449406
Xetrov72029557|Xetrov72029557|tmprss2	30.0355722	1.629314812	0.388996099	4.188511962	2.81E-05	0.000463487
Xetrov72040644|Xetrov72040644|apbb3	139.130375	1.765467828	0.421647924	4.187066332	2.83E-05	0.000465632
Xetrov72040938|Xetrov72040938	1.75667285	2.484351171	0.59360825	4.18516955	2.85E-05	0.000469127
Xetrov72011374|Xetrov72011374	2.04568485	2.4678183	0.589729341	4.184662567	2.86E-05	0.000469354
Xetrov72036384|Xetrov72036384|unnamed	13.5331833	1.47489278	0.352853504	4.179901191	2.92E-05	0.00047765
Xetrov72018842|Xetrov72018842|rimbp2	54.453494	2.02774501	0.485610133	4.175664533	2.97E-05	0.000485357
Xetrov72028364|Xetrov72028364	12.3814264	1.903239188	0.456710028	4.16728136	3.08E-05	0.000500487
Xetrov72002425|Xetrov72002425	8.33634861	2.481176894	0.595470175	4.166752591	3.09E-05	0.000501217
Xetrov72003628|Xetrov72003628|adamtsl4	130.230778	2.234445885	0.536659513	4.16361926	3.13E-05	0.000507275
Xetrov72008594|Xetrov72008594|slc9a5	335.007131	1.9153346	0.460085718	4.162995124	3.14E-05	0.000508227
Xetrov72009533|Xetrov72009533|dab1	9.64533459	2.062308788	0.495533402	4.161795717	3.16E-05	0.000510466
Xetrov72001634|Xetrov72001634|fhl5	6.64913806	2.132067125	0.513590636	4.151296724	3.31E-05	0.000531268
Xetrov72004588|Xetrov72004588	16.667944	2.164974398	0.521691053	4.149916671	3.33E-05	0.000534026
Xetrov72000014|Xetrov72000014|dnah14	13.1646974	2.111537593	0.508843954	4.1496761	3.33E-05	0.000534132
Xetrov72023316|Xetrov72023316|npr2	5.83366016	2.475791951	0.596871938	4.147944966	3.35E-05	0.000536814
Xetrov72015742|Xetrov72015742	3.25789809	2.467096471	0.59476597	4.148012153	3.35E-05	0.000536814
Xetrov72030100|Xetrov72030100|asl	284.140783	1.25912965	0.303904012	4.143182057	3.43E-05	0.000545771
Xetrov72004330|Xetrov72004330|col5a2	39.9895746	1.985014997	0.480257715	4.133228755	3.58E-05	0.000567085
Xetrov72020488|Xetrov72020488|nfic	7.95037962	2.308740468	0.558658951	4.132647414	3.59E-05	0.000568043
Xetrov72019552|Xetrov72019552|vwa5a	81.5158456	1.641552245	0.397431329	4.130404735	3.62E-05	0.00057265
Xetrov72025770|Xetrov72025770	17.4564517	1.784157986	0.432055747	4.129462459	3.64E-05	0.00057452
Xetrov72006831|Xetrov72006831	1.93900551	2.454703075	0.594983195	4.125667912	3.70E-05	0.000582122
Xetrov72043007|Xetrov72043007	16.8651233	1.84736632	0.447915938	4.124359427	3.72E-05	0.000584952
Xetrov72038266|Xetrov72038266|gria1	4.2911146	2.459735708	0.596482885	4.123732246	3.73E-05	0.000586058
Xetrov72030753|Xetrov72030753|mdh2	310.361607	1.079676999	0.261878673	4.122813766	3.74E-05	0.00058791
Xetrov72037181|Xetrov72037181	4.97945504	2.404753777	0.583388431	4.122045709	3.76E-05	0.000588892
Xetrov72034005|Xetrov72034005|arhgap28	4.7115622	2.145133756	0.520454124	4.121657715	3.76E-05	0.000589394
Xetrov72012166|Xetrov72012166|ppp2r5b	22.3844849	1.761323832	0.42741071	4.120916465	3.77E-05	0.000590802
Xetrov72032834|Xetrov72032834|cdkl5	16.9418154	2.17570279	0.528168577	4.119334025	3.80E-05	0.000593394
Xetrov72028885|Xetrov72028885	26.4539781	1.462000687	0.354897365	4.119502792	3.80E-05	0.000593394
Xetrov72028141|Xetrov72028141	2.56061564	2.373424289	0.576513021	4.116861551	3.84E-05	0.000598305
Xetrov72026148|Xetrov72026148	6.74643625	2.378219609	0.577639589	4.117134032	3.84E-05	0.000598305
Xetrov72010736|Xetrov72010736|fam192a	809.944159	1.046898968	0.254367937	4.115687615	3.86E-05	0.000600366
Xetrov72039470|Xetrov72039470|ascl1	32.7275353	1.196097776	0.290722636	4.114223065	3.88E-05	0.000603691
Xetrov72014727|Xetrov72014727|gjb1	3089.17349	1.652483563	0.401766735	4.113042267	3.90E-05	0.000606288
Xetrov72024386|Xetrov72024386	3.36966374	2.431735949	0.591704217	4.109715429	3.96E-05	0.000614077
Xetrov72021641|Xetrov72021641|sh3gl2	43.379774	1.054303898	0.256953362	4.103094384	4.08E-05	0.000631405
Xetrov72023128|Xetrov72023128	6.65994497	1.900405462	0.463223535	4.102566728	4.09E-05	0.000632327
Xetrov72042373|Xetrov72042373	4.91005264	2.163949952	0.527561239	4.101798603	4.10E-05	0.000633389
Xetrov72001316|Xetrov72001316|nr2e1	10.0584448	1.964401043	0.479601651	4.095901336	4.21E-05	0.000648669
Xetrov72025800|Xetrov72025800|lrrtm3	6.09538418	2.108697147	0.515059906	4.094081333	4.24E-05	0.000652182
Xetrov72010924|Xetrov72010924|vegfb	30.1245705	1.829729477	0.447149061	4.091989984	4.28E-05	0.000656803
Xetrov72024109|Xetrov72024109	5.3538759	2.155719664	0.526828988	4.091877461	4.28E-05	0.000656803
Xetrov72020213|Xetrov72020213|eps8l3	37.220383	1.791908575	0.437964427	4.091447761	4.29E-05	0.000657485
Xetrov72035815|Xetrov72035815	38.196067	1.76160387	0.430738966	4.08972489	4.32E-05	0.000661311
Xetrov72033738|Xetrov72033738|eomes	3366.28921	1.153376551	0.2821632	4.087622163	4.36E-05	0.000666248
Xetrov72037703|Xetrov72037703|lrrk2	250.755482	1.349923088	0.330783985	4.080980788	4.48E-05	0.000683912
Xetrov72032309|Xetrov72032309	7.25614741	2.100259683	0.514712645	4.080450915	4.49E-05	0.000684918
Xetrov72041204|Xetrov72041204|alox12b	18.3443559	2.095903524	0.513993081	4.077688208	4.55E-05	0.000691985
Xetrov72023018|Xetrov72023018|otp	32.6922172	2.284603762	0.560576926	4.075450943	4.59E-05	0.000697545
Xetrov72008039|Xetrov72008039|hydin	267.769985	1.819440844	0.446564402	4.074307845	4.62E-05	0.000700415
Xetrov72019394|Xetrov72019394|pde5a	4.1543124	2.298084526	0.564073173	4.074089381	4.62E-05	0.000700509
Xetrov72029358|Xetrov72029358|naalad2	1548.55743	1.437448391	0.352953787	4.072624929	4.65E-05	0.000703231
Xetrov72000233|Xetrov72000233	2.65563971	2.420062518	0.594788155	4.068780618	4.73E-05	0.000714359
Xetrov72028507|Xetrov72028507	75.5909225	1.184686345	0.291335778	4.066394984	4.77E-05	0.000719974
Xetrov72029883|Xetrov72029883|pvrl3	93.215862	1.528409372	0.375965782	4.065288507	4.80E-05	0.000722242
Xetrov72006044|Xetrov72006044|cers6	15.5497744	1.95461861	0.480848095	4.064939903	4.80E-05	0.000722745
Xetrov72008361|Xetrov72008361|astn1	6.91293398	2.175574676	0.535335901	4.063943166	4.83E-05	0.000725261
Xetrov72013344|Xetrov72013344|cnga2	19.8382096	2.084530126	0.513293719	4.061086368	4.88E-05	0.000733024
Xetrov72015537|Xetrov72015537	5.80950417	2.207682272	0.544029135	4.058022133	4.95E-05	0.000741524
Xetrov72027983|Xetrov72027983	175.05295	1.643744802	0.405715102	4.051475511	5.09E-05	0.000760769
Xetrov72030010|Xetrov72030010|itgbl1	4.71767006	2.316242091	0.572096156	4.048693678	5.15E-05	0.000768647
Xetrov72028484|Xetrov72028484	8.44263873	2.327362053	0.575223301	4.046014913	5.21E-05	0.000775647
Xetrov72006010|Xetrov72006010	191.833276	1.420842836	0.351319218	4.044307182	5.25E-05	0.000780088
Xetrov72b000159|Xetrov72b000159|cnrip1	357.153403	1.208880653	0.299057357	4.042303677	5.29E-05	0.000785546
Xetrov72015793|Xetrov72015793|ccdc85c	34.53357	1.773525056	0.438735873	4.042352509	5.29E-05	0.000785546
Xetrov72008036|Xetrov72008036|hmcn1	7.53172529	1.880608374	0.465637669	4.038780583	5.37E-05	0.000794849
Xetrov72032984|Xetrov72032984	174.364582	1.718203163	0.425443095	4.038620403	5.38E-05	0.000794849
Xetrov72029137|Xetrov72029137|gtf2ird1	359.786425	1.137285633	0.282252448	4.029320711	5.59E-05	0.000825659
Xetrov72026490|Xetrov72026490|hoga1	9.49314329	1.894968206	0.470612009	4.02660402	5.66E-05	0.000834467
Xetrov72034364|Xetrov72034364|abhd3	51.2052506	1.329300353	0.330141443	4.026457082	5.66E-05	0.000834467
Xetrov72003110|Xetrov72003110	14.7621565	1.685588252	0.418711654	4.025654017	5.68E-05	0.000836011

Xetrov72008038|Xetrov72008038	4.26343838	2.214203801	0.550203432	4.024336585	5.71E-05	0.000840049
Xetrov72032338|Xetrov72032338|sdc3	95.6886225	1.824581468	0.453529854	4.023068056	5.74E-05	0.000843579
Xetrov72037494|Xetrov72037494	6.34967027	2.140228646	0.532000525	4.022982208	5.75E-05	0.000843579
Xetrov72029536|Xetrov72029536|mid1	91.8190222	1.356892812	0.337554025	4.019779678	5.83E-05	0.000854462
Xetrov72b000110|Xetrov72b000110|steap1	1.71133582	2.382071928	0.592787788	4.01842274	5.86E-05	0.00085806
Xetrov72036845|Xetrov72036845	7.28714104	1.844513344	0.459179722	4.01697474	5.90E-05	0.000862677
Xetrov72024167|Xetrov72024167	59.7627791	1.318980228	0.328401721	4.016362108	5.91E-05	0.00086425
Xetrov72032492|Xetrov72032492	4.95520326	2.359029948	0.58775665	4.013616774	5.98E-05	0.000873013
Xetrov72028450|Xetrov72028450|cyp26c1	66.148314	1.875120105	0.467355304	4.012193913	6.02E-05	0.000877613
Xetrov72032421|Xetrov72032421	10.1298234	1.929496113	0.481117496	4.010446785	6.06E-05	0.000883448
Xetrov72023886|Xetrov72023886	43.449823	1.528282605	0.381257187	4.008534549	6.11E-05	0.000889942
Xetrov72038147|Xetrov72038147|pdzrn4	21.8798987	1.826904593	0.456282617	4.003888218	6.23E-05	0.000906211
Xetrov72032980|Xetrov72032980	14.8564875	2.32925474	0.581952473	4.002482762	6.27E-05	0.000910909
Xetrov72036907|Xetrov72036907	8.68578578	2.32926341	0.58226268	4.000365285	6.32E-05	0.00091839
Xetrov72018824|Xetrov72018824	629.780947	1.723006554	0.43089329	3.998685046	6.37E-05	0.000924221
Xetrov72025178|Xetrov72025178|wdfy4	34.8685148	1.70473545	0.426605788	3.996043882	6.44E-05	0.000932758
Xetrov72003615|Xetrov72003615	3.47800443	2.36691234	0.592758091	3.993049401	6.52E-05	0.000941397
Xetrov72018749|Xetrov72018749|nav1	116.913484	1.609135309	0.40336034	3.989324557	6.63E-05	0.000955274
Xetrov72008524|Xetrov72008524|ccdc66	299.628276	1.03790484	0.260248218	3.988134278	6.66E-05	0.000958174
Xetrov72025101|Xetrov72025101|pkd2l1	10.1957706	2.164727409	0.542779349	3.988227286	6.66E-05	0.000958174
Xetrov72036964|Xetrov72036964	99.1478271	1.485931853	0.372933507	3.984441802	6.76E-05	0.00097023
Xetrov72041022|Xetrov72041022|socs2	10.1338117	2.017070316	0.506657993	3.981127989	6.86E-05	0.00098087
Xetrov72002923|Xetrov72002923|fndc4	3.10387135	2.371183619	0.595562531	3.981418401	6.85E-05	0.00098087
Xetrov72025137|Xetrov72025137|cdhr1	22.9082579	1.823820697	0.458266242	3.979827732	6.90E-05	0.000984812
Xetrov72010848|Xetrov72010848	20.7822986	1.698357522	0.426788377	3.979390289	6.91E-05	0.000985821
Xetrov72018971|Xetrov72018971|arhgef40	67.0879428	1.285138046	0.323090075	3.977646309	6.96E-05	0.000991433
Xetrov72016001|Xetrov72016001	3.96829165	2.307489583	0.580135608	3.977500352	6.96E-05	0.000991433
Xetrov72023368|Xetrov72023368	2.09176102	2.364420055	0.594540293	3.976887826	6.98E-05	0.000992489
Xetrov72011781|Xetrov72011781	5.5113838	1.990173436	0.500765888	3.974259198	7.06E-05	0.000999868
Xetrov72010720|Xetrov72010720	12.1609546	2.060869272	0.518541356	3.974358548	7.06E-05	0.000999868
Xetrov72027131|Xetrov72027131	472.833607	1.798703915	0.452591933	3.974228849	7.06E-05	0.000999868
Xetrov72036485|Xetrov72036485	4.99211321	2.244664464	0.564966633	3.973092096	7.09E-05	0.001003412
Xetrov72032611|Xetrov72032611	5.56733916	1.919254265	0.483704111	3.967827068	7.25E-05	0.001022491
Xetrov72022850|Xetrov72022850|unnamed	251.642879	1.027208018	0.258864658	3.968127697	7.24E-05	0.001022491
Xetrov72012429|Xetrov72012429|kiaa1409	12.0094215	1.938061957	0.488442914	3.967837188	7.25E-05	0.001022491
Xetrov72034884|Xetrov72034884|rbms3	4.38844279	2.236065796	0.563880098	3.965498702	7.32E-05	0.001030981
Xetrov72009242|Xetrov72009242|ces2	104.644677	1.491507472	0.376291079	3.963706707	7.38E-05	0.001037204
Xetrov72039500|Xetrov72039500|fchsd1	17.4522859	1.445123435	0.364622332	3.963343185	7.39E-05	0.001038011
Xetrov72017222|Xetrov72017222|b4galnt2	38.3298073	1.53585321	0.387728432	3.961157042	7.46E-05	0.001046002
Xetrov72011938|Xetrov72011938	3.30640652	2.306752136	0.582829506	3.957850647	7.56E-05	0.001057434
Xetrov72022502|Xetrov72022502|cer1	467.494117	1.289314886	0.327053691	3.942211695	8.07E-05	0.001122168
Xetrov72b000160|Xetrov72b000160|fam36a	37.4387887	1.391679862	0.353041546	3.941971921	8.08E-05	0.001122462
Xetrov72003349|Xetrov72003349	17.2069941	1.55911991	0.395968006	3.937489613	8.23E-05	0.001140914
Xetrov72010051|Xetrov72010051|slc7a10	6.67833514	1.902561476	0.483512575	3.934874864	8.32E-05	0.001149372
Xetrov72042548|Xetrov72042548	19.8014017	1.840816033	0.467931082	3.933946912	8.36E-05	0.001152131
Xetrov72012775|Xetrov72012775	14.6498015	2.150647485	0.546748811	3.933520184	8.37E-05	0.001153335
Xetrov72005686|Xetrov72005686|foxb1	956.968809	1.475425346	0.375112378	3.933288881	8.38E-05	0.001153602
Xetrov72013161|Xetrov72013161|atpbd4	82.8001014	1.019213972	0.259441694	3.928489503	8.55E-05	0.001173433
Xetrov72009807|Xetrov72009807|ak5	2.90580316	2.33611457	0.59475667	3.927849303	8.57E-05	0.001174848
Xetrov72026897|Xetrov72026897|etv2	364.839263	1.457628886	0.371147983	3.927352307	8.59E-05	0.001176421
Xetrov72011067|Xetrov72011067|cyba	17.3321767	1.723996285	0.43899709	3.927124635	8.60E-05	0.001176679
Xetrov72042752|Xetrov72042752	9.60957484	2.119464128	0.540074104	3.924395028	8.69E-05	0.001189236
Xetrov72033015|Xetrov72033015	4.02425721	2.336454346	0.595590406	3.922921394	8.75E-05	0.001195668
Xetrov72020803|Xetrov72020803|adra2c	15.0527086	2.067697578	0.527764003	3.917845033	8.93E-05	0.001216979
Xetrov72016688|Xetrov72016688	67.9813443	1.982452769	0.506012856	3.917791309	8.94E-05	0.001216979
Xetrov72014908|Xetrov72014908|unnamed	2.50035759	2.330801989	0.594954741	3.917612263	8.94E-05	0.001217003
Xetrov72023361|Xetrov72023361	11.1382591	1.763266463	0.450543148	3.913646161	9.09E-05	0.001234501
Xetrov72041205|Xetrov72041205|art1	9.52341682	2.297809638	0.587680611	3.909963331	9.23E-05	0.001252571
Xetrov72016354|Xetrov72016354|adamtsl2	25.0576018	2.136474341	0.54654621	3.909046121	9.27E-05	0.001256431
Xetrov72000783|Xetrov72000783|esr1	3.25794755	2.181291803	0.558420271	3.90618306	9.38E-05	0.001270489
Xetrov72037170|Xetrov72037170|nxnl1	3.54001677	2.26044753	0.578753904	3.905714528	9.39E-05	0.001272038
Xetrov72004216|Xetrov72004216|scn3a	13.7342265	1.969313808	0.504644657	3.90237721	9.53E-05	0.001287578
Xetrov72008021|Xetrov72008021	83.0205588	1.162256123	0.297842085	3.902256196	9.53E-05	0.001287578
Xetrov72042273|Xetrov72042273	37.9629447	1.350729855	0.346315581	3.900286124	9.61E-05	0.001296032
Xetrov72018967|Xetrov72018967|fam13a	290.539904	1.007057987	0.25820994	3.900151899	9.61E-05	0.001296032
Xetrov72015078|Xetrov72015078|grem1	2.71407503	2.297842189	0.589509188	3.897890374	9.70E-05	0.001305389
Xetrov72021815|Xetrov72021815|cyb5r1	4.14948926	2.245989478	0.57626352	3.897504181	9.72E-05	0.001306538
Xetrov72018886|Xetrov72018886|cntnap4	4.21874108	2.127708954	0.546058378	3.896486236	9.76E-05	0.001311104
Xetrov72030241|Xetrov72030241|manea	67.5185467	1.559727583	0.400789318	3.891639603	9.96E-05	0.001334722
Xetrov72014847|Xetrov72014847	146.196	1.49781529	0.38509228	3.889497063	0.00010045	0.001345602
Xetrov72006361|Xetrov72006361	29.693353	1.53710904	0.395227589	3.889174445	0.00010059	0.001346422
Xetrov72040479|Xetrov72040479	29.8383817	1.545460994	0.397752539	3.885483668	0.00010213	0.001363181
Xetrov72033715|Xetrov72033715|dtna	149.986354	1.16854759	0.301371791	3.877428554	0.00010557	0.001403131
Xetrov72042725|Xetrov72042725|dhcr7	3113.09883	1.323261259	0.341570746	3.874047398	0.00010704	0.001418747
Xetrov72028426|Xetrov72028426	2.27906284	2.287429816	0.590540442	3.873451594	0.00010731	0.001421222
Xetrov72016201|Xetrov72016201|nova2	191.689309	1.656095503	0.427585857	3.873129746	0.00010745	0.001422101

Xetrov72041582|Xetrov72041582|cyp11b2	5.5708846	2.004140857	0.51768558	3.871347657	0.00010824	0.001430529
Xetrov72036442|Xetrov72036442|or56a1	11.1362129	1.796845375	0.464692891	3.866737387	0.0001103	0.001455789
Xetrov72023942|Xetrov72023942	5.9317113	2.283946377	0.590907029	3.865153508	0.00011102	0.001461173
Xetrov72024794|Xetrov72024794	28.9970398	1.745445575	0.451678382	3.86435491	0.00011138	0.001464938
Xetrov72035666|Xetrov72035666	38.3347521	1.693937792	0.438441385	3.863544481	0.00011175	0.001468783
Xetrov72000289|Xetrov72000289|fam83b	51.1708854	1.551347658	0.401707879	3.86188009	0.00011252	0.001476767
Xetrov72007647|Xetrov72007647|slc38a5	83.3609064	1.212748395	0.314153909	3.860363851	0.00011322	0.001484926
Xetrov72012830|Xetrov72012830|col27a1	38.929186	1.855117624	0.481843758	3.850039757	0.0001181	0.00153716
Xetrov72015574|Xetrov72015574	4.66643567	2.2873207	0.594256038	3.849049152	0.00011858	0.001542323
Xetrov72008372|Xetrov72008372	12.0258256	2.118056428	0.550675279	3.846289288	0.00011992	0.001554423
Xetrov72041261|Xetrov72041261	171.268608	1.611892702	0.419070125	3.846355548	0.00011989	0.001554423
Xetrov72000646|Xetrov72000646	30.2969275	2.075231432	0.539984948	3.84312829	0.00012148	0.001572424
Xetrov72010854|Xetrov72010854|lrrc19	7.47428583	2.171075157	0.564984839	3.842714009	0.00012168	0.001574
Xetrov72029601|Xetrov72029601|zc3h12a	17.3590872	1.789221082	0.465663376	3.842305785	0.00012188	0.001575539
Xetrov72016957|Xetrov72016957|gga3	122.340578	1.124737898	0.292741225	3.842089195	0.00012199	0.001575849
Xetrov72007765|Xetrov72007765	177.653059	1.418172972	0.369433126	3.838781292	0.00012365	0.001593948
Xetrov72000977|Xetrov72000977|vit	1.50085968	2.265525521	0.590489553	3.83669027	0.0001247	0.001605437
Xetrov72026363|Xetrov72026363|wnt4	55.1561173	1.498379127	0.39059239	3.836170815	0.00012497	0.001607406
Xetrov72039496|Xetrov72039496|glt8d2	4.78511717	2.198113581	0.574472148	3.826318805	0.00013007	0.001664273
Xetrov72011066|Xetrov72011066|rgs16	438.294382	1.085321851	0.283686807	3.825774844	0.00013036	0.001666821
Xetrov72006912|Xetrov72006912|ciita	1.59348809	2.27564666	0.594893685	3.825299743	0.00013061	0.001668905
Xetrov72027970|Xetrov72027970	28.3881578	1.888206933	0.493721258	3.824439197	0.00013107	0.00167361
Xetrov72013786|Xetrov72013786|ism2	434.432871	1.511235883	0.395588978	3.82021736	0.00013333	0.001700213
Xetrov72017290|Xetrov72017290|tom1l1	132.653363	1.80499567	0.472623383	3.819099385	0.00013394	0.001705627
Xetrov72039444|Xetrov72039444|tmem173	3.50958571	2.210357905	0.578881819	3.818323241	0.00013436	0.00170869
Xetrov72036336|Xetrov72036336|fam189b	9.84438647	1.809756637	0.474137166	3.816947431	0.00013511	0.001715925
Xetrov72022849|Xetrov72022849	5.00450427	2.136407707	0.559704626	3.817027066	0.00013507	0.001715925
Xetrov72032840|Xetrov72032840|abcc4	12.5022048	1.368891388	0.359006996	3.812993626	0.00013729	0.001742445
Xetrov72006609|Xetrov72006609	34.1923769	1.288916721	0.338246043	3.810589203	0.00013864	0.001755931
Xetrov72012507|Xetrov72012507|kif26a	667.609111	1.495616513	0.392527934	3.810216762	0.00013885	0.001757397
Xetrov72007805|Xetrov72007805	1.61417302	2.224171221	0.584287726	3.806636905	0.00014087	0.001781822
Xetrov72009497|Xetrov72009497|p4htm	5.1279247	2.097817752	0.551597344	3.8031687	0.00014286	0.00180333
Xetrov72037759|Xetrov72037759|dock4	27.8294148	1.450410252	0.381461346	3.802246985	0.00014339	0.001807631
Xetrov72016033|Xetrov72016033	14.6488854	2.034876513	0.53526542	3.801621472	0.00014375	0.00181099
Xetrov72024928|Xetrov72024928|ncam1	150.210131	1.899196373	0.499962958	3.798674165	0.00014547	0.001831433
Xetrov72000121|Xetrov72000121|ltbp1	5.59463312	2.046284045	0.53912749	3.795547591	0.00014732	0.001853431
Xetrov72027693|Xetrov72027693|cacng7	4.09958115	2.263338933	0.596357118	3.795274449	0.00014748	0.001854234
Xetrov72001970|Xetrov72001970	129.733707	1.114896495	0.294058242	3.791413868	0.00014979	0.001877036
Xetrov72004692|Xetrov72004692|adam23	7.57405124	2.02407351	0.534028379	3.790198406	0.00015053	0.001882487
Xetrov72003731|Xetrov72003731	7.77933032	1.820599956	0.480399596	3.789761631	0.00015079	0.001883849
Xetrov72018755|Xetrov72018755|spef2	79.9478422	1.231107991	0.324857254	3.789689089	0.00015084	0.001883849
Xetrov72033525|Xetrov72033525|cdh17	3.06388092	2.241326022	0.591614544	3.788490402	0.00015157	0.001889202
Xetrov72011589|Xetrov72011589	31.9538	2.192592129	0.578941407	3.787243581	0.00015233	0.001897448
Xetrov72032356|Xetrov72032356|unnamed	6.5986048	2.034614577	0.538465183	3.778544354	0.00015775	0.00196107
Xetrov72019923|Xetrov72019923|slc28a3	51.7374301	1.182196461	0.312991139	3.777092424	0.00015867	0.001968635
Xetrov72004766|Xetrov72004766|loc388210	42.8879642	1.870515628	0.495417791	3.77563273	0.0001596	0.001978897
Xetrov72033012|Xetrov72033012	134.474456	1.174836783	0.311276851	3.774250411	0.00016049	0.001986302
Xetrov72023242|Xetrov72023242	6.893192	2.128402735	0.563933345	3.774209762	0.00016052	0.001986302
Xetrov72002721|Xetrov72002721	6.80707235	2.253538597	0.597119301	3.774017341	0.00016064	0.001986531
Xetrov72043496|Xetrov72043496	35.4504627	1.249733444	0.331169436	3.773698019	0.00016085	0.001987593
Xetrov72016913|Xetrov72016913|aoc3	5.84511509	1.889329439	0.500676039	3.773556733	0.00016094	0.001987593
Xetrov72016567|Xetrov72016567	47.0052831	1.161694869	0.308000395	3.771731753	0.00016212	0.001998462
Xetrov72010923|Xetrov72010923|igf2	1823.64958	1.845325777	0.489254879	3.771706442	0.00016214	0.001998462
Xetrov72023501|Xetrov72023501|sh2d4a	75.0660736	1.179250134	0.312674171	3.771498395	0.00016227	0.001998821
Xetrov72023474|Xetrov72023474|fam190a	6.39659442	1.844522731	0.48924204	3.770164014	0.00016314	0.002008225
Xetrov72040897|Xetrov72040897	13.8292661	1.66932993	0.442813658	3.769824844	0.00016336	0.002009643
Xetrov72015512|Xetrov72015512	18.1530278	1.234473358	0.32748732	3.769530246	0.00016356	0.002010703
Xetrov72042561|Xetrov72042561|gpr33	2.31300587	2.179701505	0.578315391	3.769053255	0.00016387	0.002013235
Xetrov72003077|Xetrov72003077	7.34713496	1.88613512	0.500671033	3.767214387	0.00016508	0.002024155
Xetrov72035700|Xetrov72035700	24.5045376	1.695591973	0.450188498	3.766404474	0.00016562	0.002029408
Xetrov72002499|Xetrov72002499	6.00910801	2.103510014	0.55864066	3.765408004	0.00016628	0.002036195
Xetrov72015494|Xetrov72015494	2.90600213	2.212073571	0.58774076	3.763689231	0.00016743	0.002047585
Xetrov72015791|Xetrov72015791	10.8162717	2.042318104	0.543212052	3.759706906	0.00017011	0.002078987
Xetrov72014934|Xetrov72014934|clec4e	104.14967	1.039044804	0.276374139	3.759558718	0.00017021	0.002078987
Xetrov72032279|Xetrov72032279	52.0059625	1.420151119	0.377938419	3.757625705	0.00017153	0.002090779
Xetrov72005662|Xetrov72005662	3.42113905	2.237740757	0.596381923	3.752194137	0.00017529	0.002131362
Xetrov72013772|Xetrov72013772|olfm1	22.3699707	1.536399044	0.409520625	3.751701253	0.00017564	0.00213418
Xetrov72042674|Xetrov72042674|unnamed	3.38851513	2.209167146	0.589328513	3.748617444	0.00017781	0.002153641
Xetrov72033178|Xetrov72033178	47.4218543	1.703132817	0.454330276	3.748666791	0.00017778	0.002153641
Xetrov72025466|Xetrov72025466	23.010839	1.211851112	0.323350159	3.747798095	0.00017839	0.002157911
Xetrov72032117|Xetrov72032117|unnamed	26.3374102	1.734618614	0.463520444	3.74226992	0.00018237	0.002200302
Xetrov72003335|Xetrov72003335	2091.50294	1.300055318	0.347575501	3.740353722	0.00018376	0.002214308
Xetrov72023913|Xetrov72023913	23.7460838	1.429987528	0.382359859	3.739899718	0.00018409	0.002216893
Xetrov72005026|Xetrov72005026|grk7	15.5037266	1.576587595	0.421586044	3.73965794	0.00018427	0.002217608
Xetrov72028322|Xetrov72028322	4.13140532	1.876108416	0.501989831	3.737343466	0.00018598	0.002235258
Xetrov72005701|Xetrov72005701|frzb	4282.48347	1.360177865	0.363964723	3.737114562	0.00018614	0.002235866

Xetrov72042660|Xetrov72042660	2.59847594	2.209054623	0.591293346	3.735970709	0.00018699	0.002241767
Xetrov72015353|Xetrov72015353	10.5961351	1.653726598	0.44268172	3.73570112	0.00018719	0.002242742
Xetrov72036573|Xetrov72036573|unnamed	10.0123193	2.173492028	0.581906885	3.735119969	0.00018763	0.002246499
Xetrov72039583|Xetrov72039583	5.37540642	2.022991585	0.541665356	3.734762735	0.00018789	0.002248261
Xetrov72030419|Xetrov72030419	5.13328091	2.086198859	0.55877421	3.733527461	0.00018882	0.002255023
Xetrov72038616|Xetrov72038616|klhl25	26.3084801	1.111894867	0.298057326	3.730473201	0.00019112	0.002279647
Xetrov72017809|Xetrov72017809	10.4392159	2.106079048	0.56463613	3.729975706	0.0001915	0.002282707
Xetrov72030660|Xetrov72030660|wnt11	38.4135411	1.968313713	0.527999904	3.727867562	0.00019311	0.002300426
Xetrov72002391|Xetrov72002391	3.23721758	2.160047389	0.579556062	3.727072376	0.00019372	0.002306235
Xetrov72000478|Xetrov72000478	9.65708884	2.080666084	0.558558396	3.725064557	0.00019527	0.0023232
Xetrov72027073|Xetrov72027073|c1orf158	15.8749967	2.094700994	0.562405355	3.724539558	0.00019567	0.00232657
Xetrov72006867|Xetrov72006867	7.0960384	1.983644949	0.532695663	3.723786554	0.00019626	0.002332052
Xetrov72040813|Xetrov72040813	9.62863663	2.158626383	0.58019297	3.72053178	0.0001988	0.002356368
Xetrov72023353|Xetrov72023353	5.27371681	1.982885273	0.532939943	3.720654266	0.00019871	0.002356368
Xetrov72031862|Xetrov72031862	76.3070575	1.687810301	0.453611797	3.72082541	0.00019857	0.002356368
Xetrov72011379|Xetrov72011379	9.63950609	2.186535211	0.588002636	3.718580627	0.00020035	0.002371656
Xetrov72003988|Xetrov72003988|or1e1	6.62530578	1.971915076	0.530283035	3.718608638	0.00020032	0.002371656
Xetrov72003227|Xetrov72003227	10.4210825	1.773280598	0.477008389	3.717504007	0.0002012	0.0023773
Xetrov72016517|Xetrov72016517	89.170619	1.569430551	0.422145867	3.717744682	0.00020101	0.0023773
Xetrov72035718|Xetrov72035718	23.3862366	1.89329315	0.509494826	3.716020366	0.00020239	0.002389796
Xetrov72012582|Xetrov72012582|pappa	21.2053001	1.670184822	0.449547267	3.715259653	0.000203	0.002392497
Xetrov72007089|Xetrov72007089	18.7951361	1.943707904	0.523160538	3.715318269	0.00020295	0.002392497
Xetrov72035830|Xetrov72035830|lrrc3b	4.54162458	2.121855514	0.57107865	3.715522394	0.00020278	0.002392497
Xetrov72018594|Xetrov72018594|svep1	23.3882577	1.578981604	0.42507605	3.714586144	0.00020354	0.002395879
Xetrov72005984|Xetrov72005984|stat4	4.61773871	2.146145172	0.578397216	3.710503981	0.00020685	0.002427263
Xetrov72002351|Xetrov72002351	7.33644926	1.938305136	0.523039242	3.705850309	0.00021068	0.002469196
Xetrov72019320|Xetrov72019320|rai14	101.905388	1.068836053	0.288503399	3.704760699	0.00021159	0.002476752
Xetrov72010797|Xetrov72010797	13.4551358	1.8520673	0.500153893	3.702994868	0.00021307	0.002492513
Xetrov72009819|Xetrov72009819|fezf2	72.0708857	2.020757667	0.545836402	3.702130636	0.0002138	0.002497917
Xetrov72032283|Xetrov72032283	53.8814644	1.115467029	0.301729807	3.696906981	0.00021824	0.002548279
Xetrov72027254|Xetrov72027254	24.9911227	2.01227061	0.544523411	3.695471246	0.00021948	0.002561136
Xetrov72038883|Xetrov72038883|gabrg2	8.96678393	1.851105197	0.501706446	3.689618126	0.00022459	0.002614305
Xetrov72041363|Xetrov72041363	4.13679982	2.165630916	0.587204958	3.688032408	0.000226	0.002626093
Xetrov72028594|Xetrov72028594	13.9086833	2.142670601	0.581665867	3.683679448	0.00022989	0.002667759
Xetrov72017513|Xetrov72017513|crhr1.2	9.41640268	2.196224358	0.596399443	3.68247218	0.00023098	0.002677129
Xetrov72021266|Xetrov72021266|shd	6.65835063	2.087865664	0.567324165	3.680198716	0.00023305	0.00269945
Xetrov72016311|Xetrov72016311	1.63814579	2.18887509	0.594955321	3.679057926	0.0002341	0.002708222
Xetrov72007212|Xetrov72007212	2.89647894	2.186311724	0.59439567	3.678209371	0.00023488	0.002713482
Xetrov72041925|Xetrov72041925	14.1352959	1.768084222	0.480706741	3.678093256	0.00023498	0.002713482
Xetrov72029927|Xetrov72029927|c1orf114	17149.5322	1.107853423	0.301275147	3.677214778	0.00023579	0.002721173
Xetrov72026780|Xetrov72026780|spib	33.3816005	2.011782604	0.547780687	3.672605935	0.00024009	0.002763965
Xetrov72043192|Xetrov72043192|sycp2	50.5297544	1.318881627	0.359200357	3.671715807	0.00024093	0.002771917
Xetrov72007520|Xetrov72007520	5.38959622	1.772447912	0.483000548	3.669660252	0.00024287	0.002792595
Xetrov72003710|Xetrov72003710	2.47559577	2.187137922	0.596036778	3.669468067	0.00024306	0.00279299
Xetrov72036045|Xetrov72036045	8.42154021	1.500828826	0.410052283	3.66009138	0.00025213	0.002883138
Xetrov72012201|Xetrov72012201	3.99174178	2.164199473	0.591939795	3.656114169	0.00025607	0.002924665
Xetrov72015754|Xetrov72015754|snapc4	94.2110404	1.14095221	0.312566348	3.650272075	0.00026196	0.002984758
Xetrov72034157|Xetrov72034157|kcng2	6.91569655	2.001118415	0.548587383	3.647766017	0.00026453	0.003011533
Xetrov72004938|Xetrov72004938|nr4a2	26.454268	1.572007525	0.431096099	3.646536188	0.0002658	0.003021158
Xetrov72001637|Xetrov72001637|plscr2	8.40311342	2.061730341	0.565706346	3.644523976	0.00026789	0.003041222
Xetrov72016816|Xetrov72016816|unnamed	12.0354735	1.818474274	0.499054301	3.643840502	0.0002686	0.003046416
Xetrov72007857|Xetrov72007857	36.9362315	1.53890484	0.422338038	3.643775129	0.00026867	0.003046416
Xetrov72043649|Xetrov72043649	14.6459866	2.092282304	0.574962839	3.63898701	0.00027371	0.003098055
Xetrov72003432|Xetrov72003432|slc34a3	8.66231928	1.831295256	0.503243553	3.638984034	0.00027372	0.003098055
Xetrov72021248|Xetrov72021248	55.8762814	1.890856066	0.519600937	3.639054381	0.00027364	0.003098055
Xetrov72028238|Xetrov72028238	6.67033201	1.753319251	0.482414797	3.634464079	0.00027856	0.003141546
Xetrov72035767|Xetrov72035767	29.7819446	1.934922715	0.532380129	3.634475838	0.00027855	0.003141546
Xetrov72018291|Xetrov72018291	26.036369	2.128073765	0.586561445	3.628049169	0.00028557	0.003212928
Xetrov72021812|Xetrov72021812	17.6819583	1.506147647	0.415163563	3.627841608	0.0002858	0.003213592
Xetrov72011539|Xetrov72011539	26.5441506	1.48344064	0.408944275	3.627488468	0.00028619	0.003216069
Xetrov72032090|Xetrov72032090	4.3605848	2.143995498	0.591127586	3.626958968	0.00028678	0.003218828
Xetrov72005126|Xetrov72005126|tgfb1i1	9.02449105	2.163824024	0.596798624	3.625718858	0.00028816	0.003232389
Xetrov72004919|Xetrov72004919	17.4715701	1.65803324	0.457640486	3.623003845	0.0002912	0.003260695
Xetrov72011650|Xetrov72011650	3.15234166	2.157827498	0.595584457	3.623041991	0.00029116	0.003260695
Xetrov72020282|Xetrov72020282|katnal2	327.066626	1.013535762	0.28005159	3.619103766	0.00029563	0.00330668
Xetrov72005653|Xetrov72005653|prss29	74.1322447	1.252324739	0.346034602	3.61907373	0.00029566	0.00330668
Xetrov72043518|Xetrov72043518	35.5598107	1.170437653	0.323461736	3.618473289	0.00029635	0.003308466
Xetrov72012876|Xetrov72012876|c5	174.121849	1.650048628	0.456406797	3.615302485	0.0003	0.003335387
Xetrov72042318|Xetrov72042318	2.20151162	2.152157058	0.595279482	3.615372479	0.00029992	0.003335387
Xetrov72043082|Xetrov72043082	48.0727371	1.34364919	0.371718595	3.614694575	0.0003007	0.003341251
Xetrov72019649|Xetrov72019649	57.03913	1.461611782	0.404588836	3.612585543	0.00030316	0.003364583
Xetrov72023652|Xetrov72023652	178.730191	1.222858485	0.338676084	3.610702213	0.00030537	0.003387115
Xetrov72014227|Xetrov72014227|fhl1	11.8370842	1.847761162	0.511809576	3.610251249	0.0003059	0.003391013
Xetrov72042755|Xetrov72042755	4.71471021	1.861475698	0.515663858	3.609862646	0.00030636	0.003394099
Xetrov72039058|Xetrov72039058|rgma	445.965656	1.069050627	0.296212934	3.609061262	0.00030731	0.003402599
Xetrov72010206|Xetrov72010206|dmbx1	275.103053	1.447960191	0.402041906	3.601515587	0.00031637	0.003488562

Xetrov72037788|Xetrov72037788|lamb1	3379.97709	1.585054231	0.440153643	3.601138507	0.00031683	0.003491583
Xetrov72035294|Xetrov72035294	16.7865885	1.707707712	0.474398479	3.599732691	0.00031854	0.003506409
Xetrov72008802|Xetrov72008802|gpr56	88.7056446	1.48378837	0.412213379	3.599563835	0.00031875	0.003506638
Xetrov72020704|Xetrov72020704|cd34	9.52862543	1.722066106	0.478735512	3.597113781	0.00032177	0.00353157
Xetrov72017770|Xetrov72017770|tmem98	13.7396629	1.339918198	0.372718249	3.594989516	0.00032441	0.003556366
Xetrov72040836|Xetrov72040836|dgki	6.14404538	1.963998506	0.546849218	3.591480869	0.0003288	0.003601007
Xetrov72040814|Xetrov72040814|rergl	8.57746038	1.756318968	0.489029526	3.591437478	0.00032886	0.003601007
Xetrov72001349|Xetrov72001349|hao1	909.02975	1.406287595	0.39161117	3.591030344	0.00032937	0.003604542
Xetrov72006623|Xetrov72006623	7.33738702	1.673621687	0.466121092	3.590529835	0.00033001	0.003609374
Xetrov72010358|Xetrov72010358|dbx1	22.2669519	1.540243239	0.429285815	3.587920182	0.00033333	0.003639343
Xetrov72007359|Xetrov72007359	7.11811499	2.099261223	0.585086707	3.58794893	0.00033329	0.003639343
Xetrov72031305|Xetrov72031305|msra.2	122.018692	1.137946678	0.317293997	3.586410995	0.00033526	0.003656222
Xetrov72030212|Xetrov72030212|gabra5	1.5440101	2.128587533	0.593768375	3.584878588	0.00033724	0.003673612
Xetrov72022200|Xetrov72022200|yjefn3	4.08136258	1.905287521	0.531480116	3.584870751	0.00033725	0.003673612
Xetrov72042385|Xetrov72042385	6.7837798	1.874790463	0.523336089	3.582383293	0.00034047	0.003702357
Xetrov72036532|Xetrov72036532	45.3379898	1.647753437	0.460312344	3.579642081	0.00034407	0.003739251
Xetrov72025601|Xetrov72025601|gpr162	1.92235366	2.130423978	0.595345972	3.57846375	0.00034562	0.003749896
Xetrov72010843|Xetrov72010843	40.5362435	1.365302634	0.382012287	3.573975706	0.0003516	0.003807712
Xetrov72022803|Xetrov72022803	28.8930599	1.837605052	0.514579202	3.571083019	0.00035551	0.003839244
Xetrov72037269|Xetrov72037269	17.9788066	1.380124967	0.386612827	3.569785764	0.00035727	0.003856095
Xetrov72042007|Xetrov72042007	1.25455373	2.066274766	0.579172345	3.56763368	0.00036022	0.003881222
Xetrov72022052|Xetrov72022052	10.4204023	2.018469006	0.566036747	3.565968138	0.00036252	0.003903725
Xetrov72037687|Xetrov72037687|reln	13.0947344	1.494990603	0.419284889	3.565572337	0.00036306	0.003907388
Xetrov72001924|Xetrov72001924|tcf21	2.78099365	2.107019454	0.591050012	3.564875071	0.00036403	0.003913318
Xetrov72042534|Xetrov72042534	1.57865152	2.121076942	0.595052698	3.564519496	0.00036452	0.003914158
Xetrov72019555|Xetrov72019555|c19orf26	86.827271	1.124971395	0.315745254	3.562908334	0.00036677	0.003933783
Xetrov72021850|Xetrov72021850|tmem119	24.3299125	1.918373838	0.538722275	3.56096996	0.00036949	0.003956182
Xetrov72008118|Xetrov72008118	26.0159766	1.181532972	0.331847394	3.560470848	0.00037019	0.003961458
Xetrov72018307|Xetrov72018307|a2ml1	111.761715	1.757067753	0.493563996	3.559959333	0.00037091	0.003966928
Xetrov72043464|Xetrov72043464	2.63621996	2.080271367	0.585136984	3.555186948	0.00037771	0.004032765
Xetrov72038274|Xetrov72038274|unc5a	23.8247692	1.558488554	0.438356132	3.555302272	0.00037755	0.004032765
Xetrov72036504|Xetrov72036504|hcn4	7.21711985	2.004664726	0.563938466	3.554757913	0.00037833	0.004037063
Xetrov72023714|Xetrov72023714	17.2226455	1.631886939	0.459260492	3.553292668	0.00038044	0.004057319
Xetrov72033979|Xetrov72033979|map3k3	14.7495552	1.721941528	0.484785867	3.551963135	0.00038237	0.004073262
Xetrov72011226|Xetrov72011226|mgp	2.74572973	2.08861237	0.588603258	3.548421357	0.00038755	0.004121442
Xetrov72028791|Xetrov72028791|lmo7	804.475206	1.156852494	0.326190241	3.54655765	0.0003903	0.004146022
Xetrov72024981|Xetrov72024981|slc27a3	21.4036925	1.592053161	0.449007356	3.545717325	0.00039155	0.004155631
Xetrov72043514|Xetrov72043514	59.1393788	1.369554772	0.386263326	3.545650541	0.00039165	0.004155631
Xetrov72023543|Xetrov72023543	16.0768827	1.334478504	0.376452375	3.544880023	0.00039279	0.004165451
Xetrov72019781|Xetrov72019781|pde8b	54.4103648	1.512708909	0.426886205	3.543588179	0.00039472	0.004181204
Xetrov72016015|Xetrov72016015	5.26549963	2.061083542	0.581623536	3.543672867	0.0003946	0.004181204
Xetrov72035440|Xetrov72035440	11.790862	1.736473329	0.49029388	3.541698969	0.00039756	0.004208895
Xetrov72012094|Xetrov72012094	4.34332414	2.095007676	0.591648055	3.540969431	0.00039866	0.004218179
Xetrov72018820|Xetrov72018820|prr14l	459.143016	1.100285992	0.310820802	3.539936786	0.00040022	0.00423234
Xetrov72030129|Xetrov72030129|fuca1	197.233041	1.146178929	0.323944252	3.538198081	0.00040287	0.00425553
Xetrov72002992|Xetrov72002992	3.56047605	2.038377003	0.576749337	3.534251145	0.00040893	0.00431717
Xetrov72032248|Xetrov72032248	10.1710525	1.453855446	0.411396445	3.533952382	0.0004094	0.004319631
Xetrov72001455|Xetrov72001455|unnamed	155.648497	2.091870324	0.59246072	3.530816903	0.00041428	0.00435895
Xetrov72042893|Xetrov72042893|xa-1	4.91823449	2.064164962	0.584949866	3.528789529	0.00041747	0.004388779
Xetrov72042579|Xetrov72042579	2.11566127	2.082681216	0.590704878	3.525755911	0.00042228	0.004433192
Xetrov72000816|Xetrov72000816|bai3	8.22217628	1.477860532	0.419301964	3.52457336	0.00042417	0.004449572
Xetrov72020387|Xetrov72020387|slc41a1	26.1844534	1.2734801	0.361323864	3.524483785	0.00042431	0.004449572
Xetrov72033171|Xetrov72033171|myom1	30.3106796	1.814656687	0.515042457	3.523314751	0.00042619	0.004465982
Xetrov72038357|Xetrov72038357|slc6a15	36.8874333	1.566485781	0.444837358	3.521479821	0.00042915	0.004485307
Xetrov72020536|Xetrov72020536|gtpbp3	23.7323239	1.274720535	0.362068109	3.52066504	0.00043047	0.004496615
Xetrov72019451|Xetrov72019451|eef2.2	51.4470784	1.154690884	0.328203943	3.518211492	0.00043447	0.004528352
Xetrov72006857|Xetrov72006857	8.1168182	1.653631313	0.470150678	3.5172369	0.00043606	0.004539987
Xetrov72032426|Xetrov72032426	1.17089759	2.061677874	0.586659089	3.51426904	0.00044097	0.004580541
Xetrov72037177|Xetrov72037177	5.3318415	1.892349595	0.539379134	3.508384874	0.00045084	0.004667978
Xetrov72027941|Xetrov72027941	76.1237717	1.150425442	0.328131578	3.505988206	0.00045492	0.004705039
Xetrov72040922|Xetrov72040922|nodal3.2	7.80284636	2.035840623	0.580712458	3.505763645	0.0004553	0.004706426
Xetrov72041983|Xetrov72041983	7.89523107	1.913359777	0.545833473	3.505391061	0.00045594	0.00470785
Xetrov72002551|Xetrov72002551	1.90320727	2.088681267	0.595824095	3.505533401	0.00045569	0.00470785
Xetrov72029538|Xetrov72029538|sh2b2	80.2008304	1.028851878	0.293574717	3.504565678	0.00045735	0.004717295
Xetrov72005651|Xetrov72005651	3.66252854	2.088251428	0.596594349	3.500286971	0.00046476	0.004784749
Xetrov72005138|Xetrov72005138|chrna7	5.34814364	1.828157243	0.52268695	3.497614096	0.00046944	0.004818218
Xetrov72010901|Xetrov72010901|crp.3	2.31327247	2.063469418	0.590458324	3.494691046	0.00047461	0.004865988
Xetrov72005402|Xetrov72005402	28.4032273	1.900328248	0.54412067	3.492475753	0.00047857	0.004895869
Xetrov72018158|Xetrov72018158	3.29393891	2.06950311	0.592893092	3.49051648	0.00048209	0.004923885
Xetrov72020787|Xetrov72020787|fam113a	94.000657	1.314200473	0.376575599	3.489871563	0.00048325	0.004933107
Xetrov72003967|Xetrov72003967	31.9435523	1.748175877	0.501978055	3.482574309	0.00049662	0.005061305
Xetrov72005546|Xetrov72005546	6.65886614	1.974110399	0.567060929	3.481302091	0.00049898	0.00507991
Xetrov72019920|Xetrov72019920|map9	94.9365213	1.294488731	0.371868177	3.481041972	0.00049947	0.005082019
Xetrov72020069|Xetrov72020069|ggt1	1276.28534	1.503938449	0.432323707	3.478732312	0.00050379	0.005120567
Xetrov72029169|Xetrov72029169|scube1	42.7215698	1.44857541	0.416506587	3.477917169	0.00050533	0.005127861
Xetrov72023170|Xetrov72023170	22.4586143	1.398817858	0.402424285	3.475977741	0.000509	0.005162306

Xetrov72037272|Xetrov72037272|znf268	48.2082194	1.087039449	0.312882813	3.474270254	0.00051225	0.00519133
Xetrov72004046|Xetrov72004046	4.10380282	2.074171776	0.597023972	3.474185078	0.00051241	0.00519133
Xetrov72023539|Xetrov72023539	4.07745759	1.856670537	0.534493686	3.473699664	0.00051334	0.005197934
Xetrov72000969|Xetrov72000969	6335.2487	1.288150881	0.371115303	3.47102604	0.00051847	0.005238699
Xetrov72020283|Xetrov72020283|hcn1	2.27020935	2.068355228	0.595888199	3.471045796	0.00051844	0.005238699
Xetrov72022817|Xetrov72022817	23.9665543	1.300479385	0.374648406	3.47119957	0.00051814	0.005238699
Xetrov72034843|Xetrov72034843|ca8	6.76470923	1.705685931	0.491617441	3.469539094	0.00052135	0.005261772
Xetrov72022984|Xetrov72022984|cmtm5	40.9409603	1.141385547	0.328985131	3.469413778	0.0005216	0.005261772
Xetrov72006686|Xetrov72006686	15.0257933	1.354248893	0.390566842	3.467393403	0.00052553	0.005295812
Xetrov72029308|Xetrov72029308|dscam	37.3162646	1.278049023	0.368845897	3.464994548	0.00053024	0.005331864
Xetrov72009475|Xetrov72009475	7.71743316	1.758097862	0.507652692	3.463190268	0.00053381	0.005362022
Xetrov72012973|Xetrov72012973	9.81524967	1.953887967	0.564281884	3.462609774	0.00053496	0.005370738
Xetrov72002364|Xetrov72002364	1.94700768	2.061499782	0.595704399	3.460608625	0.00053896	0.005402178
Xetrov72025376|Xetrov72025376|dixdc1	3.8897844	2.020361536	0.584405896	3.457120385	0.00054598	0.005460969
Xetrov72033705|Xetrov72033705	37.2896902	1.472283953	0.426033503	3.45579383	0.00054868	0.005482091
Xetrov72019580|Xetrov72019580|tgm1	7.63565316	1.917861422	0.555143727	3.454711505	0.00055088	0.005501225
Xetrov72025940|Xetrov72025940	29.0711918	1.361037747	0.394248745	3.452231024	0.00055597	0.005546169
Xetrov72000862|Xetrov72000862|epha7	35.5346532	1.960385912	0.568097844	3.450789215	0.00055895	0.005572929
Xetrov72030702|Xetrov72030702|myo18a	60.575416	1.022539493	0.296479195	3.448941814	0.00056279	0.005608227
Xetrov72010500|Xetrov72010500|ctsw	6.84968367	1.529608322	0.444152934	3.443877558	0.00057344	0.005708288
Xetrov72032509|Xetrov72032509|rabl3	7.32283811	1.68832474	0.490588019	3.441430841	0.00057865	0.005757119
Xetrov72037719|Xetrov72037719|ptprz1	4.86035922	2.053821258	0.596869023	3.440991537	0.00057959	0.005763429
Xetrov72035318|Xetrov72035318	392.055689	1.259103091	0.36597235	3.440432293	0.00058079	0.005772305
Xetrov72023342|Xetrov72023342	17.1469172	1.20143678	0.349261266	3.439937078	0.00058185	0.005779827
Xetrov72000622|Xetrov72000622|nlgn1	3.23747109	1.855550283	0.539963107	3.436439007	0.00058942	0.005848811
Xetrov72034569|Xetrov72034569|sfrp4	6.22144392	1.828853198	0.532494398	3.434502228	0.00059364	0.005884566
Xetrov72035066|Xetrov72035066	18.818798	1.826786328	0.532098703	3.433171925	0.00059656	0.005907298
Xetrov72016328|Xetrov72016328	1.34245337	2.041548753	0.594780141	3.432442698	0.00059817	0.005920094
Xetrov72038674|Xetrov72038674|unnamed	660.379216	1.139464645	0.332210478	3.429947944	0.0006037	0.00596226
Xetrov72021276|Xetrov72021276	20.5851	1.382464662	0.403161385	3.429060206	0.00060568	0.005978661
Xetrov72037337|Xetrov72037337|creb3l3	1.89228862	2.021493325	0.589616856	3.428486321	0.00060696	0.005988177
Xetrov72028729|Xetrov72028729|myh15	3.59437516	1.961133603	0.572117523	3.427850963	0.00060838	0.005996252
Xetrov72016633|Xetrov72016633|lama5	2678.82782	1.417935367	0.413653179	3.427836263	0.00060841	0.005996252
Xetrov72011948|Xetrov72011948	3.304951	2.045320356	0.596846369	3.426879112	0.00061056	0.00601428
Xetrov72024967|Xetrov72024967|prdm16	10.0367299	1.909137126	0.558145156	3.420502903	0.00062506	0.006126951
Xetrov72008928|Xetrov72008928|rhpn2	980.552941	1.091247239	0.319028426	3.420532937	0.00062499	0.006126951
Xetrov72008516|Xetrov72008516	140.14877	1.502640318	0.439762824	3.416933481	0.00063331	0.006199435
Xetrov72025562|Xetrov72025562	92.764131	1.097805632	0.321332623	3.416415123	0.00063451	0.00620158
Xetrov72003350|Xetrov72003350	1206.43131	1.542165459	0.451382404	3.416538716	0.00063423	0.00620158
Xetrov72025631|Xetrov72025631|rnf207	8.11188676	1.718819647	0.50320826	3.415722247	0.00063613	0.006214155
Xetrov72039229|Xetrov72039229|prkar2b	108.19672	1.409386437	0.412674957	3.415245857	0.00063725	0.006221807
Xetrov72018436|Xetrov72018436	1.65684057	2.032739575	0.595448185	3.413797581	0.00064064	0.006251732
Xetrov72010118|Xetrov72010118|unnamed	14.6493596	1.304761545	0.383016171	3.406544273	0.00065791	0.006403646
Xetrov72025209|Xetrov72025209|myos	173.587662	1.730160786	0.508148511	3.404832935	0.00066205	0.006437255
Xetrov72020380|Xetrov72020380|slc7a8	1345.95906	1.268552306	0.372928031	3.401600846	0.00066992	0.006503789
Xetrov72004414|Xetrov72004414|srebf1	16.7755561	1.056600474	0.310737199	3.400302503	0.00067311	0.006531385
Xetrov72039144|Xetrov72039144|plin1	1.95724196	2.011459389	0.591743356	3.399209079	0.00067581	0.006550804
Xetrov72033544|Xetrov72033544	15.2378107	1.24649893	0.366939535	3.397014522	0.00068125	0.006596776
Xetrov72012132|Xetrov72012132	6.93461759	1.725255558	0.508064804	3.395739172	0.00068444	0.006613985
Xetrov72013088|Xetrov72013088|lrfn1	11.9186179	1.752639049	0.516227837	3.395088222	0.00068607	0.006626331
Xetrov72025686|Xetrov72025686|slc43a1	1202.69896	1.038293936	0.30596119	3.393547844	0.00068994	0.006653475
Xetrov72007997|Xetrov72007997|tulp1	65.9966516	1.608237409	0.473905116	3.393585249	0.00068984	0.006653475
Xetrov72027211|Xetrov72027211|cyhr1	14.2704009	1.366286837	0.402696481	3.392845233	0.00069171	0.006660333
Xetrov72017912|Xetrov72017912	54.3618901	1.410879179	0.415824859	3.39296497	0.00069141	0.006660333
Xetrov72011441|Xetrov72011441	10.13663	1.98823886	0.586114864	3.392234152	0.00069325	0.006671015
Xetrov72023587|Xetrov72023587	1.83092183	1.974849202	0.582224048	3.391905932	0.00069408	0.006672972
Xetrov72028042|Xetrov72028042	13.6610506	1.390253997	0.409971375	3.391100167	0.00069613	0.006689208
Xetrov72015532|Xetrov72015532	7.05013826	1.788882632	0.527627192	3.39042919	0.00069783	0.006698768
Xetrov72023364|Xetrov72023364	8.39355574	1.728119915	0.50974191	3.390186057	0.00069845	0.006701297
Xetrov72042978|Xetrov72042978	21.600422	1.543790103	0.455604229	3.388445505	0.0007029	0.006740539
Xetrov72029976|Xetrov72029976|bivm	7.35832812	1.899395093	0.560770371	3.387117419	0.00070631	0.006767507
Xetrov72014630|Xetrov72014630	145.515278	1.228632618	0.362773375	3.386777264	0.00070719	0.006771314
Xetrov72029075|Xetrov72029075|fam160a2	23.8009787	1.336426492	0.394832586	3.384792793	0.00071232	0.006806614
Xetrov72009427|Xetrov72009427|unnamed	806.864858	1.11359623	0.329077556	3.383993256	0.0007144	0.006823004
Xetrov72028453|Xetrov72028453	4.28291149	1.954661135	0.577946824	3.382077819	0.0007194	0.006860321
Xetrov72035329|Xetrov72035329	18.4603847	1.664371918	0.492596154	3.378775708	0.00072809	0.006929216
Xetrov72021699|Xetrov72021699|sgtb	22.1325249	1.57785931	0.467558953	3.374674572	0.00073903	0.007015573
Xetrov72042393|Xetrov72042393|adamts12	2.51282143	2.000427108	0.592869153	3.374146047	0.00074045	0.007025516
Xetrov72009009|Xetrov72009009|mmp2	6.70985289	2.010713827	0.596207721	3.372505511	0.00074488	0.007063508
Xetrov72020929|Xetrov72020929|msr1	5.22076044	1.9908067	0.590415565	3.371873671	0.00074659	0.007069818
Xetrov72031875|Xetrov72031875	50.1357236	1.083811423	0.321428271	3.371860915	0.00074662	0.007069818
Xetrov72036061|Xetrov72036061	4.06485751	1.963458426	0.58272098	3.369465825	0.00075314	0.007124382
Xetrov72024130|Xetrov72024130	32.2427307	2.011704969	0.597492289	3.366913692	0.00076015	0.007187031
Xetrov72035341|Xetrov72035341	182.375094	1.086163656	0.322734101	3.365506318	0.00076403	0.00721655
Xetrov72013908|Xetrov72013908|foxa1	1755.70488	1.032093805	0.306828507	3.363748088	0.00076892	0.007251768
Xetrov72042847|Xetrov72042847	6.18895869	1.855981884	0.551742547	3.363854926	0.00076862	0.007251768

Xetrov72002457|Xetrov72002457	15.5952072	1.79851561	0.535369235	3.359392906	0.00078114	0.007349706
Xetrov72005007|Xetrov72005007|fzd5	11.758146	1.441077254	0.428996055	3.359185327	0.00078173	0.00735049
Xetrov72007631|Xetrov72007631	2.0203395	2.002399226	0.596249082	3.358326721	0.00078416	0.007368246
Xetrov72000005|Xetrov72000005|syne1	56.772047	1.608919539	0.479120595	3.358068	0.00078489	0.007368246
Xetrov72014827|Xetrov72014827|prrt1	36.4077287	1.462268923	0.43546033	3.357984238	0.00078513	0.007368246
Xetrov72031546|Xetrov72031546	2.98662745	1.996330537	0.59481808	3.356203523	0.0007902	0.007411704
Xetrov72034592|Xetrov72034592	22.3976763	1.321552663	0.394214304	3.352371156	0.00080123	0.007496412
Xetrov72036486|Xetrov72036486	1.65636352	1.930230199	0.576073486	3.350666616	0.00080617	0.007538958
Xetrov72032931|Xetrov72032931	19.0257819	1.199280745	0.357943691	3.350473199	0.00080674	0.007540481
Xetrov72026457|Xetrov72026457	5.96574253	1.685266175	0.503374684	3.347935898	0.00081416	0.007591543
Xetrov72000796|Xetrov72000796|tbx18	9.45458223	1.560354021	0.466126893	3.347487659	0.00081548	0.007599544
Xetrov72029060|Xetrov72029060|tubgcp5	176.185142	1.087991884	0.32505662	3.347084228	0.00081666	0.007603089
Xetrov72003609|Xetrov72003609	5.02386865	1.992066632	0.595299899	3.346324494	0.00081891	0.007620186
Xetrov72002900|Xetrov72002900	6.57811492	1.650583824	0.493450578	3.34498306	0.00082288	0.007642034
Xetrov72015471|Xetrov72015471	35.0830549	1.440473136	0.430696116	3.344523164	0.00082424	0.007650943
Xetrov72030122|Xetrov72030122	6.23373515	1.935486968	0.579365439	3.340701458	0.00083567	0.007734159
Xetrov72024020|Xetrov72024020|cers4	9.91358622	1.604778997	0.480519712	3.339673604	0.00083877	0.007757895
Xetrov72035897|Xetrov72035897	2.51209971	1.971947495	0.590753367	3.338021593	0.00084377	0.007793821
Xetrov72034126|Xetrov72034126|entpd3	21.0882232	1.381945933	0.414097092	3.337250993	0.00084612	0.007811632
Xetrov72032428|Xetrov72032428	381.393375	1.327049933	0.398050962	3.333869424	0.00085647	0.007899475
Xetrov72026993|Xetrov72026993	2.52783108	1.862762164	0.559277103	3.330660516	0.0008664	0.007983275
Xetrov72037598|Xetrov72037598	5.12453097	1.790357073	0.537718567	3.329542966	0.00086989	0.008007547
Xetrov72001128|Xetrov72001128|foxa2	568.067649	1.313677051	0.394548818	3.329567826	0.00086981	0.008007547
Xetrov72031998|Xetrov72031998	34.0986314	1.321693339	0.397094209	3.32841252	0.00087342	0.008036186
Xetrov72042518|Xetrov72042518	13.0323416	1.986527002	0.596995449	3.327541282	0.00087616	0.008057421
Xetrov72002742|Xetrov72002742	3.98643514	1.86946175	0.561911498	3.326968319	0.00087796	0.008066129
Xetrov72029602|Xetrov72029602|kcnq4	185.688791	1.288612105	0.387730309	3.323475295	0.00088903	0.008151677
Xetrov72004624|Xetrov72004624|c2orf67	36.2689194	1.362037161	0.410423924	3.318610544	0.00090467	0.008267085
Xetrov72023944|Xetrov72023944	3.66260423	1.979420043	0.596655778	3.317524303	0.00090819	0.008295273
Xetrov72028470|Xetrov72028470|gcgr	1.92710162	1.960083373	0.591217052	3.315336332	0.00091533	0.008340257
Xetrov72014309|Xetrov72014309|nkx2-1	4.36024793	1.684639734	0.508117913	3.31545039	0.00091496	0.008340257
Xetrov72021097|Xetrov72021097	10.563703	1.654289763	0.499018727	3.315085533	0.00091615	0.008343707
Xetrov72043386|Xetrov72043386	8.56262115	1.96766359	0.593865413	3.313315687	0.00092197	0.008388577
Xetrov72010125|Xetrov72010125	1.66413311	1.972812258	0.595503997	3.312844698	0.00092352	0.008394605
Xetrov72038380|Xetrov72038380|sema3e	1.90136938	1.970465941	0.595127047	3.311000482	0.00092963	0.008441977
Xetrov72032818|Xetrov72032818	2.19971668	1.959283443	0.591896008	3.310181886	0.00093235	0.008458549
Xetrov72035785|Xetrov72035785|reck	258.177879	1.265683464	0.38239748	3.309863502	0.00093342	0.008464099
Xetrov72035107|Xetrov72035107	3.26055208	1.855874362	0.560813433	3.309254472	0.00093545	0.008478452
Xetrov72000020|Xetrov72000020	12.5059686	1.466621396	0.443677942	3.305599078	0.00094774	0.008573323
Xetrov72042272|Xetrov72042272	7.6315603	1.663379936	0.504047416	3.300046551	0.00096669	0.008719636
Xetrov72023380|Xetrov72023380	1.32634391	1.873887991	0.567918898	3.299569706	0.00096833	0.008726105
Xetrov72028613|Xetrov72028613	6.23982487	1.71318131	0.519243896	3.299376892	0.000969	0.008727926
Xetrov72013709|Xetrov72013709|pip5kl1	13.9662704	1.636788494	0.496750092	3.294993842	0.00098424	0.008848279
Xetrov72033704|Xetrov72033704	12.2840324	1.354266868	0.411066651	3.294518939	0.0009859	0.008857065
Xetrov72009106|Xetrov72009106|itfg1	27.0079521	1.402144663	0.425608534	3.294446775	0.00098616	0.008857065
Xetrov72006127|Xetrov72006127|socs1	83.3246115	1.582441751	0.480359462	3.294286628	0.00098672	0.008857889
Xetrov72032937|Xetrov72032937	151.065698	1.211171128	0.367781068	3.293185085	0.00099059	0.008884199
Xetrov72036307|Xetrov72036307	12.9283193	1.394131959	0.423412611	3.292608492	0.00099263	0.008898199
Xetrov72020628|Xetrov72020628|palm2	6.64842458	1.418906189	0.431166805	3.29085211	0.00099884	0.008936926
Xetrov72028600|Xetrov72028600|dnhd1	20.3630303	1.077705047	0.327930793	3.286379537	0.00101484	0.009065141
Xetrov72037493|Xetrov72037493	4.44979658	1.876604281	0.571243432	3.285121853	0.00101938	0.009094768
Xetrov72018326|Xetrov72018326	9.9230832	1.628383224	0.495860885	3.283951754	0.00102362	0.009128287
Xetrov72033075|Xetrov72033075|tg	4.55469435	1.897595864	0.577906048	3.283571562	0.00102501	0.009136283
Xetrov72035000|Xetrov72035000|ptpla	4.76117894	1.946799723	0.593479044	3.280317549	0.0010369	0.009232799
Xetrov72013406|Xetrov72013406|traf3	16.8371322	1.161670175	0.354161846	3.280054548	0.00103787	0.009233466
Xetrov72012270|Xetrov72012270	52.2619959	1.6972348	0.517566395	3.279260046	0.0010408	0.009255131
Xetrov72004671|Xetrov72004671|iqca1	35.3259976	1.801111872	0.549345006	3.278653401	0.00104304	0.009257564
Xetrov72017962|Xetrov72017962	5.68565811	1.541936052	0.470341022	3.278336311	0.00104421	0.009263605
Xetrov72011535|Xetrov72011535|sec16b	7.71112168	1.813853466	0.553620793	3.27634635	0.0010516	0.009311586
Xetrov72028803|Xetrov72028803|col2a1	15.4965087	1.763614669	0.539512385	3.268904883	0.00107965	0.009515232
Xetrov72043583|Xetrov72043583	1491.38255	1.275441026	0.391071778	3.261398799	0.00110864	0.009752511
Xetrov72036309|Xetrov72036309	1.2835722	1.844504154	0.565993571	3.25887828	0.00111854	0.0098258
Xetrov72016245|Xetrov72016245|ldlrad2	26.3769445	1.524977561	0.468260909	3.25668347	0.00112722	0.00988825
Xetrov72010077|Xetrov72010077|b3galt2	2.422932	1.939547458	0.59594283	3.254586447	0.00113558	0.009952274
Xetrov72029839|Xetrov72029839	4.40882476	1.768683318	0.543593706	3.25368616	0.00113918	0.009975769
Xetrov72041670|Xetrov72041670	21.6247265	1.480622963	0.455064891	3.253652376	0.00113932	0.009975769
Xetrov72032470|Xetrov72032470|cnga4	34.8534574	1.573886674	0.483765997	3.25340492	0.00114031	0.009979821

Appendix III

Differential expression analysis of LiCl- and UV-treated embryos at gastrula stage (NF11.5)

Genes up-regulated in UV-treated embryos
Differential analysis using DESeq2
fc> 2, padj. <0.01

Gene	baseMean	log2FoldChan	lfcSE	stat	pvalue	padj
Xetrov72013731|Xetrov72013731|olfm4	1445.53534	-3.1107165	0.23676178	-13.138592	1.98E-39	1.86E-35
Xetrov72034206|Xetrov72034206|tfap2a	14475.0918	-2.4889449	0.22245881	-11.18834	4.65E-29	1.09E-25
Xetrov72039428|Xetrov72039428|wnt8a	5500.65442	-3.1396011	0.29388338	-10.683153	1.22E-26	2.09E-23
Xetrov72032930|Xetrov72032930	166.283654	-3.5389594	0.34256531	-10.330758	5.12E-25	7.41E-22
Xetrov72037431|Xetrov72037431|ndel1	210.016842	-1.4796726	0.14371296	-10.296028	7.34E-25	9.22E-22
Xetrov72030238|Xetrov72030238|klf5	1981.79676	-2.4080827	0.23490405	-10.251346	1.17E-24	1.29E-21
Xetrov72022004|Xetrov72022004	1692.69288	-3.6539613	0.35757026	-10.218862	1.63E-24	1.71E-21
Xetrov72043094|Xetrov72043094|slc17a9	317.04323	-2.0603023	0.20240998	-10.178857	2.46E-24	2.44E-21
Xetrov72027348|Xetrov72027348|LOC100495414	1105.89507	-2.1896213	0.21534818	-10.167819	2.76E-24	2.48E-21
Xetrov72040301|Xetrov72040301|atp6v1f	208.070725	-2.2361076	0.2199199	-10.167827	2.76E-24	2.48E-21
Xetrov72018049|Xetrov72018049	80.6316919	-2.1781402	0.21438326	-10.160029	2.99E-24	2.56E-21
Xetrov72013980|Xetrov72013980|bmp4	4801.06584	-1.2535448	0.12358037	-10.143558	3.54E-24	2.77E-21
Xetrov72017149|Xetrov72017149|fam83d	318.271262	-1.9447315	0.1922632	-10.114944	4.74E-24	3.44E-21
Xetrov72026085|Xetrov72026085|styk1	397.5499	-3.1868102	0.32296884	-9.8672375	5.77E-23	4.03E-20
Xetrov72017350|Xetrov72017350|tfap2c	19634.2945	-2.4195528	0.24599296	-9.8358621	7.89E-23	5.31E-20
Xetrov72001125|Xetrov72001125|t	10361.1977	-1.1203717	0.11691952	-9.5824177	9.48E-22	5.58E-19
Xetrov72029880|Xetrov72029880|krt5.7	14133.0588	-3.2338795	0.3430034	-9.4281266	4.17E-21	2.38E-18
Xetrov72003648|Xetrov72003648|gabpb2	2929.21674	-1.4630621	0.15592068	-9.3833738	6.39E-21	3.25E-18
Xetrov72006138|Xetrov72006138|hes6.1	5062.74555	-2.0035823	0.21578798	-9.2849576	1.62E-20	8.02E-18
Xetrov72034773|Xetrov72034773|dlx5	4175.75298	-3.2005009	0.34550658	-9.2632128	1.98E-20	9.58E-18
Xetrov72020617|Xetrov72020617|ptger4	642.783034	-2.5016414	0.2701446	-9.260379	2.04E-20	9.59E-18
Xetrov72010111|Xetrov72010111|fen1	624.693668	-1.09404	0.11920899	-9.1774955	4.41E-20	1.98E-17
Xetrov72030413|Xetrov72030413|lims1	275.963244	-1.4949254	0.16381315	-9.1257964	7.12E-20	3.05E-17
Xetrov72021606|Xetrov72021606|pnhd	4067.34007	-1.1933357	0.13098126	-9.1107364	8.18E-20	3.37E-17
Xetrov72013649|Xetrov72013649|flvcr2	296.000436	-1.4553308	0.1603956	-9.0733835	1.15E-19	4.62E-17
Xetrov72001392|Xetrov72001392|vash2	50.94414	-3.0953339	0.34369609	-9.0060201	2.14E-19	8.05E-17
Xetrov72021834|Xetrov72021834|gas1	1522.48967	-1.4220697	0.15831478	-8.9825454	2.65E-19	9.77E-17
Xetrov72010328|Xetrov72010328|sertad4	46.8974603	-2.7077767	0.30342787	-8.9239552	4.50E-19	1.60E-16
Xetrov72026742|Xetrov72026742|tmem45b	442.137592	-2.2791776	0.25854747	-8.8153157	1.19E-18	4.01E-16
Xetrov72034152|Xetrov72034152|evx1	715.148804	-3.6292978	0.4127731	-8.7924766	1.46E-18	4.83E-16
Xetrov72021366|Xetrov72021366|slc35d2	207.866371	-2.4646737	0.28109301	-8.7681786	1.82E-18	5.80E-16
Xetrov72000818|Xetrov72000818|sptlc3	244.043796	-2.8285836	0.33421849	-8.4632768	2.60E-17	7.62E-15
Xetrov72034934|Xetrov72034934|bambi	10747.8423	-2.089403	0.24821802	-8.4176123	3.84E-17	1.08E-14
Xetrov72016951|Xetrov72016951|krt12	5289.6775	-2.848162	0.33980538	-8.3817449	5.21E-17	1.42E-14
Xetrov72003469|Xetrov72003469|bspry	935.410782	-3.7295315	0.44835851	-8.3181904	8.93E-17	2.37E-14
Xetrov72029688|Xetrov72029688|grhl3	10042.85	-2.2713323	0.27325222	-8.3122189	9.39E-17	2.42E-14
Xetrov72002596|Xetrov72002596	24.118979	-4.3187106	0.52189559	-8.2750471	1.28E-16	3.22E-14
Xetrov72014027|Xetrov72014027|rnf128	446.025617	-1.33401	0.16246123	-8.2112514	2.19E-16	5.29E-14
Xetrov72018107|Xetrov72018107|krt	27308.9286	-3.0530329	0.37191133	-8.2090344	2.23E-16	5.32E-14
Xetrov72021147|Xetrov72021147|smad7	601.228621	-2.1147325	0.25806392	-8.1946075	2.51E-16	5.87E-14
Xetrov72000684|Xetrov72000684|grhl1	797.986212	-2.8792759	0.35138555	-8.1940645	2.53E-16	5.87E-14
Xetrov72039865|Xetrov72039865|msx2	1215.026	-3.1354959	0.38420999	-8.1608911	3.33E-16	7.55E-14
Xetrov72014892|Xetrov72014892|vgll1	118.404477	-3.3110689	0.40649476	-8.1454159	3.78E-16	8.47E-14
Xetrov72006474|Xetrov72006474|ap1s3	360.873847	-2.433596	0.30154749	-8.0703575	7.01E-16	1.55E-13
Xetrov72007776|Xetrov72007776	455.410174	-2.3450351	0.29436176	-7.9665072	1.63E-15	3.38E-13
Xetrov72029606|Xetrov72029606|elf1	775.491221	-2.7961167	0.35106462	-7.9646783	1.66E-15	3.39E-13
Xetrov72020426|Xetrov72020426|ugt3a2	2898.80478	-3.1970663	0.40435349	-7.9066123	2.64E-15	5.14E-13
Xetrov72018069|Xetrov72018069|syngr2	38.0497923	-2.5969331	0.32952265	-7.8808941	3.25E-15	6.13E-13
Xetrov72032929|Xetrov72032929	42.4620483	-3.5340749	0.44844139	-7.8807956	3.25E-15	6.13E-13
Xetrov72016136|Xetrov72016136|lonrf3	40.6879124	-2.2881028	0.29051759	-7.8759528	3.38E-15	6.24E-13
Xetrov72020138|Xetrov72020138|fzd10	2576.83921	-2.4773296	0.31460397	-7.8744383	3.42E-15	6.26E-13
Xetrov72010707|Xetrov72010707|mob2.1	807.214381	-1.1650844	0.14836742	-7.8526972	4.07E-15	7.37E-13
Xetrov72008577|Xetrov72008577|aldh1l1	1160.44215	-2.8583889	0.36408019	-7.8509871	4.13E-15	7.40E-13
Xetrov72034292|Xetrov72034292|fam83a	26.4668582	-2.9940369	0.38250989	-7.8273451	4.98E-15	8.85E-13
Xetrov72039646|Xetrov72039646|c5orf15	647.127872	-2.0419136	0.26096044	-7.8246094	5.09E-15	8.96E-13
Xetrov72000591|Xetrov72000591|dll1	3540.39719	-1.3686321	0.17594793	-7.7786198	7.33E-15	1.26E-12
Xetrov72034061|Xetrov72034061|sp8	547.091631	-1.9309363	0.24935708	-7.7436595	9.66E-15	1.60E-12
Xetrov72043369|Xetrov72043369	134.572151	-2.2848291	0.2957921	-7.7244424	1.12E-14	1.82E-12
Xetrov72009488|Xetrov72009488|slc7a5	1795.90189	-2.1061969	0.27497196	-7.6596787	1.86E-14	2.93E-12
Xetrov72036251|Xetrov72036251	176.594703	-2.3497206	0.30685391	-7.6574569	1.90E-14	2.95E-12
Xetrov72021417|Xetrov72021417|xbp1	13119.5848	-1.618897	0.21156784	-7.6519047	1.98E-14	3.06E-12
Xetrov72041369|Xetrov72041369	23.9388601	-2.5417954	0.33271419	-7.6395761	2.18E-14	3.34E-12
Xetrov72038483|Xetrov72038483|rasef	560.788449	-1.7064663	0.22358568	-7.6322701	2.31E-14	3.48E-12
Xetrov72010727|Xetrov72010727|cd82	175.6034	-1.6725877	0.21980952	-7.6092596	2.76E-14	4.09E-12
Xetrov72027391|Xetrov72027391|hes3.3	324.888452	-3.4519873	0.45412824	-7.6013491	2.93E-14	4.28E-12

Xetrov72033670|Xetrov72033670|fzd6	522.400716	-3.053496	0.40475499	-7.5440602	4.56E-14	6.45E-12
Xetrov72041367|Xetrov72041367|unnamed	204.405448	-3.606461	0.47950304	-7.5212473	5.43E-14	7.49E-12
Xetrov72005915|Xetrov72005915|unnamed	160.897511	-1.7541779	0.23377926	-7.5035654	6.21E-14	8.42E-12
Xetrov72027542|Xetrov72027542|cnfn.1	3712.98222	-1.2289995	0.16440327	-7.4755175	7.69E-14	1.03E-11
Xetrov72003454|Xetrov72003454|unnamed	199.183502	-3.1124158	0.41660041	-7.4709858	7.96E-14	1.06E-11
Xetrov72039732|Xetrov72039732|mespb	1651.86566	-2.123736	0.28633949	-7.4168463	1.20E-13	1.54E-11
Xetrov72038189|Xetrov72038189	1716.45899	-3.0220111	0.40843109	-7.399072	1.37E-13	1.72E-11
Xetrov72034083|Xetrov72034083|cndp1	171.735434	-3.1024213	0.41926855	-7.3996042	1.37E-13	1.72E-11
Xetrov72003455|Xetrov72003455	223.747378	-3.4850678	0.47163378	-7.3893515	1.48E-13	1.82E-11
Xetrov72014283|Xetrov72014283|unnamed	756.398586	-2.1769298	0.29476546	-7.3852948	1.52E-13	1.86E-11
Xetrov72025856|Xetrov72025856|trim29	1131.02178	-2.8602406	0.38766966	-7.3780357	1.61E-13	1.94E-11
Xetrov72009180|Xetrov72009180|faah.2	212.561958	-3.6669277	0.49791329	-7.3645909	1.78E-13	2.12E-11
Xetrov72035022|Xetrov72035022|unnamed	2278.86944	-3.1548437	0.43234327	-7.2970807	2.94E-13	3.32E-11
Xetrov72036159|Xetrov72036159|esrp1	587.1712	-2.2167969	0.3041811	-7.2877534	3.15E-13	3.53E-11
Xetrov72011430|Xetrov72011430|gadd45a	6763.86808	-1.1925523	0.16396255	-7.2733212	3.51E-13	3.91E-11
Xetrov72033063|Xetrov72033063|dsp	3575.60746	-2.8539889	0.39302067	-7.2616763	3.82E-13	4.19E-11
Xetrov72b000175|Xetrov72b000175|c8orf4	178.459729	-2.1865025	0.30233158	-7.2321339	4.75E-13	5.06E-11
Xetrov72032954|Xetrov72032954|unnamed	72.7170569	-1.792399	0.24915475	-7.1939189	6.30E-13	6.52E-11
Xetrov72010954|Xetrov72010954|h1fx	2978.06641	-1.353398	0.18903737	-7.1594202	8.10E-13	8.29E-11
Xetrov72006199|Xetrov72006199|ag1	5233.95287	-3.2404107	0.45414287	-7.1352232	9.66E-13	9.63E-11
Xetrov72025654|Xetrov72025654|neurl	134.365784	-2.1358917	0.30034683	-7.1114176	1.15E-12	1.11E-10
Xetrov72031247|Xetrov72031247|upk1b	9451.28319	-1.3573633	0.19149082	-7.0883992	1.36E-12	1.30E-10
Xetrov72028867|Xetrov72028867|erbb3	260.308001	-2.5835833	0.3656615	-7.0655055	1.60E-12	1.51E-10
Xetrov72011194|Xetrov72011194	94.3039814	-2.3114174	0.32765583	-7.0544065	1.73E-12	1.61E-10
Xetrov72014430|Xetrov72014430|degs3	484.364315	-2.79221	0.39697062	-7.0337949	2.01E-12	1.84E-10
Xetrov72015022|Xetrov72015022|unnamed	241.328565	-2.80811	0.39975727	-7.0245376	2.15E-12	1.94E-10
Xetrov72021940|Xetrov72021940|msx1	1692.37805	-3.3429197	0.47616186	-7.0205532	2.21E-12	1.99E-10
Xetrov72012878|Xetrov72012878|actn1	1442.22368	-1.2209777	0.17399363	-7.0173702	2.26E-12	2.03E-10
Xetrov72036954|Xetrov72036954|vtcn1	232.517754	-3.1767416	0.45370532	-7.0017727	2.53E-12	2.25E-10
Xetrov72038705|Xetrov72038705|slc22a4	1819.08757	-2.371902	0.33891788	-6.9984565	2.59E-12	2.29E-10
Xetrov72000605|Xetrov72000605|dvl3	1128.17809	-1.6623634	0.23785868	-6.9888703	2.77E-12	2.44E-10
Xetrov72012759|Xetrov72012759	449.654175	-2.6927138	0.38587062	-6.9782815	2.99E-12	2.62E-10
Xetrov72029432|Xetrov72029432|ripk4	229.295315	-1.1852523	0.17034717	-6.9578633	3.45E-12	2.98E-10
Xetrov72011734|Xetrov72011734|gata2	14240.8925	-2.0077099	0.28931684	-6.939485	3.94E-12	3.34E-10
Xetrov72029399|Xetrov72029399	164.699097	-3.1112604	0.45196937	-6.8837861	5.83E-12	4.81E-10
Xetrov72002242|Xetrov72002242|tp63	75.407778	-3.6036993	0.52376924	-6.8803188	5.97E-12	4.89E-10
Xetrov72000894|Xetrov72000894|angel2	191.825874	-1.2403275	0.1803505	-6.8773165	6.10E-12	4.97E-10
Xetrov72041412|Xetrov72041412|stard10	1514.45727	-1.9213656	0.27957729	-6.8723951	6.31E-12	5.13E-10
Xetrov72002073|Xetrov72002073|sh3bgrl2	190.363222	-1.2947888	0.18856108	-6.8666811	6.57E-12	5.31E-10
Xetrov72006498|Xetrov72006498	462.798599	-2.7074862	0.39444009	-6.8641253	6.69E-12	5.38E-10
Xetrov72016218|Xetrov72016218|znf534	308.893102	-3.4961195	0.50978903	-6.8579733	6.98E-12	5.60E-10
Xetrov72037027|Xetrov72037027	300.906225	-2.8708911	0.42043903	-6.8283173	8.59E-12	6.77E-10
Xetrov72b000276|Xetrov72b000276|upk3a	4046.74409	-1.028424	0.15088675	-6.8158666	9.37E-12	7.35E-10
Xetrov72006242|Xetrov72006242|msgn1	1268.24626	-3.1936036	0.47278421	-6.7548863	1.43E-11	1.09E-09
Xetrov72015207|Xetrov72015207|unnamed	483.110584	-1.5142652	0.2246911	-6.7393199	1.59E-11	1.20E-09
Xetrov72009072|Xetrov72009072	15803.1008	-1.805583	0.26795851	-6.738293	1.60E-11	1.21E-09
Xetrov72017868|Xetrov72017868|arf1	286.884487	-1.1624839	0.17335324	-6.7058675	2.00E-11	1.49E-09
Xetrov72034932|Xetrov72034932|dlx6	179.687575	-3.1513088	0.47190549	-6.6778389	2.42E-11	1.78E-09
Xetrov72037025|Xetrov72037025|ap1m2	149.664273	-2.6170444	0.39218563	-6.6729737	2.51E-11	1.82E-09
Xetrov72013920|Xetrov72013920	1509.18836	-2.9887093	0.44810474	-6.6696667	2.56E-11	1.86E-09
Xetrov72036953|Xetrov72036953|loc100130701	51.9491319	-2.4047845	0.36119785	-6.6578041	2.78E-11	2.01E-09
Xetrov72019767|Xetrov72019767|tbx3	647.230384	-2.9175032	0.43843819	-6.6543091	2.85E-11	2.03E-09
Xetrov72031403|Xetrov72031403|ndfip2	954.774459	-1.0744679	0.16147687	-6.6540053	2.85E-11	2.03E-09
Xetrov72014952|Xetrov72014952|ttc9b	34.5123348	-2.5299846	0.38055907	-6.6480734	2.97E-11	2.11E-09
Xetrov72005483|Xetrov72005483|sp5	1134.91573	-2.7925804	0.42294736	-6.6026667	4.04E-11	2.83E-09
Xetrov72009247|Xetrov72009247	198.73164	-1.460257	0.22119648	-6.6016286	4.07E-11	2.83E-09
Xetrov72009945|Xetrov72009945|klf17	6557.17254	-1.5191463	0.23184045	-6.5525507	5.66E-11	3.89E-09
PAC:20701767	53.9282227	-3.0863204	0.47151246	-6.5455755	5.93E-11	4.06E-09
Xetrov72031806|Xetrov72031806|mid1ip1	69.5389603	-2.2149619	0.33889841	-6.5357695	6.33E-11	4.32E-09
Xetrov72021223|Xetrov72021223|elovl7	2474.84002	-1.8966731	0.29034719	-6.5324315	6.47E-11	4.40E-09
Xetrov72011200|Xetrov72011200|rnf11	223.896711	-1.0150156	0.15574005	-6.51737	7.16E-11	4.83E-09
Xetrov72043357|Xetrov72043357|pvrl4	105.362368	-2.6733211	0.41096855	-6.5049288	7.77E-11	5.19E-09
Xetrov72017993|Xetrov72017993|fam100b	555.495523	-1.0720334	0.16498245	-6.4978631	8.15E-11	5.42E-09
Xetrov72004308|Xetrov72004308|dip2a	356.147562	-2.2121846	0.34165716	-6.4748668	9.49E-11	6.18E-09
Xetrov72033062|Xetrov72033062|nbeal2	108.865713	-2.4496379	0.37867115	-6.4690377	9.86E-11	6.41E-09
Xetrov72020853|Xetrov72020853|gcnt4	75.8631412	-2.676359	0.41375196	-6.4685107	9.90E-11	6.41E-09
Xetrov72017857|Xetrov72017857|dlx3	83.3390419	-3.0898672	0.47823244	-6.4610155	1.04E-10	6.71E-09
Xetrov72041776|Xetrov72041776|b4galt3	3040.04794	-1.3664548	0.21181305	-6.4512302	1.11E-10	7.13E-09
Xetrov72031776|Xetrov72031776|dynlt3	29.7356669	-3.4630326	0.5382906	-6.4333886	1.25E-10	7.97E-09
Xetrov72005022|Xetrov72005022	744.614948	-2.25216	0.35024647	-6.4302148	1.27E-10	8.08E-09
Xetrov72023029|Xetrov72023029	40.2418167	-2.1322371	0.33222457	-6.4180595	1.38E-10	8.64E-09

Xetrov72005788|Xetrov72005788|hoxd1	3622.56635	-2.1260038	0.33136405	-6.4159157	1.40E-10	8.73E-09
Xetrov72003647|Xetrov72003647|vsig8	279.597059	-3.3671361	0.52688236	-6.3906791	1.65E-10	1.01E-08
Xetrov72031271|Xetrov72031271|tspo	1323.84684	-1.6313268	0.25681779	-6.3520789	2.12E-10	1.28E-08
Xetrov72011760|Xetrov72011760|elovl1	116.061457	-2.091626	0.32941347	-6.3495461	2.16E-10	1.29E-08
Xetrov72008444|Xetrov72008444|rabgap1l	2341.74485	-1.3930242	0.21953294	-6.3453995	2.22E-10	1.32E-08
Xetrov72007505|Xetrov72007505	24.0102656	-2.7169473	0.42823044	-6.3445917	2.23E-10	1.33E-08
Xetrov72029876|Xetrov72029876|mfsd2a	246.389014	-1.5769436	0.24868865	-6.3410354	2.28E-10	1.35E-08
Xetrov72026724|Xetrov72026724|ventx3.2	1047.36615	-2.0642172	0.32754128	-6.3021589	2.94E-10	1.72E-08
Xetrov72000561|Xetrov72000561|myb	1359.23394	-2.6235624	0.41669388	-6.2961386	3.05E-10	1.78E-08
Xetrov72023338|Xetrov72023338|rbm47	295.508042	-1.5326687	0.24390053	-6.283991	3.30E-10	1.91E-08
Xetrov72017537|Xetrov72017537|fam83c	553.879579	-1.872636	0.29820395	-6.2797157	3.39E-10	1.95E-08
Xetrov72025347|Xetrov72025347|xarp	2501.24069	-1.5266759	0.24399632	-6.2569626	3.93E-10	2.21E-08
Xetrov72036708|Xetrov72036708|unnamed	72.5778983	-2.6371931	0.42183798	-6.2516729	4.06E-10	2.28E-08
Xetrov72032154|Xetrov72032154|rhbdl2	87.9962528	-1.9019006	0.30470002	-6.2418789	4.32E-10	2.41E-08
Xetrov72038749|Xetrov72038749|znf703	6842.65123	-1.8625557	0.29885574	-6.2322902	4.60E-10	2.54E-08
Xetrov72036727|Xetrov72036727|unnamed	1334.32182	-2.5931818	0.41633191	-6.2286407	4.70E-10	2.58E-08
Xetrov72026530|Xetrov72026530|anxa4	2380.39643	-1.6167343	0.26000418	-6.218109	5.03E-10	2.75E-08
Xetrov72024531|Xetrov72024531	17.2860794	-3.4319739	0.55310053	-6.2049731	5.47E-10	2.98E-08
Xetrov72027642|Xetrov72027642|LOC733709	385.09188	-2.0742309	0.33514762	-6.1890067	6.05E-10	3.26E-08
Xetrov72026749|Xetrov72026749|ventx1.1	7802.72117	-1.866222	0.30158913	-6.1879618	6.09E-10	3.27E-08
Xetrov72021382|Xetrov72021382|ccno	1106.27724	-2.501505	0.40501996	-6.1762511	6.56E-10	3.50E-08
Xetrov72033689|Xetrov72033689|unnamed	323.470471	-2.1203345	0.34344436	-6.173735	6.67E-10	3.55E-08
Xetrov72029799|Xetrov72029799|sh3d21	301.554601	-2.3676077	0.38422723	-6.1619985	7.18E-10	3.79E-08
Xetrov72003017|Xetrov72003017	162.526732	-1.4018239	0.22798986	-6.1486241	7.82E-10	4.10E-08
Xetrov72010031|Xetrov72010031	362.934617	-2.8191443	0.4585413	-6.1480706	7.84E-10	4.10E-08
Xetrov72029975|Xetrov72029975|bace2	680.594595	-1.098649	0.1788634	-6.1423914	8.13E-10	4.24E-08
Xetrov72026836|Xetrov72026836|ventx1.2	5063.6638	-1.6957189	0.27608843	-6.1419411	8.15E-10	4.24E-08
Xetrov72021876|Xetrov72021876|cldn23	31.9825228	-2.2548324	0.36741062	-6.1370911	8.40E-10	4.35E-08
Xetrov72028704|Xetrov72028704|crybg3	60.7736817	-2.3947301	0.39042879	-6.1335899	8.59E-10	4.43E-08
Xetrov72034304|Xetrov72034304|myc	1597.61551	-1.531999	0.25081721	-6.10803	1.01E-09	5.15E-08
Xetrov72018136|Xetrov72018136|osbpl2	97.2584757	-2.6745814	0.44136082	-6.0598524	1.36E-09	6.81E-08
Xetrov72014664|Xetrov72014664|cdx4	4798.26388	-2.0435662	0.3379107	-6.0476518	1.47E-09	7.28E-08
Xetrov72016646|Xetrov72016646|evpl	1317.98276	-2.6030131	0.43087987	-6.0411573	1.53E-09	7.54E-08
Xetrov72035138|Xetrov72035138|tspan13	344.074001	-2.0214616	0.33501203	-6.033997	1.60E-09	7.85E-08
Xetrov72030272|Xetrov72030272|sp7	195.766034	-2.5008835	0.41465563	-6.0312301	1.63E-09	7.96E-08
Xetrov72020269|Xetrov72020269|ptbp1	4682.3276	-1.1101441	0.18424772	-6.0252798	1.69E-09	8.24E-08
Xetrov72039848|Xetrov72039848|cdx1	2828.90051	-2.2761917	0.37815248	-6.0192432	1.75E-09	8.51E-08
Xetrov72002394|Xetrov72002394|id2	640.944636	-1.973364	0.32843422	-6.0083994	1.87E-09	9.00E-08
Xetrov72021249|Xetrov72021249	99.140883	-1.5385089	0.25633578	-6.0019279	1.95E-09	9.32E-08
Xetrov72021419|Xetrov72021419|ogfod2	1305.84958	-1.4197782	0.23675114	-5.9969226	2.01E-09	9.56E-08
Xetrov72021167|Xetrov72021167|foxi4.1	239.692589	-2.7460185	0.45856673	-5.9882637	2.12E-09	1.00E-07
Xetrov72002567|Xetrov72002567	9.31425622	-3.0938057	0.51684855	-5.9859038	2.15E-09	1.02E-07
Xetrov72025690|Xetrov72025690|znf503	216.455962	-1.6081583	0.26913367	-5.9753144	2.30E-09	1.08E-07
Xetrov72008785|Xetrov72008785	87.7877483	-1.1164125	0.18771415	-5.9474076	2.72E-09	1.27E-07
Xetrov72003657|Xetrov72003657|anxa9	56.7191723	-3.1918578	0.53798496	-5.9329871	2.97E-09	1.38E-07
Xetrov72038568|Xetrov72038568|retsat	324.750713	-1.7292735	0.29151352	-5.9320525	2.99E-09	1.38E-07
Xetrov72010211|Xetrov72010211	14.6376242	-2.757002	0.46490262	-5.9302785	3.02E-09	1.39E-07
Xetrov72027495|Xetrov72027495	52.1821452	-1.7715069	0.29908484	-5.9230916	3.16E-09	1.44E-07
Xetrov72032967|Xetrov72032967	51.1963065	-1.5223734	0.25742629	-5.9138225	3.34E-09	1.52E-07
Xetrov72017053|Xetrov72017053|c20orf151	379.394529	-2.1589957	0.36657908	-5.889577	3.87E-09	1.74E-07
Xetrov72017394|Xetrov72017394|bmp7.1	826.298605	-2.4441722	0.41605268	-5.8746701	4.24E-09	1.89E-07
Xetrov72010329|Xetrov72010329|pim1	3681.20981	-1.1684239	0.19921643	-5.865098	4.49E-09	1.99E-07
Xetrov72029142|Xetrov72029142|sytl2	1224.13678	-2.0682868	0.35282672	-5.862047	4.57E-09	2.02E-07
Xetrov72032891|Xetrov72032891|dscr6	187.293487	-2.9237593	0.50066807	-5.839716	5.23E-09	2.30E-07
Xetrov72041997|Xetrov72041997	12421.0984	-1.4653767	0.25187504	-5.8178718	5.96E-09	2.59E-07
Xetrov72016257|Xetrov72016257|rgl3	618.361454	-2.376732	0.41018207	-5.7943342	6.86E-09	2.93E-07
Xetrov72013268|Xetrov72013268|dlc	4463.34658	-1.7310685	0.29943382	-5.7811389	7.42E-09	3.14E-07
Xetrov72042539|Xetrov72042539|lmo4.2	3328.98562	-2.0358501	0.35219558	-5.7804534	7.45E-09	3.15E-07
Xetrov72005156|Xetrov72005156|slc19a2	71.9357196	-2.6864223	0.4683176	-5.7363258	9.68E-09	4.04E-07
Xetrov72021228|Xetrov72021228|klf2	1162.9176	-1.1691863	0.20386578	-5.7350789	9.75E-09	4.06E-07
Xetrov72028183|Xetrov72028183	34.5028563	-2.1460606	0.37452479	-5.7300896	1.00E-08	4.15E-07
Xetrov72038446|Xetrov72038446|atp6v0a4	24.7761356	-3.2788959	0.57268494	-5.7254795	1.03E-08	4.24E-07
Xetrov72035015|Xetrov72035015|cthrc1	24.19456	-3.0855	0.53958603	-5.7182725	1.08E-08	4.40E-07
Xetrov72002680|Xetrov72002680	560.900171	-1.561608	0.27361995	-5.7072153	1.15E-08	4.68E-07
Xetrov72028175|Xetrov72028175|tectb	27.7279234	-2.4074927	0.42187681	-5.7066249	1.15E-08	4.68E-07
Xetrov72016928|Xetrov72016928|jup	3031.19647	-1.0819342	0.18962079	-5.7057781	1.16E-08	4.69E-07
Xetrov72029463|Xetrov72029463|tm9sf2	1152.37742	-1.5380833	0.26959894	-5.705079	1.16E-08	4.69E-07
Xetrov72027234|Xetrov72027234|hes5.1	215.72737	-2.5755863	0.4520264	-5.697867	1.21E-08	4.85E-07
Xetrov72039422|Xetrov72039422|wnt5b	1345.73866	-1.0666168	0.18734778	-5.6932451	1.25E-08	4.95E-07
Xetrov72000620|Xetrov72000620	108.299434	-2.9436676	0.5176991	-5.6860589	1.30E-08	5.15E-07
Xetrov72014474|Xetrov72014474|zfp36	276.227774	-2.3324342	0.41085113	-5.6770786	1.37E-08	5.40E-07

Xetrov72031077|Xetrov72031077|slc25a30	3860.12429	-1.3362725	0.235387	-5.6769171	1.37E-08	5.40E-07
Xetrov72028678|Xetrov72028678|aim1l	97.682044	-2.7190548	0.47980818	-5.6669622	1.45E-08	5.70E-07
Xetrov72010880|Xetrov72010880	843.279295	-1.8748128	0.33316728	-5.6272418	1.83E-08	7.10E-07
Xetrov72030993|Xetrov72030993	21.7070474	-2.8455088	0.50904147	-5.5899351	2.27E-08	8.71E-07
Xetrov72005893|Xetrov72005893	52.9689003	-2.8810241	0.51578059	-5.5857552	2.33E-08	8.87E-07
Xetrov72022102|Xetrov72022102	479.413203	-1.5542199	0.27844895	-5.581705	2.38E-08	9.03E-07
Xetrov72006787|Xetrov72006787	456.908534	-1.8947061	0.34126667	-5.5519812	2.82E-08	1.05E-06
Xetrov72035942|Xetrov72035942|twsg1	167.924763	-1.2944807	0.23355404	-5.542532	2.98E-08	1.10E-06
Xetrov72039030|Xetrov72039030|gata3	1178.16661	-2.5836925	0.46755849	-5.5259236	3.28E-08	1.21E-06
Xetrov72021451|Xetrov72021451|klf3	136.065514	-2.3524105	0.42600214	-5.5220627	3.35E-08	1.23E-06
Xetrov72031167|Xetrov72031167	764.089034	-1.63956	0.29709917	-5.5185612	3.42E-08	1.25E-06
Xetrov72010729|Xetrov72010729|kctd15	1204.73229	-1.2578606	0.22838482	-5.5076365	3.64E-08	1.31E-06
Xetrov72033622|Xetrov72033622|zbtb10	11421.9059	-1.0048466	0.18247729	-5.5066939	3.66E-08	1.32E-06
Xetrov72042851|Xetrov72042851|unnamed	175.434489	-2.8942712	0.52615446	-5.5008014	3.78E-08	1.36E-06
Xetrov72031544|Xetrov72031544|cldn4	8415.9859	-1.1474506	0.20903858	-5.4891811	4.04E-08	1.44E-06
Xetrov72006253|Xetrov72006253|unnamed	300.899204	-2.6665157	0.48677244	-5.4779512	4.30E-08	1.53E-06
Xetrov72040869|Xetrov72040869|helb	30.6831641	-2.0701785	0.37793736	-5.4775702	4.31E-08	1.53E-06
Xetrov72017806|Xetrov72017806|tk1	2798.8855	-1.0867337	0.19889812	-5.4637706	4.66E-08	1.64E-06
Xetrov72042741|Xetrov72042741	7.81840827	-2.6762192	0.49024936	-5.4588939	4.79E-08	1.68E-06
Xetrov72034895|Xetrov72034895|unnamed	176.86995	-2.6388157	0.48512438	-5.4394621	5.34E-08	1.86E-06
Xetrov72038929|Xetrov72038929	33.6745849	-2.6600893	0.48948553	-5.4344596	5.50E-08	1.90E-06
Xetrov72005090|Xetrov72005090|unnamed	155.751752	-1.9556505	0.36010199	-5.430824	5.61E-08	1.93E-06
Xetrov72017671|Xetrov72017671|cant1	766.858075	-1.1725585	0.21595681	-5.4295973	5.65E-08	1.93E-06
Xetrov72039344|Xetrov72039344|dusp6	1907.67554	-1.0871335	0.20060136	-5.4193724	5.98E-08	2.04E-06
Xetrov72038814|Xetrov72038814|tcp11l2	700.845304	-1.1296622	0.20860061	-5.4154309	6.11E-08	2.07E-06
Xetrov72008551|Xetrov72008551|cdh1	1023.60938	-1.7082479	0.31603955	-5.4051713	6.47E-08	2.17E-06
Xetrov72006428|Xetrov72006428|emp2	321.923144	-2.3713852	0.43984981	-5.3913521	6.99E-08	2.34E-06
Xetrov72040736|Xetrov72040736|kitlg	138.875958	-1.9872946	0.36897267	-5.3860211	7.20E-08	2.40E-06
Xetrov72007936|Xetrov72007936	1119.6209	-1.3364894	0.24824852	-5.3836751	7.30E-08	2.42E-06
Xetrov72037995|Xetrov72037995|wdr72	15.2106339	-2.8994632	0.53979585	-5.3714071	7.81E-08	2.57E-06
Xetrov72017393|Xetrov72017393|krt16	7.568057	-2.8381392	0.52844673	-5.3707196	7.84E-08	2.58E-06
Xetrov72039319|Xetrov72039319|inpp5a.2	43.0435233	-1.8421695	0.34334756	-5.36532	8.08E-08	2.65E-06
Xetrov72026559|Xetrov72026559|c1galt1c1	326.08285	-1.5562369	0.29031992	-5.3604206	8.30E-08	2.71E-06
Xetrov72005248|Xetrov72005248|unnamed	253.087191	-2.8238366	0.52781583	-5.3500415	8.79E-08	2.85E-06
Xetrov72034931|Xetrov72034931|psmg2	193.521007	-1.0477782	0.19639118	-5.3351592	9.55E-08	3.07E-06
Xetrov72019117|Xetrov72019117|tdrd7	1200.8732	-1.2551826	0.23556825	-5.3283184	9.91E-08	3.18E-06
Xetrov72004255|Xetrov72004255|ppl	1000.49575	-1.7490747	0.32928926	-5.3116666	1.09E-07	3.43E-06
Xetrov72004826|Xetrov72004826|cd2ap	129.69019	-1.4601462	0.27501097	-5.3094106	1.10E-07	3.47E-06
Xetrov72018443|Xetrov72018443|mfsd6l	145.776927	-1.3835293	0.26065337	-5.307928	1.11E-07	3.49E-06
Xetrov72011709|Xetrov72011709	78.8313671	-1.2289832	0.23289171	-5.2770585	1.31E-07	4.05E-06
Xetrov72014957|Xetrov72014957|neurog2	349.616433	-1.7419917	0.33042478	-5.2719767	1.35E-07	4.15E-06
Xetrov72b000232|Xetrov72b000232|atp6v1g3	16.6226673	-2.7246145	0.51757562	-5.2641863	1.41E-07	4.32E-06
Xetrov72036480|Xetrov72036480|prss8	682.247558	-1.5176125	0.28899243	-5.2513918	1.51E-07	4.60E-06
Xetrov72038246|Xetrov72038246|fes	118.453892	-1.4356032	0.27421398	-5.2353392	1.65E-07	4.99E-06
Xetrov72012797|Xetrov72012797	137.85826	-1.9652911	0.37646369	-5.2204001	1.79E-07	5.37E-06
Xetrov72038789|Xetrov72038789	1751.37009	-1.5582389	0.30198151	-5.1600474	2.47E-07	7.19E-06
Xetrov72005256|Xetrov72005256|tuba3e	1634.80287	-2.5629331	0.49669228	-5.1600019	2.47E-07	7.19E-06
Xetrov72026860|Xetrov72026860|unnamed	38.8372702	-2.3232235	0.45028717	-5.1594264	2.48E-07	7.20E-06
Xetrov72000636|Xetrov72000636|tab2	159.336781	-1.0289133	0.1996684	-5.1531105	2.56E-07	7.42E-06
Xetrov72028104|Xetrov72028104|cdknx	783.009872	-1.9243668	0.37550113	-5.1247963	2.98E-07	8.51E-06
Xetrov72021245|Xetrov72021245|lef1	432.975112	-1.2915931	0.25262037	-5.1127831	3.17E-07	9.05E-06
Xetrov72043445|Xetrov72043445	98.6653508	-1.9021716	0.37680626	-5.0481422	4.46E-07	1.24E-05
Xetrov72033177|Xetrov72033177|mst1r	2756.44992	-1.2761562	0.25280713	-5.0479438	4.47E-07	1.24E-05
Xetrov72007537|Xetrov72007537	15.5405702	-2.4355813	0.48671593	-5.0041125	5.61E-07	1.53E-05
Xetrov72031288|Xetrov72031288|cdx2	3771.5127	-1.9375897	0.38724678	-5.0035012	5.63E-07	1.53E-05
Xetrov72028213|Xetrov72028213	104.54194	-1.4386516	0.28837968	-4.9887414	6.08E-07	1.64E-05
Xetrov72023161|Xetrov72023161|cetn1	725.512991	-1.8840065	0.37879667	-4.9736618	6.57E-07	1.76E-05
Xetrov72000867|Xetrov72000867|slc33a1	365.710525	-1.4606795	0.29383522	-4.971084	6.66E-07	1.77E-05
Xetrov72036422|Xetrov72036422	55.7067852	-1.5543404	0.31428028	-4.9457139	7.59E-07	1.98E-05
Xetrov72002931|Xetrov72002931	16.7426685	-2.4039655	0.48865786	-4.9195269	8.68E-07	2.24E-05
Xetrov72039789|Xetrov72039789|szl	1568.5382	-1.9880929	0.40447603	-4.9152305	8.87E-07	2.28E-05
Xetrov72023840|Xetrov72023840|acsl1	460.521297	-1.0866016	0.22115609	-4.9132791	8.96E-07	2.30E-05
Xetrov72038071|Xetrov72038071|kiaa1324l	1847.86491	-1.979406	0.40293762	-4.9124377	9.00E-07	2.30E-05
Xetrov72024265|Xetrov72024265	197.803025	-2.0300074	0.4135434	-4.9088134	9.16E-07	2.34E-05
Xetrov72006150|Xetrov72006150|arl6ip1	199.768913	-1.2656408	0.25788921	-4.9076918	9.22E-07	2.35E-05
Xetrov72031615|Xetrov72031615|upk3b	3420.5296	-1.0695134	0.21811171	-4.903512	9.41E-07	2.39E-05
Xetrov72019175|Xetrov72019175|rnf31	224.877723	-1.2839663	0.26186828	-4.9030997	9.43E-07	2.39E-05
Xetrov72006165|Xetrov72006165|pdgfa	1085.90219	-1.4000484	0.28682471	-4.8811988	1.05E-06	2.65E-05
Xetrov72005942|Xetrov72005942|slc9a3r2	20.4819578	-2.4148484	0.49649401	-4.8638017	1.15E-06	2.87E-05
Xetrov72026612|Xetrov72026612|hmx3	61.9124328	-2.4664482	0.5084446	-4.8509675	1.23E-06	3.03E-05
Xetrov72043331|Xetrov72043331	7785.68887	-1.2431438	0.25630834	-4.8501887	1.23E-06	3.03E-05

Xetrov72036736|Xetrov72036736	15.8141961	-2.6867891	0.55439423	-4.8463512	1.26E-06	3.08E-05
Xetrov72009545|Xetrov72009545|spata1	83.5038516	-1.9120951	0.39499142	-4.8408523	1.29E-06	3.16E-05
Xetrov72026423|Xetrov72026423|gnb3	3036.42989	-1.590959	0.32974339	-4.8248399	1.40E-06	3.41E-05
Xetrov72016429|Xetrov72016429	699.510248	-1.5515739	0.32251685	-4.8108305	1.50E-06	3.63E-05
Xetrov72039534|Xetrov72039534|cdc123	109.804596	-1.4184287	0.29502971	-4.8077486	1.53E-06	3.68E-05
Xetrov72005612|Xetrov72005612|gbx2.2	646.040627	-2.4207419	0.50589494	-4.7850684	1.71E-06	4.07E-05
Xetrov72016406|Xetrov72016406|rab25	214.280943	-2.7098978	0.56800898	-4.7708714	1.83E-06	4.35E-05
Xetrov72015217|Xetrov72015217	349.592898	-1.6319106	0.34233728	-4.7669671	1.87E-06	4.41E-05
Xetrov72033128|Xetrov72033128|rreb1	4266.5078	-1.0631651	0.22320323	-4.7632156	1.91E-06	4.49E-05
Xetrov72025906|Xetrov72025906|atp6v1b1	33.921292	-2.4296498	0.51126793	-4.7522046	2.01E-06	4.71E-05
Xetrov72028370|Xetrov72028370	1259.92922	-1.6672597	0.35101782	-4.7497864	2.04E-06	4.76E-05
Xetrov72017250|Xetrov72017250|foxj1	1130.67482	-1.8067723	0.38087264	-4.7437702	2.10E-06	4.89E-05
Xetrov72001031|Xetrov72001031	561.666083	-1.4904048	0.31422612	-4.7430963	2.10E-06	4.90E-05
Xetrov72027641|Xetrov72027641	45.2165046	-1.2772465	0.27063969	-4.7193615	2.37E-06	5.40E-05
Xetrov72b000199|Xetrov72b000199|efna4	42.6330504	-1.1938068	0.25329003	-4.7132011	2.44E-06	5.55E-05
Xetrov72006270|Xetrov72006270	1870.19027	-1.0731827	0.22833463	-4.7000434	2.60E-06	5.89E-05
Xetrov72028552|Xetrov72028552	49.9454728	-1.6807835	0.35793162	-4.6958229	2.66E-06	5.99E-05
Xetrov72041631|Xetrov72041631|shroom4	903.136572	-1.4068206	0.2997871	-4.6927324	2.70E-06	6.07E-05
Xetrov72042825|Xetrov72042825	6.82186979	-2.7166531	0.57953377	-4.6876528	2.76E-06	6.19E-05
Xetrov72010384|Xetrov72010384	6.4498804	-2.5849738	0.55142518	-4.6878052	2.76E-06	6.19E-05
Xetrov72026036|Xetrov72026036|tead4	1268.38776	-1.0513598	0.22513958	-4.6698131	3.01E-06	6.65E-05
Xetrov72020681|Xetrov72020681|mknk2	2593.33121	-1.0380466	0.22249221	-4.6655414	3.08E-06	6.75E-05
Xetrov72013461|Xetrov72013461|sptlc2	438.502643	-1.5315214	0.32840026	-4.6635815	3.11E-06	6.80E-05
Xetrov72022451|Xetrov72022451|mad2l1	103.497695	-1.034233	0.22206627	-4.657317	3.20E-06	6.98E-05
Xetrov72027411|Xetrov72027411|hes9.1	176.889961	-1.8374491	0.39537913	-4.6473094	3.36E-06	7.30E-05
Xetrov72043598|Xetrov72043598	395.097802	-1.9550702	0.42161217	-4.6371294	3.53E-06	7.64E-05
Xetrov72000077|Xetrov72000077|greb1	250.353747	-2.2314511	0.48230904	-4.6266001	3.72E-06	7.97E-05
Xetrov72034068|Xetrov72034068	6634.52398	-1.3416418	0.29005587	-4.6254599	3.74E-06	8.01E-05
Xetrov72005843|Xetrov72005843|dlx2	79.9755241	-1.6124449	0.34866099	-4.6246782	3.75E-06	8.03E-05
Xetrov72037468|Xetrov72037468	8.88137403	-2.4190942	0.52626158	-4.5967524	4.29E-06	9.06E-05
Xetrov72043595|Xetrov72043595|eppk1	884.493993	-1.8969756	0.41273262	-4.5961367	4.30E-06	9.08E-05
Xetrov72023052|Xetrov72023052	10.9964405	-2.6199429	0.57093154	-4.5888915	4.46E-06	9.38E-05
Xetrov72017709|Xetrov72017709|lasp1	64.8561646	-1.0323195	0.22579846	-4.5718624	4.83E-06	0.00010125
Xetrov72007013|Xetrov72007013	13.5777856	-1.8329294	0.40163643	-4.5636533	5.03E-06	0.00010474
Xetrov72024698|Xetrov72024698|myo9a	139.461105	-1.1185098	0.24537483	-4.5583723	5.16E-06	0.00010681
Xetrov72003116|Xetrov72003116	77.4429748	-1.2039982	0.26437381	-4.5541507	5.26E-06	0.0001085
Xetrov72042623|Xetrov72042623|capns1	122.679957	-1.7009959	0.37503478	-4.5355682	5.74E-06	0.00011723
Xetrov72025509|Xetrov72025509|acsbg1	16.9462866	-2.1650949	0.47755001	-4.5337552	5.79E-06	0.00011805
Xetrov72040463|Xetrov72040463	87.5933594	-1.1091533	0.24711627	-4.4883863	7.18E-06	0.00014333
Xetrov72036399|Xetrov72036399	115.298378	-1.3668821	0.30478385	-4.4847589	7.30E-06	0.00014523
Xetrov72027607|Xetrov72027607|hes8	447.26319	-2.2933761	0.51199059	-4.4793325	7.49E-06	0.00014805
Xetrov72042371|Xetrov72042371	44.9403679	-1.2416792	0.27791259	-4.4678768	7.90E-06	0.00015467
Xetrov72001947|Xetrov72001947|hspc159	1198.63801	-1.6315286	0.36585589	-4.4594844	8.22E-06	0.00015986
Xetrov72005615|Xetrov72005615|gbx2.1	426.468384	-2.2201405	0.4996048	-4.4437933	8.84E-06	0.00017039
Xetrov72010075|Xetrov72010075	85.9920756	-1.0632147	0.23941385	-4.4409074	8.96E-06	0.00017251
Xetrov72002865|Xetrov72002865|unnamed	16.7907911	-2.052775	0.46447736	-4.4195373	9.89E-06	0.00018742
Xetrov72016298|Xetrov72016298	107.137786	-1.3706212	0.31043929	-4.4151021	1.01E-05	0.00019072
Xetrov72037160|Xetrov72037160|dnajb1	121.926485	-1.8268954	0.41436559	-4.4088974	1.04E-05	0.00019529
Xetrov72029943|Xetrov72029943|krt8	6825.7542	-1.2494493	0.28480699	-4.3870036	1.15E-05	0.00021262
Xetrov72007047|Xetrov72007047	91.3633853	-2.5398989	0.57919545	-4.385219	1.16E-05	0.00021353
Xetrov72017754|Xetrov72017754|hoxb4	74.3499476	-2.2843102	0.52175713	-4.3781102	1.20E-05	0.00021975
Xetrov72026284|Xetrov72026284	19.882441	-1.8907947	0.43192464	-4.3776031	1.20E-05	0.00022005
Xetrov72027308|Xetrov72027308|upk2	4718.48612	-1.1907971	0.27235201	-4.372272	1.23E-05	0.00022484
Xetrov72035506|Xetrov72035506|c7orf44	38.8721624	-1.0586733	0.2422793	-4.3696399	1.24E-05	0.00022734
Xetrov72043196|Xetrov72043196|cdh26	589.183119	-1.3906694	0.31922489	-4.3563941	1.32E-05	0.00024084
Xetrov72010982|Xetrov72010982|tmed10	325.354775	-1.6165907	0.37167547	-4.3494683	1.36E-05	0.0002469
Xetrov72020305|Xetrov72020305|slc45a3	18.2583329	-2.4197232	0.55663404	-4.3470629	1.38E-05	0.00024938
Xetrov72014526|Xetrov72014526|tmem164	942.390786	-1.1764737	0.27102946	-4.3407594	1.42E-05	0.00025616
Xetrov72005251|Xetrov72005251|tuba1a	1469.78343	-2.4154973	0.55720765	-4.3350038	1.46E-05	0.00026195
Xetrov72032084|Xetrov72032084	145.455725	-1.688873	0.38982564	-4.3323806	1.48E-05	0.00026484
Xetrov72017911|Xetrov72017911	8.17692568	-2.2989833	0.53204109	-4.3210635	1.55E-05	0.00027694
Xetrov72043395|Xetrov72043395	563.512013	-1.7989672	0.41656588	-4.318566	1.57E-05	0.0002793
Xetrov72026516|Xetrov72026516|oaf	379.504929	-1.0464644	0.24247113	-4.3158308	1.59E-05	0.00028225
Xetrov72025964|Xetrov72025964|wrap73	224.275432	-2.1602445	0.50119258	-4.3102084	1.63E-05	0.00028844
Xetrov72012057|Xetrov72012057	12.3186131	-1.8378066	0.42693619	-4.3046401	1.67E-05	0.00029496
Xetrov72034353|Xetrov72034353|unnamed	177.783181	-1.4411398	0.33500746	-4.301814	1.69E-05	0.00029761
Xetrov72016659|Xetrov72016659|fer1l4	292.444191	-1.5866804	0.37041618	-4.2835073	1.84E-05	0.00031905
Xetrov72007370|Xetrov72007370|sdc1	64.3159034	-1.2339456	0.28923355	-4.2662604	1.99E-05	0.00034125
Xetrov72021202|Xetrov72021202	1136.07589	-2.5250156	0.59249954	-4.2616331	2.03E-05	0.00034747
Xetrov72020505|Xetrov72020505|foxn4	562.80467	-2.0476678	0.4806057	-4.2605983	2.04E-05	0.00034845
Xetrov72042742|Xetrov72042742|zbtb7b	18.9326554	-2.0878991	0.49075488	-4.2544643	2.10E-05	0.0003562

Xetrov72040867|Xetrov72040867|mesp2	3.86725544	-2.4759933	0.58360758	-4.2425653	2.21E-05	0.00037405
Xetrov72004891|Xetrov72004891|map3k2	174.653619	-1.1465914	0.27059836	-4.2372444	2.26E-05	0.00038188
Xetrov72014783|Xetrov72014783|gch1	502.753809	-2.2088918	0.52203102	-4.231342	2.32E-05	0.00039099
Xetrov72019728|Xetrov72019728|gas2l1	358.491435	-1.032794	0.24489629	-4.217271	2.47E-05	0.00041397
Xetrov72042612|Xetrov72042612|foxh1	1947.6299	-1.0964964	0.26134471	-4.1955945	2.72E-05	0.00045082
Xetrov72017277|Xetrov72017277|unnamed	24.6635422	-1.9736666	0.47240605	-4.1779028	2.94E-05	0.00048142
Xetrov72017287|Xetrov72017287|ubp1	209.193968	-2.4197583	0.57949205	-4.1756541	2.97E-05	0.00048536
Xetrov72016724|Xetrov72016724|erbb2	639.050035	-1.4464019	0.34655875	-4.1736125	3.00E-05	0.0004893
Xetrov72017684|Xetrov72017684|afmid	10.1086506	-2.1907648	0.52545042	-4.1693083	3.06E-05	0.00049734
Xetrov72042628|Xetrov72042628	43.6067684	-1.9030956	0.45665031	-4.1675119	3.08E-05	0.00050041
Xetrov72028521|Xetrov72028521|unnamed	282.917822	-1.1508118	0.27625557	-4.1657505	3.10E-05	0.00050299
Xetrov72027644|Xetrov72027644|c15orf17	23.2636728	-1.6168599	0.38903431	-4.1560855	3.24E-05	0.00052249
Xetrov72009964|Xetrov72009964|elavl4	33.9431522	-1.864905	0.44945701	-4.14924	3.34E-05	0.00053469
Xetrov72035937|Xetrov72035937|unnamed	54.5802764	-1.8208167	0.43923006	-4.1454737	3.39E-05	0.00054126
Xetrov72013484|Xetrov72013484|syt16	81.4137359	-1.9488809	0.47026965	-4.1441774	3.41E-05	0.00054387
Xetrov72034338|Xetrov72034338|fam69c	30.9733092	-2.1059529	0.5096816	-4.1318991	3.60E-05	0.00056942
Xetrov72024328|Xetrov72024328|emx1.2	15.5950809	-2.067338	0.50083302	-4.127799	3.66E-05	0.00057792
Xetrov72017932|Xetrov72017932|eif1	4577.7467	-1.1651649	0.28282671	-4.1197131	3.79E-05	0.00059339
Xetrov72035701|Xetrov72035701	15.163566	-2.2575128	0.54833853	-4.1170056	3.84E-05	0.00059831
Xetrov72035876|Xetrov72035876|unnamed	172.682997	-1.7525895	0.4262245	-4.1118929	3.92E-05	0.00060881
Xetrov72036556|Xetrov72036556|fzd3	673.843662	-1.2020959	0.29305889	-4.1018921	4.10E-05	0.00063339
Xetrov72018129|Xetrov72018129|slc25a19	97.9760989	-1.4326051	0.34933875	-4.1009053	4.12E-05	0.00063532
Xetrov72005689|Xetrov72005689	6.29568802	-2.1547605	0.52675295	-4.0906472	4.30E-05	0.00065922
Xetrov72002283|Xetrov72002283	6.30548862	-2.3346075	0.57097555	-4.0888046	4.34E-05	0.0006634
Xetrov72b000086|Xetrov72b000086	303.411154	-1.4267789	0.34937813	-4.083767	4.43E-05	0.00067631
Xetrov72026791|Xetrov72026791|elovl3	12.0095004	-2.1049331	0.51640065	-4.0761627	4.58E-05	0.00069598
Xetrov72006613|Xetrov72006613|unnamed	83.1662673	-2.4072741	0.59247166	-4.0631042	4.84E-05	0.00072729
Xetrov72001200|Xetrov72001200|fam82a1	37.08796	-1.0022405	0.24796032	-4.0419392	5.30E-05	0.00078615
Xetrov72012075|Xetrov72012075	52.3289613	-1.4476216	0.35826602	-4.0406332	5.33E-05	0.00078992
Xetrov72021445|Xetrov72021445|gmpr2	48.5965897	-1.6266349	0.40303079	-4.0360065	5.44E-05	0.00080312
Xetrov72005926|Xetrov72005926|hagh	44.6461708	-1.0634242	0.26414152	-4.025964	5.67E-05	0.00083556
Xetrov72000541|Xetrov72000541|capn13	528.523884	-1.6611476	0.41572556	-3.9957792	6.45E-05	0.00093276
Xetrov72036576|Xetrov72036576|unnamed	82.7448221	-2.3470132	0.58833942	-3.9892162	6.63E-05	0.00095527
Xetrov72001957|Xetrov72001957|fam177b	17.5386253	-1.3252624	0.33240098	-3.9869388	6.69E-05	0.00096228
Xetrov72004305|Xetrov72004305|col18a1	3859.48501	-1.2641107	0.3176306	-3.9798139	6.90E-05	0.00098481
Xetrov72029630|Xetrov72029630	642.962226	-1.1096351	0.27901793	-3.9769312	6.98E-05	0.00099249
Xetrov72019280|Xetrov72019280|kit	1481.28459	-1.6983079	0.42726886	-3.9747992	7.04E-05	0.00099976
Xetrov72008632|Xetrov72008632|kifc3	757.587246	-1.0126647	0.25477169	-3.9747929	7.04E-05	0.00099976
Xetrov72033472|Xetrov72033472|vill	100.811312	-2.3055969	0.58033828	-3.97285	7.10E-05	0.00100341
Xetrov72026535|Xetrov72026535|slc25a16	322.635297	-1.0976154	0.27712376	-3.960741	7.47E-05	0.00104627
Xetrov72016351|Xetrov72016351	2.32444472	-2.3289348	0.5887556	-3.9556903	7.63E-05	0.00106624
Xetrov72020061|Xetrov72020061|epb41l4a	75.4212235	-1.3653144	0.34675942	-3.9373535	8.24E-05	0.00114091
Xetrov72040856|Xetrov72040856	11.3265538	-1.7610462	0.44751529	-3.9351643	8.31E-05	0.00114912
Xetrov72020429|Xetrov72020429|lpcat4	298.585928	-1.4802601	0.37622536	-3.9345037	8.34E-05	0.00115031
Xetrov72027545|Xetrov72027545	6.12144164	-2.3211894	0.59053256	-3.9306712	8.47E-05	0.00116368
Xetrov72027174|Xetrov72027174|c1orf93	224.218089	-1.002099	0.25721811	-3.8959117	9.78E-05	0.00131328
Xetrov72038242|Xetrov72038242|cnnm3	278.499404	-1.1052488	0.28431919	-3.8873519	0.00010134	0.00135465
Xetrov72036687|Xetrov72036687|cyp2a13	161.424582	-1.4891161	0.38402265	-3.8776778	0.00010546	0.00140268
Xetrov72030691|Xetrov72030691|p2ry2	760.048438	-1.0707481	0.27628642	-3.8755001	0.00010641	0.00141329
Xetrov72039181|Xetrov72039181|epb49	8.74171971	-1.6984689	0.43929168	-3.8663808	0.00011046	0.00145588
Xetrov72010708|Xetrov72010708|pmm2	2772.06359	-1.1639381	0.3010307	-3.8665095	0.0001104	0.00145588
Xetrov72011932|Xetrov72011932|slc22a20	5.45603346	-2.2039297	0.57054721	-3.862835	0.00011208	0.00147203
Xetrov72023912|Xetrov72023912|s1pr3	11.3255105	-1.8873279	0.48965707	-3.8543872	0.00011602	0.00151429
Xetrov72042153|Xetrov72042153	48.5512363	-1.6182291	0.41992352	-3.8536282	0.00011638	0.00151794
Xetrov72010968|Xetrov72010968|tnni2	35.6289407	-1.3222659	0.34317772	-3.8530063	0.00011668	0.00152075
Xetrov72020621|Xetrov72020621|mmp11	41.5404928	-2.0206473	0.52542849	-3.8457131	0.0001202	0.00155701
Xetrov72007986|Xetrov72007986	107.705314	-1.1165919	0.29072374	-3.8407319	0.00012267	0.00158242
Xetrov72010303|Xetrov72010303	29.6649213	-2.1369973	0.55808231	-3.8291794	0.00012857	0.00164841
Xetrov72016215|Xetrov72016215|lgals3	1188.57297	-1.0589802	0.27675443	-3.8264252	0.00013002	0.00166427
Xetrov72018434|Xetrov72018434	21.1979893	-1.7294804	0.45288968	-3.8187675	0.00013412	0.00170677
Xetrov72027085|Xetrov72027085|scn3b	10.2055255	-2.0260263	0.53166956	-3.8106871	0.00013858	0.00175593
Xetrov72038842|Xetrov72038842|atp6v1b2	499.097398	-1.1287513	0.29745029	-3.794756	0.00014779	0.00185687
Xetrov72018725|Xetrov72018725|myo5b	829.480741	-1.3800207	0.3638855	-3.7924587	0.00014916	0.00187164
Xetrov72037045|Xetrov72037045	27.2137305	-1.3241925	0.34929866	-3.7910037	0.00015004	0.00187889
Xetrov72017187|Xetrov72017187|cpne1	753.194339	-1.0103776	0.26668155	-3.7887045	0.00015143	0.00188882
Xetrov72006244|Xetrov72006244|unnamed	12.831364	-1.7278149	0.45691705	-3.7814629	0.00015591	0.0019395
Xetrov72005792|Xetrov72005792|hoxd13	10.3969025	-1.9516237	0.5174106	-3.7719052	0.00016201	0.00199846
Xetrov72035352|Xetrov72035352|frat1	7.86336347	-1.6240353	0.43148374	-3.7638389	0.00016732	0.00204759
Xetrov72003666|Xetrov72003666|golph3l	953.780306	-1.1128105	0.29603738	-3.7590203	0.00017058	0.00208212
Xetrov72027478|Xetrov72027478|esr10	113.670398	-1.3933419	0.37161709	-3.7494021	0.00017726	0.00215106
Xetrov72005493|Xetrov72005493|foxj1.2	233.427702	-2.1918007	0.58468883	-3.7486618	0.00017778	0.00215364

Xetrov72017641|Xetrov72017641|hoxb1	25.2544748	-2.1501451	0.574244	-3.7443058	0.00018089	0.00218394
Xetrov72b000108|Xetrov72b000108|agr2	262.488026	-1.8154699	0.48756286	-3.7235607	0.00019643	0.00233267
Xetrov72019210|Xetrov72019210|kiaa1324	468.704476	-1.7045764	0.45965899	-3.70835	0.00020861	0.00244648
Xetrov72008965|Xetrov72008965|irak2	22.6940515	-1.725796	0.46579015	-3.7050934	0.00021131	0.00247504
Xetrov72026079|Xetrov72026079|sgms1	1696.50786	-1.2651899	0.34171921	-3.7024256	0.00021355	0.00249656
Xetrov72032066|Xetrov72032066	13876.0566	-1.0096035	0.27482035	-3.6736854	0.00023908	0.00275529
Xetrov72028093|Xetrov72028093|unnamed	31.1674755	-1.9706475	0.53777793	-3.6644261	0.00024789	0.00284338
Xetrov72037807|Xetrov72037807|cep152	1036.29006	-1.1708904	0.31960191	-3.6635903	0.0002487	0.00285094
Xetrov72014018|Xetrov72014018|nr6a1	4404.28454	-1.3989929	0.38221945	-3.6601823	0.00025204	0.00288314
Xetrov72018222|Xetrov72018222	32.3736698	-1.0278242	0.28136428	-3.6530018	0.00025919	0.00295856
Xetrov72024689|Xetrov72024689	181.689262	-2.1655799	0.59314824	-3.6509927	0.00026123	0.0029782
Xetrov72012134|Xetrov72012134	18.1897118	-1.3506193	0.3712957	-3.6375839	0.00027521	0.00311205
Xetrov72025319|Xetrov72025319|gbp1	17.1009511	-1.1806493	0.32472896	-3.6357991	0.00027712	0.00313094
Xetrov72017884|Xetrov72017884|myl9	61.5035713	-1.0869997	0.29904692	-3.6348802	0.00027811	0.00314024
Xetrov72003655|Xetrov72003655|creb3l4	208.004514	-2.1680891	0.59676204	-3.6330882	0.00028005	0.00315646
Xetrov72017538|Xetrov72017538	386.046581	-1.3695071	0.37704864	-3.6321763	0.00028104	0.00316575
Xetrov72013135|Xetrov72013135|hsp90aa1.2	10.4892096	-1.9358006	0.53367578	-3.6272972	0.0002864	0.00321653
Xetrov72026858|Xetrov72026858|unnamed	5.2737444	-2.1424065	0.59433482	-3.604713	0.0003125	0.00345196
Xetrov72042530|Xetrov72042530	34.5134593	-2.0553817	0.57127828	-3.5978642	0.00032084	0.00352345
Xetrov72031134|Xetrov72031134|phox2a	87.0717936	-1.0142916	0.28206234	-3.5959837	0.00032317	0.00354487
Xetrov72010856|Xetrov72010856|fam3a	977.258726	-1.3615958	0.38052858	-3.5781697	0.00034601	0.00375172
Xetrov72038238|Xetrov72038238|fam13b	173.819992	-1.0003036	0.27992701	-3.5734446	0.00035232	0.00381132
Xetrov72018433|Xetrov72018433	6810.38546	-1.3313888	0.37308944	-3.5685512	0.00035896	0.00387078
Xetrov72017707|Xetrov72017707|hoxb5	11.1957687	-2.0693524	0.58149828	-3.5586561	0.00037276	0.0039844
Xetrov72013752|Xetrov72013752|znf329	108.32329	-1.4751373	0.41803786	-3.528717	0.00041758	0.00438878
Xetrov72006674|Xetrov72006674|chpf	270.260241	-1.2042932	0.34136847	-3.5278396	0.00041897	0.00440089
Xetrov72042984|Xetrov72042984|fblim1	61.2975022	-1.5971725	0.45345673	-3.5222158	0.00042796	0.00447962
Xetrov72001104|Xetrov72001104|pdia6	1343.60554	-1.0277666	0.2924658	-3.5141428	0.00044118	0.00458054
Xetrov72036913|Xetrov72036913|hs3st3a1	171.318817	-1.3048033	0.37139915	-3.5132103	0.00044273	0.00459411
Xetrov72021872|Xetrov72021872|slc25a22	205.098072	-1.3860706	0.39455847	-3.5129662	0.00044313	0.00459581
Xetrov72020174|Xetrov72020174|slain2	336.832377	-1.068072	0.30445506	-3.5081433	0.00045125	0.00466965
Xetrov72023443|Xetrov72023443|camk1g	11.6850162	-1.5059436	0.42965669	-3.5049927	0.00045662	0.00471232
Xetrov72012756|Xetrov72012756|iqsec2	54.30814	-1.2741915	0.36449358	-3.4957858	0.00047267	0.00484871
Xetrov72020878|Xetrov72020878|gcnt1	78.2504035	-1.0866101	0.31111835	-3.4925942	0.00047835	0.00489587
Xetrov72011491|Xetrov72011491	208.695902	-1.2246581	0.35078483	-3.4911946	0.00048087	0.00491674
Xetrov72016080|Xetrov72016080	363.765167	-1.2762017	0.36559029	-3.4907976	0.00048158	0.00492137
Xetrov72041478|Xetrov72041478|tfcp2l1	376.735999	-1.4410543	0.41520538	-3.4707025	0.0005191	0.0052422
Xetrov72037659|Xetrov72037659|trpv6	12.6914415	-1.9364281	0.55897214	-3.4642659	0.00053168	0.00534348
Xetrov72031953|Xetrov72031953	265.656367	-1.2883383	0.37220121	-3.4614028	0.00053737	0.005392
Xetrov72027323|Xetrov72027323|hes3.1	2036.14364	-1.1187134	0.32324012	-3.4609362	0.0005383	0.00539848
Xetrov72042859|Xetrov72042859|unnamed	208.733484	-2.0240884	0.58913013	-3.4357238	0.00059097	0.00586118
Xetrov72032691|Xetrov72032691	276.329224	-1.4557188	0.42389478	-3.4341512	0.00059441	0.00588909
Xetrov72039904|Xetrov72039904|unnamed	454.022225	-1.9031162	0.55616751	-3.42184	0.00062199	0.00610769
Xetrov72040162|Xetrov72040162|sap30l	19.8960648	-1.2124256	0.35480111	-3.417198	0.00063269	0.00619663
Xetrov72012187|Xetrov72012187|adap1	900.607733	-1.0064217	0.29505571	-3.4109549	0.00064736	0.00630712
Xetrov72035057|Xetrov72035057|chmp4c	76.4368893	-1.4331027	0.42115552	-3.4027874	0.00066702	0.00647895
Xetrov72033573|Xetrov72033573|casd1	150.849574	-1.7828627	0.52665027	-3.3852877	0.00071104	0.0067978
Xetrov72014019|Xetrov72014019|chst4	283.318665	-1.1206416	0.33120284	-3.3835507	0.00071555	0.00683055
Xetrov72034324|Xetrov72034324	46.2911855	-1.818535	0.53759745	-3.3827076	0.00071775	0.00684808
Xetrov72036962|Xetrov72036962	3.13809594	-2.0132289	0.59564238	-3.379929	0.00072505	0.00691068
Xetrov72013642|Xetrov72013642	40.3956593	-1.2958385	0.38379133	-3.3764143	0.00073437	0.00697487
Xetrov72038928|Xetrov72038928|slc18a2	47.5807158	-2.0009918	0.59334639	-3.3723839	0.00074521	0.00706351
Xetrov72021587|Xetrov72021587	12.760488	-1.9459992	0.57819999	-3.3656161	0.00076373	0.00721655
Xetrov72007774|Xetrov72007774	14.8044	-1.20412	0.35827533	-3.3608788	0.00077695	0.00732019
Xetrov72029860|Xetrov72029860|cyp4f22	60.485332	-1.8445189	0.55063652	-3.349794	0.00080872	0.00755524
Xetrov72020407|Xetrov72020407|kcna1	28.014804	-1.2498167	0.37339643	-3.3471576	0.00081645	0.00760309
Xetrov72036590|Xetrov72036590|tdh	24.9568319	-1.4045906	0.41984795	-3.3454745	0.00082142	0.00763604
Xetrov72034683|Xetrov72034683|hoxa1	431.75623	-1.5219162	0.45639799	-3.3346251	0.00085414	0.0078819
Xetrov72022127|Xetrov72022127	9.275179	-1.5786567	0.47501998	-3.3233479	0.00088944	0.00815168
Xetrov72026902|Xetrov72026902|hmx2	38.355637	-1.9817074	0.59704227	-3.3192079	0.00090273	0.00825342
Xetrov72010158|Xetrov72010158|fa2h	91.9575414	-1.7914712	0.54033635	-3.3154741	0.00091488	0.00834026
Xetrov72002030|Xetrov72002030	24.177272	-1.7248241	0.52046672	-3.3139951	0.00091973	0.00837227
Xetrov72036278|Xetrov72036278|axin2	22.6735237	-1.5558808	0.46974842	-3.3121576	0.00092579	0.00841119
Xetrov72010040|Xetrov72010040|syt8	594.513727	-1.451108	0.43983162	-3.2992353	0.00096949	0.00872815
Xetrov72016788|Xetrov72016788|arhgap27	338.190491	-1.1321988	0.34453099	-3.2862031	0.00101548	0.00906514
Xetrov72016332|Xetrov72016332|rab3d	78.8445567	-1.6747285	0.51110003	-3.2767137	0.00105023	0.00930823
Xetrov72010152|Xetrov72010152|foxf1	100.037452	-1.7740458	0.54192852	-3.273579	0.00106195	0.00939001
Xetrov72018611|Xetrov72018611|dmxl1	164.018939	-1.0698204	0.32707889	-3.2708329	0.00107231	0.00946138
Xetrov72022781|Xetrov72022781|ypel1	12.4225859	-1.5009288	0.46064903	-3.2582914	0.00112085	0.00983697

Bibliography

Abdollah, S, M Macías-Silva, T Tsukazaki, H Hayashi, L Attisano, and J L Wrana (1997). "TbetaRI phosphorylation of Smad2 on Ser465 and Ser467 is required for Smad2-Smad4 complex formation and signaling." In: *The Journal of biological chemistry* 272.44, pp. 27678–27685.

Aberle, H, A Bauer, J Stappert, A Kispert, and R Kemler (1997). "beta-catenin is a target for the ubiquitin-proteasome pathway." In: *The EMBO journal* 16.13, pp. 3797–3804.

Agius, E, M Oelgeschläger, O Wessely, C Kemp, and E M de Robertis (2000). "Endodermal Nodal-related signals and mesoderm induction in Xenopus." In: *Development* 127.6, pp. 1173–1183.

Akiyama, Haruhiko, Jon P Lyons, Yuko Mori-Akiyama, Xiaohong Yang, Ren Zhang, Zhaoping Zhang, Jian Min Deng, Makoto M Taketo, Takashi Nakamura, Richard R Behringer, Pierre D McCrea, and Benoit de Crombrugghe (2004). "Interactions between Sox9 and beta-catenin control chondrocyte differentiation." In: *Genes & Development* 18.9, pp. 1072–1087.

Al-Salihi, Mazin A, Lina Herhaus, Thomas Macartney, and Gopal P Sapkota (2012). "USP11 augments TGFβ signalling by deubiquitylating ALK5." In: *Open Biology* 2.6, p. 120063.

Alarcón, Claudio, Alexia-Ileana Zaromytidou, Qiaoran Xi, Sheng Gao, Jianzhong Yu, Sho Fujisawa, Afsar Barlas, Alexandria N Miller, Katia Manova-Todorova, Maria J Macias, Gopal Sapkota, Duojia Pan, and Joan Massagué (2009). "Nuclear CDKs drive Smad transcriptional activation and turnover in BMP and TGF-beta pathways." In: *Cell* 139.4, pp. 757–769.

Albert, Istvan, Travis N Mavrich, Lynn P Tomsho, Ji Qi, Sara J Zanton, Stephan C Schuster, and B Franklin Pugh (2007). "Translational and rotational settings of H2A.Z nucleosomes across the Saccharomyces cerevisiae genome". In: *Nature* 446.7135, pp. 572–576.

Amin, Nirav M, Todd M Greco, Lauren M Kuchenbrod, Maggie M Rigney, Mei-I Chung, John B Wallingford, Ileana M Cristea, and Frank L Conlon (2014). "Proteomic profiling of cardiac tissue by isolation of nuclei tagged in specific cell types (INTACT)." In: *Development* 141.4, pp. 962–973.

Anders, S, P T Pyl, and W Huber (2015). "HTSeq–a Python framework to work with high-throughput sequencing data". In: *Bioinformatics (Oxford, England)* 31.2, pp. 166–169.

Arce, Laura, Kira T Pate, and Marian L Waterman (2009). "Groucho binds two conserved regions of LEF-1 for HDAC-dependent repression." In: *BMC cancer* 9.1, p. 159.

Artinger, M, I Blitz, K Inoue, U Tran, and K W Cho (1997). "Interaction of goosecoid and brachyury in Xenopus mesoderm patterning." In: *Mechanisms of Development* 65.1-2, pp. 187–196.

Asashima, M, H Nakano, H Uchiyama, H Sugino, T Nakamura, Y Eto, D Ejima, S Nishimatsu, N Ueno, and K Kinoshita (1991). "Presence of activin (erythroid differentiation factor) in unfertilized eggs and blastulae of Xenopus laevis." In: *Proceedings of the National Academy of Sciences of the United States of America* 88.15, pp. 6511–6514.

B nziger, Carla, Davide Soldini, Corina Sch tt, Peder Zipperlen, George Hausmann, and Konrad Basler (2006). "Wntless, a Conserved Membrane Protein Dedicated to the Secretion of Wnt Proteins from Signaling Cells". In: *Cell* 125.3, pp. 509–522.

Backstrom, S (1954). "Morphogenetic effects of Li on the embryonic development of *Xenopus*". In: *Arch. Zool.* 6, pp. 527–536.

Baker, N E (1987). "Molecular cloning of sequences from wingless, a segment polarity gene in Drosophila: the spatial distribution of a transcript in embryos." In: *The EMBO journal* 6.6, pp. 1765–1773.

Banerjee, Santanu, Laura Gordon, Thomas M Donn, Caterina Berti, Cecilia B Moens, Steven J Burden, and Michael Granato (2011). "A novel role for MuSK and non-canonical Wnt signaling during segmental neural crest cell migration." In: *Development* 138.15, pp. 3287–3296.

Barker, N, A Hurlstone, H Musisi, A Miles, M Bienz, and H Clevers (2001). "The chromatin remodelling factor Brg-1 interacts with beta-catenin to promote target gene activation." In: *The EMBO journal* 20.17, pp. 4935–4943.

Barrett, Caitlyn W, J Joshua Smith, Lauren C Lu, Nicholas Markham, Kristy R Stengel, Sarah P Short, Baolin Zhang, Aubrey A Hunt, Barbara M Fingleton, Robert H Carnahan, Michael E Engel, Xi Chen, R Daniel Beauchamp, Keith T Wilson, Scott W Hiebert, Albert B Reynolds, and Christopher S Williams (2012). "Kaiso directs the transcriptional corepressor MTG16 to the Kaiso binding site in target promoters." In: *PloS one* 7.12, e51205.

Barski, Artem, Suresh Cuddapah, Kairong Cui, Tae-Young Roh, Dustin E Schones, Zhibin Wang, Gang Wei, Iouri Chepelev, and Keji Zhao (2007). "High-resolution profiling of histone methylations in the human genome." In: *Cell* 129.4, pp. 823–837.

Bartscherer, Kerstin, Nadège Pelte, Dierk Ingelfinger, and Michael Boutros (2006). "Secretion of Wnt Ligands Requires Evi, a Conserved Transmembrane Protein". In: *Cell* 125.3, pp. 523–533.

Beddington, R S P, P Rashbass, and V Wilson (1992). "Brachyury - a gene affecting mouse gastrulation and early organogenesis". In: *Development* 116.Supplement, pp. 157–165.

Belenkaya, Tatyana Y, Yihui Wu, Xiaofang Tang, Bo Zhou, Longqiu Cheng, Yagya V Sharma, Dong Yan, Erica M Selva, and Xinhua Lin (2008). "The Retromer Complex Influences Wnt Secretion by Recycling Wntless from Endosomes to the Trans-Golgi Network". In: *Developmental Cell* 14.1, pp. 120–131.

Bhanot, P, M Brink, C H Samos, J C Hsieh, Y Wang, J P Macke, D Andrew, J Nathans, and R Nusse (1996). "A new member of the frizzled family from Drosophila functions as a Wingless receptor." In: *Nature* 382.6588, pp. 225–230.

Biggin, Mark D (2011). "Animal transcription networks as highly connected, quantitative continua." In: *Developmental Cell* 21.4, pp. 611–626.

Bilic, Josipa, Ya-Lin Huang, Gary Davidson, Timo Zimmermann, Cristina-Maria Cruciat, Mariann Bienz, and Christof Niehrs (2007). "Wnt induces LRP6 signalosomes and promotes dishevelled-dependent LRP6 phosphorylation." In: *Science* 316.5831, pp. 1619–1622.

Birsoy, Bilge, Matt Kofron, Kyle Schaible, Chris Wylie, and Janet Heasman (2006). "Vg 1 is an essential signaling molecule in Xenopus development." In: *Development (Cambridge, England)* 133.1, pp. 15–20.

Blitz, Ira L, Kitt D Paraiso, Ilya Patrushev, William T Y Chiu, Ken W Y Cho, and Michael J Gilchrist (2017). "A catalog of Xenopus tropicalis transcription factors and their regional expression in the early gastrula stage embryo." In: *Developmental Biology* 426.2, pp. 409–417.

Blythe, Shelby A, Sang-Wook Cha, Emmanuel Tadjuidje, Janet Heasman, and Peter S Klein (2010). "beta-Catenin primes organizer gene expression by recruiting a histone H3 arginine 8 methyltransferase, Prmt2." In: *Developmental Cell* 19.2, pp. 220–231.

Bogdanović, Ozren, Arne H Smits, Elisa de la Calle-Mustienes, Juan J Tena, Ethan Ford, Ruth Williams, Upeka Senanayake, Matthew D Schultz, Saartje Hontelez, Ila van Kruijsbergen, Teresa Rayon, Felix Gnerlich, Thomas Carell, Gert Jan C Veenstra, Miguel Manzanares, Tatjana Sauka-Spengler, Joseph R Ecker, Michiel Vermeulen, José Luis Gómez-Skarmeta, and Ryan Lister (2016). "Active DNA demethylation at enhancers during the vertebrate phylotypic period." In: *Nature Publishing Group*.

Bollag, R J, Z Siegfried, J A Cebra-Thomas, N Garvey, E M Davison, and L M Silver (1994). "An ancient family of embryonically expressed mouse genes sharing a conserved protein motif with the T locus." In: *Nature genetics* 7.3, pp. 383–389.

Bonn, Stefan, Robert P Zinzen, Alexis Perez-Gonzalez, Andrew Riddell, Anne-Claude Gavin, and Eileen E M Furlong (2012a). "Cell type-specific chromatin immunoprecipitation from multicellular complex samples using BiTS-ChIP". In: *Nature Protocols* 7.5, pp. 978–994.

Bonn, Stefan, Robert P Zinzen, Charles Girardot, E Hilary Gustafson, Alexis Perez-Gonzalez, Nicolas Delhomme, Yad Ghavi-Helm, Bartek Wilczyński, Andrew Riddell, and Eileen E M Furlong (2012b). "Tissue-specific analysis of chromatin state identifies temporal signatures of enhancer activity during embryonic development". In: *Nature Publishing Group* 44.2, pp. 148–156.

Boucher, D M, M Schäffer, K Deissler, C A Moore, J D Gold, C A Burdsal, J J Meneses, R A Pedersen, and M Blum (2000). "goosecoid expression represses Brachyury in embryonic stem cells and affects craniofacial development in chimeric mice." In: *The International journal of developmental biology* 44.3, pp. 279–288.

Bragdon, Beth, Oleksandra Moseychuk, Sven Saldanha, Daniel King, Joanne Julian, and Anja Nohe (2011). "Bone morphogenetic proteins: a critical review." In: *Cellular signalling* 23.4, pp. 609–620.

Brannon, M and D Kimelman (1996). "Activation of Siamois by the Wnt pathway." In: *Dev Biol* 180.1, pp. 344–347.

Brannon, M, M Gomperts, L Sumoy, R T Moon, and D Kimelman (1997). "A beta-catenin/XTcf-3 complex binds to the siamois promoter to regulate dorsal axis specification in Xenopus." In: *Genes & Development* 11.18, pp. 2359–2370.

Brunner, E, O Peter, L Schweizer, and K Basler (1997). "pangolin encodes a Lef-1 homologue that acts downstream of Armadillo to transduce the Wingless signal in Drosophila." In: *Nature* 385.6619, pp. 829–833.

Buechling, Tina, Varun Chaudhary, Kerstin Spirohn, Matthias Weiss, and Michael Boutros (2011). "p24 proteins are required for secretion of Wnt ligands." In: *Nature Publishing Group* 12.12, pp. 1265–1272.

Cabrera, C V, M C Alonso, P Johnston, R G Phillips, and P A Lawrence (1987). "Phenocopies induced with antisense RNA identify the wingless gene." In: *Cell* 50.4, pp. 659–663.

Carreira, S, T J Dexter, U Yavuzer, D J Easty, and C R Goding (1998). "Brachyury-related transcription factor Tbx2 and repression of the melanocyte-specific TRP-1 promoter." In: *Molecular and cellular biology* 18.9, pp. 5099–5108.

Casey, E S, M A O'Reilly, F L Conlon, and J C Smith (1998). "The T-box transcription factor Brachyury regulates expression of eFGF through binding to a non-palindromic response element." In: *Development* 125.19, pp. 3887–3894.

Cha, Sang-Wook, Emmanuel Tadjuidje, Qinghua Tao, Christopher Wylie, and Janet Heasman (2008). "Wnt5a and Wnt11 interact in a maternal Dkk1-regulated fashion to activate both canonical and non-canonical signaling in Xenopus axis formation." In: *Development (Cambridge, England)* 135.22, pp. 3719–3729.

Charney, Rebekah M, Elmira Forouzmand, Jin Sun Cho, Jessica Cheung, Kitt D Paraiso, Yuuri Yasuoka, Shuji Takahashi, Masanori Taira, Ira L Blitz, Xiaohui Xie, and Ken W Y Cho (2017). "Foxh1 Occupies cis -Regulatory Modules Prior to Dynamic Transcription Factor Interactions Controlling the Mesendoderm Gene Program". In: *Developmental Cell* 40.6, 595–607.e4.

Cheifetz, S, J A Weatherbee, MLS Tsang, and J K Anderson (1987). "The transforming growth factor-β system, a complex pattern of cross-reactive ligands and receptors". In: *Cell* 48.3, pp. 409–415.

Chen, Hong Bing, Jonathan G Rud, Kai Lin, and Lan Xu (2005). "Nuclear targeting of transforming growth factor-beta-activated Smad complexes." In: *The Journal of biological chemistry* 280.22, pp. 21329–21336.

Chen, Jiakun, Qicong Luo, Yuanyang Yuan, Xiaoli Huang, Wangyu Cai, Chao Li, Tongzhen Wei, Ludi Zhang, Meng Yang, Qingfeng Liu, Guodong Ye, Xing Dai, and Boan Li (2010). "Pygo2 Associates with MLL2 Histone Methyltransferase and GCN5 Histone Acetyltransferase Complexes To Augment Wnt Target Gene Expression and Breast Cancer Stem-Like Cell Expansion". In: *Molecular and cellular biology* 30.24, pp. 5621–5635.

Chen, R H and R Derynck (1994). "Homomeric interactions between type II transforming growth factor-beta receptors." In: *The Journal of biological chemistry* 269.36, pp. 22868–22874.

Chen, X, M J Rubock, and M Whitman (1996). "A transcriptional partner for MAD proteins in TGF-beta signalling." In: *Nature* 383.6602, pp. 691–696.

Chen, X, E Weisberg, V Fridmacher, M Watanabe, G Naco, and M Whitman (1997). "Smad4 and FAST-1 in the assembly of activin-responsive factor." In: *Nature* 389.6646, pp. 85–89.

Chesley, Paul (1935). "Development of the short-tailed mutant in the house mouse". In: *Journal of Experimental Zoology* 70.3, pp. 429–459.

Chiu, William T, Rebekah Charney Le, Ira L Blitz, Margaret B Fish, Yi Li, Jacob Biesinger, Xiaohui Xie, and Ken W Y Cho (2014). "Genome-wide view of TGFβ/Foxh1 regulation of the early mesendoderm program." In: *Development* 141.23, pp. 4537–4547.

Cho, Ken W Y, Bruce Blumberg, Herbert Steinbeisser, and Eddy M De Robertis (1991). "Molecular nature of Spemann's organizer: the role of the Xenopus homeobox gene goosecoid". In: *Cell* 67.6, pp. 1111–1120.

Christian, J L and R T Moon (1993). "Interactions between Xwnt-8 and Spemann organizer signaling pathways generate dorsoventral pattern in the embryonic mesoderm of Xenopus." In: *Genes & Development* 7.1, pp. 13–28.

Christian, J L, J A McMahon, A P McMahon, and R T Moon (1991). "Xwnt-8, a Xenopus Wnt-1/int-1-related gene responsive to mesoderm-inducing growth factors, may play a role in ventral mesodermal patterning during embryogenesis." In: *Development (Cambridge, England)* 111.4, pp. 1045–1055.

Clements, Debbie, Hazel C Taylor, Bernhard G Herrmann, and David Stott (1996). "Distinct regulatory control of the Brachyury gene in axial and non-axial mesoderm suggests separation of mesoderm lineages early in mouse gastrulation". In: *Mechanisms of Development* 56.1-2, pp. 139–149.

Collart, C, N D L Owens, L Bhaw-Rosun, B Cooper, E De Domenico, I Patrushev, A K Sesay, J N Smith, J C Smith, and M J Gilchrist (2014). "High-resolution analysis of gene activity during the Xenopus mid-blastula transition". In: *Development* 141.9, pp. 1927–1939.

Conlon, F L, S G Sedgwick, K M Weston, and J C Smith (1996). "Inhibition of Xbra transcription activation causes defects in mesodermal patterning and reveals autoregulation of Xbra in dorsal mesoderm." In: *Development* 122.8, pp. 2427–2435.

Conlon, F L, L Fairclough, B M Price, E S Casey, and J C Smith (2001). "Determinants of T box protein specificity." In: *Development* 128.19, pp. 3749–3758.

Constam, Daniel B (2014). "Regulation of TGFβ and related signals by precursor processing." In: *Seminars in cell & developmental biology* 32, pp. 85–97.

Cooke, J and E J Smith (1988). "The restrictive effect of early exposure to lithium upon body pattern in Xenopus development, studied by quantitative anatomy and immunofluorescence." In: *Development* 102.1, pp. 85–99.

Cooke, J and J C Smith (1987). "The midblastula cell cycle transition and the character of mesoderm in u.v.-induced nonaxial Xenopus development." In: *Development* 99.2, pp. 197–210.

Cooke, J, K Symes, and E J Smith (1989). "Potentiation by the lithium ion of morphogenetic responses to a Xenopus inducing factor." In: *Development* 105.3, pp. 549–558.

Cunliffe, V and J C Smith (1992). "Ectopic mesoderm formation in Xenopus embryos caused by widespread expression of a Brachyury homologue." In: *Nature* 358.6385, pp. 427–430.

Cunliffe, V and J C Smith (1994). "Specification of mesodermal pattern in Xenopus laevis by interactions between Brachyury, noggin and Xwnt-8." In: *The EMBO journal* 13.2, pp. 349–359.

Dale, L, J C Smith, and J M Slack (1985). "Mesoderm induction in Xenopus laevis: a quantitative study using a cell lineage label and tissue-specific antibodies." In: *Journal of embryology and experimental morphology* 89, pp. 289–312.

Daniels, Danette L and William I Weis (2005). "Beta-catenin directly displaces Groucho/TLE repressors from Tcf/Lef in Wnt-mediated transcription activation." In: *Nature structural & molecular biology* 12.4, pp. 364–371.

Danilchik, Michael V (2011). "Manipulating and imaging the early Xenopus laevis embryo." In: *Methods in molecular biology (Clifton, N.J.)* 770, pp. 21–54.

Dassow, G von, J E Schmidt, and D Kimelman (1993). "Induction of the Xenopus organizer: expression and regulation of Xnot, a novel FGF and activin-regulated homeo box gene." In: *Genes & Development* 7.3, pp. 355–366.

Datta, Pran K and Harold L Moses (2000). "STRAP and Smad7 Synergize in the Inhibition of Transforming Growth Factor β Signaling". In: *Molecular and cellular biology* 20.9, pp. 3157–3167.

De Domenico, Elena, Nick D L Owens, Ian M Grant, Rosa Gomes-Faria, and Michael J Gilchrist (2015). "Molecular asymmetry in the 8-cell stage Xenopus tropicalis

embryo described by single blastomere transcript sequencing." In: *Developmental Biology* 408.2, pp. 252–268.

De Robertis, Edward M and Hiroki Kuroda (2004). "Dorsal-ventral patterning and neural induction in Xenopus embryos". In: *Annual Review of Cell and Developmental Biology* 20.1, pp. 285–308.

Deal, Roger B and Steven Henikoff (2010a). "A Simple Method for Gene Expression and Chromatin Profiling of Individual Cell Types within a Tissue". In: *Developmental Cell* 18.6, pp. 1030–1040.

Deal, Roger B and Steven Henikoff (2010b). "The INTACT method for cell type–specific gene expression and chromatin profiling in Arabidopsis thaliana". In: *Nature Protocols* 6.1, pp. 56–68.

Dennler, Sylviane, Susumu Itoh, Denis Vivien, Peter ten Dijke, Stéphane Huet, and Jean Michel Gauthier (1998). "Direct binding of Smad3 and Smad4 to critical TGFβ-inducible elements in the promoter of human plasminogen activator inhibitor-type 1 gene". In: *The EMBO journal* 17.11, pp. 3091–3100.

Derynck, R and L Rhee (1987). "Sequence of the porcine transforming growth factor-beta precursor." In: *Nucleic Acids Research* 15.7, p. 3187.

Derynck, R, J A Jarrett, E Y Chen, D H Eaton, J R Bell, R K Assoian, A B Roberts, M B Sporn, and D V Goeddel (1985). "Human transforming growth factor-beta complementary DNA sequence and expression in normal and transformed cells." In: *Nature* 316.6030, pp. 701–705.

Derynck, R, W M Gelbart, R M Harland, C H Heldin, S E Kern, J Massague, D A Melton, M Mlodzik, R W Padgett, A B Roberts, J Smith, G H Thomsen, B Vogelstein, and X F Wang (1996). "Nomenclature: vertebrate mediators of TGFbeta family signals." In: *Cell* 87.2, p. 173.

Ding, Yi, Gabriele Colozza, Kelvin Zhang, Yuki Moriyama, Diego Ploper, Eric A Sosa, Maria D J Benitez, and Edward M De Robertis (2016). "Genome-wide analysis of dorsal and ventral transcriptomes of the Xenopus laevis gastrula." In: *Developmental Biology*.

Ding, Yi, Diego Ploper, Eric A Sosa, Gabriele Colozza, Yuki Moriyama, Maria D J Benitez, Kelvin Zhang, Daria Merkurjev, and Edward M De Robertis (2017). "Spemann organizer transcriptome induction by early beta-catenin, Wnt, Nodal, and Siamois signals in Xenopus laevis." In: *Proceedings of the National Academy of Sciences* 114.15, E3081–E3090.

Dobrovolskaia-Zavadskaia, N (1927). "Sur la mortification spontanée de la queue che la souris nouveau-née et sur l'existence d'un caracter e (facteur) héréditaire "non viable"". In: *Crit. Rev. Soc. Biol* 97, pp. 114–112.

Dominguez, I, K Itoh, and S Y Sokol (1995). "Role of glycogen synthase kinase 3 beta as a negative regulator of dorsoventral axis formation in Xenopus embryos." In: *Proceedings of the National Academy of Sciences of the United States of America* 92.18, pp. 8498–8502.

Dosch, R and C Niehrs (2000). "Requirement for anti-dorsalizing morphogenetic protein in organizer patterning." In: *Mechanisms of Development* 90.2, pp. 195–203.

Dosch, R, V Gawantka, H Delius, C Blumenstock, and C Niehrs (1997). "Bmp-4 acts as a morphogen in dorsoventral mesoderm patterning in Xenopus". In: ...

Doubravska, Lenka, Michaela Krausova, Dietmar Gradl, Martina Vojtechova, Lucie Tumova, Jan Lukas, Tomas Valenta, Vendula Pospichalova, Bohumil Fafilek, Jiri Plachy, Ondrej Sebesta, and Vladimir Korinek (2011). "Fatty acid modification of Wnt1 and Wnt3a at serine is prerequisite for lipidation at cysteine and is essential for Wnt signalling". In: *Cellular signalling* 23.5, pp. 837–848.

Ebisawa, T, M Fukuchi, G Murakami, T Chiba, K Tanaka, T Imamura, and K Miyazono (2001). "Smurf1 interacts with transforming growth factor-beta type I receptor through Smad7 and induces receptor degradation." In: *The Journal of biological chemistry* 276.16, pp. 12477–12480.

Ehrlich, Marcelo, Orit Gutman, Petra Knaus, and Yoav I Henis (2012). "Oligomeric interactions of TGF-β and BMP receptors." In: *FEBS letters* 586.14, pp. 1885–1896.

Elinson, R P (1975). "Site of sperm entry and a cortical contraction associated with egg activation in the frog Rana pipiens." In: *Dev Biol* 47.2, pp. 257–268.

Elinson, R P and M E Manes (1978). "Morphology of the site of sperm entry on the frog egg." In: *Dev Biol* 63.1, pp. 67–75.

Elinson, R P and B Rowning (1988). "A transient array of parallel microtubules in frog eggs: potential tracks for a cytoplasmic rotation that specifies the dorso-ventral axis." In: *Developmental Biology* 128.1, pp. 185–197.

Elinson, Richard P (1980). "The amphibian egg cortex in fertilization and early development". In: *Symp. Dev. Biol.* 38, pp. 217–234.

Faial, T, A S Bernardo, S Mendjan, E Diamanti, D Ortmann, G E Gentsch, V L Mascetti, M W B Trotter, J C Smith, and R A Pedersen (2015). "Brachyury and SMAD signalling collaboratively orchestrate distinct mesoderm and endoderm gene regulatory networks in differentiating human embryonic stem cells". In: *Development*.

Fainsod, A, H Steinbeisser, and E M de Robertis (1994). "On the function of BMP-4 in patterning the marginal zone of the Xenopus embryo." In: *The EMBO journal* 13.21, pp. 5015–5025.

Farin, Henner F, Ingrid Jordens, Mohammed H Mosa, Onur Basak, Jeroen Korving, Daniele V F Tauriello, Karin de Punder, Stephane Angers, Peter J Peters, Madelon M Maurice, and Hans Clevers (2016). "Visualization of a short-range Wnt gradient in the intestinal stem-cell niche". In: *Nature* 530.7590, pp. 340–343.

Faunes, Fernando, Natalia Sánchez, Mauricio Moreno, Gonzalo H Olivares, Dasfne Lee-Liu, Leonardo Almonacid, Alex W Slater, Tomas Norambuena, Ryan J Taft, John S Mattick, Francisco Melo, and Juan Larrain (2011). "Expression of Transposable Elements in Neural Tissues during Xenopus Development". In: *PLoS ONE* 6.7, e22569.

Faure, S, M A Lee, T Keller, P ten Dijke, and M Whitman (2000). "Endogenous patterns of TGFbeta superfamily signaling during early Xenopus development." In: *Development (Cambridge, England)* 127.13, pp. 2917–2931.

Feng, Jianxing, Tao Liu, and Yong Zhang (2002). *Using MACS to Identify Peaks from ChIP-Seq Data*. Hoboken, NJ, USA: John Wiley & Sons, Inc.

Feng, Jianxing, Tao Liu, Bo Qin, Yong Zhang, and Xiaole Shirley Liu (2012). "Identifying ChIP-seq enrichment using MACS." In: *Nature Protocols* 7.9, pp. 1728–1740.

Feng, Xin-Hua and Rik Derynck (2005). "Specificity and versatility in tgf-beta signaling through Smads." In: *Annual Review of Cell and Developmental Biology* 21, pp. 659–693.

Fernando Pérez, Brian E. Granger (2007). "IPython: A System for Interactive Scientific Computing, Computing in Science and Engineering". In: *Computing in Science and Engineering* 9.3, pp. 21–29.

Finkielstein, C V, A L Lewellyn, and J L Maller (2001). "The midblastula transition in Xenopus embryos activates multiple pathways to prevent apoptosis in response to DNA damage." In: *Proceedings of the National Academy of Sciences of the United States of America* 98.3, pp. 1006–1011.

Flachsova, Monika, Radek Sindelka, and Mikael Kubista (2013). "Single blastomere expression profiling of Xenopus laevis embryos of 8 to 32-cells reveals developmental asymmetry." In: *Scientific reports* 3, p. 2278.

Ford, Ethan, Chrysa Nikopoulou, Antonis Kokkalis, and Dimitris Thanos (2014). "A method for generating highly multiplexed ChIP-seq libraries". In: 7.1, pp. 1–5.

Franch-Marro, Xavier, Franz Wendler, Sonia Guidato, Janice Griffith, Alberto Baena-Lopez, Nobue Itasaki, Madelon M Maurice, and Jean-Paul Vincent (2008). "Wingless secretion requires endosome-to-Golgi retrieval of Wntless/Evi/Sprinter by the retromer complex". In: *Nature cell biology* 10.2, pp. 170–177.

Frolik, C A, L M Wakefield, D M Smith, and M B Sporn (1984). "Characterization of a membrane receptor for transforming growth factor-beta in normal rat kidney fibroblasts." In: *The Journal of biological chemistry* 259.17, pp. 10995–11000.

Funayama, N, F Fagotto, P McCrea, and B M Gumbiner (1995). "Embryonic axis induction by the armadillo repeat domain of beta-catenin: evidence for intracellular signaling." In: *The Journal of Cell Biology* 128.5, pp. 959–968.

Furuhashi, M, K Yagi, H Yamamoto, Y Furukawa, S Shimada, Y Nakamura, A Kikuchi, K Miyazono, and M Kato (2001). "Axin facilitates Smad3 activation in the transforming growth factor beta signaling pathway." In: *Molecular and cellular biology* 21.15, pp. 5132–5141.

Gao, Hong, Bin Wu, Roger Giese, and Zhenglun Zhu (2007). "Xom interacts with and stimulates transcriptional activity of LEF1/TCFs: implications for ventral cell fate determination during vertebrate embryogenesis". In: *Cell research* 17.4, pp. 345–356.

Garner, M M and A Revzin (1981). "A gel electrophoresis method for quantifying the binding of proteins to specific DNA regions: application to components of the Escherichia coli lactose operon regulatory system." In: *Nucleic Acids Research* 9.13, pp. 3047–3060.

Garnett, A T, Aaron T Garnett, Tina M Han, T M Han, M J Gilchrist, Michael J Gilchrist, J C Smith, James C Smith, Michael B Eisen, M B Eisen, F C Wardle, Fiona C Wardle, Sharon L Amacher, and S L Amacher (2009). "Identification of direct T-box target genes in the developing zebrafish mesoderm." In: *Development (Cambridge, England)* 136.5, pp. 749–760.

Gawantka, V, H Delius, K Hirschfeld, C Blumenstock, and C Niehrs (1995). "Antagonizing the Spemann organizer: role of the homeobox gene Xvent-1." In: *The EMBO journal* 14.24, pp. 6268–6279.

Genderen, C van, R M Okamura, I Fariñas, R G Quo, T G Parslow, L Bruhn, and R Grosschedl (1994). "Development of several organs that require inductive epithelial-mesenchymal interactions is impaired in LEF-1-deficient mice." In: *Genes & Development* 8.22, pp. 2691–2703.

Gentsch, G E, R S Monteiro, and J C Smith (2016). "Cooperation Between T-Box Factors Regulates the Continuous Segregation of Germ Layers During Vertebrate Embryogenesis". In: Elsevier.

Gentsch, George E, Ilya Patrushev, and James C Smith (2015). "Genome-wide snapshot of chromatin regulators and states in Xenopus embryos by ChIP-Seq." In: *Journal of visualized experiments : JoVE* 96, e52535–e52535.

Gentsch, George E and James C Smith (2014). "Investigating physical chromatin associations across the Xenopus genome by chromatin immunoprecipitation." In: *Cold Spring Harbor protocols* 2014.5, pdb.prot080614.

Gentsch, George E and James C Smith (2017). "Efficient Preparation of High-Complexity ChIP-Seq Profiles from Early Xenopus Embryos." In: *Methods in molecular biology (Clifton, N.J.)* 1507, pp. 23–42.

Gentsch, George E, Nick D L Owens, Stephen R Martin, Paul Piccinelli, Tiago Faial, Matthew W B Trotter, Michael J Gilchrist, and James C Smith (2013). "In vivo T-box transcription factor profiling reveals joint regulation of embryonic neuromesodermal bipotency." In: *CellReports* 4.6, pp. 1185–1196.

Georgiou, Georgios and Simon J van Heeringen (2016). "fluff: exploratory analysis and visualization of high-throughput sequencing data." In: *PeerJ* 4, e2209.

Gerhart, J, M Danilchik, T Doniach, S Roberts, B Rowning, and R Stewart (1989). "Cortical rotation of the Xenopus egg: consequences for the anteroposterior pattern of embryonic dorsal development." In: *Development* 107 Suppl, pp. 37–51.

Germain, S, M Howell, G M Esslemont, and C S Hill (2000). "Homeodomain and winged-helix transcription factors recruit activated Smads to distinct promoter elements via a common Smad interaction motif." In: *Genes & Development* 14.4, pp. 435–451.

Giese, K, A Amsterdam, and R Grosschedl (1991). "DNA-binding properties of the HMG domain of the lymphoid-specific transcriptional regulator LEF-1." In: *Genes & Development* 5.12B, pp. 2567–2578.

Gilboa, Lilach, Rebecca G Wells, Harvey F Lodish, and Yoav I Henis (1998). "Oligomeric Structure of Type I and Type II Transforming Growth Factor β Receptors: Homodimers Form in the ER and Persist at the Plasma Membrane". In: *The Journal of Cell Biology* 140.4, pp. 767–777.

Gilmour, D S and J T Lis (1984). "Detecting protein-DNA interactions in vivo: distribution of RNA polymerase on specific bacterial genes." In: *Proceedings of the National Academy of Sciences of the United States of America* 81.14, pp. 4275–4279.

Gilmour, D S and J T Lis (1985). "In vivo interactions of RNA polymerase II with genes of Drosophila melanogaster." In: *Molecular and cellular biology* 5.8, pp. 2009–2018.

Goodman, Robyn M, Shreya Thombre, Zeynep Firtina, Dione Gray, Daniella Betts, Jamie Roebuck, Eric P Spana, and Erica M Selva (2006). "Sprinter: a novel transmembrane protein required for Wg secretion and signaling". In: *Development (Cambridge, England)* 133.24, pp. 4901–4911.

Goto, Satoshi, Misako Taniguchi, Masatoshi Muraoka, Hidenao Toyoda, Yukiko Sado, Masao Kawakita, and Shigeo Hayashi (2001). "UDP—[ndash]—sugar transporter implicated in glycosylation and processing of Notch". In: *Nature cell biology* 3.9, pp. 816–822.

Graff, J M (1997). "Embryonic patterning: to BMP or not to BMP, that is the question." In: *Cell* 89.2, pp. 171–174.

Graff, J M, A Bansal, and D A Melton (1996). "Xenopus Mad proteins transduce distinct subsets of signals for the TGF beta superfamily." In: *Cell* 85.4, pp. 479–487.

Graham, T A, C Weaver, F Mao, D Kimelman, and W Xu (2000). "Crystal structure of a beta-catenin/Tcf complex." In: *Cell* 103.6, pp. 885–896.

Grant, P and J F Wacaster (1972). "The amphibian gray crescent region–a site of developmental information?" In: *Developmental Biology* 28.3, pp. 454–471.

Green, J B, H V New, and J C Smith (1992). "Responses of embryonic Xenopus cells to activin and FGF are separated by multiple dose thresholds and correspond to distinct axes of the mesoderm." In: *Cell* 71.5, pp. 731–739.

Green, J B and J C Smith (1990). "Graded changes in dose of a Xenopus activin A homologue elicit stepwise transitions in embryonic cell fate." In: *Nature* 347.6291, pp. 391–394.

Green, J B, J C Smith, and J C Gerhart (1994). "Slow emergence of a multithreshold response to activin requires cell-contact-dependent sharpening but not prepattern." In: *Development (Cambridge, England)* 120.8, pp. 2271–2278.

Groppe, Jay, Jason Greenwald, Ezra Wiater, Joaquin Rodriguez-Leon, Aris N Economides, Witek Kwiatkowski, Markus Affolter, Wylie W Vale, Juan Carlos Izpisua Belmonte, and Senyon Choe (2002). "Structural basis of BMP signalling inhibition by the cystine knot protein Noggin." In: *Nature* 420.6916, pp. 636–642.

Gross, Julia Christina, Varun Chaudhary, Kerstin Bartscherer, and Michael Boutros (2012). "Active Wnt proteins are secreted on exosomes." In: *Nature cell biology* 14.10, pp. 1036–1045.

Grotewold, L, M Plum, R Dildrop, T Peters, and U Rüther (2001). "Bambi is coexpressed with Bmp-4 during mouse embryogenesis." In: *Mechanisms of development* 100.2, pp. 327–330.

Guo, Xing, Alejandro Ramirez, David S Waddell, Zhizhong Li, Xuedong Liu, and Xiao-Fan Wang (2008). "Axin and GSK3- control Smad3 protein stability and modulate TGF- signaling." In: *Genes & Development* 22.1, pp. 106–120.

Gupta, Rakhi, Andrea Wills, Duygu Ucar, and Julie Baker (2014). "Developmental enhancers are marked independently of zygotic Nodal signals in Xenopus." In: *Developmental Biology* 395.21, pp. 2227–2241.

Gurdon, J B, A Mitchell, and D Mahony (1995). "Direct and continuous assessment by cells of their position in a morphogen gradient." In: *Nature* 376.6540, pp. 520–521.

Gurdon, J B, P Harger, A Mitchell, and P Lemaire (1994). "Activin signalling and response to a morphogen gradient." In: *Nature* 371.6497, pp. 487–492.

Hall, Thomas S (1942). "The mode of action of lithium salts in amphibian development". In: *Journal of Experimental Zoology Part A: Ecological Genetics and Physiology* 89.1, pp. 1–35.

Hämmerlein, A, J Weiske, and O Huber (2005). "A second protein kinase CK1-mediated step negatively regulates Wnt signalling by disrupting the lymphocyte enhancer factor-1/beta-catenin complex." In: *Cellular and molecular life sciences : CMLS* 62.5, pp. 606–618.

Haramoto, Yoshikazu, Kousuke Tanegashima, Yasuko Onuma, Shuji Takahashi, Hiroyuki Sekizaki, and Makoto Asashima (2004). "Xenopus tropicalis nodal-related gene 3 regulates BMP signaling: an essential role for the pro-region". In: *Developmental Biology* 265.1, pp. 155–168.

Harland, Richard and John Gerhart (1997). "Formation and function of Spemann's organizer". In: *Annual Review of Cell and Developmental Biology* 13.1, pp. 611–667.

Hasegawa, Yoshimi, Kiyotoshi Satoh, Akiko Iizuka-Kogo, Atsushi Shimomura, Ryuji Nomura, Tetsu Akiyama, and Takao Senda (2007). "Loss of ICAT gene function leads to arrest of ureteric bud branching and renal agenesis". In: *Biochemical and Biophysical Research Communications* 362.4, pp. 988–994.

Hayashi, H, S Abdollah, Y Qiu, J Cai, Y Y Xu, B W Grinnell, M A Richardson, J N Topper, M A Gimbrone, J L Wrana, and D Falb (1997). "The MAD-related protein Smad7 associates with the TGFbeta receptor and functions as an antagonist of TGFbeta signaling." In: *Cell* 89.7, pp. 1165–1173.

Hayata, T, A Eisaki, H Kuroda, and M Asashima (1999). "Expression of Brachyury-like T-box transcription factor, Xbra3 in Xenopus embryo." In: *Development genes and evolution* 209.9, pp. 560–563.

Hayes, M, M Naito, A Daulat, S Angers, and B Ciruna (2013). "Ptk7 promotes non-canonical Wnt/PCP-mediated morphogenesis and inhibits Wnt/ -catenin-dependent cell fate decisions during vertebrate development". In: *Development (Cambridge, England)* 140.10, pp. 2245–2245.

Heasman, J (1997). "Patterning the Xenopus blastula." In: *Development* 124.21, pp. 4179–4191.

Hecht, Andreas, Kris Vleminckx, Marc P Stemmler, Frans van Roy, and Rolf Kemler (2000). "The p300/CBP acetyltransferases function as transcriptional coactivators of β-catenin in vertebrates". In: *The EMBO journal* 19.8, pp. 1839–1850.

Heeringen, Simon J van, Robert C Akkers, Ila van Kruijsbergen, M Asif Arif, Lars L P Hanssen, Nilofar Sharifi, and Gert Jan C Veenstra (2014). "Principles of nucleation of H3K27 methylation during embryonic development." In: *Genome Research* 24.3, pp. 401–410.

Heintzman, Nathaniel D, Rhona K Stuart, Gary Hon, Yutao Fu, Christina W Ching, R David Hawkins, Leah O Barrera, Sara Van Calcar, Chunxu Qu, Keith A Ching, Wei Wang, Zhiping Weng, Roland D Green, Gregory E Crawford, and Bing Ren (2007). "Distinct and predictive chromatin signatures of transcriptional promoters and enhancers in the human genome." In: *Nature genetics* 39.3, pp. 311–318.

Heinz, Sven, Christopher Benner, Nathanael Spann, Eric Bertolino, Yin C Lin, Peter Laslo, Jason X Cheng, Cornelis Murre, Harinder Singh, and Christopher K Glass (2010). "Simple combinations of lineage-determining transcription factors prime cis-regulatory elements required for macrophage and B cell identities." In: *Molecular cell* 38.4, pp. 576–589.

Heldin, Carl-Henrik and Aristidis Moustakas (2016). "Signaling Receptors for TGF-β Family Members." In: *Cold Spring Harbor perspectives in biology* 8.8, a022053–34.

Hemmati-Brivanlou, Ali and Gerald H Thomsen (1995). "Ventral mesodermal patterning inXenopus embryos: Expression patterns and activities of BMP-2 and BMP-4". In: *Developmental Genetics* 17.1, pp. 78–89.

Henis, Y I, A Moustakas, H Y Lin, and H F Lodish (1994). "The types II and III transforming growth factor-beta receptors form homo-oligomers." In: *The Journal of Cell Biology* 126.1, pp. 139–154.

Henningfeld, Kristine A, Henner Friedle, Sepand Rastegar, and Walter Knöchel (2002). "Autoregulation of Xvent-2B; direct interaction and functional cooperation of Xvent-2 and Smad1." In: *The Journal of biological chemistry* 277.3, pp. 2097–2103.

Henry, Gilbert L, Fred P Davis, Serge Picard, and Sean R Eddy (2012). "Cell type-specific genomics of Drosophila neurons." In: *Nucleic Acids Research* 40.19, pp. 9691–9704.

Herr, Patrick and Konrad Basler (2012). "Porcupine-mediated lipidation is required for Wnt recognition by Wls". In: *Developmental Biology* 361.2, pp. 392–402.

Herrmann, Bernhard G, Siegfried Labeit, Annemarie Poustka, Thomas R King, and Hans Lehrach (1990). "Cloning of the T gene required in mesoderm formation in the mouse". In: *Nature* 343.6259, pp. 617–622.

Hikasa, Hiroki and Sergei Y Sokol (2011). "Phosphorylation of TCF proteins by homeodomain-interacting protein kinase 2." In: *The Journal of biological chemistry* 286.14, pp. 12093–12100.

Hikasa, Hiroki and Sergei Y Sokol (2013). "Wnt Signaling in Vertebrate Axis Specification". In: *Cold Spring Harbor perspectives in biology* 5.1, a007955.

Hikasa, Hiroki, Jerome Ezan, Keiji Itoh, Xiaotong Li, Michael W Klymkowsky, and Sergei Y Sokol (2010). "Regulation of TCF3 by Wnt-dependent phosphorylation during vertebrate axis specification." In: *Developmental Cell* 19.4, pp. 521–532.

Hofmann, K (2000). "A superfamily of membrane-bound O-acyltransferases with implications for wnt signaling." In: *Trends in biochemical sciences* 25.3, pp. 111–112.

Hontelez, Saartje, Ila van Kruijsbergen, Georgios Georgiou, Simon J van Heeringen, Ozren Bogdanović, Ryan Lister, and Gert Jan C Veenstra (2015). "Embryonic transcription is controlled by maternally defined chromatin state". In: *Nature communications* 6.

Horb, M E and G H Thomsen (1997). "A vegetally localized T-box transcription factor in Xenopus eggs specifies mesoderm and endoderm and is essential for embryonic mesoderm formation." In: *Development* 124.9, pp. 1689–1698.

Howell, M, T J Mohun, and C S Hill (2001). "Xenopus Smad3 is specifically expressed in the chordoneural hinge, notochord and in the endocardium of the developing heart." In: *Mechanisms of Development* 104.1-2, pp. 147–150.

Howell, M, F Itoh, C E Pierreux, S Valgeirsdottir, S Itoh, P ten Dijke, and C S Hill (1999). "Xenopus Smad4beta is the co-Smad component of developmentally regulated transcription factor complexes responsible for induction of early mesodermal genes." In: *Dev Biol* 214.2, pp. 354–369.

Huber, A H, W J Nelson, and W I Weis (1997). "Three-dimensional structure of the armadillo repeat region of beta-catenin." In: *Cell* 90.5, pp. 871–882.

Isaacs, H V, M E Pownall, and J M Slack (1994). "eFGF regulates Xbra expression during Xenopus gastrulation." In: *The EMBO journal* 13.19, pp. 4469–4481.

Ishibashi, Hideyuki, Noriko Matsumura, Hiroshi Hanafusa, Kunihiro Matsumoto, E M De Robertis, and Hiroki Kuroda (2008). "Expression of Siamois and Twin in the blastula Chordin/Noggin signaling center is required for brain formation in Xenopus laevis embryos". In: *Mechanisms of Development* 125.1-2, pp. 58–66.

Itoh, K, J Jacob, and Y Sokol S (1998). "A role for Xenopus Frizzled 8 in dorsal development." In: *Mechanisms of development* 74.1-2, pp. 145–157.

Janda, Claudia Y, Deepa Waghray, Aron M Levin, Christoph Thomas, and K Christopher Garcia (2012). "Structural basis of Wnt recognition by Frizzled." In: *Science* 337.6090, pp. 59–64.

Janda, Claudia Y, Luke T Dang, Changjiang You, Junlei Chang, Wim de Lau, Zhendong A Zhong, Kelley S Yan, Owen Marecic, Dirk Siepe, Xingnan Li, James D Moody, Bart O Williams, Hans Clevers, Jacob Piehler, David Baker, Calvin J Kuo, and K Christopher Garcia (2017). "Surrogate Wnt agonists that phenocopy canonical Wnt and β-catenin signalling". In: *Nature* 545.7653, pp. 234–237.

Johnson, David S, Ali Mortazavi, Richard M Myers, and Barbara Wold (2007). "Genome-wide mapping of in vivo protein-DNA interactions." In: *Science* 316.5830, pp. 1497–1502.

Joly, J S, C Joly, S Schulte-Merker, H Boulekbache, and H Condamine (1993). "The ventral and posterior expression of the zebrafish homeobox gene eve1 is perturbed in dorsalized and mutant embryos." In: *Development* 119.4, pp. 1261–1275.

Jones, C M and J C Smith (1998). "Establishment of a BMP-4 morphogen gradient by long-range inhibition." In: *Dev Biol* 194.1, pp. 12–17.

Jones, C M and J C Smith (1999). "Mesoderm induction assays." In: *Methods in molecular biology (Clifton, N.J.)* 97, pp. 341–350.

Jones, Philip, David Binns, Hsin-Yu Chang, Matthew Fraser, Weizhong Li, Craig McAnulla, Hamish McWilliam, John Maslen, Alex Mitchell, Gift Nuka, Sebastien Pesseat, Antony F Quinn, Amaia Sangrador-Vegas, Maxim Scheremetjew, Siew-Yit

Yong, Rodrigo Lopez, and Sarah Hunter (2014). "InterProScan 5: genome-scale protein function classification." In: *Bioinformatics (Oxford, England)* 30.9, pp. 1236–1240.

Jonk, Luigi J C, Susumu Itoh, Carl-Henrik Heldin, Peter ten Dijke, and Wiebe Kruijer (1998). "Identification and Functional Characterization of a Smad Binding Element (SBE) in the JunB Promoter That Acts as a Transforming Growth Factor-β, Activin, and Bone Morphogenetic Protein-inducible Enhancer". In: *The Journal of biological chemistry* 273.33, pp. 21145–21152.

Joubin, K and C D Stern (1999). "Molecular interactions continuously define the organizer during the cell movements of gastrulation." In: *Cell* 98.5, pp. 559–571.

Kang, Jong Seok, Elise F Saunier, Rosemary J Akhurst, and Rik Derynck (2008). "The type I TGF-beta receptor is covalently modified and regulated by sumoylation." In: *Nature cell biology* 10.6, pp. 654–664.

Kao, K R and R P Elinson (1988). "The entire mesodermal mantle behaves as Spemann's organizer in dorsoanterior enhanced Xenopus laevis embryos." In: *Developmental Biology* 127.1, pp. 64–77.

Kao, K R, Y Masui, and R P Elinson (1986). "Lithium-induced respecification of pattern in Xenopus laevis embryos." In: *Nature* 322.6077, pp. 371–373.

Karpinka, J Brad, Joshua D Fortriede, Kevin A Burns, Christina James-Zorn, Virgilio G Ponferrada, Jacqueline Lee, Kamran Karimi, Aaron M Zorn, and Peter D Vize (2015). "Xenbase, the Xenopus model organism database; new virtualized system, data types and genomes." In: *Nucleic Acids Research* 43.Database issue, pp. D756–63.

Kavsak, P, R K Rasmussen, C G Causing, S Bonni, H Zhu, G H Thomsen, and J L Wrana (2000). "Smad7 binds to Smurf2 to form an E3 ubiquitin ligase that targets the TGF beta receptor for degradation." In: *Molecular cell* 6.6, pp. 1365–1375.

Kawahara, A, T Wilm, L Solnica-Krezel, and I B Dawid (2000). "Functional interaction of vega2 and goosecoid homeobox genes in zebrafish." In: *genesis* 28.2, pp. 58–67.

Keklikoglou, I, C Koerner, C Schmidt, J D Zhang, D Heckmann, A Shavinskaya, H Allgayer, B Gückel, T Fehm, A Schneeweiss, Ö Sahin, S Wiemann, and U Tschulena (2012). "MicroRNA-520—[sol]—373 family functions as a tumor suppressor in estrogen receptor negative breast cancer by targeting NF-—[kappa]—B and TGF-—[beta]— signaling pathways". In: *Oncogene* 31.37, pp. 4150–4163.

Keller, R (1991). "Early embryonic development of Xenopus laevis". In: *Methods in cell biology.*

Keller, R and M Danilchik (1988). "Regional expression, pattern and timing of convergence and extension during gastrulation of Xenopus laevis." In: *Development (Cambridge, England)* 103.1, pp. 193–209.

Keller, R E (1984). "The Cellular Basis of Gastrulation in Xenopus laevis: Active, Postinvolution Convergence and Extension by Mediolateral Interdigitation". In: *Integrative and Comparative Biology* 24.3, pp. 589–603.

Kharchenko, Peter V, Michael Y Tolstorukov, and Peter J Park (2008). "Design and analysis of ChIP-seq experiments for DNA-binding proteins." In: *Nature Biotechnology* 26.12, pp. 1351–1359.

Kiecker, C and C Niehrs (2001). "AP neural patterning by a Wnt gradient". In: pp. 1–13.

Kim, C H, T Oda, M Itoh, D Jiang, K B Artinger, S C Chandrasekharappa, W Driever, and A B Chitnis (2000). "Repressor activity of Headless/Tcf3 is essential for vertebrate head formation." In: *Nature* 407.6806, pp. 913–916.

Kim, Daehwan, Geo Pertea, Cole Trapnell, Harold Pimentel, Ryan Kelley, and Steven L Salzberg (2013). "TopHat2: accurate alignment of transcriptomes inthe presence of insertions, deletions and genefusions". In: *Genome Biology* 14.4, R36.

Kim, Si Wan, Se-Jin Yoon, Edward Chuong, Chuba Oyolu, Andrea E Wills, Rakhi Gupta, and Julie Baker (2011). "Chromatin and transcriptional signatures for Nodal signaling during endoderm formation in hESCs." In: *Developmental Biology* 357.2, pp. 492–504.

Kim, Tae Hoon, Leah O Barrera, Ming Zheng, Chunxu Qu, Michael A Singer, Todd A Richmond, Yingnian Wu, Roland D Green, and Bing Ren (2005). "A high-resolution map of active promoters in the human genome." In: *Nature* 436.7052, pp. 876–880.

Kim, Tae Hoon, Ziedulla K Abdullaev, Andrew D Smith, Keith A Ching, Dmitri I Loukinov, Roland D Green, Michael Q Zhang, Victor V Lobanenkov, and Bing Ren (2007). "Analysis of the vertebrate insulator protein CTCF-binding sites in the human genome." In: *Cell* 128.6, pp. 1231–1245.

Kimelman, D, J L Christian, and R T Moon (1992). "Synergistic principles of development: overlapping patterning systems in Xenopus mesoderm induction." In: *Development* 116.1, pp. 1–9.

Kimelman, D and M Kirschner (1987). "Synergistic induction of mesoderm by FGF and TGF-beta and the identification of an mRNA coding for FGF in the early Xenopus embryo." In: *Cell* 51.5, pp. 869–877.

Kinoshita, K and M Asashima (1995). "Effect of activin and lithium on isolated Xenopus animal blastomeres and response alteration at the midblastula transition." In: *Development* 121.6, pp. 1581–1589.

Kinzler, K W, M C Nilbert, L K Su, B Vogelstein, T M Bryan, D B Levy, K J Smith, A C Preisinger, P Hedge, and D McKechnie (1991). "Identification of FAP locus genes from chromosome 5q21." In: *Science* 253.5020, pp. 661–665.

Kirsch, T, W Sebald, and M K Dreyer (2000). "Crystal structure of the BMP-2-BRIA ectodomain complex." In: *Nature structural biology* 7.6, pp. 492–496.

Kispert, A and B G Herrmann (1993). "The Brachyury gene encodes a novel DNA binding protein." In: *The EMBO journal* 12.8, pp. 3211–3220.

Kitagawa, M, S Hatakeyama, M Shirane, M Matsumoto, N Ishida, K Hattori, I Nakamichi, A Kikuchi, and K Nakayama (1999). "An F-box protein, FWD1, mediates ubiquitin-dependent proteolysis of beta-catenin." In: *The EMBO journal* 18.9, pp. 2401–2410.

Klein, P S and D A Melton (1996). "A molecular mechanism for the effect of lithium on development." In: *Proceedings of the National Academy of Sciences of the United States of America* 93.16, pp. 8455–8459.

Knippschild, Uwe, Andreas Gocht, Sonja Wolff, Nadine Huber, Jürgen Löhler, and Martin Stöter (2005). "The casein kinase 1 family: participation in multiple cellular processes in eukaryotes." In: *Cellular signalling* 17.6, pp. 675–689.

Kok, Fatma O, Masahiro Shin, Chih-Wen Ni, Ankit Gupta, Ann S Grosse, Andreas van Impel, Bettina C Kirchmaier, Josi Peterson-Maduro, George Kourkoulis, Ira Male, Dana F DeSantis, Sarah Sheppard-Tindell, Lwaki Ebarasi, Christer Betsholtz, Stefan Schulte-Merker, Scot A Wolfe, and Nathan D Lawson (2015). "Reverse Genetic Screening RevealsPoor Correlation between Morpholino-Induced and Mutant Phenotypes in Zebrafish". In: *Developmental Cell* 32.1, pp. 97–108.

Komekado, Hideyuki, Hideki Yamamoto, Tsutomu Chiba, and Akira Kikuchi (2007). "Glycosylation and palmitoylation of Wnt-3a are coupled to produce an active form of Wnt-3a." In: *Genes to cells : devoted to molecular & cellular mechanisms* 12.4, pp. 521–534.

Korchynskyi, Olexander and Peter ten Dijke (2002). "Identification and functional characterization of distinct critically important bone morphogenetic protein-specific response elements in the Id1 promoter." In: *The Journal of biological chemistry* 277.7, pp. 4883–4891.

Korkut, Ceren, Bulent Ataman, Preethi Ramachandran, James Ashley, Romina Barria, Norberto Gherbesi, and Vivian Budnik (2009). "Trans-Synaptic Transmission of Vesicular Wnt Signals through Evi/Wntless". In: *Cell* 139.2, pp. 393–404.

Köster, M, S Plessow, J H Clement, A Lorenz, H Tiedemann, and W Knöchel (1991). "Bone morphogenetic protein 4 (BMP-4), a member of the TGF-beta family, in early embryos of Xenopus laevis: analysis of mesoderm inducing activity." In: *Mechanisms of development* 33.3, pp. 191–199.

Kratochwil, Klaus, Juan Galceran, Sabine Tontsch, Wera Roth, and Rudolf Grosschedl (2002). "FGF4, a direct target of LEF1 and Wnt signaling, can rescue the arrest of tooth organogenesis in Lef1−/− mice". In: *Genes & Development* 16.24, pp. 3173–3185.

Kretzschmar, M, J Doody, and J Massague (1997). "Opposing BMP and EGF signalling pathways converge on the TGF-beta family mediator Smad1." In: *Nature* 389.6651, pp. 618–622.

Ku, M and D A Melton (1993). "Xwnt-11: a maternally expressed Xenopus wnt gene." In: *Development (Cambridge, England)* 119.4, pp. 1161–1173.

Kurata, T, J Nakabayashi, T S Yamamoto, M Mochii, and N Ueno (2001). "Visualization of endogenous BMP signaling during Xenopus development." In: *Differentiation; research in biological diversity* 67.1-2, pp. 33–40.

Kurayoshi, Manabu, Hideki Yamamoto, Shunsuke Izumi, and Akira Kikuchi (2007). "Post-translational palmitoylation and glycosylation of Wnt-5a are necessary for its signalling". In: *Biochemical Journal* 402.3, pp. 515–523.

Kurisaki, A, S Kose, Y Yoneda, C H Heldin, and A Moustakas (2001). "Transforming growth factor-beta induces nuclear import of Smad3 in an importin-beta1 and Ran-dependent manner." In: *Molecular biology of the cell* 12.4, pp. 1079–1091.

Kurisaki, Akira, Keiko Kurisaki, Marcin Kowanetz, Hiromu Sugino, Yoshihiro Yoneda, Carl-Henrik Heldin, and Aristidis Moustakas (2006). "The mechanism of nuclear export of Smad3 involves exportin 4 and Ran." In: *Molecular and cellular biology* 26.4, pp. 1318–1332.

Kuroda, Hiroki, Oliver Wessely, and E M De Robertis (2004). "Neural Induction in Xenopus: Requirement for Ectodermal and Endomesodermal Signals via Chordin, Noggin, β-Catenin, and Cerberus". In: *PLoS Biology* 2.5, e92.

Labbé, E, A Letamendia, and L Attisano (2000). "Association of Smads with lymphoid enhancer binding factor 1/T cell-specific factor mediates cooperative signaling by the transforming growth factor-beta and wnt pathways." In: *Proceedings of the National Academy of Sciences of the United States of America* 97.15, pp. 8358–8363.

Labbé, Etienne, Lisa Lock, Ainhoa Letamendia, Agnieszka E Gorska, Robert Gryfe, Steven Gallinger, Harold L Moses, and Liliana Attisano (2007). "Transcriptional cooperation between the transforming growth factor-beta and Wnt pathways in mammary and intestinal tumorigenesis." In: *Cancer research* 67.1, pp. 75–84.

Landt, S G, G K Marinov, A Kundaje, P Kheradpour, F Pauli, S Batzoglou, B E Bernstein, P Bickel, J B Brown, P Cayting, Y Chen, G DeSalvo, C Epstein, K I Fisher-Aylor, G Euskirchen, M Gerstein, J Gertz, A J Hartemink, M M Hoffman, V R Iyer, Y L Jung, S Karmakar, M Kellis, P V Kharchenko, Q Li, T Liu, X S Liu, L Ma, A Milosavljevic, R M Myers, P J Park, M J Pazin, M D Perry, D Raha, T E

Reddy, J Rozowsky, N Shoresh, A Sidow, M Slattery, J A Stamatoyannopoulos, M Y Tolstorukov, K P White, S Xi, P J Farnham, J D Lieb, B J Wold, and M Snyder (2012). "ChIP-seq guidelines and practices of the ENCODE and modENCODE consortia". In: *Genome Research* 22.9, pp. 1813–1831.

Langmead, B, C Trapnell, M Pop, and S L Salzberg (2009). "Ultrafast and memory-efficient alignment of short DNA sequences to the human genome". In: *Genome Biology*.

Langmead, Ben (2010). "Aligning short sequencing reads with Bowtie." In: *Current protocols in bioinformatics / editoral board, Andreas D. Baxevanis ... [et al.]* Chapter 11, Unit 11.7.

Larabell, C A, M Torres, B A Rowning, C Yost, J R Miller, M Wu, D Kimelman, and R T Moon (1997). "Establishment of the dorso-ventral axis in Xenopus embryos is presaged by early asymmetries in beta-catenin that are modulated by the Wnt signaling pathway." In: *The Journal of Cell Biology* 136.5, pp. 1123–1136.

Larco, J E de and G J Todaro (1978). "Growth factors from murine sarcoma virus-transformed cells." In: *Proceedings of the National Academy of Sciences of the United States of America* 75.8, pp. 4001–4005.

Latinkic, B V and J C Smith (1999). "Goosecoid and mix.1 repress Brachyury expression and are required for head formation in Xenopus." In: *Development* 126.8, pp. 1769–1779.

Latinkic, B V, M Umbhauer, K A Neal, W Lerchner, J C Smith, and V Cunliffe (1997). "The Xenopus Brachyury promoter is activated by FGF and low concentrations of activin and suppressed by high concentrations of activin and by paired-type homeodomain proteins." In: *Genes & Development* 11.23, pp. 3265–3276.

Laudet, V, D Stehelin, and H Clevers (1993). "Ancestry and diversity of the HMG box superfamily." In: *Nucleic Acids Research* 21.10, pp. 2493–2501.

Laurent, Micheline N, Ira L Blitz, Chikara Hashimoto, U Rothbacher, and K W Cho (1997). "The Xenopus homeobox gene twin mediates Wnt induction of goosecoid in establishment of Spemann's organizer". In: *Development* 124.23, pp. 4905–4916.

Lee, E, A Salic, and M W Kirschner (2001). "Physiological regulation of [beta]-catenin stability by Tcf3 and CK1epsilon." In: *The Journal of Cell Biology* 154.5, pp. 983–993.

Lee, Ethan, Adrian Salic, Roland Krüger, Reinhart Heinrich, and Marc W Kirschner (2003). "The roles of APC and Axin derived from experimental and theoretical analysis of the Wnt pathway." In: *PLoS Biology* 1.1, E10.

Lee, M A, J Heasman, and M Whitman (2001). "Timing of endogenous activin-like signals and regional specification of the Xenopus embryo." In: *Development (Cambridge, England)* 128.15, pp. 2939–2952.

Lele, Z, M Nowak, and M Hammerschmidt (2001). "Zebrafish admp is required to restrict the size of the organizer and to promote posterior and ventral development." In: *Developmental Dynamics* 222.4, pp. 681–687.

Lemaire, Patrick, Nigel Garrett, and J B Gurdon (1995). "Expression cloning of Siamois, a xenopus homeobox gene expressed in dorsal-vegetal cells of blastulae and able to induce a complete secondary axis". In: *Cell* 81.1, pp. 85–94.

Lerchner, W, B V Latinkic, J E Remacle, D Huylebroeck, and J C Smith (2000). "Region-specific activation of the Xenopus brachyury promoter involves active repression in ectoderm and endoderm: a study using transgenic frog embryos." In: *Development* 127.12, pp. 2729–2739.

LeSueur, J A and J M Graff (1999). "Spemann organizer activity of Smad10." In: *Development (Cambridge, England)* 126.1, pp. 137–146.

Leyns, L, T Bouwmeester, S H Kim, S Piccolo, and E M de Robertis (1997). "Frzb-1 is a secreted antagonist of Wnt signaling expressed in the Spemann organizer." In: *Cell* 88.6, pp. 747–756.

Li, Feng-Qian, Adaobi Mofunanya, Kimberley Harris, and Ken-Ichi Takemaru (2008). "Chibby cooperates with 14-3-3 to regulate beta-catenin subcellular distribution and signaling activity." In: *The Journal of Cell Biology* 181.7, pp. 1141–1154.

Li, Heng, Bob Handsaker, Alec Wysoker, Tim Fennell, Jue Ruan, Nils Homer, Gabor Marth, Goncalo Abecasis, Richard Durbin, and 1000 Genome Project Data Processing Subgroup (2009). "The Sequence Alignment/Map format and SAMtools." In: *Bioinformatics (Oxford, England)* 25.16, pp. 2078–2079.

Li, Jiong and Cun-Yu Wang (2008). "TBL1?TBLR1 and ?-catenin recruit each other to Wnt target-gene promoter for transcription activation and oncogenesis". In: *Nature cell biology* 10.2, pp. 160–169.

Li, Yang I, David A Knowles, and Jonathan K Pritchard (2016). "LeafCutter: Annotation-free quantification of RNA splicing". In:

Li, Zhenfei, Fen Nie, Sheng Wang, and Lin Li (2011). "Histone H4 Lys 20 monomethylation by histone methylase SET8 mediates Wnt target gene activation." In: *Proceedings of the National Academy of Sciences* 108.8, pp. 3116–3123.

Lin, H Y and X F Wang (1992). "Expression cloning of TGF-beta receptors." In: *Molecular Reproduction and Development* 32.2, pp. 105–110.

Lin, H Y, X F Wang, E Ng-Eaton, R A Weinberg, and H F Lodish (1992). "Expression cloning of the TGF-beta type II receptor, a functional transmembrane serine/threonine kinase." In: *Cell* 68.4, pp. 775–785.

Liu, Chunming, Yiming Li, Mikhail Semenov, Chun Han, Gyeong Hun Baeg, Yi Tan, Zhuohua Zhang, Xinhua Lin, and Xi He (2002). "Control of beta-catenin phosphorylation/degradation by a dual-kinase mechanism." In: *Cell* 108.6, pp. 837–847.

Liu, Fei, Olaf van den Broek, Olivier Destrée, and Stefan Hoppler (2005). "Distinct roles for Xenopus Tcf/Lef genes in mediating specific responses to Wnt/β-catenin signalling in mesoderm development". In: *Development (Cambridge, England)* 132.24, pp. 5375–5385.

Liu, Guizhong, Anna Bafico, Violaine K Harris, and Stuart A Aaronson (2003). "A novel mechanism for Wnt activation of canonical signaling through the LRP6 receptor." In: *Molecular and cellular biology* 23.16, pp. 5825–5835.

Liu, X, Y Sun, S N Constantinescu, E Karam, R A Weinberg, and H F Lodish (1997). "Transforming growth factor beta-induced phosphorylation of Smad3 is required for growth inhibition and transcriptional induction in epithelial cells." In: *Proceedings of the National Academy of Sciences of the United States of America* 94.20, pp. 10669–10674.

Lo, R S, Y G Chen, Y Shi, N P Pavletich, and J Massague (1998). "The L3 loop: a structural motif determining specific interactions between SMAD proteins and TGF-beta receptors." In: *The EMBO journal* 17.4, pp. 996–1005.

Lolas, Macarena, Pablo D T Valenzuela, Robert Tjian, and Zhe Liu (2014). "Charting Brachyury-mediated developmental pathways during early mouse embryogenesis." In: *Proceedings of the National Academy of Sciences* 111.12, pp. 4478–4483.

López-Casillas, F, J L Wrana, and J Massague (1993). "Betaglycan presents ligand to the TGF beta signaling receptor." In: *Cell* 73.7, pp. 1435–1444.

Love, Damon, Feng-Qian Li, Michael C Burke, Benjamin Cyge, Masao Ohmitsu, Jeffrey Cabello, Janet E Larson, Steven L Brody, J Craig Cohen, and Ken-Ichi Takemaru (2010). "Altered Lung Morphogenesis, Epithelial Cell Differentiation and Mechanics

in Mice Deficient in the Wnt/β-Catenin Antagonist Chibby". In: *PLoS ONE* 5.10, e13600.

Love, Michael I, Wolfgang Huber, and Simon Anders (2014). "Moderated estimation of fold change and dispersion for RNA-seq data with DESeq2". In: *Genome Biology* 15.12, p. 550.

Loveland, Kate Lakoski, Marilyn Bakker, Terri Meehan, Elizabeth Christy, Viktoria von Schönfeldt, Ann Drummond, and David de Kretser (2003). "Expression of Bambi is widespread in juvenile and adult rat tissues and is regulated in male germ cells." In: *Endocrinology* 144.9, pp. 4180–4186.

Luo, Kunxin (2017). "Signaling Cross Talk between TGF-β/Smad and Other Signaling Pathways." In: *Cold Spring Harbor perspectives in biology* 9.1, a022137.

Luo, Kunxin and Harvey F Lodish (1997). "Positive and negative regulation of type II TGF-β receptor signal transduction by autophosphorylation on multiple serine residues". In: *The EMBO journal* 16.8, pp. 1970–1981.

Luo, Ting, Mami Matsuo-Takasaki, Megan L Thomas, Daniel L Weeks, and Thomas D Sargent (2002). "Transcription factor AP-2 is an essential and direct regulator of epidermal development in Xenopus." In: *Dev Biol* 245.1, pp. 136–144.

Luo, Ting, Young-Hoon Lee, Jean-Pierre Saint-Jeannet, and Thomas D Sargent (2003). "Induction of neural crest in Xenopus by transcription factor AP2alpha." In: *Proceedings of the National Academy of Sciences of the United States of America* 100.2, pp. 532–537.

Lustig, K D, K L Kroll, E E Sun, and M W Kirschner (1996). "Expression cloning of a Xenopus T-related gene (Xombi) involved in mesodermal patterning and blastopore lip formation." In: *Development* 122.12, pp. 4001–4012.

Ma, Jingqun and Vikki Marie Weake (2014). "Affinity-based isolation of tagged nuclei from Drosophila tissues for gene expression analysis." In: *Journal of visualized experiments : JoVE* 85, e51418–e51418.

Ma, Pengcheng, Xiangcai Yang, Qinghua Kong, Chaocui Li, Shuangjuan Yang, Yan Li, and Bingyu Mao (2014). "The ubiquitin ligase RNF220 enhances canonical Wnt signaling through USP7-mediated deubiquitination of β-catenin." In: *Molecular and cellular biology* 34.23, pp. 4355–4366.

Maechler, Martin, Peter Rousseeuw, Anja Struyf, Mia Hubert, and Kurt Hornik (2013). *cluster: Cluster Analysis Basics and Extensions*. R package version 1.14.4 — For new features, see the 'Changelog' file (in the package source).

Mahmoudi, Tokameh, Sylvia F Boj, Pantelis Hatzis, Vivian S W Li, Nadia Taouatas, Robert G J Vries, Hans Teunissen, Harry Begthel, Jeroen Korving, Shabaz Mohammed, Albert J R Heck, and Hans Clevers (2010). "The leukemia-associated Mllt10/Af10-Dot1l are Tcf4/β-catenin coactivators essential for intestinal homeostasis." In: *PLoS Biology* 8.11, e1000539.

Malacinski, G M, C D Allis, and H M Chung (1974). "Correction of developmental abnormalities resulting from localized ultra-violet irradiation of an amphibian egg. 1." In: *Journal of Experimental Zoology* 189.2, pp. 249–254.

Manes, Mario E and Richard P Elinson (1980). "Ultraviolet light inhibits grey crescent formation on the frog egg." In: *Wilhelm Roux's archives of developmental biology* 189.1, pp. 73–76.

Mao, B, W Wu, Y Li, D Hoppe, P Stannek, A Glinka, and C Niehrs (2001). "LDL-receptor-related protein 6 is a receptor for Dickkopf proteins." In: *Nature* 411.6835, pp. 321–325.

Marcellini, Sylvain (2006). "When Brachyury meets Smad1: the evolution of bilateral symmetry during gastrulation". In: *BioEssays : news and reviews in molecular, cellular and developmental biology* 28.4, pp. 413–420.

Martello, Graziano, Luca Zacchigna, Masafumi Inui, Marco Montagner, Maddalena Adorno, Anant Mamidi, Leonardo Morsut, Sandra Soligo, Uyen Tran, Sirio Dupont, Michelangelo Cordenonsi, Oliver Wessely, and Stefano Piccolo (2007). "MicroRNA control of Nodal signalling". In: *Nature* 449.7159, pp. 183–188.

Masiakowski, P and R D Carroll (1992). "A novel family of cell surface receptors with tyrosine kinase-like domain." In: *The Journal of biological chemistry* 267.36, pp. 26181–26190.

Massague, J (1998). "TGF-beta signal transduction." In: *Annual review of biochemistry* 67, pp. 753–791.

Massague, J and B Like (1985). "Cellular receptors for type beta transforming growth factor. Ligand binding and affinity labeling in human and rodent cell lines." In: *The Journal of biological chemistry* 260.5, pp. 2636–2645.

Massagué, Joan (2012). "TGF—[beta]— signalling in context". In: *Nature reviews. Molecular cell biology* 13.10, pp. 616–630.

Masuyama, N, H Hanafusa, M Kusakabe, H Shibuya, and E Nishida (1999). "Identification of two Smad4 proteins in Xenopus. Their common and distinct properties." In: *The Journal of biological chemistry* 274.17, pp. 12163–12170.

McClure, Colin D and Tony D Southall (2015). "Getting Down to Specifics: Profiling Gene Expression and Protein-DNA Interactions in a Cell Type-Specific Manner." In: *Advances in genetics* 91, pp. 103–151.

McCrea, P D, C W Turck, and B Gumbiner (1991). "A homolog of the armadillo protein in Drosophila (plakoglobin) associated with E-cadherin." In: *Science* 254.5036, pp. 1359–1361.

McDonald, N Q and W A Hendrickson (1993). "A structural superfamily of growth factors containing a cystine knot motif." In: *Cell* 73.3, pp. 421–424.

McGough, Ian John and Jean-Paul Vincent (2016). "Exosomes in developmental signalling". In: *Development (Cambridge, England)* 143.14, pp. 2482–2493.

McKinney, Wes. "pandas: a Foundational Python Library for Data Analysis and Statistics". In:

McMahon, A P and R T Moon (1989). "Ectopic expression of the proto-oncogene int-1 in Xenopus embryos leads to duplication of the embryonic axis." In: *Cell* 58.6, pp. 1075–1084.

Meno, C, Y Saijoh, H Fujii, M Ikeda, T Yokoyama, M Yokoyama, Y Toyoda, and H Hamada (1996). "Left-right asymmetric expression of the TGF beta-family member lefty in mouse embryos." In: *Nature* 381.6578, pp. 151–155.

Merrill, Bradley J, H Amalia Pasolli, Lisa Polak, Michael Rendl, Maria J García-García, Kathryn V Anderson, and Elaine Fuchs (2004). "Tcf3: a transcriptional regulator of axis induction in the early embryo." In: *Development (Cambridge, England)* 131.2, pp. 263–274.

Messenger, Nigel J, Christin Kabitschke, Robert Andrews, Donna Grimmer, Ricardo Núñez Miguel, Tom L Blundell, James C Smith, and Fiona C Wardle (2005). "Functional specificity of the Xenopus T-domain protein Brachyury is conferred by its ability to interact with Smad1." In: *Developmental Cell* 8.4, pp. 599–610.

Mestdagh, Pieter, Anna-Karin Boström, Francis Impens, Erik Fredlund, Gert Van Peer, Pasqualino De Antonellis, Kristoffer von Stedingk, Bart Ghesquière, Stefanie Schulte, Michael Dews, Andrei Thomas-Tikhonenko, Johannes H Schulte, Massimo Zollo, Alexander Schramm, Kris Gevaert, Håkan Axelson, Frank Speleman, and Jo

Vandesompele (2010). "The miR-17-92 microRNA cluster regulates multiple components of the TGF-β pathway in neuroblastoma." In: *Molecular cell* 40.5, pp. 762–773.

Mikkelsen, Tarjei S, Manching Ku, David B Jaffe, Biju Issac, Erez Lieberman, Georgia Giannoukos, Pablo Alvarez, William Brockman, Tae-Kyung Kim, Richard P Koche, William Lee, Eric Mendenhall, Aisling O'Donovan, Aviva Presser, Carsten Russ, Xiaohui Xie, Alexander Meissner, Marius Wernig, Rudolf Jaenisch, Chad Nusbaum, Eric S Lander, and Bradley E Bernstein (2007). "Genome-wide maps of chromatin state in pluripotent and lineage-committed cells." In: *Nature* 448.7153, pp. 553–560.

Miller, J R, B A Rowning, C A Larabell, J A Yang-Snyder, R L Bates, and R T Moon (1999). "Establishment of the Dorsal-Ventral Axis inXenopus Embryos Coincides with the Dorsal Enrichment of Dishevelled That Is Dependent on Cortical Rotation". In: *The Journal of Cell Biology* 146.2, pp. 427–438.

Mohan, Man, Hans-Martin Herz, Yoh-Hei Takahashi, Chengqi Lin, Ka Chun Lai, Ying Zhang, Michael P Washburn, Laurence Florens, and Ali Shilatifard (2010). "Linking H3K79 trimethylation to Wnt signaling through a novel Dot1-containing complex (DotCom)." In: *Genes & Development* 24.6, pp. 574–589.

Mohun, T J, S Brennan, N Dathan, S Fairman, and J B Gurdon (1984). "Cell type-specific activation of actin genes in the early amphibian embryo." In: *Nature* 311.5988, pp. 716–721.

Molenaar, M, M van de Wetering, M Oosterwegel, J Peterson-Maduro, S Godsave, V Korinek, J Roose, O Destrée, and H Clevers (1996). "XTcf-3 transcription factor mediates beta-catenin-induced axis formation in Xenopus embryos." In: *Cell* 86.3, pp. 391–399.

Moore, Amy C, Joseph M Amann, Christopher S Williams, Emilios Tahinci, Tiffany E Farmer, J Andres Martinez, Genyan Yang, K Scott Luce, Ethan Lee, and Scott W Hiebert (2008). "Myeloid Translocation Gene Family Members Associate with T-Cell Factors (TCFs) and Influence TCF-Dependent Transcription". In: *Molecular and cellular biology* 28.3, pp. 977–987.

Moos, M, S Wang, and M Krinks (1995). "Anti-dorsalizing morphogenetic protein is a novel TGF-beta homolog expressed in the Spemann organizer." In: *Development* 121.12, pp. 4293–4301.

Morgan, Richard, Ali-Morsi El-Kadi, and Christopher Theokli (2003). "Flamingo, a cadherin-type receptor involved in the Drosophila planar polarity pathway, can block signaling via the canonical wnt pathway in Xenopus laevis." In: *The International journal of developmental biology* 47.4, pp. 245–252.

Morin, P J, A B Sparks, V Korinek, N Barker, H Clevers, B Vogelstein, and K W Kinzler (1997). "Activation of beta-catenin-Tcf signaling in colon cancer by mutations in beta-catenin or APC." In: *Science* 275.5307, pp. 1787–1790.

Morley, Rosalind H, Kim Lachani, Damian Keefe, Michael J Gilchrist, Paul Flicek, James C Smith, and Fiona C Wardle (2009). "A gene regulatory network directed by zebrafish No tail accounts for its roles in mesoderm formation." In: *Proceedings of the National Academy of Sciences of the United States of America* 106.10, pp. 3829–3834.

Moustakas, A, H Y Lin, Y I Henis, J Plamondon, M D O'Connor-McCourt, and H F Lodish (1993). "The transforming growth factor beta receptors types I, II, and III form hetero-oligomeric complexes in the presence of ligand." In: *The Journal of biological chemistry* 268.30, pp. 22215–22218.

Moustakas, Aristidis and Carl-Henrik Heldin (2009). "The regulation of TGFbeta signal transduction." In: *Development* 136.22, pp. 3699–3714.

Müller, C W and B G Herrmann (1997). "Crystallographic structure of the T domain-DNA complex of the Brachyury transcription factor." In: *Nature* 389.6653, pp. 884–888.

Nakamura, Yukio and Stefan Hoppler (2017). "Genome-wide analysis of canonical Wnt target gene regulation in Xenopus tropicalis challenges β-catenin paradigm." In: *genesis* 55.1-2.

Nakamura, Yukio, Eduardo de Paiva Alves, Gert Jan C Veenstra, and Stefan Hoppler (2016). "Tissue- and stage-specific Wnt target gene expression is controlled subsequent to β-catenin recruitment to cis-regulatory modules." In: *Development* 143.11, pp. 1914–1925.

Nakano, Naoko, Susumu Itoh, Yukihide Watanabe, Kota Maeyama, Fumiko Itoh, and Mitsuyasu Kato (2010). "Requirement of TCF7L2 for TGF-beta-dependent transcriptional activation of the TMEPAI gene." In: *The Journal of biological chemistry* 285.49, pp. 38023–38033.

Nakao, A, M Afrakhte, A Morén, T Nakayama, J L Christian, R Heuchel, S Itoh, M Kawabata, N E Heldin, C H Heldin, and P ten Dijke (1997). "Identification of Smad7, a TGFbeta-inducible antagonist of TGF-beta signalling." In: *Nature* 389.6651, pp. 631–635.

Nakayama, T, H Gardner, L K Berg, and J L Christian (1998). "Smad6 functions as an intracellular antagonist of some TGF-beta family members during Xenopus embryogenesis." In: *Genes to cells : devoted to molecular & cellular mechanisms* 3.6, pp. 387–394.

Newport, J and M Kirschner (1982a). "A major developmental transition in early Xenopus embryos: I. characterization and timing of cellular changes at the midblastula stage." In: *Cell* 30.3, pp. 675–686.

Newport, J and M Kirschner (1982b). "A major developmental transition in early Xenopus embryos: II. Control of the onset of transcription." In: *Cell* 30.3, pp. 687–696.

Niehrs, C (2001). "The Spemann organizer and embryonic head induction." In: *The EMBO journal* 20.4, pp. 631–637.

Nieuwkoop, P D and G A Ubbels (1969). "The formation of the mesoderm in urodelean amphibians. I. Induction by the Endoderm." In: *Wilhelm Roux' Archiv für Entwicklungsmechanik der Organismen* 162, pp. 341–373.

Nieuwkoop, Pieter D and Jacob Faber (1994). *Normal Table of Xenopus Laevis (Daudin).* A Systematical and Chronological Survey of the Development from the Fertilized Egg Till the End of Metamorphosis. Garland Science.

Nishisho, I, Y Nakamura, Y Miyoshi, Y Miki, H Ando, A Horii, K Koyama, J Utsunomiya, S Baba, and P Hedge (1991). "Mutations of chromosome 5q21 genes in FAP and colorectal cancer patients." In: *Science* 253.5020, pp. 665–669.

Noordermeer, J, J Klingensmith, N Perrimon, and R Nusse (1994). "dishevelled and armadillo act in the wingless signalling pathway in Drosophila." In: *Nature* 367.6458, pp. 80–83.

Nusse, R and H E Varmus (1982). "Many tumors induced by the mouse mammary tumor virus contain a provirus integrated in the same region of the host genome." In: *Cell* 31.1, pp. 99–109.

Nusse, Roel and Hans Clevers (2017). "Wnt/β-Catenin Signaling, Disease, and Emerging Therapeutic Modalities". In: *Cell* 169.6, pp. 985–999.

Nüsslein-Volhard, C and E Wieschaus (1980). "Mutations affecting segment number and polarity in Drosophila." In: *Nature* 287.5785, pp. 795–801.

Onichtchouk, D, Y G Chen, R Dosch, V Gawantka, H Delius, J Massague, and C Niehrs (1999). "Silencing of TGF-beta signalling by the pseudoreceptor BAMBI." In: *Nature* 401.6752, pp. 480–485.

Onjiko, Rosemary M, Sally A Moody, and Peter Nemes (2015). "Single-cell mass spectrometry reveals small molecules that affect cell fates in the 16-cell embryo." In: *Proceedings of the National Academy of Sciences* 112.21, pp. 6545–6550.

Onuma, Yasuko, Chang-Yeol Yeo, and Malcolm Whitman (2006). "XCR2, one of three Xenopus EGF-CFC genes, has a distinct role in the regulation of left-right patterning". In: *Development (Cambridge, England)* 133.2, pp. 237–250.

O'Reilly, M A, J C Smith, and V Cunliffe (1995). "Patterning of the mesoderm in Xenopus: dose-dependent and synergistic effects of Brachyury and Pintallavis." In: *Development* 121.5, pp. 1351–1359.

Orlando, V and R Paro (1993). "Mapping Polycomb-repressed domains in the bithorax complex using in vivo formaldehyde cross-linked chromatin". In: *Cell* 75.6, pp. 1187–1198.

Ou, Chen-Yin, Melissa J LaBonte, Philipp C Manegold, Alex Yick-Lun So, Irina Ianculescu, Daniel S Gerke, Keith R Yamamoto, Robert D Ladner, Michael Kahn, Jeong Hoon Kim, and Michael R Stallcup (2011). "A coactivator role of CARM1 in the dysregulation of β-catenin activity in colorectal cancer cell growth and gene expression." In: *Molecular cancer research : MCR* 9.5, pp. 660–670.

Ouchi, Noriyuki, Yasuhide Asaumi, Koji Ohashi, Akiko Higuchi, Saki Sono-Romanelli, Yuichi Oshima, and Kenneth Walsh (2010). "DIP2A functions as a FSTL1 receptor." In: *The Journal of biological chemistry* 285.10, pp. 7127–7134.

Owens, Nick D L, Ira L Blitz, Maura A Lane, Ilya Patrushev, John D Overton, Michael J Gilchrist, Ken W Y Cho, and Mustafa K Khokha (2016). "Measuring Absolute RNA Copy Numbers at High Temporal Resolution Reveals Transcriptome Kinetics in Development." In: *CellReports* 14.3, pp. 632–647.

Padgett, R W, R D St Johnston, and W M Gelbart (1987). "A transcript from a Drosophila pattern gene predicts a protein homologous to the transforming growth factor-beta family." In: *Nature* 325.6099, pp. 81–84.

Palecek, J, G A Ubbels, and K Rzehak (1978). "Changes of the external and internal pigment pattern upon fertilization in the egg of Xenopus laevis." In: *Journal of embryology and experimental morphology* 45, pp. 203–214.

Papaioannou, Virginia E (2014). "The T-box gene family: emerging roles in development, stem cells and cancer." In: *Development* 141.20, pp. 3819–3833.

Paranjpe, Sarita S, Ulrike G Jacobi, Simon J van Heeringen, and Gert Jan C Veenstra (2013). "A genome-wide survey of maternal and embryonic transcripts during Xenopus tropicalis development." In: *BMC genomics* 14.1, p. 762.

Pasteels, J (1945). *Recherches sur l'action du LiCl sur les oeufs des Amphibiens*. Arch. Biol.

Peifer, M, C Rauskolb, M Williams, B Riggleman, and E Wieschaus (1991). "The segment polarity gene armadillo interacts with the wingless signaling pathway in both embryonic and adult pattern formation." In: *Development (Cambridge, England)* 111.4, pp. 1029–1043.

Peterson-Nedry, Wynne, Naz Erdeniz, Susan Kremer, Jessica Yu, Shahana Baig-Lewis, and Marcel Wehrli (2008). "Unexpectedly robust assembly of the Axin destruction complex regulates Wnt/Wg signaling in Drosophila as revealed by analysis in vivo." In: *Developmental Biology* 320.1, pp. 226–241.

Piccolo, S, Y Sasai, B Lu, and E M de Robertis (1996). "Dorsoventral patterning in Xenopus: inhibition of ventral signals by direct binding of chordin to BMP-4." In: *Cell* 86.4, pp. 589–598.

Piccolo, S, E Agius, L Leyns, S Bhattacharyya, H Grunz, T Bouwmeester, and E M de Robertis (1999). "The head inducer Cerberus is a multifunctional antagonist of Nodal, BMP and Wnt signals." In: *Nature* 397.6721, pp. 707–710.

Pierreux, C E, F J Nicolás, and C S Hill (2000). "Transforming growth factor beta-independent shuttling of Smad4 between the cytoplasm and nucleus." In: *Molecular and cellular biology* 20.23, pp. 9041–9054.

Pinson, K I, J Brennan, S Monkley, B J Avery, and W C Skarnes (2000). "An LDL-receptor-related protein mediates Wnt signalling in mice." In: *Nature* 407.6803, pp. 535–538.

Popov, Ivan K, Taejoon Kwon, David K Crossman, Michael R Crowley, John B Wallingford, and Chenbei Chang (2016). "Identification of new regulators of embryonic patterning and morphogenesis in Xenopus gastrulae by RNA sequencing." In: *Developmental Biology*.

Port, Fillip, George Hausmann, and Konrad Basler (2011). "A genome-wide RNA interference screen uncovers two p24 proteins as regulators of Wingless secretion." In: *Nature Publishing Group* 12.11, pp. 1144–1152.

Port, Fillip, Marco Kuster, Patrick Herr, Edy Furger, Carla Bänziger, George Hausmann, and Konrad Basler (2008). "Wingless secretion promotes and requires retromer-dependent cycling of Wntless". In: *Nature cell biology* 10.2, pp. 178–185.

Quinlan, Aaron R and Ira M Hall (2010). "BEDTools: a flexible suite of utilities for comparing genomic features." In: *Bioinformatics (Oxford, England)* 26.6, pp. 841–842.

R Core Team (2013). *R: A Language and Environment for Statistical Computing*. R Foundation for Statistical Computing. Vienna, Austria. URL: `http://www.R-project.org/`.

Radaev, Sergei, Zhongcheng Zou, Tao Huang, Eileen M Lafer, Andrew P Hinck, and Peter D Sun (2010). "Ternary complex of transforming growth factor-beta1 reveals isoform-specific ligand recognition and receptor recruitment in the superfamily." In: *The Journal of biological chemistry* 285.19, pp. 14806–14814.

Raftery, L A, V Twombly, K Wharton, and W M Gelbart (1995). "Genetic screens to identify elements of the decapentaplegic signaling pathway in Drosophila." In: *Genetics* 139.1, pp. 241–254.

Ramírez, Fidel, Devon P Ryan, Björn Grüning, Vivek Bhardwaj, Fabian Kilpert, Andreas S Richter, Steffen Heyne, Friederike Dündar, and Thomas Manke (2016). "deepTools2: a next generation web server for deep-sequencing data analysis." In: *Nucleic Acids Research* 44.W1, W160–5.

Rankin, Scott A, Jay Kormish, Matt Kofron, Anil Jegga, and Aaron M Zorn (2011). "A gene regulatory network controlling hhex transcription in the anterior endoderm of the organizer". In: *Developmental Biology* 351.2, pp. 297–310.

Reis, Alice H, Bryan T MacDonald, Kerstin Feistel, Jose M Brito, Nathalia G Amado, Chiwei Xu, Jose G Abreu, and Xi He (2014). "Expression and evolution of the Tiki1 and Tiki2 genes in vertebrates." In: *The International journal of developmental biology* 58.5, pp. 355–362.

Reversade, Bruno and E M de Robertis (2005). "Regulation of ADMP and BMP2/4/7 at opposite embryonic poles generates a self-regulating morphogenetic field." In: *Cell* 123.6, pp. 1147–1160.

Reya, Tannishtha, Mary O'Riordan, Ross Okamura, Erik Devaney, Karl Willert, Roel Nusse, and Rudolf Grosschedl (2000). "Wnt Signaling Regulates B Lymphocyte Proliferation through a LEF-1 Dependent Mechanism". In: *Immunity* 13.1, pp. 15–24.

Rhee, Ho Sung and B Franklin Pugh (2011). "Comprehensive genome-wide protein-DNA interactions detected at single-nucleotide resolution." In: *Cell* 147.6, pp. 1408–1419.

Rhee, Ho Sung and B Franklin Pugh (2012). "Genome-wide structure and organization of eukaryotic pre-initiation complexes." In: *Nature* 483.7389, pp. 295–301.

Rijsewijk, F, M Schuermann, E Wagenaar, P Parren, D Weigel, and R Nusse (1987). "The Drosophila homolog of the mouse mammary oncogene int-1 is identical to the segment polarity gene wingless." In: *Cell* 50.4, pp. 649–657.

Roberts, S G and M R Green (1996). "Purification and analysis of functional preinitiation complexes." In: *Methods in enzymology* 273, pp. 110–118.

Robertson, Gordon, Martin Hirst, Matthew Bainbridge, Misha Bilenky, Yongjun Zhao, Thomas Zeng, Ghia Euskirchen, Bridget Bernier, Richard Varhol, Allen Delaney, Nina Thiessen, Obi L Griffith, Ann He, Marco Marra, Michael Snyder, and Steven Jones (2007). "Genome-wide profiles of STAT1 DNA association using chromatin immunoprecipitation and massively parallel sequencing." In: *Nature Methods* 4.8, pp. 651–657.

Robinson, James T, Helga Thorvaldsdottir, Wendy Winckler, Mitchell Guttman, Eric S Lander, Gad Getz, and Jill P Mesirov (2011). "Integrative genomics viewer." In: *Nature Biotechnology* 29.1, pp. 24–26.

Rosa, F M (1989). "Mix.1, a homeobox mRNA inducible by mesoderm inducers, is expressed mostly in the presumptive endodermal cells of Xenopus embryos." In: *Cell* 57.6, pp. 965–974.

Ross-Innes, Caryn S, Rory Stark, Andrew E Teschendorff, Kelly A Holmes, H Raza Ali, Mark J Dunning, Gordon D Brown, Ondrej Gojis, Ian O Ellis, Andrew R Green, Simak Ali, Suet-Feung Chin, Carlo Palmieri, Carlos Caldas, and Jason S Carroll (2012). "Differential oestrogen receptor binding is associated with clinical outcome in breast cancer." In: *Nature* 481.7381, pp. 389–393.

Rossi, Andrea, Zacharias Kontarakis, Claudia Gerri, Hendrik Nolte, Soraya Hölper, Marcus Krüger, and Didier Y R Stainier (2015). "Genetic compensation induced by deleterious mutations but not gene knockdowns." In: *Nature* 524.7564, pp. 230–233.

Rowning, B A, J Wells, M Wu, J C Gerhart, R T Moon, and C A Larabell (1997). "Microtubule-mediated transport of organelles and localization of beta-catenin to the future dorsal side of Xenopus eggs." In: *Proceedings of the National Academy of Sciences of the United States of America* 94.4, pp. 1224–1229.

Rubinfeld, B, D A Tice, and P Polakis (2001). "Axin-dependent phosphorylation of the adenomatous polyposis coli protein mediated by casein kinase 1epsilon." In: *The Journal of biological chemistry* 276.42, pp. 39037–39045.

Rubinfeld, B, I Albert, E Porfiri, C Fiol, S Munemitsu, and P Polakis (1996). "Binding of GSK3beta to the APC-beta-catenin complex and regulation of complex assembly." In: *Science* 272.5264, pp. 1023–1026.

Ryan, K, N Garrett, A Mitchell, and J B Gurdon (1996). "Eomesodermin, a key early gene in Xenopus mesoderm differentiation." In: *Cell* 87.6, pp. 989–1000.

Rzehak, K (1972). "Changes in the pigment pattern of eggs of Xenopus laevis following fertilization." In: *Folia biologica* 20.4, pp. 409–416.

Sakai, M (1996). "The vegetal determinants required for the Spemann organizer move equatorially during the first cell cycle." In: *Development* 122.7, pp. 2207–2214.

Sakanaka, C, P Leong, L Xu, S D Harrison, and L T Williams (1999). "Casein kinase iepsilon in the wnt pathway: regulation of beta-catenin function." In: *Proceedings of the National Academy of Sciences of the United States of America* 96.22, pp. 12548–12552.

Salic, A N, K L Kroll, L M Evans, and M W Kirschner (1997). "Sizzled: a secreted Xwnt8 antagonist expressed in the ventral marginal zone of Xenopus embryos." In: *Development (Cambridge, England)* 124.23, pp. 4739–4748.

Sander, Veronika, Bruno Reversade, and E M de Robertis (2007). "The opposing homeobox genes Goosecoid and Vent1/2 self-regulate Xenopus patterning." In: *The EMBO journal* 26.12, pp. 2955–2965.

Sasai, Y (1994). "Xenopus chordin: A novel dorsalizing factor activated by organizer-specific homeobox genes". In: *Cell* 79.5, pp. 779–790.

Satow, Reiko, Akira Kurisaki, Te-chuan Chan, Tatsuo S Hamazaki, and Makoto Asashima (2006). "Dullard promotes degradation and dephosphorylation of BMP receptors and is required for neural induction." In: *Developmental Cell* 11.6, pp. 763–774.

Savage, C, P Das, A L Finelli, S R Townsend, C Y Sun, S E Baird, and R W Padgett (1996). "Caenorhabditis elegans genes sma-2, sma-3, and sma-4 define a conserved family of transforming growth factor beta pathway components." In: *Proceedings of the National Academy of Sciences of the United States of America* 93.2, pp. 790–794.

Scharf, S R and J C Gerhart (1980). "Determination of the dorsal-ventral axis in eggs of Xenopus laevis: complete rescue of uv-impaired eggs by oblique orientation before first cleavage." In: *Developmental Biology* 79.1, pp. 181–198.

Scharf, S R, B Rowning, M Wu, and J C Gerhart (1989). "Hyperdorsoanterior embryos from Xenopus eggs treated with D2O". In: *Developmental Biology* 134.1, pp. 175–188.

Schmidl, Christian, Christian Schmidl, André F Rendeiro, André F Rendeiro, Nathan C Sheffield, Nathan C Sheffield, Christoph Bock, and Christoph Bock (2015). "ChIPmentation: fast, robust, low-input ChIP-seq for histones and transcription factors." In: *Nature Methods* 12.10, pp. 963–965.

Schneider, S, H Steinbeisser, R M Warga, and P Hausen (1996). "Beta-catenin translocation into nuclei demarcates the dorsalizing centers in frog and fish embryos." In: *Mechanisms of Development* 57.2, pp. 191–198.

Schrons, H, E Knust, and J A Campos-Ortega (1992). "The Enhancer of split complex and adjacent genes in the 96F region of Drosophila melanogaster are required for segregation of neural and epidermal progenitor cells." In: *Genetics* 132.2, pp. 481–503.

Schulte-Merker, S and J C Smith (1995). "Mesoderm formation in response to Brachyury requires FGF signalling." In: *Current Biology* 5.1, pp. 62–67.

Schulte-Merker, S, F J van Eeden, M E Halpern, C B Kimmel, and C Nüsslein-Volhard (1994). "no tail (ntl) is the zebrafish homologue of the mouse T (Brachyury) gene." In: *Development (Cambridge, England)* 120.4, pp. 1009–1015.

Sebald, Walter, Joachim Nickel, Jin-Li Zhang, and Thomas D Mueller (2004). "Molecular recognition in bone morphogenetic protein (BMP)/receptor interaction." In: *Biological chemistry* 385.8, pp. 697–710.

Sekiya, Takashi, Takeaki Oda, Ken Matsuura, and Tetsu Akiyama (2004). "Transcriptional regulation of the TGF-beta pseudoreceptor BAMBI by TGF-beta signaling." In: *Biochemical and Biophysical Research Communications* 320.3, pp. 680–684.

Seyres, Denis, Yad Ghavi-Helm, Guillaume Junion, Ouarda Taghli-Lamallem, Céline Guichard, Laurence Röder, Charles Girardot, Eileen E M Furlong, and Laurent Perrin (2016). "Identification and in silico modeling of enhancers reveals new features of the cardiac differentiation network." In: *Development* 143.23, pp. 4533–4542.

Shao, Zhen, Yijing Zhang, Guo-Cheng Yuan, Stuart H Orkin, and David J Waxman (2012). "MAnorm: a robust model for quantitative comparison of ChIP-Seq data sets." In: *Genome Biology* 13.3, R16.

Shi, Weibin, Chuanxi Sun, Bin He, Wencheng Xiong, Xingming Shi, Dachun Yao, and Xu Cao (2004). "GADD34-PP1c recruited by Smad7 dephosphorylates TGFbeta type I receptor." In: *The Journal of Cell Biology* 164.2, pp. 291–300.

Shimizu, H, M A Julius, M Giarré, Z Zheng, A M Brown, and J Kitajewski (1997). "Transformation by Wnt family proteins correlates with regulation of beta-catenin." In: *Cell growth & differentiation : the molecular biology journal of the American Association for Cancer Research* 8.12, pp. 1349–1358.

Showell, Chris, Kathleen S Christine, Elizabeth M Mandel, and Frank L Conlon (2006). "Developmental expression patterns of Tbx1, Tbx2, Tbx5, and Tbx20 in Xenopus tropicalis." In: *Developmental Dynamics* 235.6, pp. 1623–1630.

Siegfried, E, E L Wilder, and N Perrimon (1994). "Components of wingless signalling in Drosophila." In: *Nature* 367.6458, pp. 76–80.

Sierra, Jose, Tomonori Yoshida, Claudio A Joazeiro, and Katherine A Jones (2006). "The APC tumor suppressor counteracts β-catenin activation and H3K4 methylation at Wnt target genes". In: *Genes & Development* 20.5, pp. 586–600.

Slack, J M (1994). "Inducing factors in Xenopus early embryos." In: *CURBIO* 4.2, pp. 116–126.

Slack, J M and D Forman (1980). "An interaction between dorsal and ventral regions of the marginal zone in early amphibian embryos." In: *Journal of embryology and experimental morphology* 56, pp. 283–299.

Slack, J M, B G Darlington, J K Heath, and S F Godsave (1987). "Mesoderm induction in early Xenopus embryos by heparin-binding growth factors." In: *Nature* 326.6109, pp. 197–200.

Smith, J (1997). "Brachyury and the T-box genes." In: *Current Opinion in Genetics & Development* 7.4, pp. 474–480.

Smith, J (1999). "T-box genes: what they do and how they do it". In: *Trends in Genetics*.

Smith, J C (1987). "A mesoderm-inducing factor is produced by Xenopus cell line." In: *Development* 99.1, pp. 3–14.

Smith, J C, L Dale, and J M Slack (1985). "Cell lineage labels and region-specific markers in the analysis of inductive interactions." In: *Journal of embryology and experimental morphology* 89 Suppl, pp. 317–331.

Smith, J C and J M Slack (1983). "Dorsalization and neural induction: properties of the organizer in Xenopus laevis." In: *Journal of embryology and experimental morphology* 78, pp. 299–317.

Smith, J C, B M Price, K Van Nimmen, and D Huylebroeck (1990). "Identification of a potent Xenopus mesoderm-inducing factor as a homologue of activin A." In: *Nature* 345.6277, pp. 729–731.

Smith, J C, B M J Price, J B A Green, D Weigel, and B G Herrmann (1991). "Expression of a xenopus homolog of Brachyury (T) is an immediate-early response to mesoderm induction". In: *Cell* 67.1, pp. 79–87.

Smith, W C and R M Harland (1992). "Expression cloning of noggin, a new dorsalizing factor localized to the Spemann organizer in Xenopus embryos." In: *Cell* 70.5, pp. 829–840.

Smits, Arne H, Rik G H Lindeboom, Matteo Perino, Simon J van Heeringen, Gert Jan C Veenstra, and Michiel Vermeulen (2014). "Global absolute quantification reveals tight regulation of protein expression in single Xenopus eggs." In: *Nucleic Acids Research* 42.15, pp. 9880–9891.

Sokol, S Y (1993). "Mesoderm formation in Xenopus ectodermal explants overexpressing Xwnt8: evidence for a cooperating signal reaching the animal pole by gastrulation." In: *Development (Cambridge, England)* 118.4, pp. 1335–1342.

Sokol, S Y, J Klingensmith, N Perrimon, and K Itoh (1995). "Dorsalizing and neuralizing properties of Xdsh, a maternally expressed Xenopus homolog of dishevelled." In: *Development (Cambridge, England)* 121.6, pp. 1637–1647.

Sokol, Sergei Y and Stefan Hoppler (2014). *Wnt Signaling in Early Vertebrate Development*. Vol. 5. From Fertilization to Gastrulation. Hoboken, NJ, USA: John Wiley & Sons, Inc.

Solomon, M J, P L Larsen, and A Varshavsky (1988). "Mapping protein-DNA interactions in vivo with formaldehyde: evidence that histone H4 is retained on a highly transcribed gene." In: *Cell* 53.6, pp. 937–947.

Song, Haiyun, Sandra Goetze, Johannes Bischof, Chloe Spichiger-Haeusermann, Marco Kuster, Erich Brunner, and Konrad Basler (2010). "Coop functions as a corepressor of Pangolin and antagonizes Wingless signaling." In: *Genes & Development* 24.9, pp. 881–886.

Souchelnytskyi, S, P ten Dijke, K Miyazono, and C H Heldin (1996). "Phosphorylation of Ser165 in TGF-beta type I receptor modulates TGF-beta1-induced cellular responses." In: *The EMBO journal* 15.22, pp. 6231–6240.

Spitz, François and Eileen E M Furlong (2012). "Transcription factors: from enhancer binding to developmental control". In: *Nature reviews. Genetics* 13.9, pp. 613–626.

Stambolic, V, L Ruel, and J R Woodgett (1996). "Lithium inhibits glycogen synthase kinase-3 activity and mimics wingless signalling in intact cells." In: *CURBIO* 6.12, pp. 1664–1668.

Steiner, F A, P B Talbert, S Kasinathan, R B Deal, and S Henikoff (2012). "Cell-type-specific nuclei purification from whole animals for genome-wide expression and chromatin profiling". In: *Genome Research* 22.4, pp. 766–777.

Stennard, F, G Carnac, and J B Gurdon (1996). "The Xenopus T-box gene, Antipodean, encodes a vegetally localised maternal mRNA and can trigger mesoderm formation." In: *Development* 122.12, pp. 4179–4188.

Stennard, F, A M Zorn, K Ryan, N Garrett, and J B Gurdon (1999). "Differential expression of VegT and Antipodean protein isoforms in Xenopus." In: *Mechanisms of Development* 86.1-2, pp. 87–98.

Stott, D, A Kispert, and B G Herrmann (1993). "Rescue of the tail defect of Brachyury mice." In: *Genes & Development* 7.2, pp. 197–203.

Subramanyam, Deepa, Samy Lamouille, Robert L Judson, Jason Y Liu, Nathan Bucay, Rik Derynck, and Robert Blelloch (2011). "Multiple targets of miR-302 and miR-372 promote reprogramming of human fibroblasts to induced pluripotent stem cells." In: *Nature Biotechnology* 29.5, pp. 443–448.

Summerton, James and Dwight Weller (1997). "Morpholino Antisense Oligomers: Design, Preparation, and Properties". In: *Antisense and Nucleic Acid Drug Development* 7.3, pp. 187–195.

Summerton, James E (2017). "Invention and Early History of Morpholinos: From Pipe Dream to Practical Products". In: *Gene Regulatory Networks*. New York, NY: Springer New York, pp. 1–15.

Sun, B I, S M Bush, L A Collins-Racie, E R LaVallie, E A DiBlasio-Smith, N M Wolfman, J M McCoy, and H L Sive (1999). "derrière: a TGF-beta family member required for posterior development in Xenopus." In: *Development (Cambridge, England)* 126.7, pp. 1467–1482.

Sun, Y, F T Kolligs, M O Hottiger, R Mosavin, E R Fearon, and G J Nabel (2000). "Regulation of beta -catenin transformation by the p300 transcriptional coactivator." In: *Proceedings of the National Academy of Sciences of the United States of America* 97.23, pp. 12613–12618.

Sussman, D J, J Klingensmith, P Salinas, P S Adams, R Nusse, and N Perrimon (1994). "Isolation and characterization of a mouse homolog of the Drosophila segment polarity gene dishevelled." In: *Dev Biol* 166.1, pp. 73–86.

Suzuki, A, C Chang, J M Yingling, X F Wang, and A Hemmati-Brivanlou (1997). "Smad5 induces ventral fates in Xenopus embryo." In: *Dev Biol* 184.2, pp. 402–405.

Symes, K, C Yordán, and M Mercola (1994). "Morphological differences in Xenopus embryonic mesodermal cells are specified as an early response to distinct threshold concentrations of activin." In: *Development (Cambridge, England)* 120.8, pp. 2339–2346.

Tada, M, M A O'Reilly, and J C Smith (1997). "Analysis of competence and of Brachyury autoinduction by use of hormone-inducible Xbra." In: *Development* 124.11, pp. 2225–2234.

Tada, M and J C Smith (2000). "Xwnt11 is a target of Xenopus Brachyury: regulation of gastrulation movements via Dishevelled, but not through the canonical Wnt pathway." In: *Development* 127.10, pp. 2227–2238.

Tada, M, E S Casey, L Fairclough, and J C Smith (1998). "Bix1, a direct target of Xenopus T-box genes, causes formation of ventral mesoderm and endoderm." In: *Development* 125.20, pp. 3997–4006.

Tago, K, T Nakamura, M Nishita, J Hyodo, S Nagai, Y Murata, S Adachi, S Ohwada, Y Morishita, H Shibuya, and T Akiyama (2000). "Inhibition of Wnt signaling by ICAT, a novel beta-catenin-interacting protein." In: *Genes & Development* 14.14, pp. 1741–1749.

Takacs, Carter M, Jason R Baird, Edward G Hughes, Sierra S Kent, Hassina Benchabane, Raehum Paik, and Yashi Ahmed (2008). "Dual positive and negative regulation of wingless signaling by adenomatous polyposis coli." In: *Science* 319.5861, pp. 333–336.

Takahashi, S, C Yokota, K Takano, K Tanegashima, Y Onuma, J Goto, and M Asashima (2000). "Two novel nodal-related genes initiate early inductive events in Xenopus Nieuwkoop center." In: *Development* 127.24, pp. 5319–5329.

Takemaru, K I and R T Moon (2000). "The transcriptional coactivator CBP interacts with beta-catenin to activate gene expression." In: *The Journal of Cell Biology* 149.2, pp. 249–254.

Takemaru, Ken-Ichi, Shinji Yamaguchi, Young Sik Lee, Yang Zhang, Richard W Carthew, and Randall T Moon (2003). "Chibby, a nuclear beta-catenin-associated antagonist of the Wnt/Wingless pathway." In: *Nature* 422.6934, pp. 905–909.

Tamai, K, M Semenov, Y Kato, R Spokony, C Liu, Y Katsuyama, F Hess, J P Saint-Jeannet, and X He (2000). "LDL-receptor-related proteins in Wnt signal transduction." In: *Nature* 407.6803, pp. 530–535.

Tamai, Keiko, Xin Zeng, Chunming Liu, Xinjun Zhang, Yuko Harada, Zhijie Chang, and Xi He (2004). "A mechanism for Wnt coreceptor activation." In: *Molecular cell* 13.1, pp. 149–156.

Tanaka, Masao, Kosaku Murakami, Shoichi Ozaki, Yoshitaka Imura, Xiao-Peng Tong, Takuo Watanabe, Toshioki Sawaki, Takafumi Kawanami, Daisuke Kawabata, Takao Fujii, Takashi Usui, Yasufumi Masaki, Toshihiro Fukushima, Zhe-Xiong Jin, Hisanori Umehara, and Tsuneyo Mimori (2010). "DIP2 disco-interacting protein 2 homolog A (Drosophila) is a candidate receptor for follistatin-related protein/follistatin-like 1–analysis of their binding with TGF-β superfamily proteins." In: *The FEBS journal* 277.20, pp. 4278–4289.

Tang, Xiaofang, Yihui Wu, Tatyana Y Belenkaya, Qinzhu Huang, Lorraine Ray, Jia Qu, and Xinhua Lin (2012). "Roles of N-glycosylation and lipidation in Wg secretion and signaling". In: *Developmental Biology* 364.1, pp. 32–41.

Tao, Qinghua, Chika Yokota, Helbert Puck, Matt Kofron, Bilge Birsoy, Dong Yan, Makoto Asashima, Christopher C Wylie, Xinhua Lin, and Janet Heasman (2005). "Maternal wnt11 activates the canonical wnt signaling pathway required for axis formation in Xenopus embryos." In: *Cell* 120.6, pp. 857–871.

Tauriello, Daniele V F, Ingrid Jordens, Katharina Kirchner, Jerry W Slootstra, Tom Kruitwagen, Britta A M Bouwman, Maria Noutsou, Stefan G D Rüdiger, Klaus Schwamborn, Alexandra Schambony, and Madelon M Maurice (2012). "Wnt/β-catenin signaling requires interaction of the Dishevelled DEP domain and C terminus with a discontinuous motif in Frizzled." In: *Proceedings of the National Academy of Sciences* 109.14, E812–20.

Taylor, Neil A, Wim J M Van De Ven, and John W M Creemers (2003). "Curbing activation: proprotein convertases in homeostasis and pathology." In: *FASEB journal : official publication of the Federation of American Societies for Experimental Biology* 17.10, pp. 1215–1227.

Thorvaldsdottir, Helga, James T Robinson, and Jill P Mesirov (2013). "Integrative Genomics Viewer (IGV): high-performance genomics data visualization and exploration." In: *Briefings in bioinformatics* 14.2, pp. 178–192.

Todaro, G J and R J Huebner (1972). "The viral oncogene hypothesis: New evidence". In: *Proceedings of the National ...*

Tolwinski, N S and E Wieschaus (2001). "Armadillo nuclear import is regulated by cytoplasmic anchor Axin and nuclear anchor dTCF/Pan." In: *Development (Cambridge, England)* 128.11, pp. 2107–2117.

Tolwinski, Nicholas S, Marcel Wehrli, Anna Rives, Naz Erdeniz, Stephen DiNardo, and Eric Wieschaus (2003). "Wg/Wnt signal can be transmitted through arrow/LRP5,6 and Axin independently of Zw3/Gsk3beta activity." In: *Developmental Cell* 4.3, pp. 407–418.

Topol, Lilia, Wen Chen, Hai Song, Timothy F Day, and Yingzi Yang (2009). "Sox9 inhibits Wnt signaling by promoting beta-catenin phosphorylation in the nucleus." In: *The Journal of biological chemistry* 284.5, pp. 3323–3333.

Trinh, Le A, Vanessa Chong-Morrison, Daria Gavriouchkina, Tatiana Hochgreb-Hägele, Upeka Senanayake, Scott E Fraser, and Tatjana Sauka-Spengler (2017). "Biotagging of Specific Cell Populations in Zebrafish Reveals Gene Regulatory Logic Encoded in the Nuclear Transcriptome". In: *CellReports* 19.2, pp. 425–440.

Tsuda, Hiroshi, Noriaki Sasai, Mami Matsuo-Takasaki, Makoto Sakuragi, Yoshinobu Murakami, and Yoshiki Sasai (2002). "Dorsalization of the neural tube by Xenopus tiarin, a novel patterning factor secreted by the flanking nonneural head ectoderm." In: *Neuron* 33.4, pp. 515–528.

Tsukazaki, Tomoo, Theodore A Chiang, Anne F Davison, Liliana Attisano, and Jeffrey L Wrana (1998). "SARA, a FYVE Domain Protein that Recruits Smad2 to the TGFβ Receptor". In: *Cell* 95.6, pp. 779–791.

Tucker, R F, E L Branum, G D Shipley, R J Ryan, and H L Moses (1984). "Specific binding to cultured cells of 125I-labeled type beta transforming growth factor from human platelets." In: *Proceedings of the National Academy of Sciences of the United States of America* 81.21, pp. 6757–6761.

Ubbels, G A, K Hara, C H Koster, and M W Kirschner (1983). "Evidence for a functional role of the cytoskeleton in determination of the dorsoventral axis in Xenopus laevis eggs." In: *Journal of embryology and experimental morphology* 77, pp. 15–37.

Ulloa, Fausto and Elisa Martí (2010). "Wnt won the war: antagonistic role of Wnt over Shh controls dorso-ventral patterning of the vertebrate neural tube." In: *Developmental Dynamics* 239.1, pp. 69–76.

Umulis, David, Michael B O'Connor, and Seth S Blair (2009). "The extracellular regulation of bone morphogenetic protein signaling." In: *Development* 136.22, pp. 3715–3728.

Untergasser, Andreas, Ioana Cutcutache, Triinu Koressaar, Jian Ye, Brant C Faircloth, Maido Remm, and Steven G Rozen (2012). "Primer3–new capabilities and interfaces." In: *Nucleic Acids Research* 40.15, e115.

Varelas, Xaralabos, Rui Sakuma, Payman Samavarchi-Tehrani, Raheem Peerani, Balaji M Rao, Joanna Dembowy, Michael B Yaffe, Peter W Zandstra, and Jeffrey L Wrana (2008). "TAZ controls Smad nucleocytoplasmic shuttling and regulates human embryonic stem-cell self-renewal." In: *Nature cell biology* 10.7, pp. 837–848.

Vincent, J P and J C Gerhart (1987). "Subcortical rotation in Xenopus eggs: an early step in embryonic axis specification." In: *Developmental Biology* 123.2, pp. 526–539.

Vincent, J P, G F Oster, and J C Gerhart (1986). "Kinematics of gray crescent formation in Xenopus eggs: the displacement of subcortical cytoplasm relative to the egg surface." In: *Developmental Biology* 113.2, pp. 484–500.

Vinson, C R and P N Adler (1987). "Directional non-cell autonomy and the transmission of polarity information by the frizzled gene of Drosophila." In: *Nature* 329.6139, pp. 549–551.

Visel, Axel, Matthew J Blow, Zirong Li, Tao Zhang, Jennifer A Akiyama, Amy Holt, Ingrid Plajzer-Frick, Malak Shoukry, Crystal Wright, Feng Chen, Veena Afzal, Bing Ren, Edward M Rubin, and Len A Pennacchio (2009). "ChIP-seq accurately predicts tissue-specific activity of enhancers." In: *Nature* 457.7231, pp. 854–858.

Vitorino, Marta, Ana Cristina Silva, José Manuel Inácio, José Silva Ramalho, Michal Gur, Abraham Fainsod, Herbert Steinbeisser, and José António Belo (2015). " Xenopus Pkdcc1 and Pkdcc2 Are Two New Tyrosine Kinases Involved in the Regulation of JNK Dependent Wnt/PCP Signaling Pathway". In: *PLoS ONE* 10.8, e0135504.

Vonica, Alin and Barry M Gumbiner (2002). "Zygotic Wnt Activity Is Required for Brachyury Expression in the Early Xenopus laevis Embryo". In: *Developmental Biology* 250.1, pp. 112–127.

Voss, Ty C and Gordon L Hager (2014). "Dynamic regulation of transcriptional states by chromatin and transcription factors." In: *Nature reviews. Genetics* 15.2, pp. 69–81.

Waskom, Michael, Olga Botvinnik, Paul Hobson, John B. Cole, Yaroslav Halchenko, Stephan Hoyer, Alistair Miles, Tom Augspurger, Tal Yarkoni, Tobias Megies, Luis Pedro Coelho, Daniel Wehner, cynddl, Erik Ziegler, diego0020, Yury V. Zaytsev, Travis Hoppe, Skipper Seabold, Phillip Cloud, Miikka Koskinen, Kyle Meyer, Adel

Qalieh, and Dan Allan (2014). *seaborn: v0.5.0 (November 2014)*. DOI: 10.5281/zenodo.12710. URL: https://doi.org/10.5281/zenodo.12710.

Watanabe, M, N Masuyama, M Fukuda, and E Nishida (2000). "Regulation of intracellular dynamics of Smad4 by its leucine-rich nuclear export signal." In: *EMBO reports* 1.2, pp. 176–182.

Weaver, C (2004). "Move it or lose it: axis specification in Xenopus". In: *Development* 131.15, pp. 3491–3499.

Weeks, D L and D A Melton (1987). "A maternal mRNA localized to the vegetal hemisphere in Xenopus eggs codes for a growth factor related to TGF-beta." In: *Cell* 5, pp. 861–867.

Wehrli, M, S T Dougan, K Caldwell, L O'Keefe, S Schwartz, D Vaizel-Ohayon, E Schejter, A Tomlinson, and S DiNardo (2000). "arrow encodes an LDL-receptor-related protein essential for Wingless signalling." In: *Nature* 407.6803, pp. 527–530.

Weiss, Alexander and Liliana Attisano (2013). "The TGFbeta Superfamily Signaling Pathway". In: *Wiley interdisciplinary reviews. Developmental biology* 2.1, pp. 47–63.

Wells, Rebecca G, Lilach Gilboa, Yin Sun, Xuedong Liu, Yoav I Henis, and Harvey F Lodish (1999). "Transforming Growth Factor-β Induces Formation of a Dithiothreitol-resistant Type I/Type II Receptor Complex in Live Cells". In: *The Journal of biological chemistry* 274.9, pp. 5716–5722.

Wessely, Oliver, Eric Agius, Michael Oelgeschläger, Edgar M Pera, and E M de Robertis (2001). "Neural Induction in the Absence of Mesoderm: β-Catenin-Dependent Expression of Secreted BMP Antagonists at the Blastula Stage in Xenopus". In: *Developmental Biology* 234.1, pp. 161–173.

Wessely, Oliver, James I Kim, Douglas Geissert, Uyen Tran, and E M de Robertis (2004). "Analysis of Spemann organizer formation in Xenopus embryos by cDNA macroarrays." In: *Developmental Biology* 269.2, pp. 552–566.

Wetering, M van de, R Cavallo, D Dooijes, M van Beest, J van Es, J Loureiro, A Ypma, D Hursh, T Jones, A Bejsovec, M Peifer, M Mortin, and H Clevers (1997). "Armadillo coactivates transcription driven by the product of the Drosophila segment polarity gene dTCF." In: *Cell* 88.6, pp. 789–799.

Wicks, Stephen J, Katherine Haros, Marjorie Maillard, Ling Song, Robert E Cohen, Peter Ten Dijke, and Andrew Chantry (2005). "The deubiquitinating enzyme UCH37 interacts with Smads and regulates TGF-beta signalling." In: *Oncogene* 24.54, pp. 8080–8084.

Willot, V, J Mathieu, Yan Lu, B Schmid, S Sidi, Yi-Lin Yan, J H Postlethwait, M Mullins, F Rosa, and N Peyriéras (2002). "Cooperative action of ADMP- and BMP-mediated pathways in regulating cell fates in the zebrafish gastrula." In: *Developmental Biology* 241.1, pp. 59–78.

Wills, Andrea E and Julie C Baker (2015). "E2a Is Necessary for Smad2/3-Dependent Transcription and the Direct Repression of lefty during Gastrulation". In: *Developmental Cell* 32.3, pp. 345–357.

Wilson, P A and D A Melton (1994). "Mesodermal patterning by an inducer gradient depends on secondary cell-cell communication." In: *CURBIO* 4.8, pp. 676–686.

Wolpert, Lewis and Cheryll Tickle (2011). *Principles of Development*. 4th. Oxford University Press.

Wong, G T, B J Gavin, and A P McMahon (1994). "Differential transformation of mammary epithelial cells by Wnt genes." In: *Molecular and cellular biology* 14.9, pp. 6278–6286.

Wozney, J M, V Rosen, A J Celeste, L M Mitsock, M J Whitters, R W Kriz, R M Hewick, and E A Wang (1988). "Novel regulators of bone formation: molecular clones and activities." In: *Science* 242.4885, pp. 1528–1534.

Wrana, J L, L Attisano, J Cárcamo, A Zentella, J Doody, M Laiho, X F Wang, and J Massague (1992). "TGF beta signals through a heteromeric protein kinase receptor complex." In: *Cell* 71.6, pp. 1003–1014.

Wrana, J L, L Attisano, R Wieser, F Ventura, and J Massague (1994). "Mechanism of activation of the TGF-beta receptor." In: *Nature* 370.6488, pp. 341–347.

Wu, Beibei, Sarah Piloto, Weihua Zeng, Nate P Hoverter, Thomas F Schilling, and Marian L Waterman (2013). "Ring Finger Protein 14 is a new regulator of TCF/β-catenin-mediated transcription and colon cancer cell survival." In: *Nature Publishing Group* 14.4, pp. 347–355.

Wu, G, Y G Chen, B Ozdamar, C A Gyuricza, P A Chong, J L Wrana, J Massague, and Y Shi (2000). "Structural basis of Smad2 recognition by the Smad anchor for receptor activation." In: *Science* 287.5450, pp. 92–97.

Wühr, Martin, Robert M Freeman, Marc Presler, Marko E Horb, Leonid Peshkin, Steven P Gygi, and Marc W Kirschner (2014). "Deep proteomics of the Xenopus laevis egg using an mRNA-derived reference database." In: *Current biology : CB* 24.13, pp. 1467–1475.

Xi, Qiaoran, Wei He, Xiang H-F Zhang, Hong-Van Le, and Joan Massagué (2008). "Genome-wide impact of the BRG1 SWI/SNF chromatin remodeler on the transforming growth factor beta transcriptional program." In: *The Journal of biological chemistry* 283.2, pp. 1146–1155.

Xiao, Z, X Liu, and H F Lodish (2000). "Importin beta mediates nuclear translocation of Smad 3." In: *The Journal of biological chemistry* 275.31, pp. 23425–23428.

Xiao, Z, N Watson, C Rodriguez, and H F Lodish (2001). "Nucleocytoplasmic shuttling of Smad1 conferred by its nuclear localization and nuclear export signals." In: *The Journal of biological chemistry* 276.42, pp. 39404–39410.

Xiao, Zhan, Robert Latek, and Harvey F Lodish (2003). "An extended bipartite nuclear localization signal in Smad4 is required for its nuclear import and transcriptional activity." In: *Oncogene* 22.7, pp. 1057–1069.

Xiao, Zhan, Amy M Brownawell, Ian G Macara, and Harvey F Lodish (2003). "A novel nuclear export signal in Smad1 is essential for its signaling activity." In: *The Journal of biological chemistry* 278.36, pp. 34245–34252.

Xing, Yi, Wilson K Clements, David Kimelman, and Wenqing Xu (2003). "Crystal structure of a beta-catenin/axin complex suggests a mechanism for the beta-catenin destruction complex." In: *Genes & Development* 17.22, pp. 2753–2764.

Xing, Yi, Wilson K Clements, Isolde Le Trong, Thomas R Hinds, Ronald Stenkamp, David Kimelman, and Wenqing Xu (2004). "Crystal structure of a beta-catenin/APC complex reveals a critical role for APC phosphorylation in APC function." In: *Molecular cell* 15.4, pp. 523–533.

Xu, Lan, Yibin Kang, Seda Cöl, and Joan Massagué (2002). "Smad2 nucleocytoplasmic shuttling by nucleoporins CAN/Nup214 and Nup153 feeds TGFbeta signaling complexes in the cytoplasm and nucleus." In: *Molecular cell* 10.2, pp. 271–282.

Xu, Lan, Claudio Alarcón, Seda Cöl, and Joan Massagué (2003). "Distinct domain utilization by Smad3 and Smad4 for nucleoporin interaction and nuclear import." In: *The Journal of biological chemistry* 278.43, pp. 42569–42577.

Xu, Lan, Xiaohao Yao, Xiaochu Chen, Peiyuan Lu, Biliang Zhang, and Y Tony Ip (2007). "Msk is required for nuclear import of TGF-beta/BMP-activated Smads." In: *The Journal of Cell Biology* 178.6, pp. 981–994.

Yamashita, H, P ten Dijke, P Franzén, K Miyazono, and C H Heldin (1994). "Formation of hetero-oligomeric complexes of type I and type II receptors for transforming growth factor-beta." In: *The Journal of biological chemistry* 269.31, pp. 20172–20178.

Yan, Xiaohua and Ye-Guang Chen (2011). "Smad7: not only a regulator, but also a cross-talk mediator of TGF-β signalling." In: *Biochemical Journal* 434.1, pp. 1–10.

Yan, Xiaohua, Zhenghong Lin, Feng Chen, Xingang Zhao, Hua Chen, Yuanheng Ning, and Ye-Guang Chen (2009). "Human BAMBI Cooperates with Smad7 to Inhibit Transforming Growth Factor-β Signaling". In: *The Journal of biological chemistry* 284.44, pp. 30097–30104.

Yanagawa, Shin-ichi, Yukihiro Matsuda, Jong-Seo Lee, Hiroko Matsubayashi, Sonoka Sese, Tatsuhiko Kadowaki, and Akinori Ishimoto (2002). "Casein kinase I phosphorylates the Armadillo protein and induces its degradation in Drosophila." In: *The EMBO journal* 21.7, pp. 1733–1742.

Yang, Hao, Feng Fang, Ruimin Chang, and Lianyue Yang (2013). "MicroRNA-140-5p suppresses tumor growth and metastasis by targeting transforming growth factor β receptor 1 and fibroblast growth factor 9 in hepatocellular carcinoma." In: *Hepatology (Baltimore, Md.)* 58.1, pp. 205–217.

Yasuoka, Yuuri, Yutaka Suzuki, Shuji Takahashi, Haruka Someya, Norihiro Sudou, Yoshikazu Haramoto, Ken W Cho, Makoto Asashima, Sumio Sugano, and Masanori Taira (2014). "Occupancy of tissue-specific cis-regulatory modules by Otx2 and TLE/Groucho for embryonic head specification." In: *Nature communications* 5, p. 4322.

Yoon, Se-Jin, Andrea E Wills, Edward Chuong, Rakhi Gupta, and Julie C Baker (2011). "HEB and E2A function as SMAD/FOXH1 cofactors." In: *Genes & Development* 25.15, pp. 1654–1661.

Yost, C, M Torres, J R Miller, E Huang, D Kimelman, and R T Moon (1996). "The axis-inducing activity, stability, and subcellular distribution of beta-catenin is regulated in Xenopus embryos by glycogen synthase kinase 3." In: *Genes & Development* 10.12, pp. 1443–1454.

Zakin, Lise and E M de Robertis (2010). "Extracellular regulation of BMP signaling." In: *Current biology : CB* 20.3, R89–92.

Zawel, Leigh, Jia Le Dai, Phillip Buckhaults, Shibin Zhou, Kenneth W Kinzler, Bert Vogelstein, and Scott E Kern (1998). "Human Smad3 and Smad4 Are Sequence-Specific Transcription Activators". In: *Molecular cell* 1.4, pp. 611–617.

Zeng, L, F Fagotto, T Zhang, W Hsu, T J Vasicek, W L Perry, J J Lee, S M Tilghman, B M Gumbiner, and F Costantini (1997). "The mouse Fused locus encodes Axin, an inhibitor of the Wnt signaling pathway that regulates embryonic axis formation." In: *Cell* 90.1, pp. 181–192.

Zeng, Xin, Keiko Tamai, Brad Doble, Shitao Li, He Huang, Raymond Habas, Heidi Okamura, Jim Woodgett, and Xi He (2005). "A dual-kinase mechanism for Wnt co-receptor phosphorylation and activation." In: *Nature* 438.7069, pp. 873–877.

Zhai, Linda, Deepti Chaturvedi, and Susan Cumberledge (2004). "Drosophila wnt-1 undergoes a hydrophobic modification and is targeted to lipid rafts, a process that requires porcupine." In: *The Journal of biological chemistry* 279.32, pp. 33220–33227.

Zhang, Chen U and Ken M Cadigan (2014). *An Overview of Gene Regulation by Wnt/β-Catenin Signaling*. Vol. 18. Molecular Mechanisms and Biological Functions. Hoboken, NJ, USA: John Wiley & Sons, Inc.

Zhang, J and M L King (1996). "Xenopus VegT RNA is localized to the vegetal cortex during oogenesis and encodes a novel T-box transcription factor involved in mesodermal patterning." In: *Development* 122.12, pp. 4119–4129.

Zhang, J, D W Houston, M L King, C Payne, C Wylie, and J Heasman (1998a). "The role of maternal VegT in establishing the primary germ layers in Xenopus embryos." In: *Cell* 94.4, pp. 515–524.

Zhang, Jian, Douglas W Houston, Mary Lou King, Christopher Payne, Christopher Wylie, and Janet Heasman (1998b). "The Role of Maternal VegT in Establishing the Primary Germ Layers in Xenopus Embryos". In: *Cell* 94.4, pp. 515–524.

Zhang, Lei, Jianhang Jia, Bing Wang, Kazuhito Amanai, Keith A Wharton, and Jin Jiang (2006). "Regulation of wingless signaling by the CKI family in Drosophila limb development." In: *Dev Biol* 299.1, pp. 221–237.

Zhang, Long, FangFang Zhou, Yvette Drabsch, Rui Gao, B Ewa Snaar-Jagalska, Craig Mickanin, Huizhe Huang, Kelly-Ann Sheppard, Jeff A Porter, Chris X Lu, and Peter ten Dijke (2012a). "USP4 is regulated by AKT phosphorylation and directly deubiquitylates TGF-β type I receptor." In: *Nature cell biology* 14.7, pp. 717–726.

Zhang, Long, FangFang Zhou, Amaya García de Vinuesa, Esther M de Kruijf, Wilma E Mesker, Li Hui, Yvette Drabsch, Yihao Li, Andreas Bauer, Adrien Rousseau, Kelly-Ann Sheppard, Craig Mickanin, Peter J K Kuppen, Chris X Lu, and Peter ten Dijke (2013). "TRAF4 promotes TGF-β receptor signaling and drives breast cancer metastasis." In: *Molecular cell* 51.5, pp. 559–572.

Zhang, Wei, Yaxin Jiang, Qiang Wang, Xinyong Ma, Zeyu Xiao, Wei Zuo, Xiaohong Fang, and Ye-Guang Chen (2009). "Single-molecule imaging reveals transforming growth factor-beta-induced type II receptor dimerization." In: *Proceedings of the National Academy of Sciences* 106.37, pp. 15679–15683.

Zhang, Xinjun, Jose Garcia Abreu, Chika Yokota, Bryan T MacDonald, Sasha Singh, Karla Loureiro Almeida Coburn, Seong-Moon Cheong, Mingzi M Zhang, Qi-Zhuang Ye, Howard C Hang, Hanno Steen, and Xi He (2012b). "Tiki1 is required for head formation via Wnt cleavage-oxidation and inactivation." In: *Cell* 149.7, pp. 1565–1577.

Zhang, Xinjun, Bryan T MacDonald, Huilan Gao, Michael Shamashkin, Anthony J Coyle, Robert V Martinez, and Xi He (2016). "Characterization of Tiki, a New Family of Wnt-specific Metalloproteases." In: *The Journal of biological chemistry* 291.5, pp. 2435–2443.

Zhang, Yong, Tao Liu, Clifford A Meyer, Jérôme Eeckhoute, David S Johnson, Bradley E Bernstein, Chad Nussbaum, Richard M Myers, Myles Brown, Wei Li, and X Shirley Liu (2008). "Model-based Analysis of ChIP-Seq (MACS)". In: *Genome Biology* 9.9, R137.

Zimmerman, L B, J M De Jesús-Escobar, and R M Harland (1996). "The Spemann organizer signal noggin binds and inactivates bone morphogenetic protein 4." In: *Cell* 86.4, pp. 599–606.

Zuo, Wei, Fei Huang, Y Jeffrey Chiang, Meng Li, Jun Du, Yi Ding, Ting Zhang, Hyuk Woo Lee, Lak Shin Jeong, Yuling Chen, Haiteng Deng, Xin-Hua Feng, Shiwen Luo, Chunji Gao, and Ye-Guang Chen (2013). "c-Cbl-mediated neddylation antagonizes ubiquitination and degradation of the TGF-β type II receptor." In: *Molecular cell* 49.3, pp. 499–510.